



UNIVERSITAT DE
BARCELONA

From *corpora amylacea* to wasteosomes

Marta Riba Baques



Aquesta tesi doctoral està subjecta a la llicència **Reconeixement- NoComercial – SenseObraDerivada 4.0. Espanya de Creative Commons.**

Esta tesis doctoral está sujeta a la licencia **Reconocimiento - NoComercial – SinObraDerivada 4.0. España de Creative Commons.**

This doctoral thesis is licensed under the **Creative Commons Attribution-NonCommercial-NoDerivs 4.0. Spain License.**



UNIVERSITAT DE
BARCELONA

Facultat de Farmàcia i Ciències de l'Alimentació

Departament de Bioquímica i Fisiologia

From *corpora amylacea* to wasteosomes

MARTA RIBA BAQUES

2022



UNIVERSITAT DE BARCELONA

Facultat de Farmàcia i Ciències de l'Alimentació

Departament de Bioquímica i Fisiologia

Programa de doctorat:

Recerca, desenvolupament i control de medicaments

From corpora amylacea to wasteosomes

Memòria presentada per **Marta Riba Baques** per optar al títol de doctor per la
Universitat de Barcelona

Dra. Carme Pelegrí i Gabaldà
(Directora)

Dr. Jordi Vilaplana i Hortensi
(Director)

Marta Riba Baques
(Doctoranda)

MARTA RIBA BAQUES

2022

Aquesta tesi ha estat finançada per:

Projecte 2017 SGR 625

Generalitat de Catalunya

Projecte BFU2016-78398-P

Ministerio de Economía y Competitividad

Projecte PID2020-115475GB-I00

Agencia Estatal de Investigación

La doctoranda ha gaudit dels següents ajuts predoctorals durant la realització d'aquesta tesi:

Ajuts destinats a universitats, centres de recerca i fundacions hospitalàries per contractar personal investigador novell (FI)

Agència de Gestió d'Ajuts Universitaris i de Recerca (AGAUR)

Ayudas para la Formación de Profesorado Universitario (FPU)

Ministerio de Ciencia, Innovación y Universidades

Ayudas complementarias de movilidad destinadas a beneficiarios del programa de

Formación del Profesorado Universitario (FPU)

Ministerio de Ciencia, Innovación y Universidades

ÍNDEX:

ABSTRACT

I. INTRODUCCIÓ	1
1. COSSOS AMILACIS CEREBRALS	3
1.1. Morfologia	4
1.2. Localització	5
1.3. Composició	6
1.4. Presència de neo-epítops	9
1.5. Característiques ultraestructurals	11
1.6. Origen cel·lular	12
1.7. Variacions amb l'edat i en determinades patologies	13
1.8. Significat fisiopatològic i postulats referents a la funció	14
II. OBJECTIUS	21
III. RESULTATS	25
1. ARTICLE 1 <i>Corpora amylacea act as containers that remove waste products from the brain</i>	27
2. ARTICLE 2 <i>Corpora amylacea in the human brain exhibit neoepitopes of a carbohydrate nature</i>	45
3. ARTICLE 3 <i>From corpora amylacea to wasteosomes: history and perspectives</i>	65

4. ARTICLE 4 *Wasteosomes (corpora amylacea) of human brain are phagocytosed by non-inflammatory macrophages* 81

IV. DISCUSSIÓ133

V. CONCLUSIONS151

VI. BIBLIOGRAFIA157

VII. ANNEX171

ÍNDIX DE FIGURES

Figura 1.	Primeres il·lustracions dels CA.....	4
Figura 2.	CA de la zona subpial glial de l'escorça cerebral tenyits amb PAS-hematoxilina.....	5
Figura 3.	Distribució dels CA al cervell humà.....	6
Figura 4.	CA d'una secció d'hipocamp humà marcats amb IgM de ratolí i els astròcits marcats amb un anticòs dirigit contra GFAP.....	9
Figura 5.	Imatges de microscòpia electrònica de transmissió (MET) de CA d'hipocamp de cervell humà.....	12
Figura 6.	Proposta esquematitzada de sortida dels CA del cervell cap a la sang.....	17
Figura 7.	Immunomarcats de CA de l'hipocamp humà amb GS, p62 i Ubi.....	18
Figura 8.	Via proposada d'eliminació de substàncies de rebuig del cervell basada en el sistema <i>wasteosome</i>	138
Figura 9.	Sistema <i>wasteosome</i> : esquema del procés implicat en la generació i eliminació dels <i>wasteosomes</i>	148

ABREVIATURES

Aβ	<i>amyloid-β peptide</i> , pèptid β -amiloide	LCR	líquid cefalorraquidi
APP	<i>amyloid-β protein precursor</i> , proteïna precursora de β -amiloide	Man	mannosa
BHE	barrera hematoencefàlica	MBL	<i>mannose binding lectin</i> , lectina d'unió a mannososa
CA	<i>corpora amylacea</i> , cossos amilacis	MER	microscòpia electrònica de rastreig
CD	clúster de diferenciació	MET	microscòpia electrònica de transmissió
ConA	concanavalina A	MMP2	<i>matrix-metalloproteinase-2</i> , metal·loproteasa de matriu 2
FcμR	receptor de la fracció constant μ	MS-IgM	<i>myeloma serum IgM</i> , IgM de sèrum de mieloma
Fru	fructosa	NE	neo-epítop
Gal	galactosa	NFT	<i>Neurofibrillary tangles</i> , cabdells neurofibril·lars
GalNAc	N-acetilgalactosamina	NHS	N-hidroxisuccinimida
GFAP	<i>glial fibrillary acidic protein</i> , proteïna àcida fibril·lar glial	NS-IgM	<i>normal serum IgM</i> , IgM de sèrum normal
Glc	glucosa	PAS	<i>periodic acid Schiff</i> , àcid periòdic de Schiff
GlcNAc	N-acetilglucosamina	SNC	sistema nerviós central
GS	glicogen sintasa	Ubi	ubiquitina
Ig	immunoglobulina		

ABSTRACT

Corpora amylacea (CA) in the human brain are polyglucosan aggregates that were first described by J.E. Purkinje in 1837. They are intracellular astrocytic bodies that accumulate mainly in the perivascular, periventricular and subpial regions of the aging brain, but are also present in large numbers in specific areas of the brain in neurodegenerative conditions. Different studies suggest that the function of CA seems to be directed towards trapping products derived from aging or degenerative processes. While essentially constituted of polymerized hexoses, primarily glucose, a wide range of components have been described in CA, some of them derived from neurons, astrocytes, oligodendrocytes or blood, or even related to viral, fungal or microbial infections. Their location in the perivascular, periventricular and subpial regions of the brain, all of them connected or close to cavities filled with cerebrospinal fluid (CSF), suggests that CA can be extruded from these regions into the CSF. Furthermore, CA contain neo-epitopes (NE) of an unknown nature that are recognized by natural antibodies of IgM type. This IgM-NE interaction indicates that if CA were released from the central nervous system (CNS), they could interact with the natural immune system, which could intervene in their elimination. This body of evidence allowed us to consider that CA not only entrap residual products, but also act as waste containers involved in a cleaning mechanism that removes residual substances from the CNS. Accordingly, this thesis aimed to verify this hypothesis. Our studies revealed the presence of CA in the CSF and in the cervical lymph nodes, into which CSF drains through the meningeal lymphatic system. In the cervical lymph nodes, we observed CA making contact with certain cells that, according to their location, shape, and staining properties may be macrophages. Subsequent *in vitro* studies showed that CA are phagocytosed and degraded by macrophages. We also observed that there may be redundant mechanisms involved in triggering the phagocytosis process, which would ensure the elimination of CA. Moreover, these mechanisms are related to non-inflammatory responses, which allow the elimination of CA without tissue damage. On the other hand, we pointed out that the NE present in CA, which may act as “eat-me” signals that would enhance the phagocytosis of CA, have a carbohydrate nature. Taken together, these findings support the above-mentioned hypothesis, indicating that CA can act as containers that remove waste products from the brain and are involved in a mechanism that cleans the CNS. According to these results, the present thesis was later extended to find out the function of the CA from other organs and tissues. In this regard, we aimed to establish a global and integrative hypothesis about the function and significance of CA in the whole organism. The results allowed us to suggest that CA in the different organs are created by specific cells, which collect waste products and amass them within a glycan structure, and secrete them into the external medium or interstitial spaces being, in this second case, phagocytosed by macrophages. Overall, we suggested considering CA from the different tissues of the human body as waste containers.

Lastly, to avoid the ambiguity of the terms amyloid or amyloids (that indicate starch-like structures but can also refer to insoluble fibrillary proteins), we proposed renaming CA as “wasteosomes”, emphasizing the waste products they entrap rather than their misleading amyloid properties.

I. INTRODUCCIÓ

1. COSSOS AMILACIS CEREBRALS

Els cossos amilacis o *corpora amylacea* (CA) són uns agregats glicoproteics que s'acumulen al cervell humà durant l'envelliment i algunes malalties neurodegeneratives, com la malaltia d'Alzheimer, la malaltia de Huntington, la malaltia de Parkinson, l'esclerosi múltiple i l'epilèpsia del lòbul temporal (Averback *et al.*, 1981; Cavanagh, 1999; Cissé *et al.*, 1993; Fleming *et al.*, 1987; Leel-Össy *et al.*, 1998; Loiseau *et al.*, 1992; Nishio *et al.*, 2001; Selmaj *et al.*, 2008; Singhrao *et al.*, 1995; Wilhelmus *et al.*, 2011).

Els CA presenten una llarga història d'abandonament per part dels neuropatòlegs derivada de la seva aparent irrellevància en les malalties del sistema nerviós (Cavanagh, 1999). L'anatomista que va descobrir aquestes estructures al sistema nerviós central (SNC) va ser Purkinje (1837). Anys més tard, Virchow (1854) va descriure aquests cossos al cervell i a la medul·la espinal sota el nom de "corpúscles cel·lulòsics", ja que va observar similituds entre aquestes estructures i la cel·lulosa de les plantes. Aquest reconegut patòleg va assenyalar que els cossos es trobaven propers a l'epèndima cerebral, motiu que el va portar a plantejar que aquestes estructures només es formarien en les proximitats de la zona ependimària. Morgagni havia descrit prèviament formes semblants a la pròstata i les havia anomenades "*corpora amylacea*", per les seves similituds amb el midó (en llatí *amylum*) (Morgagni, 1723). Posteriorment, el mateix Virchow (1855) va apuntar que les estructures que ell mateix havia descrit al SNC presentaven la mateixa naturalesa que les descrites a la pròstata per Morgagni, per això, va passar a anomenar-les també *corpora amylacea*. En referència a la seva formació, el mateix autor va postular que els CA del SNC s'originarien a partir d'un procés secretor (Virchow, 1871).

Posteriorment, els oftalmòlegs Leber (1875) i Treitel (1876) van trobar CA al nervi òptic, i van plantejar per primera vegada la formació dels CA a l'interior dels nervis. Leyden (1880) va descriure aquests cossos a la substància grisa en degeneració de la medul·la espinal d'individus d'edat avançada. Ceci (1881) va postular que els CA sorgien de la coagulació i de la remodelació de la medul·la. D'altra banda, Kelbs (1889) i Redlich (1891) van considerar que aquestes estructures es formaven en cèl·lules gials. Schaffer (1890) va examinar els CA de la medul·la espinal de casos de malaltia de Lyssa, també coneguda com la ràbia, i va proposar que la formació dels cossos derivava d'una transformació química dels axons i de la beina de mielina que donava lloc a la fusió d'aquestes dues estructures. Wichmann (1893), va indicar que els CA contenien components provinents dels vasos sanguinis i va postular que en condicions normals del metabolisme del teixit nerviós aquests components serien consumits pel propi teixit, però que en condicions patològiques, les estructures nervioses no els consumirien i els dipositarien en el teixit formant els CA.

D'altra banda, Robertson (1900) va assenyalar que aquests cossos eren productes de degeneració de la mesoglia, tipus cel·lular que anys més tard del Río-Hortega (1919) va

anomenar micròglia. Wolf (1901) va plantejar que la degeneració cel·lular de les fibres nervioses donaria lloc a la formació dels CA. Aquests cossos no van passar desapercebuts per Catola i Achúcarro (1906) que van representar-los a l'interior d'axons cilíndrics considerant-los d'origen neuronal (Figura 1).

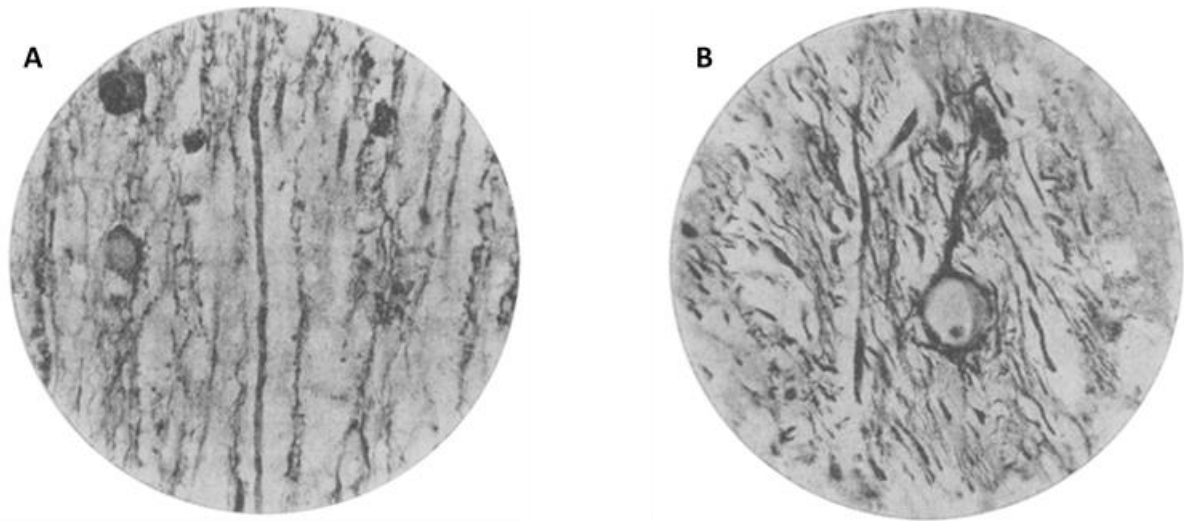


Figura 1. Primeres il·lustracions dels CA. Representacions dels CA de seccions longitudinals de la medulla espinal d'un cas de *paralysis agitans* o malaltia de Parkinson. A) S'observen CA poligonals. B) CA envoltat per una càpsula dins d'un axó cilíndric. S'observen cèl·lules glials i inflamació al voltant de l'axó (Catola i Achúcarro, 1906).

Anys més tard, Ellis (1920) va descriure que els CA es trobaven associats a l'envelliment normal. Buzzard i Greenfield (1921) van descartar que aquests cossos tinguessin un significat neuropatològic, fet que va provocar que durant molt de temps es consideressin irrelevants. En aquesta línia, Ferraro i Damon (1931) van revisar els resultats obtinguts fins al moment sobre l'origen d'aquests cossos en diversos teixits i van proposar que es tractava d'artefactes *post-mortem*. En aquell moment, cap estudi suggeria una funció clara o un significat biològic consistent per a aquests cossos. No va ser fins anys més tard que l'aplicació de noves tècniques d'histoquímica, ultraestructura i immunohistoquímica va motivar un interès en la naturalesa dels CA i la seva relació amb determinades malalties (Cavanagh, 1999). Aquests estudis més recents, que seran comentats en els propers apartats, han proposat diverses hipòtesis envers l'origen dels CA i les seves possibles implicacions. Malgrat tot, les teories que giren entorn a aquestes estructures no han estat demostrades de manera coherent i consistent i la seva funció segueix sent una incògnita per a la comunitat científica.

1.1. Morfologia

Els CA del SNC són unes estructures esfèriques o ovalades que mesuren entre 2 i 20 μm de diàmetre, tot i que poden arribar a 50 μm en alguns casos. Generalment, la seva mida mitjana

gira al voltant de 10-12 μm (Cavanagh, 1999). Tot i això, s'ha descrit que a l'escorça, al nucli estriat i a la matèria gris de la medul·la espinal els CA són més petits que en altres zones, d'una mida d'1,5 μm o menys, i només ocasionalment arriben a 10-12 μm (Averback, 1981; Leheskoki *et al.*, 1991; Takahashi *et al.*, 1975). Sovint, els CA presenten anells concèntrics o forma de diana i la zona central sembla presentar una coloració més intensa que la perifèria quan es tenyeixen amb la tinció de l'àcid periòdic de Schiff (*periodic acid Schiff*, PAS) (Figura 2). En alguns casos, fins i tot, s'han arribat a observar dos o més cossos molt propers, els quals semblen fusionar-se. Pel que fa a la seva superfície, normalment, és llisa, però no és infreqüent que es presenti irregular, com si es tractés d'una coberta (Cavanagh, 1999).

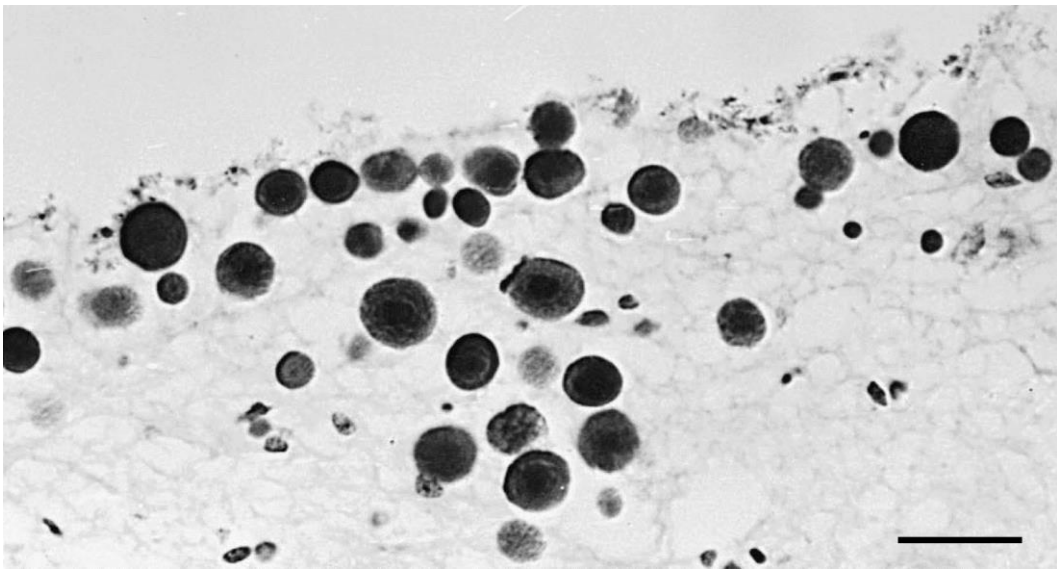


Figura 2. CA de la zona subpial glial de l'escorça cerebral tenyits amb PAS-hematoxilina. Mostra provinent d'un home de 56 anys. Barra d'escala: 20 μm (Cavanagh, 1999).

1.2. Localització

En persones d'edat avançada, els CA es troben pràcticament en totes les regions del SNC. No obstant això, els CA semblen concentrar-se en determinades regions, el que mostra que la seva distribució no és aleatòria sinó que té un paper rellevant en la seva formació i el seu desenvolupament (Cavanagh, 1999). De fet, s'ha observat que els CA tendeixen a acumular-se al recobriment glial sota l'epèndima dels ventricles, concretament sota el cos callós, al sostre i, en menor mesura, al terra del tercer i quart ventricles i al sostre de l'aqüeducte cerebral. A més a més, també s'ha descrit l'acumulació de CA en les superfícies més externes del cervell, generalment, en el recobriment glial sota la piamàter, en les superfícies medials dels lòbuls temporals i sobre l'hipocamp (Figura 3) (Alder, 1951; Cavanagh, 1999; Cissé i Schipper; 1995; Navarro *et al.*, 2018; Sakai *et al.*, 1969; Schipper i Cissé, 1995; Suzuki *et al.*, 2012).

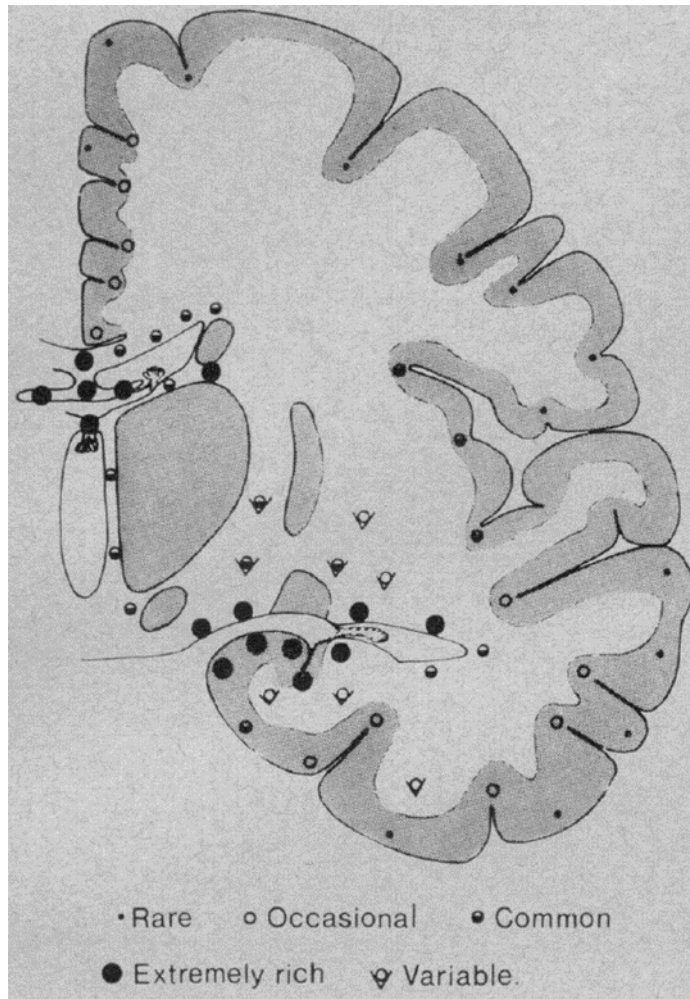


Figura 3. Distribució dels CA al cervell humà. Estudi realitzat amb mostres de 4 persones de 70 anys. Els CA van ser determinats mitjançant la tinció de blau alcian (Sakai *et al.*, 1969).

D'altra banda, els CA, a la matèria blanca, tendeixen a concentrar-se a les zones perivasculars, al voltant de vasos de mida mitjana i gran, i se n'han trobat també a l'espai de Virchow-Robin (Cavanagh, 1999; Navarro *et al.*, 2018). Al cerebel, se n'han descrit a la capa de Purkinje, situats a l'espai entre les cèl·lules de Purkinje (Mittal i Olszewski, 1985). Al bulb raquidi també han estat descrits (Fujii *et al.*, 1996). Tal i com ja havia descrit Virchow (1854), a la medulla espinal també s'observen CA, els quals es localitzen propers a les superfícies, en el recobriment glial sota la piamèter o entre fibres nervioses mielinitzades (Cavanagh, 1999).

En definitiva, els CA s'acumulen principalment a les regions periventriculars, perivasculars i subpials del cervell, caracteritzades per la seva proximitat al líquid cefalorraquidi (LCR) i en major nombre en zones on aquest líquid es produeix (Sakai *et al.*, 1969).

1.3. Composició

Tot i que alguns estudis han mostrat certa controvèrsia pel que fa a alguns components dels CA del SNC, en general, hi ha consens en que el component principal d'aquestes estructures

són hexoses polimeritzades, principalment glucosa (Glc), les quals constitueixen l'esquelet de poliglucosà (Cavanagh, 1999; Sakai *et al.*, 1969). De fet, una característica rellevant dels CA és que es tenyeixen amb la tinció de PAS, la qual s'utilitza per a la detecció d'estructures amb un elevat contingut en polisacàrids, com ara el glicogen. A més a més, els CA es tenyeixen amb concanavalina A (ConA), una lectina d'origen vegetal que reconeix principalment mannanosa (Man) i Glc (Liu *et al.*, 1987). S'ha observat que la digestió amb α -amilasa redueix lleugerament aquesta tinció, fet que assenyala un elevat grau de compactació i/o ramificació en l'estructura glucídica que dificulta la digestió enzimàtica. L'anàlisi bioquímic dels CA ha estimat que les hexoses constitueixen un 68,4% del seu pes, mentre que les proteïnes representen un 8,1% i el 23,5% no ha estat determinat (Sakai *et al.*, 1969). Posteriorment, Stam i Roukema (1973) van descriure també la presència de petites quantitats de sulfats, a banda de corroborar la presència de fosfats, i van determinar que aquests fosfats i sulfats es troben units a les hexoses del poliglucosà.

Histoquímicament, es va demostrar que els CA no contenen ADN, ARN o lípids (Sakai *et al.* 1969; Stam i Roukema, 1973). D'altra banda, tècniques de microanàlisi de rajos X van indicar la presència d'àtoms de Na, P, S, Ca, Fe, Cu i Cl units als CA (Singhrao *et al.*, 1993; Tokutake *et al.*, 1995).

Pel que fa al contingut proteic dels CA, Steyaert *et al.* (1990) van aïllar CA del teixit cerebral utilitzant gradients de sacarosa i, mitjançant l'SDS-PAGE, van mostrar la presència de diferents bandes polipeptídiques de pesos moleculars entre 24 i 133 KDa. Cissé *et al.* (1991) van examinar la seqüència d'aminoàcids dels polipèptids de 24 i 42 KDa i van assenyalar que aquests polipèptids presenten certa homologia amb l'extrem N-terminal de la ubiquitina (Ubi) humana. Tot i això, es va indicar que els pesos moleculars d'aquests polipèptids són superiors als de la Ubi (8,5 KDa), fet que va posar de manifest que algunes proteïnes presents en els CA es troben conjugades a aquesta proteïna. Posteriorment, Selmaj *et al.* (2008) van realitzar un estudi de proteòmica mitjançant tècniques d'electroforesi i de *matrix-assisted laser desorption/ionization time-of-flight mass spectrometry* (MALDI-TOF) amb CA provinents de zones lesionades del cervell de pacients d'esclerosi múltiple i van observar el contingut de 24 proteïnes, algunes del citoesquelet, principalment actina i tubulina, i d'altres implicades en la motilitat i la plasticitat cel·lular i en processos d'apoptosi i senescència.

Darrerament, s'han realitzat un gran nombre d'estudis immunohistoquímics per determinar la composició dels CA. Aquests estudis han revelat una gran diversitat de substàncies en els CA, provinents de diferents tipus cel·lulars.

Alguns estudis immunohistoquímics han indicat la presència d'espècies de proteïna tau en els CA (Day *et al.*, 2015; Loeffler *et al.*, 1993; Wander *et al.*, 2020; Wilhelmus *et al.*, 2011; Xu *et al.*, 2021), però altres autors no han estat capaços de reproduir aquests resultats (Augé *et al.*, 2017; Notter i Knuesel, 2013). A més, s'han observat resultats contradictoris pel que fa al

pèptid β -amiloide (*amyloid- β* , A β) o la proteïna precursora d'aquest (*amyloid- β protein precursor*, APP). Els estudis de Notter i Knuesel (2013) van determinar la presència d'A β i APP i Tate-Ostroff *et al.* (1989) la presència del domini extracitoplasmàtic de l'APP. En canvi, Augé *et al.* (2017), Pirici i Mărgăritescu (2014) i Wilhelmus *et al.* (2011) no van trobar presència d'A β en els CA. S'han observat també altres proteïnes d'origen neuronal, com ara l' α -sinucleïna (Buervenich *et al.*, 2001; Notter i Knuesel, 2013; Wilhelmus *et al.*, 2011), la proteïna associada a microtúbuls 2 (MAP2) (Nam *et al.*, 2012; Notter i Knuesel, 2013), la nestina (Buervenich *et al.*, 2001), l'antigen del nucli neuronal (NeuN) (Buervenich *et al.*, 2001; Korzhevskii i Giliarov, 2007; Pirici i Mărgăritescu, 2014), neurofilaments (Pirici i Mărgăritescu, 2014), la proteïna parkina (Wilhelmus *et al.*, 2011), la reelina (Notter i Knuesel, 2013) i proteïnes del citoesquelet com la β -tubulina classe III i β -actina (Wilhelmus *et al.*, 2011).

S'han descrit, també mitjançant assaigs d'immunohistoquímica, components relacionats amb oligodendròcits com ara mielina (Singh Rao *et al.*, 1994) i proteïnes vinculades amb els astròcits com l'aquaporina 4 (AQP4) (Pirici i Mărgăritescu, 2014), l'S100 (Buervenich *et al.*, 2001; Hoyaux *et al.*, 2000; Pirici i Mărgăritescu, 2014) o la proteïna àcida fibril·lar glial (*glial fibrillary acidic protein*, GFAP) la qual alguns autors l'han descrit distribuïda en la totalitat de l'estructura dels CA (Buervenich *et al.*, 2001; Pirici i Mărgăritescu, 2014; Xu *et al.*, 2021), mentre que altres han revelat que aquesta proteïna es localitza només a la perifèria (Augé *et al.*, 2018; Augé *et al.*, 2019; Bakić i Jovanović, 2017; Nam *et al.*, 2012; Notter i Knuesel, 2013; Pirici *et al.*, 2014; Suzuki *et al.*, 2012). S'ha posat de manifest la presència de proteïnes de xoc tèrmic o *heat shock proteins* (Cissé *et al.*, 1993; Buervenich *et al.*, 2001; Gáti i Leel-Ossy, 2001; Martin *et al.*, 1991), tot i que aquest marcatge no va poder ser reproduït per Erdamar *et al.* (2000). D'altra banda, en els CA s'han observat proteïnes sanguínies com l'*A disintegrin-like and metalloprotease with thrombospondin type 1 repeat motifs 13* (ADAMTS13), la trombopondina-1 i el receptor de l'endotelina B (Meng *et al.*, 2009; Vasaikar *et al.*, 2018), components del sistema complement (Singh Rao *et al.*, 1995), epítops mitocondrials i factors transcripcionals (Botez i Rami, 2001), productes finals de glicosilació avançada (Iwaki *et al.*, 1996) i proteoglicans (Liu *et al.*, 1987). Pel que fa a derivats d'agents infecciosos, s'ha descrit la presència de proteïnes d'herpesvirus (Libard *et al.*, 2014) i proteïnes d'algunes espècies fúngiques (Pisa *et al.*, 2016). Aquests estudis immunohistoquímics que van indicar la presència de proteïnes fúngiques en els CA van ser recolzats posteriorment pels resultats obtinguts mitjançant tècniques de proteòmica (Pisa *et al.*, 2018).

Tot i que la presència d'Ubi ja havia estat apuntada per diversos estudis (Cissé *et al.*, 1993; Day *et al.*, 2015; Pirici i Mărgăritescu, 2014; Pirici *et al.*, 2014; Wilhelmus *et al.*, 2011), els assaigs d'Augé *et al.* (2018) van corroborar la presència d'aquesta proteïna i van posar de manifest la presència de l'enzim glicogen sintasa (GS), de la proteïna p62 o seqüestrosoma-1, la cadena lleugera 3 de la proteïna associada a microtúbul (*microtubule-associated protein light chain 3*, LC3) i la metal·loproteasa de matriu 2 (*matrix-metalloproteinase-2*, MMP2). En

aquest mateix estudi, Augé *et al.* (2018) van revisar la presència de la major part de components que havien estat descrits en els CA mitjançant mètodes immunohistoquímics i van posar de manifest la controvèrsia entre alguns dels resultats publicats. A més a més, van apuntar que aquesta discordança podria derivar de l'obtenció de falsos marcatges causats per la presència de neo-epítops (NE) i anticossos naturals dirigits contra aquests NE que es comenten a l'apartat següent.

1.4. Presència de neo-epítops

En els estudis d'Augé *et al.* (2017) i Augé *et al.* (2019), es va descriure la presència d'uns epítops als CA del cervell humà, que no es trobaven en altres estructures del cervell i es generaven durant el procés de formació dels propis cossos, de manera que es tractava d'epítops de nova formació, és a dir, de NE. A més a més, es va observar que aquests NE eren reconeguts per immunoglobulines (Ig) de l'isotip IgM (Figura 4). Es va observar que aquestes IgM eren de tipus natural ja que d'una banda, es va demostrar que eren interespecífiques, és a dir, les IgM provinents de sèrums d'animals de diferents espècies eren capaces de reconèixer els NE dels CA, i d'altra banda, es trobaven presents en el sèrum de cordó umbilical i per tant, eren generades pel fetus prèviament al contacte amb agents externs.

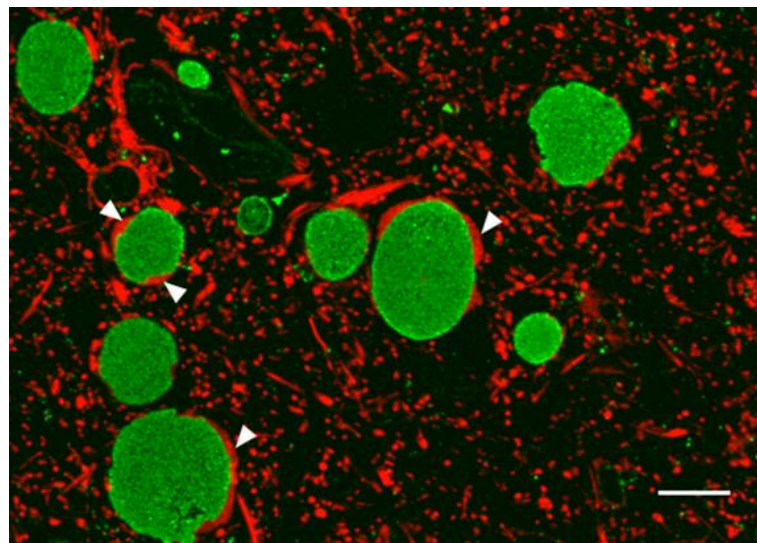


Figura 4. CA d'una secció d'hipocamp humà marcats amb IgM de ratolí (verd) i els astròcits marcats amb un anticòs dirigit contra GFAP (vermell). S'observa com els NE reconeguts per les IgM es localitzen en tota l'estructura dels CA. Els CA apareixen envoltats de filaments astrocítics de GFAP (puntes de fletxa). Barra d'escala: 10 µm (Augé *et al.*, 2019).

La presència de NE que són reconeguts per IgM naturals havia estat prèviament descrita en uns agregats de poliglucosà que apareixen al cervell de ratolins envellits, que s'anomenen grànuls PAS o grànuls *corpora amylacea-like* (CAL) i que presenten certes similituds amb els CA humans. Aquests estudis amb grànuls PAS de ratolí van demostrar l'existència d'IgM en

el plasma dels animals dirigides contra els NE dels grànuls PAS propis, la qual cosa va demostrar que es tractava d'autoanticossos. No obstant això, es va determinar que a causa de la barrera hematoencefàlica (BHE), aquestes IgM del plasma no eren capaces d'unir-se als NE dels grànuls del mateix animal *in vivo* (Manich *et al.*, 2014a; Manich *et al.*, 2014b; Manich *et al.*, 2015).

D'acord amb els resultats descrits amb els grànuls PAS del cervell de ratolí, es va estudiar si en el cas dels CA del cervell humà, les IgM del plasma humà serien capaces d'arribar als NE dels CA *in vivo*. Per això, es va afegir directament a una secció d'hipocamp un anticòs dirigit contra IgM marcat amb fluorescència. Aquest assaig no va mostrar marcatge, per tant, de la mateixa manera que amb els grànuls PAS de ratolí, la BHE impedeix que, *in vivo*, les pròpies IgM accedeixin al SNC i contactin amb els NE dels CA (Augé *et al.*, 2017).

D'altra banda, aquests estudis van assenyalar que la presència d'aquests NE reconeguts per IgM naturals podrien ser la causa de falsos marcatges positius en els CA en assaigs immunohistoquímics que haurien donat lloc a l'obtenció de conclusions errònies. Prèviament a aquests estudis, Manich *et al.*, (2014b) havien descrit la presència d'IgM contaminants en un elevat nombre d'anticossos comercials de tipus IgG. Aquests autors van demostrar que algunes d'aquestes IgM contaminants eren dirigides contra els NE dels grànuls PAS del cervell de ratolí, fet que provocava falsos marcatges positius quan es duïen a terme estudis immunohistoquímics. Concretament, aquestes IgM contaminants dirigides contra els NE dels grànuls PAS s'unien a aquestes estructures i eren posteriorment reconegudes per anticossos secundaris dirigits contra IgG, policlonals i no isotip específics. De la mateixa manera, aquestes interaccions també es produïen entre les IgM dirigides contra els NE dels CA i els anticossos secundaris dirigits contra IgG, policlonals no isotip específics, i eren les causants dels falsos marcatges positius descrits en els CA (Augé *et al.*, 2017). En aquest sentit, es van revisar els marcatges de les proteïnes tau i A β , prèviament descrits en els CA, utilitzant anticossos secundaris isotip específics dirigits contra la cadena pesada de les IgG, els quals no reconeixen les IgM. Pel que fa a la proteïna tau, a l'utilitzar un anticòs primari IgG dirigit contra tau i un anticòs secundari específic contra la cadena pesada de les IgG, es va observar marcatge dels característics cabdells neurofibril·lars (*neurofibrillary tangles*, NFTs), però no dels CA. En canvi, a l'utilitzar el mateix anticòs primari i un anticòs secundari contra la cadena pesada de les IgM, es va observar el marcatge dels CA i no dels NFTs. Aquests resultats van posar de manifest la presència d'IgM contaminants que reconeixen els NE dels CA en l'anticòs primari utilitzat. Els mateixos resultats van ser observats en el marcatge d'A β . Conjuntament, es va corroborar doncs, que la controvèrsia descrita en alguns components dels CA podria derivar-se de la presència d'IgM contaminants en anticossos comercials i la reacció creuada dels anticossos secundaris policlonals dirigits contra IgG amb les IgM contaminants.

Malgrat tot, posteriorment a la determinació dels NE als CA, Wander *et al.* (2020) van estudiar la presència de proteïna tau en els CA amb tècniques d'immunohistoquímica

mitjançant anticossos secundaris isotip específics i van observar marcatge de tau en aquestes estructures. Cal destacar però, que les mostres van ser sotmeses a un procés de desemmascament d'antigen mitjançant l'aplicació de calor, una altra variable que caldria considerar doncs a l'hora de determinar la composició dels CA. En definitiva, aquests estudis mostren la necessitat de revisar amb detall alguns dels components descrits en els CA mitjançant estudis immunohistoquímics (Augé *et al.*, 2017; Wander *et al.*, 2020).

1.5. Característiques ultraestructurals

La ultraestructura dels CA consisteix en una agrupació de filaments lineals curts, d'entre 8 i 12 nm, que sovint es distribueixen en forma d'anells concèntrics (Palmucci *et al.*, 1982; Ramsey, 1965). Els cossos són arrodonits i es troben envoltats d'una membrana plasmàtica, que no els és pròpia, fet que demostra la seva localització intracel·lular (Augé *et al.*, 2019; Ramsey, 1965). Diversos estudis de microscòpia electrònica han associat els CA amb fibrilles glijals o els han localitzat a l'interior de processos astrocítics (Augé *et al.*, 2019; Leel-Ossy, 2001; Navarro *et al.*, 2018; Palmucci *et al.*, 1982; Ramsey, 1965; Sbarbati *et al.*, 1996). Els CA també han estat descrits a l'interior dels axons del nervi òptic (Woodford i Tso, 1980), en alguns axons del tàlem (Mizutani *et al.*, 1987), en petits axons mielinitzats de la matèria gris de la medul·la (Takahashi *et al.*, 1975) i, rarament, en processos neuronals de l'escorça orbitofrontal (Anzil *et al.*, 1974). De fet, Anzil *et al.* (1974) van destacar que la presència de CA als axons és menys freqüent que dins dels astròcits. Cal remarcar que tot i que s'han mostrat evidències que associen els CA amb els axons, mai s'han trobat CA en els somes neuronals d'individus sans i no hi ha cap dubte que en la regió subpial els CA es localitzen clarament als processos astrocítics (Cavanagh, 1999). Fins i tot, Sbarbati *et al.* (1996) van observar els CA de mostres de nervi vestibular de malaltia de Ménière en els processos astrocítics envoltats per plegaments del citoplasma glial. Aquests autors van considerar que aquests plec podrien separar-se donant lloc a l'alliberament dels cossos de la làmina basal de la *glia limitans* cap al teixit connectiu de la piamàter o cap a l'espai subpial. De fet, van ser observats al teixit connectiu de la piamàter sense estar envoltats de cap membrana.

Recentment, estudis ultraestructurals han descrit vesícules, mitocondris, restes cel·lulars, cossos multilamel·lars i estructures membranoses a l'interior dels CA i en les zones contigües als mateixos (Augé *et al.*, 2019; Navarro *et al.*, 2018). També s'han observat CA amb diferent grau de compactació, fet que es correspon probablement als diferents estadis de formació d'aquestes estructures (Figura 5) (Augé *et al.*, 2019).

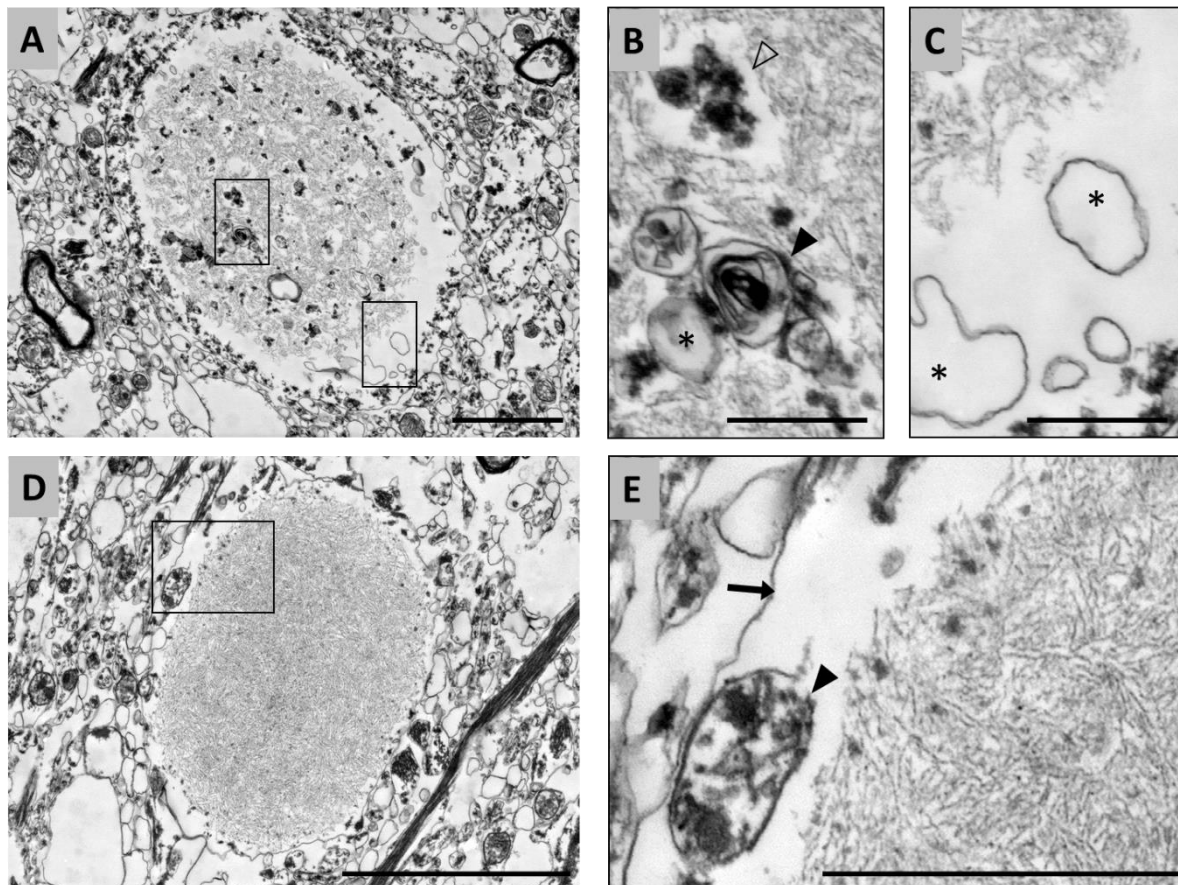


Figura 5. Imatges de microscòpia electrònica de transmissió (MET) de CA d'hipocamp de cervell humà. (A) CA immadur d'estructura poc compactada. (B i C) Ampliacions d'(A) on s'observa la presència de restes cel·lulars (cap de fletxa blanc), cossos multilamel·lars (cap de fletxa negra) i estructures membranoses (asterisc). (D) CA madur d'estructura compacta. (E) Ampliació de (D) on s'observa la presència d'una membrana plasmàtica envoltant el CA (fletxa negra) i un mitocondri (cap de fletxa negra) al costat del CA. Barres d'escala: (A) 2 µm, (B i C) 500 nm, (D) 3 µm, (E) 1 µm (Augé *et al.*, 2019).

1.6. Origen cel·lular

Tal i com s'ha indicat en els apartats anteriors, els estudis immunohistoquímics i ultraestructurals han plantejat tant un origen neuronal com un origen glial en els CA del SNC.

L'origen neuronal dels CA s'ha postulat principalment d'acord amb la presència d'aquests cossos en els axons d'algunes localitzacions del SNC, determinada mitjançant estudis ultraestructurals (Anzil *et al.*, 1974; Mizutani *et al.*, 1987; Takahashi *et al.*, 1975; Woodford i Tso, 1980). D'acord amb això, els estudis de proteòmica de Selmaj *et al.* (2008) van identificar 24 proteïnes d'origen neuronal, principalment provinents del citoesquelet, però també algunes relacionades amb processos d'apoptosi i senescència. En base a aquestes proteïnes, aquests autors van suggerir que la biogènesi dels CA prové de la degeneració i agregació de neurones. A més a més, estudis d'immunohistoquímica han descrit alguns components d'origen neuronal en els CA, fet que ha posat de manifest un origen neuronal, o almenys, la

implicació de les neurones en la formació dels CA (Buervenich *et al.*, 2001; Day *et al.*, 2015; Korzhevskii i Giliarov, 2007; Loeffler *et al.*, 1993; Nam *et al.*, 2012; Notter i Knuesel, 2013; Pirici i Mărgăritescu, 2014; Wilhelmus *et al.*, 2011). No obstant això, tal i com s'ha comentat anteriorment, cap estudi ha demostrat la presència de CA en els somes neuronals (Cavanagh, 1999).

D'altra banda, alguns autors han descrit, mitjançant estudis ultraestructurals, la presència de CA en astròcits (Augé *et al.*, 2019; Leel-Ossy, 2001; Navarro *et al.*, 2018; Palmucci *et al.*, 1982; Ramsey, 1965; Sbarbati *et al.*, 1996). Tot i que Anzil *et al.* (1974) van destacar la presència d'alguns CA en axons, van observar que era molt més freqüent localitzar-los dins d'astròcits. Tanmateix, diversos estudis han relacionat la presència de la proteïna astrocítica GFAP amb els CA (Augé *et al.*, 2018; Augé *et al.*, 2019; Bakić i Jovanović, 2017; Buervenich *et al.*, 2001; Nam *et al.*, 2012; Notter i Knuesel, 2013; Pirici i Mărgăritescu, 2014; Schipper i Cissé, 1995; Singhrao *et al.*, 1993; Suzuki *et al.*, 2012; Xu *et al.*, 2021). Alguns d'aquests estudis apunten la presència d'aquesta proteïna a l'interior del CA, mentre que la majoria d'ells la localitzen envoltant aquestes estructures.

En contrast amb els resultats que recolzen l'origen neuronal dels CA, sembla que hi ha tanta o més evidència que indica que els astròcits són importants per a la biogènesi dels CA. De fet, s'ha postulat que els CA serien d'origen astrocític però la presència de proteïnes neuronals resultaria de la fagocitosis de neurites o neurones en degeneració (Meng *et al.*, 2009; Singhrao *et al.*, 1993).

1.7. Variacions amb l'edat i en determinades patologies

Pel que fa a les variacions amb l'edat, s'ha descrit que el nombre de CA del SNC és invariablement baix en individus joves. En aquest sentit, s'han trobat molt pocs CA en mostres de medul·la espinal de nens d'entre 10 i 15 anys. A més a més, els CA descrits en nens fan la meitat del diàmetre dels CA de persones adultes. A partir dels 30-40 anys, els CA són més grans i nombrosos (Cavanagh, 1999). Els estudis de Chung i Horoupian (1996) van assenyalar una incidència baixa de CA a l'hipocamp i en la zona parahipocampal en un grup de 20 individus control d'edats entre 16 i 51 anys amb diferents malalties sense afectació cerebral. D'aquest grup, 4 individus no van presentar cap CA, coincidint amb els més joves, i a la resta dels individus, se'n van trobar 1 o 2. En els estudis de Busard *et al.* (1994), es va determinar la mitjana del nombre de CA en l'escorça frontal i temporal i es va mostrar que, a edats inferiors als 40 anys, la presència de CA era més aviat esporàdica, però a partir d'aquesta edat, el nombre de CA incrementava, tot i que de manera variable. D'altra banda no es va establir cap relació entre el nombre de CA i el sexe de l'individu. Els estudis de Maqbool i Tahir (2008), amb 60 casos d'edats entre 19 i 72 anys, també van assenyalar un increment significatiu de CA amb l'edat al lòbul frontal i a l'hipocamp. En aquest sentit, Nam

et al. (2012) van indicar un increment en el nombre de CA amb l'edat en un estudi realitzat amb 12 casos d'entre 37 i 90 anys.

Pel que fa a la relació entre el nombre de CA i determinades malalties, s'ha posat de manifest una elevada densitat d'aquestes estructures en malalties neurodegeneratives com la malaltia d'Alzheimer (Averback *et al.*, 1981; Cissé *et al.*, 1993; Fleming *et al.*, 1987; Singhrao *et al.*, 1995; Wilhelmus *et al.*, 2011), la malaltia de Huntington (Averback *et al.*, 1981), la malaltia de Parkinson (Pisa *et al.*, 2016; Wilhelmus *et al.*, 2011), la malaltia de Pick (Singhrao *et al.*, 1995), l'esclerosi lateral amiotròfica (Pisa *et al.*, 2016), l'esclerosi múltiple (Selmaj *et al.*, 2008; Singhrao *et al.*, 1995) i l'epilèpsia del lòbul temporal (Leel-Ossy *et al.*, 1998; Loiseau *et al.*, 1992; Nishio *et al.*, 2001). Tot i això, segons Leel-Össy (1991), la patologia en la qual s'ha observat el major nombre de CA és l'encefalopatia vascular. Cal considerar també que, recentment, Xu *et al.*, (2021) han assenyalat un elevat nombre de CA en l'hipocamp de casos d'apnea obstructiva del son.

1.8. Significat fisiopatològic i postulats referents a la funció

Des del seu descobriment, s'han atribuït múltiples funcions als CA del SNC d'acord amb la seva composició, localització i estudis ultraestructurals.

Els CA van ser descrits per primera vegada per Purkinje (1837) però el qui els va estudiar a fons anys més tard va ser Virchow (1854). De fet, va ser aquest patòleg qui va postular que els CA es formen a l'epèndima cerebral com a resultat d'un procés secretor (Virchow, 1871). Durant el segle XIX, els CA van ser estudiats per diferents metges i fisiòlegs i ja van ser associats amb l'edat (Leyden, 1880), amb la coagulació i processos de remodelació (Ceci, 1881), amb alteracions dels axons i la mielina (Schaffer, 1890) i amb processos de degeneració (Robertson 1900).

Anys més tard, arrel del posicionament de Buzzard i Greenfield (1921), que van considerar que els CA no tenien significat neuropatològic, i de Ferraro i Damon (1931), que van indicar que els CA eren artefactes *post-mortem*, l'estudi dels CA va quedar en un segon pla. No va ser fins a les últimes dècades de segle XX, amb l'aplicació de noves tècniques, que es va reprendre l'estudi d'aquestes estructures i es va descriure la seva relació amb certes condicions neuropatològiques.

Sakai *et al.* (1969) van realitzar un anàlisi histoquímic i bioquímic molt extensiu dels CA i van posar de manifest certes similituds entre aquestes estructures i els cossos de Lafora, uns cossos de poliglucosà presents a les neurones de malalts de malaltia de Lafora. La malaltia de Lafora és una epilèpsia mioclònica hereditària causada per un defecte genètic del metabolisme del glicogen (Cavanagh, 1999). D'acord amb aquestes observacions, Sakai *et al.* (1969) van postular que els CA, de manera similar als cossos de Lafora, s'originarien a partir d'una alteració del metabolisme del glicogen en els astròcits. En aquest sentit, aquests autors

van proposar anomenar aquest desordre que produeix la formació dels CA com a amilopectinosi cerebral. Entre d'altres observacions, van destacar que els CA es formen a les interfícies del cervell, concretament a les zones properes a la barrera cervell-LCR. D'acord amb això, van plantejar que els astròcits situats en aquestes regions es trobarien exposats a agents nocius provinents del LCR, els quals alterarien el metabolisme d'aquestes cèl·lules que donaria lloc a la formació dels CA. A més a més, van considerar que l'edat seria un altre factor que afavoriria la disrupció metabòlica dels astròcits i alteraria la transferència de material entre els astròcits i les neurones adjacents, fet que provocaria l'acumulació de material i propiciaria la formació dels CA.

D'altra banda, Singhrao *et al.* (1995), d'acord amb els seus estudis d'immunohistoquímica, van proposar que els CA són matrius inertes de mucopolisacàrid que capturen proteïnes ubiquitinades resultants de la mort o el dany de neurones, mielina i oligodendròcits, de manera que previndrien el reconeixement d'aquestes proteïnes immunogèniques per part de la micròglia i limfòcits i per tant, protegirien al SNC de més dany tissular. Així doncs, aquests autors van plantejar que els CA formarien part d'un mecanisme d'aïllament de proteïnes potencialment perilloses i de prevenció de la mort cel·lular provocada per l'envelliment i algunes malalties del SNC.

Sbarbati *et al.* (1996), en els seus estudis realitzats en mostres de nervi vestibular, van descriure CA en astròcits fibrosos essent extruïts cap al teixit connectiu de la piamàter, a través de la membrana basal de la *glia limitans*. Aquestes observacions van permetre assenyalar que els CA formarien part d'un sistema glio-pial d'eliminació de substàncies del sistema nerviós. A més a més, es va plantejar que els CA podrien ser fagocitats per cèl·lules fagocítiques de la piamàter o l'aracnoide i es va postular que, al ser transferits els CA a una zona propera a capil·lars sanguinis, aquests capil·lars podrien participar en l'eliminació dels CA. D'altra banda, d'acord amb l'observació de CA a la zona subpial i suependimal, Cavanagh (1999) va indicar que els CA podrien ser transferits de manera passiva, mitjançant els moviments regulars del teixit i les pulsacions vasculars, cap a l'espai subaracnoidal, ple de LCR. Es desconeix, però, si els CA podrien travessar les vellositats aracnoidals per sortir del SNC. No obstant això, Cavanagh (1999) va apuntar que no hi hauria necessitat que els CA sortissin del cervell, perquè aquests s'acostumen a trobar en regions, que segons aquest autor, són merament estructurals, com el sostre del sistema ventricular i les zones subpials, de manera que la presència de CA en aquestes zones no alteraria els sistemes neuronals de manera rellevant.

Contràriament a la hipòtesi plantejada per Cavanagh (1999), alguns autors han hipotetitzat que el LCR no seria una via de sortida des del sistema nerviós per als CA, sinó que aquest líquid proveiria les substàncies per a la formació d'aquestes estructures (Nam *et al.*, 2012).

D'altra banda, el mateix Cavanagh (1999), juntament amb altres autors, va proposar que en condicions fisiològiques, les molècules de glúcids podrien formar la base per a la recol·lecció i l'empaquetament de productes resultants de l'estrès oxidatiu de mitocondris i altres proteïnes, o altres materials potencialment nocius i no degradables resultat de l'envelliment (Kimura *et al.*, 1998; Iwaki *et al.*, 1996; Schipper i Cissé, 1995). En aquesta línia, Schipper (2004), d'acord amb els seus estudis, va concloure que els CA serien derivats dels grànuls peroxidasa o Gomori-positius dels astròcits, i que la seva formació podria ser mediada per l'activitat hemo-oxigenasa 1 i el dany mitocondrial. D'aquesta manera, els CA provindrien de la presència d'estrès oxidatiu i d'anomalies mitocondrials derivades de l'envelliment dels astròcits.

Selmaj *et al.* (2008) va suggerir que la biogènesi dels CA involucraria un procés de degeneració i agregació de neurones. Relacionat amb aquesta hipòtesi, Meng *et al.* (2009), arrel de l'observació de dues proteïnes sanguínies en els CA, van proposar que aquestes estructures formarien conglomeracions de proteïnes que provindrien de neurones en degeneració i d'elements sanguinis alliberats com a conseqüència d'un trencament de la BHE. Notter i Knuesel (2013), en canvi, van assenyalar els CA s'originarien a partir de l'acumulació d'òrgànuls i metabòlits proteics de neurones.

Reprement la hipòtesi d'Sbarbati *et al.* (1996) referent a la possible fagocitosis dels CA una vegada extruïts del nervi vestibular, anys més tard, Suzuki *et al.*, (2012) van observar CA essent fagocitats per macròfags infiltrants en mostres de nervi òptic i de bulb raquidi de casos de neuromielitis òptica. Aquests resultats van suggerir que els CA serien extruïts pels astròcits i fagocitats per macròfags donant lloc a un procés d'eliminació d'aquestes estructures.

Estudis recents han posat de manifest la participació del sistema glimfàtic en la formació dels CA (Navarro *et al.*, 2018). El sistema glimfàtic consisteix en una afluència de LCR a nivell periarterial que flueix cap al líquid intersticial del cervell i va a parar a l'espai perivenós formant un sistema d'eliminació de substàncies del SNC (Jessen *et al.*, 2015). Navarro *et al.* (2018) van observar que els CA es localitzen i tenen tendència a acumular-se al voltant de grans vasos sanguinis, una zona de gran activitat d'aquest sistema glimfàtic, de manera que aquest sistema transferiria substàncies de rebuig de diversos tipus cel·lulars cap als astròcits, els quals acumularien aquests productes nocius d'altres cèl·lules, a més dels propis, en els CA. A més a més, van plantejar que els CA també serien eliminats mitjançant el sistema perivascular implicant el sistema glimfàtic.

Així mateix, els estudis d'Augé *et al.* (2017), els quals van posar de manifest la presència d'uns NE als CA que són reconeguts per IgM naturals, van assenyalar que la unió entre els NE i les IgM podria donar lloc a la fagocitosis dels CA per processos d'immunitat innata i que probablement, l'eliminació dels CA es tractaria d'un procés pre-programat. Així doncs,

d'acord amb els estudis que descriuen la presència de substàncies de rebuig en els CA i el fet que els CA siguin reconeguts per IgM naturals, aquests autors van recolzar que els CA estarien involucrats en un mecanisme de neteja de productes de rebuig cerebrals. No obstant això, la unió entre les IgM i els CA dins del SNC tindria lloc en cas que es produís un trencament de la BHE o amb l'extrusió dels CA fora del cervell. Conjuntament, tal com es mostra a la Figura 6, es descriu la hipòtesi referent als CA com a contenidors involucrats en mecanismes de neteja, en els quals residus cel·lulars i altres productes nocius de diversos tipus de cèl·lules serien capturats i acumulats per ésser posteriorment eliminats per processos de fagocitosi o altres mecanismes mediat per el sistema immunitari innat.

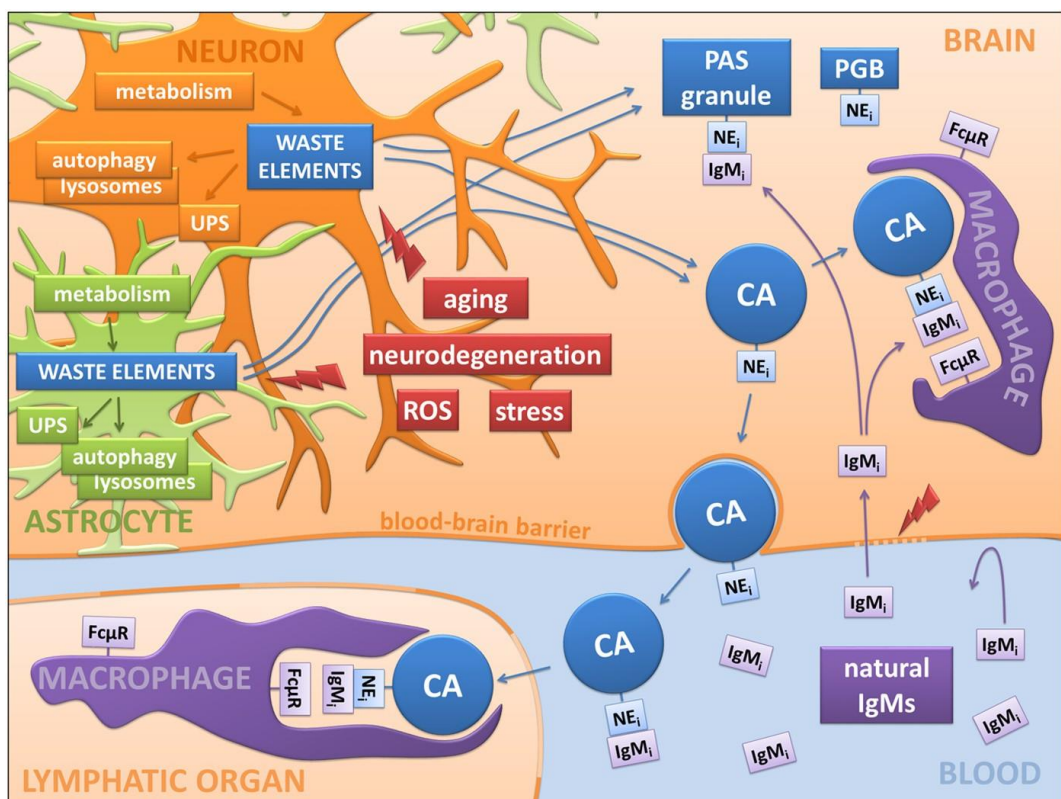


Figura 6. Proposta esquematitzada de sortida dels CA del cervell cap a la sang. Les substàncies de rebuig generades a partir de neurones, astròcits, oligodendròcits i altres cèl·lules cerebrals s'eliminen intracel·lularment a través del sistema Ubi-proteosoma (UPS) o mitjançant processos autofàgics vinculats a la digestió lisosomal. No obstant això, alguns d'aquests productes de rebuig es poden trobar en els CA de cervells humans o en el seu equivalent del cervell de ratolí, els grànuls de PAS. La producció d'elements de rebuig es veu reforçada per factors com l'envelliment, trastorns neurodegeneratius, espècies reactives d'oxigen o estrès cel·lular. Aquests CA contenen alguns neo-epítops (NEi) que són reconeguts per IgM (IgMi). Atès que en condicions fisiològiques la BHE impedeix l'accés de les IgM al parènquima cerebral, la unió entre les IgM i el CA es produeix fora del cervell després de l'extrusió dels CA o dins del cervell si es trenca la barrera, permetent el pas de les IgM. Els macròfags, que contenen receptors específics per a les IgM (FcμR), posteriorment, podrien fagocitar els CA. Així doncs s'estableix una relació entre els CA i la immunitat natural que suggereix que els CA podrien ser contenidors de substàncies de rebuig preparats per a ser eliminats mitjançant aquest sistema predeterminat (Agué *et al.*, 2017).

Paral·lelament, els mateixos autors van realitzar estudis immunohistoquímics que van localitzar a l'estructura dels CA l'enzim GS, indispensable per a la formació de l'estructura de poliglucosà dels CA, i també Ubi i p62, ambdues proteïnes associades a processos d'eliminació de substàncies de rebuig. De fet, la distribució d'aquestes proteïnes observada mitjançant microscòpia confocal va ser clau per a la interpretació dels resultats. Es va mostrar que els CA contenen un nucli central amb un elevat contingut d'Ubi, que es correspondria a una regió d'acumulació de substàncies ubiquitinades, i una zona perifèrica amb GS, p62 i Ubi, que es correspondria a una zona activa de captació de substàncies capturades per la p62 i empaquetades per part de la GS en l'esquelet de poliglucosà (Figura 7) (Augé *et al.*, 2018).

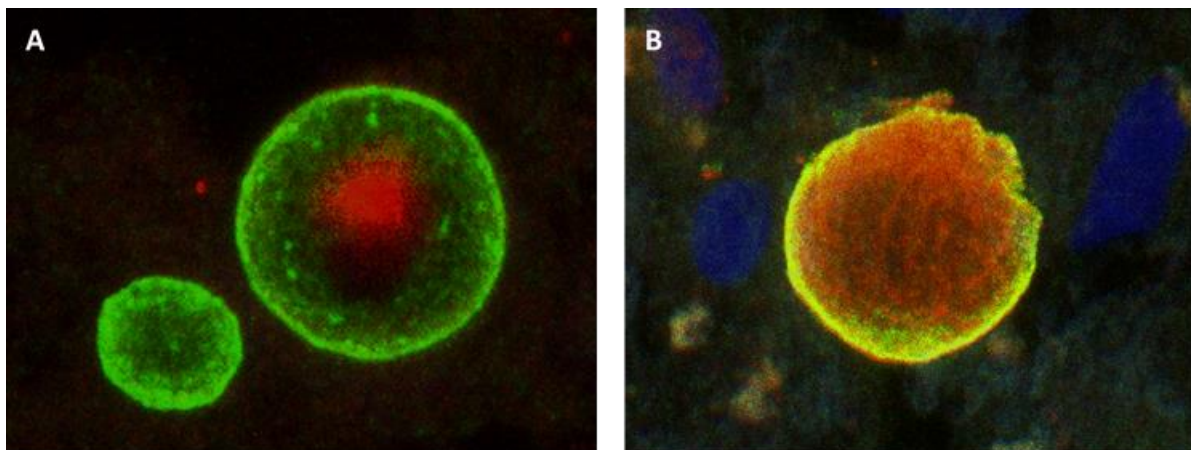


Figura 7. Immunomarcatges de CA de l'hipocamp humà amb GS, p62 i Ubi. (A) CA d'una secció d'hipocamp humà marcat amb GS (verd) a la perifèria dels CA i Ubi (vermell) en la zona central. (B) CA d'una secció d'hipocamp marcat amb GS (vermell) i p62 (verd) a la zona perifèrica de l'estructura (Augé *et al.*, 2018).

Tot i que s'han fet diverses interpretacions pel que fa a la funció dels CA del SNC, un gran nombre d'autors ha postulat la participació dels CA del SNC en el recull i acumulació de substàncies de rebuig, i la seva subseqüent eliminació. Malgrat tot, aquestes propostes provenen, en la major part, de premisses especulatives, algunes mancades de consistència. Per aquesta raó, es precisa de nous estudis que permetin l'obtenció de conclusions robustes envers el paper dels CA en el SNC.

En la present tesi, d'acord amb la localització dels CA propera a cavitats plenes de LCR (Sakai *et al.*, 1969; Cavanagh, 1999), les observacions d'extrusió dels CA des de l'interior dels astròcits del teixit cerebral cap al teixit connectiu de la piamàter (Sbarbati *et al.*, 1996) i la hipòtesi de Cavanagh (1999) que plantejava que els CA probablement arribarien al LCR, es pretén estudiar si efectivament els CA són extruïts cap al LCR. Aquest treball posa en dubte la hipòtesi recolzada per Augé *et al.* (2017) i Sbarbati *et al.* (1996) que planteja una transferència dels CA del parènquima cerebral cap a la sang, ja que aquesta via es veuria obstaculitzada per la BHE. Aquest transport cap a la sang podria donar-se en els òrgans circumventriculars, on no hi ha BHE, però els CA no han estat observats en aquestes

localitzacions. Així doncs, l'extrusió dels CA cap al LCR sembla que pren més consistència. Concretament, tal i com s'ha comentat, els CA s'acumulen en les regions perivasculars, periventriculars i subpials del cervell humà. D'acord amb això, els CA podrien ser extruïts cap a l'espai de Virchow-Robin o espai perivascular, cap als ventricles o cap a l'espai subaracnoidal, zones interconnectades entre elles i plenes de LCR. Una vegada al LCR els CA podrien sortir del SNC, accedint a la sang mitjançant les vellositats o granulacions aracnoidals, estructures clàssicament descrites com les responsables del drenatge del LCR cap a la sang. En aquest cas, però, els CA haurien de ser capaços de travessar el teixit aracnoidal i l'endoteli continu que separa el LCR dels sins venosos, fet improbable principalment a causa de la mida dels CA. Cal destacar que el LCR no drena només a través de les vellositats aracnoidals, sinó també a través dels capil·lars limfàtics de les meninges que arriben a l'espai subaracnoidal que mesuren entre 7 i 842 μm (Schwalbe, 1869; Absinta *et al.*, 2017). Des dels capil·lars limfàtics meníngis i els vasos limfàtics posteriors, la limfa travessa diferents ganglis limfàtics cervicals (Louveau *et al.*, 2015; Weller *et al.*, 2010). D'acord amb això, s'ha descrit que els vasos limfàtics de les meninges permeten l'eliminació de macromolècules del cervell en ser recol·lectades al LCR (Sweeney i Zlokovic, 2018). D'aquesta manera, el drenatge mitjançant els capil·lars limfàtics podria intervenir en l'eliminació dels CA que haurien estat alliberats del cervell cap al LCR. Des d'allà, els CA podrien accedir als ganglis limfàtics cervicals on els CA podrien ser fagocitats per cèl·lules del sistema immunitari, com ara macròfags.

II. OBJECTIUS

L'objectiu global d'aquesta tesi és determinar la funció dels CA de l'organisme humà. Aquest objectiu serà desglossat en diferents objectius específics que s'aniran detallant al llarg del desenvolupament de la tesi. Com que els objectius específics es van anar plantejant de manera seqüencial en base als resultats i a les conclusions que s'anaven obtenint, no és possible detallar tots els objectius concrets en aquest apartat.

Inicialment la tesi estava enfocada a l'estudi dels CA del SNC, però d'acord amb els resultats que es van anar obtenint, es va estendre posteriorment als CA dels altres òrgans i teixits.

Pel que fa als CA del SNC, i en base als estudis previs comentats a la introducció, s'hipotetitza que la funció dels CA és recollir i acumular substàncies de rebuig del cervell humà, i que formen part d'un sistema de recollida i eliminació de productes de rebuig del cervell.

En referència a la funció dels CA en altres òrgans o teixits, es va plantejar identificar, a partir d'una revisió bibliogràfica, les similituds i divergències entre els CA dels diferents òrgans del cos humà, i a partir d'aquesta informació establir una hipòtesi global i integradora respecte a la funció i la significança dels CA en l'organisme.

III. RESULTATS

1. ARTICLE 1

***CORPORA AMYLACEA* ACT AS CONTAINERS THAT REMOVE WASTE PRODUCTS FROM THE BRAIN**

Marta Riba, Elisabet Augé, Joan Campo-Sabariz, David Moral-Anter, Laura Molina-Porcel, Teresa Ximelis, Ruth Ferrer, Raquel Martín-Venegas, Carme Pelegrí, Jordi Vilaplana

Proceedings of the National Academy of Sciences of the United States of America 2019,
116, 26038–26048

DOI: [10.1073/pnas.1913741116](https://doi.org/10.1073/pnas.1913741116)

JCR 2019 IF: 9,412

RESUM

Antecedents: D'acord amb diversos estudis de composició i ultraestructura, alguns autors han recolzat el paper dels CA com a estructures que recullen i acumulen substàncies de rebuig del cervell incorporant-les en un esquelet glucídic. Molts d'ells han postulat que la seva funció és la d'eliminació de productes de rebuig del cervell, en base a la seva localització a prop de les interfícies cerebrals properes al LCR, l'observació del possible procés d'extrusió des dels astròcits cap al teixit connectiu de la piamàter i la presència de NE a la seva estructura, els quals podrien desencadenar processos de fagocitosis.

Objectiu: Confirmar la hipòtesi que postula que els CA formen part d'un sistema d'eliminació de substàncies de rebuig del cervell humà, el qual es basa en l'extrusió dels CA des del parènquima cerebral cap al LCR, des d'on els CA accedirien al sistema limfàtic de les meninges i arribarien als ganglis limfàtics cervicals, on serien eliminats per macròfags. D'acord amb aquesta hipòtesi, els objectius del present treball van ser determinar la presència de CA en el LCR i en els ganglis limfàtics cervicals i estudiar les interaccions entre CA i macròfags.

Material i mètodes: Per determinar la presència de CA en el LCR, es van utilitzar mostres *post-mortem* de LCR ventricular de 16 pacients amb malalties neurodegeneratives (65-91 anys). Aquestes mostres van ser processades mitjançant la tinció de PAS i tècniques d'immunofluorescència, per al seu posterior anàlisi per microscòpia de camp clar i/o de fluorescència. A més a més, es van realitzar estudis de microscòpia electrònica de transmissió (MET) i microscòpia òptica de rastreig (MER). Per examinar la presència de CA en els ganglis limfàtics cervicals, es van obtenir seccions d'aquestes estructures obtingudes de 4 pacients amb càncer (83-96 anys). Les mostres seleccionades, que no presentaven afectació tumoral, van ser processades mitjançant la tinció de PAS i tècniques d'immunofluorescència, i van ser visualitzades al microscopi de camp clar i/o de fluorescència. Es va analitzar també la relació entre el nombre de CA de cada gangli i la posició d'aquests en la zona superior, central o inferior del coll utilitzant el test ANOVA amb la correcció de Bonferroni. Per estudiar les interaccions entre CA i macròfags, es van afegir CA del LCR opsonitzats amb IgM humanes a cultius de macròfags derivats de monòcits THP-1, els quals a partir d'aquest punt s'anomenaran macròfags THP-1. Paral·lelament, com a experiment control, es va realitzar el mateix procediment amb CA sense opsonitzar amb IgM. Les mostres es van processar mitjançant tinció de PAS, marcatges amb ConA i fal·loïdina ambdues conjugades amb fluorescència, i mitjançant tècniques d'immunofluorescència amb l'anticòs dirigit contra el receptor de Man o clúster de diferenciació (CD) 206, que podia estar present en els macròfags THP-1. Tot seguit, es va procedir amb l'observació de les preparacions amb microscòpia de camp clar, de fluorescència i confocal. Es van realitzar també estudis de MER.

Resultats: D'una banda, els estudis realitzats mitjançant la tinció de PAS, juntament amb els estudis d'immunofluorescència amb IgM i amb anticossos dirigits contra la GS i els estudis

amb MET i MER, van confirmar la presència de CA al LCR. Totes les mostres de LCR analitzades contenien CA. A més a més, els estudis de MET van evidenciar que les característiques ultraestructurals dels CA del LCR ventricular eren similars a les dels CA madurs localitzats en teixit hipocampal. D'altra banda, la tinció de PAS i el marcatge amb IgM van posar de manifest la presència de CA als ganglis limfàtics cervicals. No obstant això, no totes les seccions analitzades contenien CA. Cal destacar que els CA es trobaven a l'espai subcapsular o als sins trabeculars i establien contactes amb cèl·lules adjacents, les quals per forma i localització podien ser identificades com a macròfags. Els marcatges amb anticossos dirigits contra el receptor de la fracció constant μ (Fc μ R) de les IgM i el CD35 van permetre l'observació de macròfags Fc μ R i CD35 positius, però els CA no estaven en contacte amb aquests subtipus de macròfags. Pel que fa a la relació entre el nombre de CA en els ganglis limfàtics cervicals i la localització dels mateixos a la zona del coll, l'anàlisi estadística va mostrar diferències significatives entre el nombre de CA comptabilitzats en els ganglis localitzats a la zona superior del coll respecte al nombre de CA comptabilitzats en els ganglis de la zona inferior. No es van observar diferències significatives entre el nombre de CA quantificats en els ganglis de la zona intermèdia del coll respecte als CA quantificats en les zones superior o inferior. Considerant que els CA presents als ganglis limfàtics es van trobar establint contacte amb macròfags, es va iniciar l'estudi de les interaccions entre CA i macròfags afegint CA purificats del LCR en macròfags THP-1 en cultiu. La tinció de PAS i els marcatges amb anticossos i ConA van permetre l'observació de macròfags THP-1 en contacte o envoltant els CA que havien estat prèviament opsonitzats amb IgM, i l'observació de les preparacions mitjançant microscòpia confocal i reconstrucció en tres dimensions van mostrar CA a l'interior dels macròfags. A més a més, el processament i visualització de les mostres amb MER van possibilitar l'observació de lamel·lipodis emergents dels macròfags establint contacte amb els CA opsonitzats amb IgM. Així doncs, els resultats indicaven que els CA opsonitzats amb IgM podien ser fagocitats pels macròfags THP-1. Inesperadament, però, els experiments control realitzats amb CA no opsonitzats amb IgM van mostrar els mateixos resultats, de manera que, tot i que no es va descartar que la opsonització dels CA amb IgM intervingués en procés de fagocitosis, aquesta opsonització no seria un requeriment per la fagocitosis d'aquestes estructures per part de macròfags THP-1. En aquest sentit, es va estudiar la possibilitat que els CA fossin fagocitats per altres vies. D'acord amb la composició glucídica dels CA i el seu marcatge amb ConA, es va plantejar que els CA podrien contenir Man i per tant podrien ser fagocitats mitjançant la detecció de Man per part del receptor de Man CD206. Es va confirmar la presència del receptor CD206 en els macròfags THP-1 utilitzant l'anticòs dirigit contra aquest receptor. Aquests resultats van recolzar que els macròfags THP-1 podrien fagocitar els CA mitjançant el receptor CD206.

Conclusions: Les mostres de LCR estudiades contenen CA amb les mateixes característiques de composició i ultraestructura que els CA del parènquima cerebral, la qual cosa recolza l'extrusió dels CA des del cervell cap al LCR. Des del LCR els CA podrien accedir el sistema

limfàtic de les meninges i als subseqüents vasos limfàtics del coll, on hi ha els ganglis limfàtics cervicals. En els ganglis limfàtics cervicals els CA es localitzen en zones de pas de la limfa, com ara l'espai subcapsular i els sins trabeculars, i entren en contacte amb macròfags. A més a més, els ganglis localitzats en les zones superiors del coll contenen més CA que els que es troben situats a la zona inferior, cosa que suggereix que aquests ganglis actuen com a filtres, i van eliminant els CA que hi accedeixen. Pel que fa a les interaccions dels CA amb els macròfags, s'ha confirmat que els macròfags THP-1 són capaços de fagocitar els CA del LCR i que, de fet, podria haver-hi mecanismes redundants que donarien lloc a la fagocitosis dels CA per tal de garantir-ne l'eliminació. Conseqüentment, aquest conjunt d'evidències confirma la hipòtesi que planteja que els CA són extruïts des del cervell humà cap al LCR i que, mitjançant el sistema limfàtic de les meninges, arriben als ganglis limfàtics cervicals on són fagocitats per macròfags, tot constituint un sistema d'eliminació de substàncies de rebuig cerebrals.

Després de la publicació d'aquest article, ens van demanar escriure un article de divulgació basat en aquests resultats a la plataforma The Conversation. Aquest article de divulgació s'ha republicat i difós en un total de 24 plataformes internacionals i ha arribat a més de 160.000 lectors distribuïts en 10 països.

ASÍ SACA LA BASURA EL CEREBRO

Jordi Vilaplana, Carme Pelegrí, Elisabet Augé, Marta Riba

The Conversation 2020, 129808, 1–5

<https://theconversation.com/asi-saca-la-basura-el-cerebro-129808>

Aquest article es troba a l'Annex de la present tesi.



Corpora amylacea act as containers that remove waste products from the brain

Marta Riba^{a,b,c,1}, Elisabet Augé^{a,b,c,1}, Joan Campo-Sabariz^{a,d}, David Moral-Anter^{a,d}, Laura Molina-Porcel^e, Teresa Ximelis^e, Ruth Ferrer^{a,d}, Raquel Martín-Venegas^{a,d}, Carme Pelegrí^{a,b,c,2}, and Jordi Vilaplana^{a,b,c,2}

^aSecció de Fisiologia, Departament de Bioquímica i Fisiologia, Universitat de Barcelona, 08028 Barcelona, Spain; ^bInstitut de Neurociències, Universitat de Barcelona, 08035 Barcelona, Spain; ^cCentros de Biomedicina en Red de Enfermedades Neurodegenerativas (CIBERNED), 28031 Madrid, Spain; ^dInstitut de Recerca en Nutrició i Seguretat Alimentàries (INSA-UB), Universitat de Barcelona, 08291 Barcelona, Spain; and ^eNeurological Tissue Bank of the Biobanc-Hospital Clinic-Institut d'Investigacions Biomèdiques August Pi i Sunyer (IDIBAPS), 08036 Barcelona, Spain

Edited by Lawrence Steinman, Stanford University School of Medicine, Stanford, CA, and approved November 5, 2019 (received for review August 8, 2019)

Corpora amylacea (CA) in the human brain are granular bodies formed by polyglucosan aggregates that amass waste products of different origins. They are generated by astrocytes, mainly during aging and neurodegenerative conditions, and are located predominantly in periventricular and subpial regions. This study shows that CA are released from these regions to the cerebrospinal fluid and are present in the cervical lymph nodes, into which cerebrospinal fluid drains through the meningeal lymphatic system. We also show that CA can be phagocytosed by macrophages. We conclude that CA can act as containers that remove waste products from the brain and may be involved in a mechanism that cleans the brain. Moreover, we postulate that CA may contribute in some autoimmune brain diseases, exporting brain substances that interact with the immune system, and hypothesize that CA may contain brain markers that may aid in the diagnosis of certain brain diseases.

corpora amylacea | meningeal lymphatic system | aging | phagocytosis | natural immune system

In 1837 the anatomist and physiologist J. E. Purkinje described the presence of some particular granular bodies in the brain of elderly patients (1). Virchow, in 1854, described them in more detail and observed that these bodies (*corpora* in Latin) share some similarities with starch (*amylum* in Latin) (2). These bodies, named *corpora amylacea* (CA), were initially considered to have no pathological significance and for a long time were thought to be irrelevant. In recent decades, however, this perception has changed. With the advances in technology, CA have been studied from different perspectives and a large number of theories regarding their nature have been put forward. Unfortunately, none of these theories have been demonstrated conclusively and CA remain intriguing and mysterious bodies. In the present study, several features of CA are described and a vision of their function is proposed which may have implications for clinical practice.

There is a consensus that the main components of CA are polymerized hexoses (primarily glucose) (3) and it has been estimated that hexoses constitute about 88% of their weight (4). Along with polymerized hexoses, other components originating in neurons, astrocytes, or oligodendrocytes, from blood or of fungal or viral origin, have also been described, although some of them have generated controversy (5). In 2017 we reported that CA contain neoepitopes that are recognized by natural antibodies of the immunoglobulin M (IgM) isotype (6). We also observed that these IgMs were present as contaminants in numerous commercial antibodies used for immunohistochemistry procedures and, since these contaminant IgMs are recognized by the majority of the secondary antibodies, they frequently cause false positive immunostaining in CA. These IgMs therefore account for some of the inconsistencies concerning CA composition and are the main reason for the uncertainty surrounding their origin and functions. In subsequent work, we reviewed the presence of the components previously described in CA and were able to rule out some of them, at least at levels that can be detected by immunohistochemistry (5,

6). Nonetheless, we observed that CA contain glycogen synthase (GS), an indispensable enzyme for polyglucosan formation, and also ubiquitin and protein p62, both associated with processes of elimination of waste substances (5). The relationship between CA and waste substances is recurrent in the literature. Already in 1999, after a detailed and complete review, Cavanagh indicated that “CA functions seem to be directed towards trapping and sequestration of potentially hazardous products of cellular metabolism, principally derived from the aging process, but probably also from any disease state resulting in excessive amounts of potentially harmful metabolic products” (3). Although some of these hazardous products were described after carrying out unreliable immunohistochemical procedures, the results obtained using other techniques have supported their presence. In this regard, ultrastructural studies by Sbarbati et al. (7) indicated that CA originate in astrocytes and accumulate abnormal material, and the study by Augé et al. (8) showed that CA are formed inside astrocytes by the accumulation of residual products, including degenerating mitochondria and membranous fragments originating from degenerative processes. Moreover, combining the results of human neuropathological surveys, cell culture techniques, and animal models, some authors have proposed that CA are homologous to “Gomori-positive” granules which accumulate in subcortical/periventricular regions of the rodent brain and which are derived from damaged

Significance

Aging and neurodegenerative processes induce the formation of waste substances in the brain. Some of these substances accumulate in *corpora amylacea* (CA). We reveal that CA are released from the brain into the cerebrospinal fluid and are present in the cervical lymph nodes, into which cerebrospinal fluid drains through the meningeal lymphatic system. We also show that CA can be phagocytosed by macrophages. We conclude that CA can act as waste containers and hypothesize that CA are involved in a mechanism that cleans the brain. We also postulate that CA may contain clinical markers of brain disorders and may also play significant roles in some brain autoimmune diseases. These last points merit further study due to their possible clinical implications.

Author contributions: M.R., E.A., R.M.-V., C.P., and J.V. designed research; M.R., E.A., J.C.-S., D.M.-A., L.M.-P., T.X., R.F., R.M.-V., C.P., and J.V. performed research; M.R., E.A., C.P., and J.V. analyzed data; and M.R., E.A., C.P., and J.V. wrote the paper.

The authors declare no competing interest.

This article is a PNAS Direct Submission.

This open access article is distributed under [Creative Commons Attribution-NonCommercial-NoDerivatives License 4.0 \(CC BY-NC-ND\)](https://creativecommons.org/licenses/by-nc-nd/4.0/).

¹M.R. and E.A. contributed equally to this work.

²To whom correspondence may be addressed. Email: carmepelegri@ub.edu or vilaplana@ub.edu.

This article contains supporting information online at <https://www.pnas.org/lookup/suppl/doi:10.1073/pnas.1913741116/-DCSupplemental>.

First published December 3, 2019.

mitochondria engaged in a complex macroautophagy process (9, 10). For their part, using a combination of 2D electrophoresis with matrix-assisted laser desorption/ionization time-of-flight mass spectrometry, Selmaj et al. (11) identified several proteins of suspected neuronal origin and others involved in the regulation of apoptosis and senescence, supporting the notion that the biogenesis of CA involves the degeneration and aggregation of substances, some of them of neuronal origin. Moreover, Cissé et al. (12) already described the presence of ubiquitin in CA in high-performance liquid chromatography (HPLC) studies. Taken together, this evidence indicates a relationship between CA and waste elements and reinforces the idea that CA are waste containers formed by a polyglucosan structure that amasses waste products (6).

It is well known that CA are located mainly in perivascular, periventricular, and subpial regions of the brain (4). Since the glymphatic system drains the interstitial fluid (ISF) from the perivascular regions to the cerebrospinal fluid (CSF) (13), and since both periventricular and subpial regions are close to the cavities that contain the CSF (i.e., ventricles and subarachnoid space), it is plausible that, as several authors have proposed, CA are expelled from the brain to the CSF (3–7, 14). In biopsied material from the vestibular root entry zone in cases of Ménière's disease, Sbarbati et al. (7) observed at ultrastructural level that CA were sited in astroglial processes of the glia limitans, near the pial region. Around these CA the astrocytic cytoplasmic membrane presents folds that create fissures which, according to these authors, may split the CA apart, allowing them to escape into the pial connective tissue or subpial space. In this regard, in a study with human hippocampal tissue, we observed the presence of CA in both the subependymal region and beneath the pia and,

occasionally, inside the CSF of the ventricular region. This evidence (summarized in Fig. 1) seems to indicate a possible route of escape for the CA into the CSF.

The CSF drains not only via arachnoid granulations, as classically believed, but also via the recently rediscovered meningeal lymphatic system (15). The presence of lymphatic vessels collecting CSF at the base of the skull was described for the first time by Földi et al. (16). Johnston et al. (17) reported connections between the CSF and nasal lymphatic vessels in humans and other mammals. Later, lymphatic vessels collecting CSF were also described lining the dural sinuses by Louveau et al. (18, 19), and new techniques based on magnetic resonance imaging permit their *in vivo* visualization (20). From meningeal lymphatic vessels and subsequent lymphatic vessels, lymph crosses different cervical lymph nodes (18, 21) before accessing the lymphatic duct or right thoracic duct, which ultimately drain into the brachiocephalic veins. The images in Fig. 2 sketch the structure of the meninges, including the meningeal lymphatic system, as well as the routes of the lymphatic vessels that descend to the neck and cervical lymph nodes. On this basis, it has been reported that meningeal lymphatic vessels allow the brain to eliminate macromolecules by collecting them from the CSF (22). Conceivably, in the same way as waste molecules generated in the brain, it is possible that CA released from the brain into the CSF escape from the CSF via the meningeal lymphatic system, reaching the deep cervical lymph nodes or beyond. The lymphatic capillaries are formed by overlapping cells that can act as valves leaving relatively large openings, allowing the passage of macromolecules and even cells, and thus also the passage of CA.

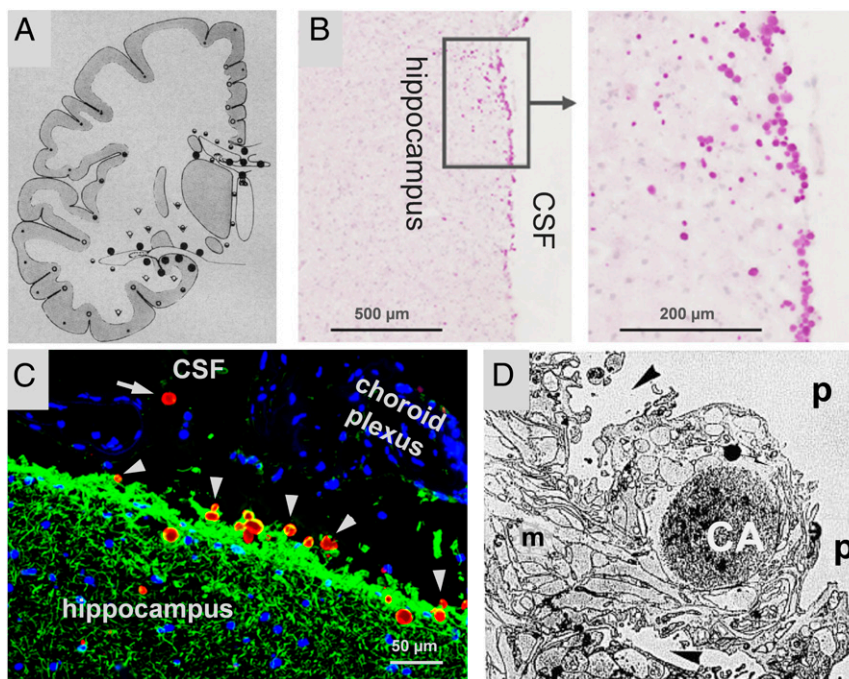


Fig. 1. Distribution of CA in human brain and possible extrusion into the CSF. (A) Distribution of CA in cerebrum of 70-y-old brains (· rare, ° occasional, ▼ common, ● extremely rich, ▼ variable). Note that CA tend to be concentrated in the proximity to CSF (mean from 4 cases). Adapted with permission from ref. 4. Copyright 1969 American Medical Association. All rights reserved. (B) Hippocampal section of human brain stained with PAS. CA (magenta spots) can be observed in the border of the hippocampus. Adapted with permission from ref. 5, which is licensed under [CC BY 4.0](https://creativecommons.org/licenses/by/4.0/). (C) Hippocampal section of human brain stained with α -glial fibrillary acidic protein (α -GFAP) (green), mouse IgMs directed against neopeptides (red), and Hoechst (blue). Note that almost all CA (stained with the IgMs) are partially encircled with astrocytic fibrils (stained with α -GFAP). Clustered nuclei (blue staining) in the ventricle are from cells from choroid plexus. Some CA seem to escape from hippocampus (arrowheads) and one is located inside the ventricle (arrow), all suggesting that CA can be extruded from brain. (D) Proposed extrusion of CA at the vestibular root entry zone. The CA is generated inside the astrocyte and, after the formation of a system of ramified scissurae around the CA, it is transferred to the pial connective tissue. m, marginal glia; p, pial connective tissue; arrowheads, scissurae of astrocyte enveloping the CA. Original image: 3,100 \times . Adapted from ref. 7 by permission of Oxford University Press.

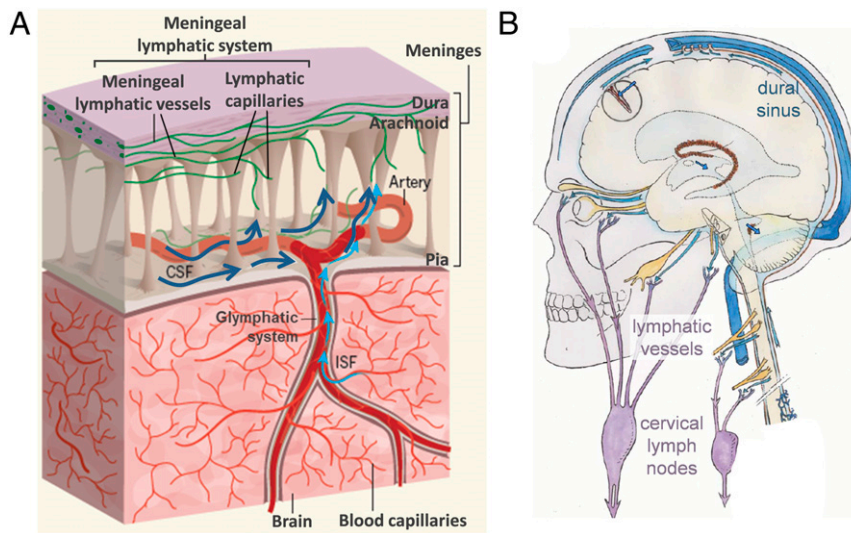


Fig. 2. Drainage of CSF via the meningeal lymphatic system. (A) Part of the CSF drains from the subarachnoid space via the lymphatic meningeal system. In turn, ISF drains to the subarachnoid space via the glymphatic system. These routes allow the elimination of waste elements and macromolecules generated in the brain tissue. Adapted by permission from ref. 22, Springer Nature: *Nature*, copyright 2018. (B) The meningeal lymphatic vessels descend to the neck, where the cervical lymph nodes are located. These nodes are involved in the elimination of waste products (the scheme does not depict the lymphatic vessels lining the dural sinuses). Adapted from ref. 23. Copyright 2011 Elsevier Masson SAS. All rights reserved.

As we indicated in previous work, CA contain neoepitopes that are recognized by natural IgM antibodies (6). Natural IgM antibodies are generated even before birth, without exposure to external antigens, and contribute to critical innate immune functions such as the maintenance of tissue homeostasis (24). Carbohydrate epitopes are targets of immune surveillance and natural IgM antibodies (25, 26). Some of these epitopes are generated *de novo* under triggering circumstances in cells or structures of the body itself, and are thus known as neoepitopes. For instance, in aging processes there is an increase in the generation of advanced glycation end products (27), which can act as neoepitopes, and neoepitopes of carbohydrates have also been described in malignant tumor cells (26, 28). In the case of CA, the interaction between IgMs and neoepitopes cannot occur inside the brain, because CA are intracellular structures and thus have a limiting membrane (7, 8). Moreover, IgMs do not cross the blood–brain barrier and so do not have access to the brain parenchyma or the CSF (6). Hence, if CA are extruded from the brain to the CSF and reach the cervical lymph nodes via the meningeal lymphatic vessels, their interaction with IgMs may take place in the cervical lymph nodes. Furthermore, since phagocytosis is one of the responses triggered by natural IgMs, it would be interesting to examine whether lymph node macrophages can phagocytose them. It must be pointed out that CA being phagocytosed by macrophages has been observed in samples from cases of neuromyelitis optica, a condition that involves tissue inflammation, vascular alterations, and probably the disruption of the blood–brain barrier (29).

Overall, this evidence suggests a mechanism for eliminating residual substances from the brain in which CA act as waste containers that are extruded from the brain to the CSF. Afterward, via the meningeal lymphatic system, CA can reach the cervical lymph nodes, and macrophages located there may play a significant role in their phagocytosis. We therefore studied the possible presence of CA in the CSF, their presence in the cervical lymph nodes, and their interactions with macrophages.

Results

CSF Contains CA. To study the presence of CA in the CSF, we analyzed several CSF samples supplied by the Biobanc-Hospital

Clinic-Institut d'Investigacions Biomèdiques August Pi i Sunyer (IDIBAPS). According to the standard protocol used at this facility, samples are centrifuged at $4,000 \times g$ at 4°C for 10 min and pellets are rejected in order to clean the CSF of unwanted insoluble particles or cell debris. The supernatants are then maintained at -80°C until used. The study by Sakai et al. (4), in which the authors isolated CA from brain tissue, indicated that centrifugation at $650 \times g$ during 10 min is enough to produce CA precipitation. Therefore, as the standard protocol used by the Biobanc would remove any CA present in the CSF, we asked for samples of noncentrifuged CSF in order to perform a prospective study. These CSF samples were extended on slides and were stained with periodic acid Schiff (PAS) or immunostained with human IgMs directed against the neoepitopes (IgM_h α -NE). In all cases, we observed round bodies with sizes and histochemical staining compatible with CA, thus suggesting the presence of CA in the CSF. Representative images of these bodies stained with PAS or with IgM_h α -NE are shown in Fig. 3A and B, respectively. As the use of noncentrifuged samples compromises the availability of CSF for other studies, the Biobanc began to collect the pellets of the CSF processed according to their protocol instead of rejecting them. These pellets were used to complete the present study. When performing the extensions from resuspended pellets of CSF, CA were also observed stained with PAS (Fig. 3C) and stained with both α -GS and IgM_h α -NE (Fig. 3D). The presence of CA in pellets of CSF was corroborated by visualizing them at an ultrastructural level using transmission electron microscopy (TEM). As shown by the representative images from Fig. 3E–J, CA from CSF comprise densely packed, randomly oriented short linear fibers, which in some cases are concentrated in the central region or in concentric ring regions of CA. Indeed, these ultrastructural features are similar to those of mature CA from the hippocampus brain tissue (8) and those of mature PAS granules from mice (30), which are equivalent to CA of human brain. CA from the brain are encircled by a plasma membrane that confirms their intracellular and cytosolic location (3, 8), but this membrane is not visible in CA from the CSF. This suggests that CA may have lost this membrane during the extrusion process. Sbarbati et al. (7) also suggested this hypothesis when describing the extrusion of CA to pial connective tissue from vestibular nerve samples. Scanning electron microscope

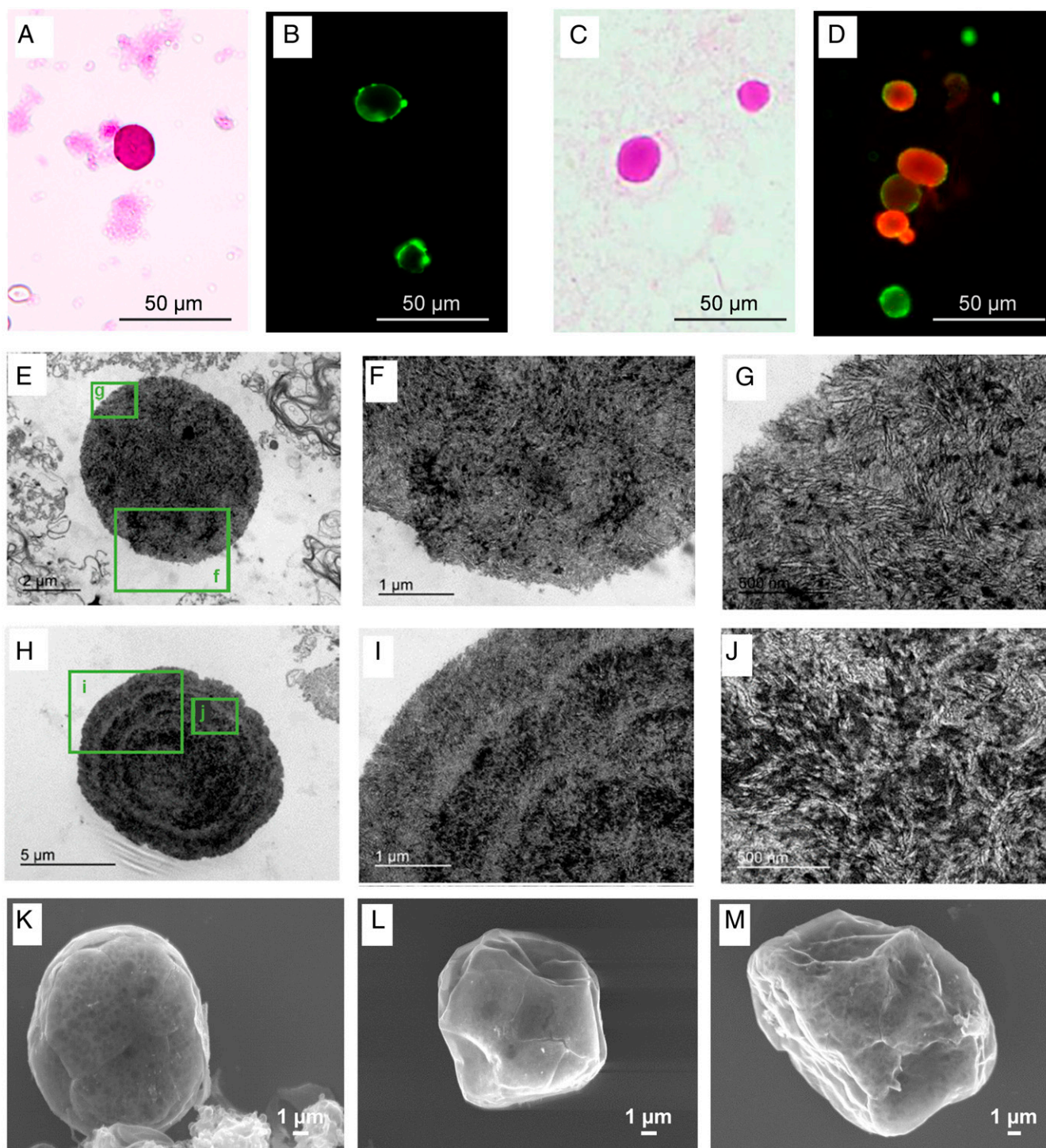


Fig. 3. Human CSF contains CA. After the extension of uncentrifuged CSF on slides, the staining with PAS (A) and with IgM_h, α -NE (B) showed the presence of CA in CSF. When performing the extension from resuspended pellets of CSF, CA were also observed stained with PAS (C) and stained with both α -GS and IgM_h, α -NE (D, red and green, respectively). This indicated that pellets of CSF contain CA. The presence of CA in pellets of CSF is corroborated by visualizing them at an ultrastructural level using TEM (E–J) and SEM (K–M).

(SEM) analysis from pellet samples also confirmed the presence of CA in CSF (Fig. 3 K–M). As reported many years ago with reference to CA isolated from brain tissue (4), these bodies present a spherical shape with a smooth surface. Ripples and crevices may be observed on the surface, but these are artifacts produced by the electron beam interacting on the sample. Altogether, these results indicate that CSF contains CA, thus demonstrating that CA are

extruded from brain to the CSF. Moreover, these results also indicate that CSF pellets can be used to analyze these bodies.

CA Are Present in the Cervical Lymph Nodes. Once the presence of CA in the CSF is established, the next question is to determine whether they are eliminated from the CSF. Due to their size (some 10 μ m in diameter) they cannot be eliminated via arachnoid

granulations to dural venous sinuses. However, as noted above, CSF and their macromolecules are also drained via the meningeal lymphatic system, and thus CA may be eliminated by this system and may then be driven to the cervical lymph nodes.

We therefore analyzed cervical lymph nodes from different cases in order to check the presence of CA. When staining paraffin-embedded sections of the cervical nodes with PAS we observed that, although not all sections contain CA, these bodies were observed in certain sections from all donors (Fig. 4). As can be seen in Fig. 4A, CA found in the cervical lymph nodes were generally sited in the subcapsular space or in the trabecular sinuses that radiate from this space through the parenchyma to the medullary sinuses. It can also be seen that, although CA are surrounded by the sinus space, they are not completely free; they show specific contacts with some lymph node cells. The localization of these lymph node cells in the trabecular sinuses and their elongated form suggest that they can be macrophages entrapping CA. We also analyzed different sections by immunofluorescence techniques. The staining with IgM_h α-NE and the secondary fluorochrome-labeled α-IgM_h antibody did not allow the visualization of CA in the nodes because of the presence of IgM_h in the tissue, which become fluorolabeled and thus masked CA visualization. However, CA were observed in the nodes when using IgMs from mouse directed against neoepitopes (IgM_m α-NE) and a secondary fluorochrome-labeled α-IgM_m (Fig. 4B). As shown in previous research (6), the α-IgM_m binds to the IgM_m but does not recognize the IgM_h. In order to determine what type of lymph node cells were in contact with CA, we used double immunostaining with IgM_m α-NE and α-FcμR on the one hand and IgM_m α-NE and α-CD35 on the other. The FcμR (or FAIM3) is an IgM receptor present in some macrophages and dendritic cells and is related to phagocytotic processes, and CD35 is a receptor for the C3b component of the complement system also present in these cells. We observed that cervical lymph nodes contain some cells that become stained with these markers, but the cells that are in contact with CA did not stain with these antibodies (Fig. 4C).

We also analyzed the relationship between the amount of CA contained in the cervical nodes and the position of these nodes in the neck, expecting that nodes sited in the lower regions would have fewer CA than those in the upper regions. We analyzed the amount of CA in the nodes sited in regions I, II, III, and IV according to Rouvière's standard anatomic description (31). Regions I and II are located in the upper plane of the neck, while region III is located in the intermediate plane and region IV in the lower plane. Data on these observations can be found in the [Dataset S1](#). Fig. 4C shows the mean number of CA per section according to the localization of the node in the neck. The mean number of CA ± SEM from sections corresponding to the upper zone (regions I and II) is 1.62 ± 0.31 ($n = 13$), from the intermediate zone (region III) 0.90 ± 0.31 ($n = 10$), and from the lower zone (region IV) 0.17 ± 0.17 ($n = 6$) (Fig. 4D). These results correspond to the mean of CA per section. Bearing in mind that each section has a thickness of 8 μm, and considering that the standard size of a node is around 3 mm in radius, the approximate mean number of CA per node is about 810 ± 155.45 in the upper zone, 450 ± 157.17 in the intermediate zone, and 85 ± 83.28 in the lower zone. Then, an ANOVA was performed with the number of CA per section as the dependent variable and the zone where the nodes are located as the independent variable. The ANOVA indicated significant differences in the number of CA according to zone ($F_{2,26} = 4.74$; $P < 0.019$). Post hoc comparisons (Bonferroni test) indicated higher numbers of CA in the nodes of the upper zone than in those of the lower zone ($P < 0.017$). There were no significant differences in the number of CA in the nodes of the intermediate zone compared with the upper and lower zones ($P > 0.05$). Overall, these results support the idea that CA reach and become entrapped in the cervical lymph nodes.

Macrophages Phagocytose and Process CA. As indicated above, CA in cervical lymph nodes were generally found in the subcapsular space or in the trabecular sinuses and have specific contacts with some lymph node cells. Although α-CD35 and α-FcμR do not seem to stain these lymph node cells, the localization of these cells in the trabecular sinuses and their elongated form suggest that they may be macrophages entrapping CA.

Subsequently, we used in vitro cultures of macrophages derived from THP-1 cells to analyze their interaction with CA. In the first attempt, we isolated CA from CSF and opsonized them with IgM_h α-NE, and then added the opsonized CA in the culture of THP-1-derived macrophages. PAS staining applied to these samples suggested that macrophages can phagocytose CA. As illustrated in Fig. 5A, some macrophages are close to CA and begin to encircle them, while in other cases macrophages completely encircle CA, suggesting that the CA have been phagocytosed. When staining the samples with fluorescent-labeled phalloidin and fluorescent-labeled α-IgM_h we also observed some CA adhering to the macrophages and others encircled by them (Fig. 5B). Using confocal microscopy and 3D reconstruction, which allow observing the structure rotating on itself, we observed some macrophages that were phagocytosing CA (Fig. 5C) and also some others containing CA inside them, indicating that the CA had been phagocytosed (Fig. 5D). Other samples were processed for visualization by SEM. SEM images also showed macrophages engulfing CA, and some filopodia were seen emerging from macrophages and coming into contact with the bodies (Fig. 5E). Altogether, these results indicate that CA opsonized with IgM_h can be phagocytosed by THP-1-derived macrophages.

Unexpectedly, however, controls performed with CA non-opsonized with IgMs were also phagocytosed by THP-1-derived macrophages (Fig. 5F). Therefore, although the possibility that opsonization with IgMs could generate some response cannot be ruled out, IgM opsonization is not a requisite for CA phagocytosis by THP-1-derived macrophages, and this process must involve other mechanisms than those triggered by IgMs and α-FcμR. Phagocytosis via the IgM activation of the complement system (32) can also be ruled out because in our experiments the complement proteins were heat inactivated. Mei Liu et al. (33) observed that CA are reactive for Con A, a lectin that binds with high affinity to mannose oligomers, and indicated that CA contain mannose-rich conjugates. Thus, as mannose conjugates can be recognized by mannose receptors sited in macrophages and can activate phagocytosis, it may be that mannose contained on the surface of CA can trigger phagocytosis via possible mannose receptors sited on THP-1-derived macrophages. Accordingly, we first verified that CA are reactive to Con A. Fig. 5G shows representative images of CA from CSF stained with Con A, which suggests the presence of mannose in CA. We then tested the presence of the mannose receptor CD206 in THP-1-derived macrophages, and observed that actually macrophages became stained with α-CD206, indicating the presence of this receptor in these cells. Fig. 5H shows a representative image of a CA (stained with fluorescent-labeled Con A) encircled by THP-1 macrophages immunostained with α-CD206. These results reinforce the notion that, in the case of THP-1 cells and with the conditions of the present study, the phagocytosis of CA is produced via the mannose receptor. However, as will be discussed below, there may be other redundant mechanisms by which macrophages can phagocytose CA.

Discussion

For decades now, several functions have been attributed to CA, all of them proposed on the basis of studies performed in brain tissue or its extracts. The presence of CA in both the CSF and the cervical lymph nodes, demonstrated in the present study, provides another perspective.

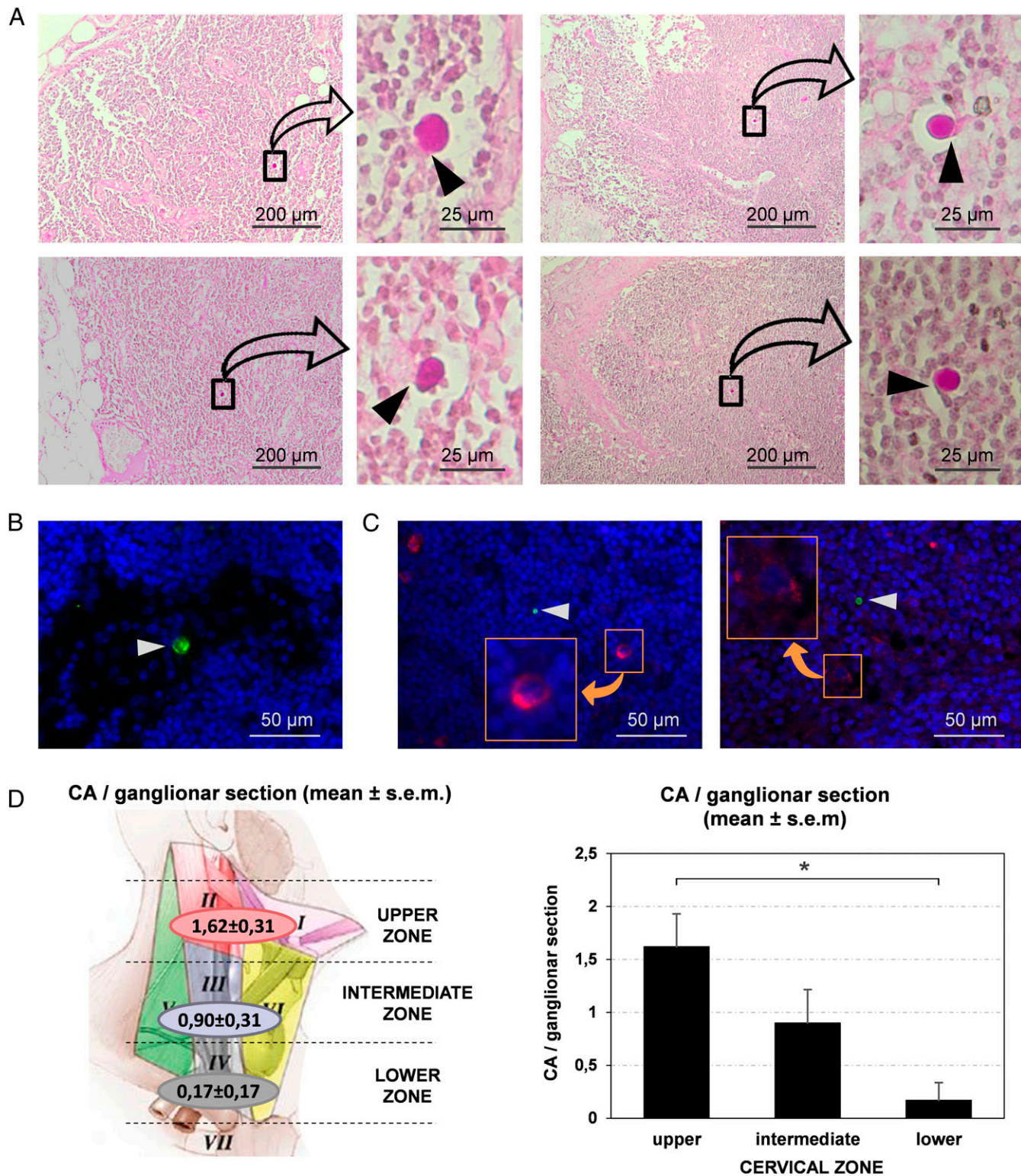


Fig. 4. CA are present in the cervical lymph nodes. (A) Images of sections from different cervical nodes stained with PAS. For each section, a region containing CA is magnified. Note that CA exhibit specific contacts with some lymph node cells (arrowheads). (B) CA (arrowhead) can also be observed by immunofluorescence when sections are immunostained by IgM_m α-NE (green). Blue staining (Hoechst) corresponds to the nuclei of lymph node cells. (C) Double staining with IgM_m α-NE and α-FcμR (green and red respectively, *Left image*), and double staining with IgM_m α-NE and α-CD35 (green and red respectively, *Right image*) indicate that some cells of the cervical lymph nodes contain FcμR and other cells express CD35 (*Insets*). However, the cells in contact with CA (arrowheads) did not stain with these antibodies. (D) Mean number (±SEM) of CA per section in the different regions of the neck. The upper region of the neck contains more CA per section than the lower one ($P < 0.05$), which suggests that brain CA reach the cervical lymph nodes, and that the nodes may retain or eliminate them.

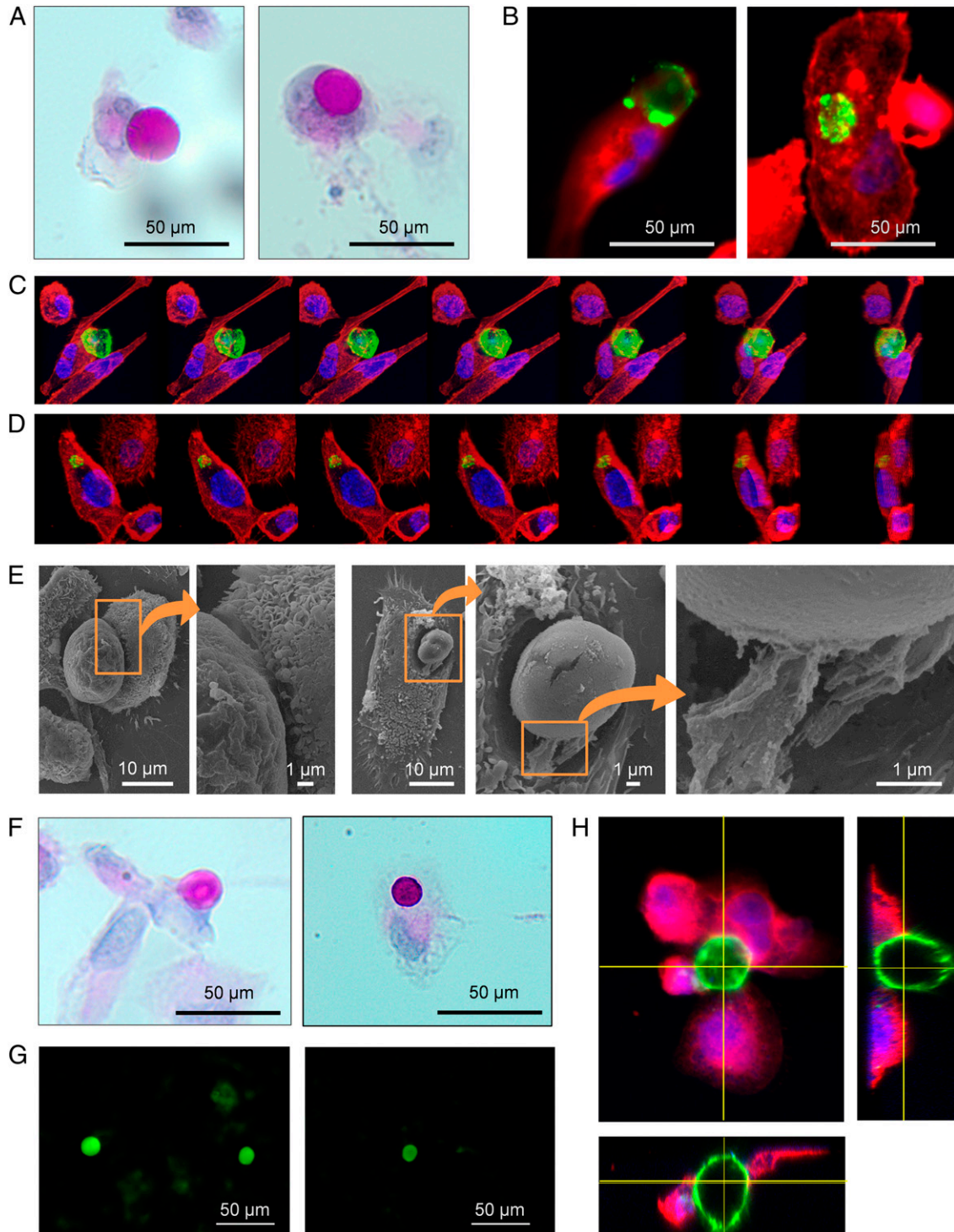


Fig. 5. CA are phagocytosed by THP-1-derived macrophages. (A) Macrophage in contact with an IgM_h-opsonized CA (Left) and an IgM_h-opsonized CA phagocytosed by macrophage (Right); PAS staining. (B) Other examples of a macrophage making contact with an IgM_h-opsonized CA (Left) and an IgM_h-opsonized CA phagocytosed by macrophage (Right). In these cases, macrophages are stained with fluorescent-labeled phalloidin (red) and IgM_h-opsonized CA are stained with fluorescent-labeled α -IgM_h (green). Nuclei are stained with Hoechst (blue). (C) Sequence of images showing a macrophage phagocytosing an IgM_h-opsonized CA from different points of view. The sequence was performed after the 3D reconstruction from images obtained by confocal microscopy. Phalloidin (red), fluorescent labeled α -IgM_h (green), and Hoechst (blue). (D) The same procedure was used to obtain a sequence of images showing an IgM_h-opsonized CA that has been phagocytosed by a macrophage. (E) SEM images also showed macrophages engulfing IgM_h-opsonized CA. Some filopodia were found emerging from macrophages and making contact with the bodies (Insets). (F) Macrophage making contact with a non IgM_h-opsonized CA (Left) and a non IgM_h-opsonized CA phagocytosed by a macrophage (Right); PAS staining. These results indicate that IgM_h opsonization of CA is not a requirement for phagocytosis by THP-1-derived macrophages. (G) CA from CSF become stained with fluorochrome-labeled Con A, which suggests that they contain mannose. (H) CA (stained with Con A, green), encircled by THP-1-derived macrophages immunostained with α -CD206 (mannose receptor, red) and Hoechst (nuclei, blue). Orthogonal views show macrophages attached to the CA. These results suggest that, in the case of THP-1-derived macrophages and with the conditions set up in the present study, CA phagocytosis is produced via the mannose receptor.

CA are formed by waste elements included in a polyglucosan structure and their presence in the CSF reveals that they may act as waste containers removing brain products from the brain to the CSF. In addition, their presence in the deep cervical lymph nodes supports the hypothesis that they can leave CSF via the meningeal lymphatic vessels and reach these nodes. As shown, the staining properties of the CA found in the cervical nodes indicate that they are compatible with those described in the CSF, and their localization in the trabecular sinuses but not in the parenchyma suggests that they are not generated in the nodes themselves. In addition, the gradient in the number of CA observed in the nodes related to their proximity to the brain also suggests that they arrive there from the CSF. As there are other structures apart from the brain that generate CA, the possibility that the CA contained in the cervical nodes come from some of these other structures must be considered. If this were the case, then: 1) these structures must generate CA that become stained with PAS and immunostained with natural IgMs; 2) these structures must expel the CA directly or indirectly into the lymph; and 3) the lymph generated must drain toward the cervical lymph nodes sited in the regions I, II, III, and IV of the neck. To our knowledge, the brain is the only structure that fulfills the 3 premises indicated. Structures or organs like mammary glands, cardiac muscle, or prostate can be ruled out, because the lymph of these structures does not drain toward the cervical lymph nodes. On the other hand, CA originating in the thyroid gland and prostate are calcified structures formed (in the case of prostate) by a calcified protein matrix (34), and thus are incompatible with the CA that we described in the cervical lymph nodes. This is also the case of calculi originating in the salivary gland, which are formed by hydroxyapatite (34).

Although it might be thought that the presence of CA in the CSF is merely circumstantial, there are certain indices that suggest that this presence is the result of some specific physiological processes. The localization of CA mainly in the periventricular and subpial regions of the brain does not seem to be casual. Moreover, as can be observed in [Movie S1](#) (adapted from ref. 5), some CA contain a central compact core with a high presence of ubiquitin and a peripheral region which contains GS, p62, and ubiquitin. The central core may correspond to a region where different ubiquitinated waste substances have accumulated, while the peripheral region may correspond to an active zone where the waste elements are collected by p62 and packaged by GS, which generates the polyglucosan component of the CA (5). In addition, the presence in CA of neoepitopes that are recognized by plasmatic natural IgMs suggested that they may be structures ready to be phagocytosed by macrophages or other immune cells if they were released from the brain (6, 8). Correspondingly, and as shown here, the CA present in the cervical lymph nodes were seen adhered to elongated cells compatible with macrophages, and CA were avidly phagocytosed by THP-1-derived macrophages. Taken together, these results extend the hypothesis proposed in Augé et al. (6), according to which CA collect residual substances and are removed from the brain and then eliminated via the immune system. Fig. 6 summarizes this route, updating the scheme proposed in 2017. The pathway begins in the astrocytes which generate CA to create a kind of waste container formed by polyglucosan aggregates that amass waste products originating not only in the astrocytes themselves, but also deriving from neighboring cells. Aging and neurodegenerative conditions increase the production of waste products, thus enhancing the process. After their release into the CSF, CA reach the cervical lymph nodes via the meningeal lymphatic vessels and the subsequent lymphatic vessels. There, mannose contained in CA can trigger the phagocytosis via mannose receptors sited on macrophages, although we do not rule out other possible mechanisms including the IgM-Fc μ R, the IgM-complement pathways, and the lectin pathway mediated by the C3b opsonization induced by mannose-binding

lectin (MBL). In any case, the immune system may provide redundant mechanisms to ensure the elimination of CA.

Due to the blood–brain barrier and the cerebrospinal fluid–brain barrier, the brain used to be considered an immune-privileged organ until the discovery of the meningeal lymphatic system. This system collects brain substances contained in the CSF, and the presence of specific brain components outside the brain can interact with the immune system with possibly fatal consequences (35, 36). It has been reported that cellular and soluble constituents of the CSF cause immune responses in the cervical lymph nodes (18), and the possible immunological implications of CSF drainage via the meningeal lymphatic system were also noted long ago by Bradbury et al. (37). In this regard, Weller et al. (21) indicated that “the lymphatic drainage of ISF and CSF and the specialized cervical lymph nodes to which they drain play significant roles in the induction of immunological tolerance and of adaptive immunological responses in the central nervous system (CNS)”. Accordingly, and given that the results of the present study indicate that CA reach the cervical lymph nodes, we cannot rule out the possibility that, in certain circumstances, the waste substances contained in CA may enhance certain immunological functions or intervene in some autoimmune alterations. Consequently, and given their possible clinical implications, the possible role of CA in immunological processes or brain autoimmune diseases needs to be investigated.

Our findings may also represent a starting point for the study of some clinical markers of brain disorders. We know that CA can contain waste substances produced in the brain and several of them may be markers of some of these disorders. We also know that CA are present in both noncentrifuged samples of CSF and pellets obtained from CSF centrifugation, and so these structures are easily accessible for study. In recent decades, the liquid fraction of the CSF has been exhaustively assessed in order to obtain brain markers. For instance, it is well established that phospho-tau181, total-tau, and amyloid β 1–42 are CSF biomarkers for Alzheimer’s disease (38). Moreover, promising new fluid biomarkers for staging and monitoring of frontotemporal dementia, such as the neurofilament light chain, are emerging (39, 40). Furthermore, CSF analysis is used to exclude other diseases in the differential diagnosis of multiple sclerosis (41). In addition, CSF biomarkers are being studied in patients with Parkinson’s and are being used in clinical trials (42). However, the solid fraction of the CSF has not been studied to obtain brain markers. Our results support the need to study CA contained in the CSF, postulating that these bodies will contain some of these markers. As CA from CSF are more accessible than those from brain tissue, their use for diagnostic purposes may become a valuable new strategy.

To sum up, our results indicate that CA can act as waste containers that allow the removal of waste products from the brain and suggest their involvement in a mechanism that cleans the brain. Moreover, we hypothesize a role for CA in some autoimmune brain diseases, exporting brain substances that interact with the immune system, and we suggest that they may be important elements in the diagnosis of certain brain diseases, since they may contain markers of brain disease.

Methods

Human CSF Samples. Postmortem CSF samples from 16 cases of neuropathologically affected patients (65 to 90 y old) were obtained from the Banc de Teixits Neurològics (Biobanc-Hospital Clínic-IDIBAPS, Barcelona). Noncentrifuged samples ($n = 7$) as well as pellets obtained after centrifugation at $4,000 \times g$ at 4°C for 10 min ($n = 9$) were used. Medical data on these cases are detailed in [SI Appendix, Table S1](#).

Human Deep Cervical Lymph Node Samples. Paraffin sections (thickness of $8\ \mu\text{m}$) of cervical lymph nodes taken by lymphadenectomy from 4 cancer patients (83 to 96 y old) were obtained from the Banc de Tumors i Anatomia Patològica (Biobanc-Hospital Clínic-IDIBAPS, Barcelona). All selected nodes

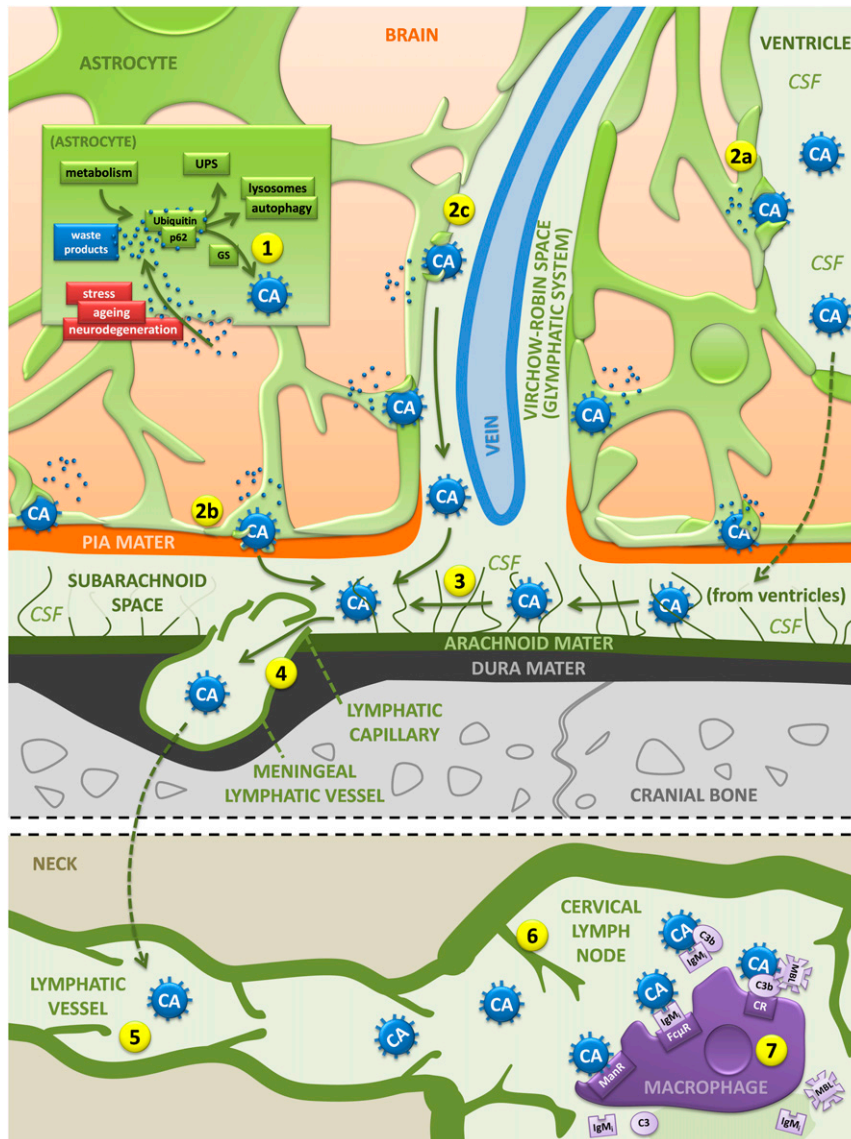


Fig. 6. Hypothesized pathway of the elimination of brain waste products based on the role of CA as waste containers. The pathway begins in the astrocytes, which generate CA building a kind of waste container formed by polyglucosan aggregates that amass waste products originated not only in the astrocytes themselves, but also derived from neighboring cells (1). CA are then released into the CSF in the ventricular region or subarachnoid space (2a and 2b) or via the glymphatic system (2c). From there (3), CA enter the meningeal lymphatic vessels (4) and the subsequent lymphatic vessels (5) and reach the cervical lymph nodes (6). There, macrophages can phagocytose CA via mannose and mannose receptors or via other possible mechanisms that might include the IgM-Fc μ R, the IgM-complement pathways, and the lectin pathway mediated by the C3b opsonization induced by MBL and C3b receptors (7). C3, C3b component of the complement system; C3b, C3b fragment generated from C3; CR, C3b receptor; ManR, mannose receptor; UPS, ubiquitin–proteasome system. (See text for details.)

were nontumor affected. Medical data on these cases are detailed in *S1 Appendix, Table S2*.

All procedures involving human samples were performed in accordance with appropriate guidelines and regulations. All experiments involving human tissue were approved by the Bioethical Committee of the University of Barcelona.

Cell Culture and Differentiation. THP-1 cells provided by ATCC were cultured as previously described (43). Cells were subcultured at a density of 5×10^4 cells/cm² on 24-well clusters with 12-mm round cover glasses. Cells were differentiated to macrophages with phorbol 12-myristate 13-acetate (PMA; Sigma-Aldrich) at a concentration of 100 nmol/L in RPMI 1640 (Sigma-Aldrich) supplemented with 10% heat-inactivated FBS (GE Healthcare Life Sciences), 50 μ M β -mercaptoethanol (Sigma-Aldrich), and penicillin (100 U/mL)/streptomycin (100 μ g/mL) (Life Technologies) for 3 d. Differentiation of PMA-treated cells was enhanced after the initial 3-d stimulus by removing the PMA-containing media and then incubating the cells in fresh supplemented RPMI 1640 for a further 3 d.

Phagocytosis Studies. To study the phagocytosis of CA by macrophages, we first obtained CA from CSF and opsonized them with IgMs. CA were obtained from CSF samples completing 5 centrifugations of CSF at $700 \times g$ for 10 min, discarding the supernatants, and resuspending the pellets with 500 μ L of PBS. Thereafter, another centrifugation at $700 \times g$ for 10 min was performed, but the resuspension was obtained with 500 μ L of PBS containing IgM_h (1:10 dilution; OBT1524; AbD Serotec). The resuspension was maintained overnight at 4 $^{\circ}$ C to obtain the IgM-opsonized CA. Controls were performed with PBS without IgMs. Thereafter, another centrifugation at $700 \times g$ for 10 min was performed, and the pellet was resuspended with 1,000 μ L of supplemented RPMI. The samples of 1,000 μ L were then added to the wells containing the THP-1-derived macrophages after removing their media.

Antibodies and Reagents. The following antibodies were used as primary antibodies: human IgM purified immunoglobulins (1:10 dilution; OBT1524; AbD Serotec), rabbit monoclonal IgG against GS (1:100; 15B1; Cell Signaling), IgMs contained as a contaminant in the OX52 antibody (obtained from mouse

ascites), rabbit polyclonal IgG against mannose receptor CD206 (1:1,200; ab64693, Abcam), mouse monoclonal IgG₁ against CD35 (1:40; E11; Thermo Scientific), and mouse monoclonal IgG₁ against Fc μ R (1:150; OT1E6; Thermo Scientific).

The following antibodies were used as secondary antibodies: Alexa Fluor (AF) 488 goat anti-human IgM heavy chain (1:200; A-21215; Life Technologies), AF488 goat anti-mouse IgM μ chain specific (1:250; 115-545-075; Jackson ImmunoResearch Laboratories), AF555 donkey anti-rabbit IgG directed against both heavy and light chains (1:250; A-31572; Life Technologies), and AF555 goat anti-mouse IgG₁ (1:250; A-21125; Life Technologies).

Fluorescein-labeled Con A (Vector Laboratories) was incubated overnight instead of primary antibodies in some immunohistochemical experiments in order to detect CA.

Tetramethyl rhodamine-isothiocyanate (TRITC)-phalloidin (Sigma-Aldrich) was used to stain F-actin from macrophages. This staining was combined with the immunohistochemical procedures and was performed by adding TRITC-phalloidin (1:500) to the secondary antibodies.

Immunofluorescence. Volumes of 40 μ L of noncentrifuged CSF or 40 μ L of resuspended CSF pellets (centrifuged 6 times at 700 \times g for 10 min and resuspended each time with PBS) were extended in slides and air dried. They were then fixed with acetone for 10 min at 4 $^{\circ}$ C to carry out the immunohistochemistry. For lymph node samples, sections were deparaffinized in xylene and an antigen retrieval step was applied with 10 mM sodium citrate buffer (pH = 6.0) heated to 100 $^{\circ}$ C for 40 min. For the cell culture, macrophages were washed with Dulbecco's PBS (DPBS; GIBCO) and fixed in 4% paraformaldehyde in PBS for 15 min.

Immunofluorescence was performed as follows: samples were rehydrated with PBS and then blocked and permeabilized with 1% BSA in PBS (Sigma-Aldrich) (blocking buffer [BB]) with 0.1% Triton X-100 (Sigma-Aldrich) for 20 min. They were then washed with PBS and incubated with the primary antibody overnight at 4 $^{\circ}$ C. Next, samples were washed and incubated for 1 h at room temperature with the secondary antibody. Nuclear staining was performed with Hoechst (2 μ g/mL, H-33258, Fluka) and samples were washed and coverslipped with Fluoromount (Electron Microscopy Sciences) or ProLong Gold (Thermo Scientific). Staining controls were performed by incubating with BB instead of the primary antibody. In double staining, controls for cross-reactivity of the antibodies were also performed.

PAS Staining. All samples were processed as described in the immunohistochemistry section, except for the macrophage cell culture, in which cells were only washed with DPBS. Then, samples were stained with PAS according to the standard procedure. Briefly, samples were fixed for 10 min in Carnoy's solution (60% ethanol, 30% chloroform, and 10% glacial acetic acid). Thereafter, the samples were pretreated for 10 min with 0.25% periodic acid (19324-50, Electron Microscopy Sciences) in distilled water followed by a washing step for 3 min. Then, the samples were immersed in Schiff's reagent (26052-06, Electron Microscopy Sciences) for 10 min. After Schiff's reagent, samples were washed for 5 min in distilled water. Nuclei were counterstained for 6 min with a hematoxylin solution according to Mayer (3870, J. T. Baker). Then, the samples were washed, dehydrated to xylene, and coverslipped with a quick mounting medium (Eukitt, Fluka Analytical).

Sample Processing for Transmission Electron Microscopy. CSF samples were postfixed for 1 h using 4% paraformaldehyde and 0.1% glutaraldehyde in phosphate buffer (PB) 0.1 M. Next, samples were centrifuged at 700 \times g for 10

min and washed 4 times with PB 0.1 M for 10 min. Then, they were stained with 1% OsO₄ in PB and containing 0.8% potassium ferricyanide for 1 h at 4 $^{\circ}$ C, dehydrated in acetone at 4 $^{\circ}$ C, and finally embedded in Spurr resin. The resin was polymerized for 48 h at 80 $^{\circ}$ C. Semithin sections (1- μ m thickness) were obtained and, after methylene blue staining, CA were localized. Ultrathin sections (70-nm thickness) were obtained using an ultramicrotome (Leica Ultracut) and a diamond knife (Diatome), and the sections were then placed on copper grids and poststained with uranyl acetate and lead citrate.

Sample Processing for Scanning Electron Microscopy. CSF samples and macrophages were postfixed using 2.5% glutaraldehyde in PB 0.1 M. Next, they were washed 3 times with PB 0.1 M for 10 min. Then, samples were stained with 1% OsO₄ in PB and containing 0.8% potassium ferricyanide for 1 h 30 min at 4 $^{\circ}$ C and dehydrated in alcohols at 4 $^{\circ}$ C. Next, they were processed either via critical point drying or air drying with hexamethyldisilazane. Finally, they were mounted and sputter coated (carbon or gold).

Image Acquisition and Processing. Images were captured with a fluorescence laser in an optical microscope (BX41, Olympus) and stored in TIFF format. All of the images were acquired using the same microscope, laser, and software settings. Exposure time was adapted to each staining, but the respective control images were acquired with the same exposure time. Image analysis and treatment were performed using the ImageJ program (NIH). Images that were modified for contrast and brightness to enhance their visualization were processed in the same way as the images corresponding to their respective controls.

In order to study the CA on cell cultures, image stacks were taken with a confocal laser scanning microscope (LSM 880, Zeiss) and 3D animations were obtained by means of the ImageJ program (NIH).

Ultrathin sections were examined using a JEOL JEM-1010 transmission electron microscope operated at an accelerating voltage of 80 kV. The images were obtained using a CCD Orius camera (Gatan).

SEM images were observed using a JEOL JSM-7001F scanning electron microscope.

Statistical Analysis. Statistical analysis was performed with the ANOVA module of the IBM SPSS Statistics (IBM). Significant differences were considered when $P < 0.05$.

Data Availability Statement. All data are available in the manuscript and supporting information.

ACKNOWLEDGMENTS. This study was funded by grant BFU2016-78398-P awarded by the Spanish Ministerio de Economía y Competitividad, by Agencia Estatal de Investigación, and by Fondo Europeo de Desarrollo Regional. We thank the Generalitat de Catalunya for funding our research group (2017/SGR625) and for awarding a predoctoral fellowship to M.R. (Ajuts per contractar personal investigador novell, Direcció General de Recerca, 2019). We thank Eva Prats and Josep Manel Rebled from Unitat de Microscòpia Electrònica (Centres Científics i Tecnològics, Universitat de Barcelona) for their professional advice and help. We are sincerely grateful to Elisenda Coll and Maria Calvo, from the Servei de Microscòpia Confocal (Centres Científics i Tecnològics, Universitat de Barcelona) for their help and availability. We are indebted to the Biobanc-Hospital Clinic-Institut d'Investigacions Biomèdiques August Pi i Sunyer (IDIBAPS), integrated in the Spanish National Biobank Network, for samples and data procurement. We are sincerely grateful to Michael Maudsley for correcting the English version of the manuscript.

- G. Catola, N. Achúcarro, Über die Entstehung de Amyloidkörperchen in Zentralnervensystem. *Virchows Arch. f. Path. Anat.* **184**, 454-469 (1906).
- R. Virchow, Ueber eine Gehirn und Rückenmark des Menschen aufgefundenene Substanz mit der chemischen Reaction der Cellulose. *Arch. Pathol. Anat. Physiol. Klin. Med.* **6**, 135-138 (1854).
- J. B. Cavanagh, Corpora-amyloidea and the family of polyglucosan diseases. *Brain Res. Brain Res. Rev.* **29**, 265-295 (1999).
- M. Sakai, J. Austin, F. Witmer, L. Trueb, Studies of corpora amyloidea. I. Isolation and preliminary characterization by chemical and histochemical techniques. *Arch. Neurol.* **21**, 526-544 (1969).
- E. Augé, J. Duran, J. J. Guinovart, C. Pelegrí, J. Vilaplana, Exploring the elusive composition of corpora amyloidea of human brain. *Sci. Rep.* **8**, 13525 (2018).
- E. Augé, I. Cabezón, C. Pelegrí, J. Vilaplana, New perspectives on corpora amyloidea in the human brain. *Sci. Rep.* **7**, 41807 (2017).
- A. Sbarbati, M. Carner, V. Colletti, F. Osculati, Extrusion of corpora amyloidea from the marginal glia at the vestibular root entry zone. *J. Neuropathol. Exp. Neurol.* **55**, 196-201 (1996).
- E. Augé et al., Corpora amyloidea in human hippocampal brain tissue are intracellular bodies that exhibit a homogeneous distribution of neo-epitopes. *Sci. Rep.* **9**, 2063 (2019).
- S. Cissé, H. M. Schipper, Experimental induction of corpora amyloidea-like inclusions in rat astroglia. *Neuropathol. Appl. Neurobiol.* **21**, 423-431 (1995).
- H. M. Schipper, S. Cissé, Mitochondrial constituents of corpora amyloidea and autofluorescent astrocytic inclusions in senescent human brain. *Glia* **14**, 55-64 (1995).
- K. Selmaj et al., Corpora amyloidea from multiple sclerosis brain tissue consists of aggregated neuronal cells. *Acta Biochim. Pol.* **55**, 43-49 (2008).
- S. Cissé, G. Lacoste-Royal, J. Laperrière, T. Cabana, D. Gauvreau, Ubiquitin is a component of polypeptides purified from corpora amyloidea of aged human brain. *Neurochem. Res.* **16**, 429-433 (1991).
- N. A. Jessen, A. S. Munk, I. Lundgaard, M. Nedergaard, The glymphatic system: A beginner's guide. *Neurochem. Res.* **40**, 2583-2599 (2015).
- D. Pirici, C. Margaritescu, Corpora amyloidea in aging brain and age-related brain disorders. *J. Aging Gerontol.* **2**, 33-57 (2014).
- F. Bucchieri, F. Farina, G. Zummo, F. Cappello, Lymphatic vessels of the dura mater: A new discovery? *J. Anat.* **227**, 702-703 (2015).
- M. Földi et al., New contributions to the anatomical connections of the brain and the lymphatic system. *Acta Anat. (Basel)* **64**, 498-505 (1966).

17. M. Johnston, A. Zakharov, C. Papaiconomou, G. Salmasi, D. Armstrong, Evidence of connections between cerebrospinal fluid and nasal lymphatic vessels in humans, non-human primates and other mammalian species. *Cerebrospinal Fluid Res.* **1**, 2 (2004).
18. A. Louveau *et al.*, Structural and functional features of central nervous system lymphatic vessels. *Nature* **523**, 337–341 (2015).
19. A. Louveau *et al.*, Understanding the functions and relationships of the glymphatic system and meningeal lymphatics. *J. Clin. Invest.* **127**, 3210–3219 (2017).
20. S. K. Ha, G. Nair, M. Absinta, N. J. Luciano, D. S. Reich, Magnetic resonance imaging and histopathological visualization of human dural lymphatic vessels. *Bio Protoc.* **8**, 1–17 (2018).
21. R. O. Weller, I. Galea, R. O. Carare, A. Minagar, Pathophysiology of the lymphatic drainage of the central nervous system: Implications for pathogenesis and therapy of multiple sclerosis. *Pathophysiology* **17**, 295–306 (2010).
22. M. D. Sweeney, B. V. Zlokovic, A lymphatic waste-disposal system implicated in Alzheimer's disease. *Nature* **560**, 172–174 (2018).
23. L. Sakka, G. Coll, J. Chazal, Anatomy and physiology of cerebrospinal fluid. *Eur. Ann. Otorhinolaryngol. Head Neck Dis.* **128**, 309–316 (2011).
24. C. Grönwall, J. Vas, G. J. Silverman, Protective roles of natural IgM antibodies. *Front. Immunol.* **3**, 66 (2012).
25. S. Brändlein *et al.*, Natural IgM antibodies and immunosurveillance mechanisms against epithelial cancer cells in humans. *Cancer Res.* **63**, 7995–8005 (2003).
26. H. P. Vollmers, S. Brändlein, Natural IgM antibodies: The orphaned molecules in immune surveillance. *Adv. Drug Deliv. Rev.* **58**, 755–765 (2006).
27. A. Goldin, J. A. Beckman, A. M. Schmidt, M. A. Creager, Advanced glycation end products: Sparking the development of diabetic vascular injury. *Circulation* **114**, 597–605 (2006).
28. B. A. Cobb, D. L. Kasper, Coming of age: Carbohydrates and immunity. *Eur. J. Immunol.* **35**, 352–356 (2005).
29. A. Suzuki *et al.*, Phagocytized corpora amylacea as a histological hallmark of astrocytic injury in neuromyelitis optica. *Neuropathology* **32**, 587–594 (2012).
30. G. Manich *et al.*, Presence of a neo-epitope and absence of amyloid beta and tau protein in degenerative hippocampal granules of aged mice. *Age (Dordr.)* **36**, 151–165 (2014).
31. H. Rouvière, A. Delmas, *Anatomie Humaine. Descriptive, Topographique, Fonctionnelle* (Masson et Cie, Paris, France, ed. 12, 1985), pp. 244–248.
32. Y. Chen, Y. B. Park, E. Patel, G. J. Silverman, IgM antibodies to apoptosis-associated determinants recruit C1q and enhance dendritic cell phagocytosis of apoptotic cells. *J. Immunol.* **182**, 6031–6043 (2009).
33. H. M. Liu, K. Anderson, B. Caterson, Demonstration of a keratan sulfate proteoglycan and a mannose-rich glycoconjugate in corpora amylacea of the brain by immunocytochemical and lectin-binding methods. *J. Neuroimmunol.* **14**, 49–60 (1987).
34. K. S. Sfanas, B. A. Wilson, A. M. De Marzo, W. B. Isaacs, Acute inflammatory proteins constitute the organic matrix of prostatic corpora amylacea and calculi in men with prostate cancer. *Proc. Natl. Acad. Sci. U.S.A.* **106**, 3443–3448 (2009).
35. A. G. Baxter, The origin and application of experimental autoimmune encephalomyelitis. *Nat. Rev. Immunol.* **7**, 904–912 (2007).
36. R. Gold, C. Lington, H. Lassmann, Understanding pathogenesis and therapy of multiple sclerosis via animal models: 70 years of merits and culprits in experimental autoimmune encephalomyelitis research. *Brain* **129**, 1953–1971 (2006).
37. M. W. Bradbury, H. F. Cserr, R. J. Westrop, Drainage of cerebral interstitial fluid into deep cervical lymph of the rabbit. *Am. J. Physiol.* **240**, F329–F336 (1981).
38. B. Olsson *et al.*, CSF and blood biomarkers for the diagnosis of Alzheimer's disease: A systematic review and meta-analysis. *Lancet Neurol.* **15**, 673–684 (2016).
39. L. H. Meeter *et al.*, Neurofilament light chain: A biomarker for genetic frontotemporal dementia. *Ann. Clin. Transl. Neurol.* **3**, 623–636 (2016).
40. L. H. Meeter, L. D. Kaat, J. D. Rohrer, J. C. van Swieten, Imaging and fluid biomarkers in frontotemporal dementia. *Nat. Rev. Neurol.* **13**, 406–419 (2017).
41. M. Stangel *et al.*, The utility of cerebrospinal fluid analysis in patients with multiple sclerosis. *Nat. Rev. Neurol.* **9**, 267–276 (2013).
42. A. Lleó *et al.*, Cerebrospinal fluid biomarkers in trials for Alzheimer and Parkinson diseases. *Nat. Rev. Neurol.* **11**, 41–55 (2015).
43. V. Martínez *et al.*, Establishment of an in vitro photoassay using THP-1 cells and IL-8 to discriminate phototoxicants from photoallergens. *Toxicol. In Vitro* **27**, 1920–1927 (2013).

2. ARTICLE 2

***CORPORA AMYLACEA* IN THE HUMAN BRAIN EXHIBIT NEOEPITOPES OF A
CARBOHYDRATE NATURE**

Marta Riba, Elisabet Augé, Iraidá Tena, Jaume del Valle, Laura Molina-Porcel, Teresa Ximelis, Jordi Vilaplana, Carme Pelegrí

Frontiers in Immunology 2021, 12, 618193

DOI: [10.3389/fimmu.2021.618193](https://doi.org/10.3389/fimmu.2021.618193)

JCR 2020 IF: 7,561

RESUM

Antecedents: Els estudis realitzats en CA d'hipocamp i de LCR han revelat la presència de NE d'origen desconegut en aquestes estructures, els quals són reconeguts per IgM naturals. S'ha postulat que aquest reconeixement podria afavorir la fagocitosi i eliminació dels CA mitjançant processos d'immunitat innata.

Objectiu: El present treball pretén determinar la naturalesa dels NE presents en els CA del SNC, els quals són reconeguts per IgM naturals i podrien intervenir en la fagocitosi i l'eliminació dels CA.

Material i mètodes: Per tal de determinar la possible naturalesa glucídica dels NE es van utilitzar seccions criostàtiques d'hipocamp humà de 4 pacients amb malalties neurodegeneratives (85-91 anys) i 2 pacients sense associació a malalties neurodegeneratives (70-86 anys) i es van realitzar estudis de preadsorció de les IgM amb concentracions creixents de monosacàrids específics per tal de determinar si la preadsorció produïa una inhibició parcial o total del marcatge dels NE dels CA amb les IgM. Com a control positiu de preadsorció, es van realitzar els mateixos procediments utilitzant la lectina ConA conjugada amb fluorescència, la qual reconeix carbohidrats complexos especialment si tenen una elevada composició de Man, i com a control negatiu de la preadsorció es va usar un anticòs dirigit contra la proteïna p62 que, pel fet d'anar dirigit contra una estructura proteica, no havia de ser interferit per la preadsorció amb sucres. Primerament, es van preparar dilucions de 0 (control), 50, 100, 200 i 400 mM de cadascun dels següents monosacàrids: Glc, Man, fructosa (Fru), galactosa (Gal), N-acetilglucosamina (GlcNAc) i N-acetilgalactosamina (GalNAc). En alguns casos també es va preparar una dilució de 800 mM. La preadsorció es va dur a terme afegint IgM, ConA o l'anticòs dirigit contra p62 a les dilucions de monosacàrid preparades i aquestes es van mantenir *overnight* en agitació. Seguidament, les dilucions de monosacàrid amb IgM, ConA o l'anticòs contra p62 van ser incubades en diferents seccions d'hipocamp i es va procedir amb estudis d'immunofluorescència. Es van obtenir imatges mitjançant microscòpia de fluorescència i es va quantificar la intensitat de fluorescència dels CA en els diferents talls i diferents condicions amb el programa FIJI. Posteriorment, es va dur a terme l'anàlisi estadístic de les dades utilitzant el test ANOVA i el test de Scheffe per comparacions *post hoc*. D'altra banda, per tal de determinar si els NE tenien naturalesa proteica o glucoproteica es van utilitzar mostres *post-mortem* de LCR ventricular de tres casos de malalties neurodegeneratives (65-92 anys) i es van realitzar estudis d'immunofluorescència incubant prèviament les mostres amb pepsina, un enzim que degrada proteïnes. Les mostres control van ser incubades amb solució tampó de fosfats en lloc de l'enzim. S'entenia que si els NE tenien naturalesa proteica o glucoproteica el marcatge dels NE amb les IgM desapareixeria. Com a control positiu de la digestió amb pepsina es va usar el marcatge amb l'anticòs contra la proteïna p62 i la sonda de marcatge proteic N-hidroxisuccinimida (NHS) èster conjugada amb fluorescència, i per tal de verificar que la

digestió amb pepsina no alterava directament l'estructura glucídica es va fer també el marcatge amb ConA conjugada amb fluorescència.

Resultats: Pel que fa als estudis de preadsorció amb sucres es va observar que, tal i com era predictable, les concentracions creixents dels monosacàrids Glc, Man, Fru i NAcGlu donaven lloc a una disminució del marcatge dels CA amb aquesta ConA, però que aquesta disminució no era visible amb la preadsorció amb la Gal ni l'NAcGal, ja que aquests dos monosacàrids no interfereixen amb la zona d'unió de la ConA amb l'estructura de carbohidrat. D'altra banda, i també com era d'esperar, el marcatge de la proteïna p62 dels CA mitjançant l'anticòs dirigit contra aquesta proteïna no es va veure interferit per cap dels monosacàrids estudiats. En relació a la preadsorció de les IgM, tots els monosacàrids testats van interferir en el marcatge dels NE dels CA en més o menys mesura. Concretament, la Glc va ser el monosacàrid que més va disminuir el marcatge dels NE dels CA amb IgM. Pel que fa a les digestions amb pepsina, les mostres de CA que van ser incubades amb l'enzim no van mostrar marcatge de p62 ni NHS ester, el que va confirmar la digestió de les proteïnes contingudes en els CA. En canvi, sí que es va observar marcatge de ConA en els CA digerits amb pepsina, el que confirmava que l'estructura glucídica dels CA quedava inalterada. De la mateixa manera que la ConA, el marcatge dels NE dels CA amb IgM no es va mostrar afectat per la digestió proteica, fet que feia descartar la naturalesa peptídica o glucopeptídica dels NE.

Conclusions: La disminució del marcatge dels CA amb ConA causada per les concentracions creixents de monosacàrids demostra que la preadsorció amb sucres és un mètode fiable per avaluar la interacció basada en el reconeixement de glúcids. A més a més, el manteniment del marcatge dels CA amb l'anticòs dirigit contra p62 tot i la preadsorció de l'anticòs amb els monosacàrids confirma que el marcatge dels CA amb anticossos dirigits contra proteïnes no es veu afectat per la presència de monosacàrids. Pel que fa a la preadsorció de les IgM amb sucres, la disminució del marcatge dels NE dels CA amb IgM amb concentracions creixents de monosacàrids, particularment amb Glc, indica que aquestes IgM reconeixen sucres, fet que suggereix que els NE dels CA són de naturalesa glucídica. D'altra banda, la interacció de les IgM, amb els monosacàrids estudiats planteja un possible efecte de la glicèmia en la reactivitat de les IgM, i per extensió, en la immunitat mediada per aquests anticossos. En referència a les digestions amb pepsina, la conservació del marcatge dels NE dels CA amb les IgM tot i la digestió proteica, descarta que els NE siguin d'origen peptídic o glucopeptídic. D'aquesta manera, el conjunt de resultats obtinguts fonamenta la naturalesa glucídica dels NE reconeguts per IgM presents en els CA. Amb tot això, globalment, la presència de NE glucídics en els CA, que són reconeguts per IgM, concorda amb la funció d'alguns glicans com a senyals *eat-me*, els quals indueixen processos fagocítics per part de macròfags.



Corpora Amylacea in the Human Brain Exhibit Neopeptides of a Carbohydrate Nature

Marta Riba^{1,2,3†}, Elisabet Augé^{1,2,3†}, Iraida Tena¹, Jaume del Valle^{1,2,3},
Laura Molina-Porcel^{4,5}, Teresa Ximelis^{4,5}, Jordi Vilaplana^{1,2,3*‡} and Carme Pelegrí^{1,2,3‡}

¹ Secció de Fisiologia, Departament de Bioquímica i Fisiologia, Universitat de Barcelona, Barcelona, Spain, ² Institut de Neurociències, Universitat de Barcelona, Barcelona, Spain, ³ Centres de Biomedicina en Red de Enfermedades Neurodegenerativas (CIBERNED), Madrid, Spain, ⁴ Alzheimer's Disease and Other Cognitive Disorders Unit, Neurology Service, Hospital Clínic, Institut d'Investigacions Biomèdiques August Pi i Sunyer (IDIBAPS), Universitat de Barcelona, Barcelona, Spain, ⁵ Neurological Tissue Bank, Biobanc-Hospital Clínic-IDIBAPS, Barcelona, Spain

OPEN ACCESS

Edited by:

Hans-Peter Hartung,
Heinrich Heine University of
Düsseldorf, Germany

Reviewed by:

Todd Cohen,
University of North Carolina at
Chapel Hill, United States
Or Kakhlon,
Hadassah Medical Center, Israel

*Correspondence:

Jordi Vilaplana
vilaplana@ub.edu

[†]These authors have contributed
equally to this work

[‡]These authors have contributed
equally to this work

Specialty section:

This article was submitted to
Multiple Sclerosis and
Neuroimmunology,
a section of the journal
Frontiers in Immunology

Received: 11 November 2020

Accepted: 10 June 2021

Published: 28 June 2021

Citation:

Riba M, Augé E, Tena I, del Valle J,
Molina-Porcel L, Ximelis T, Vilaplana J
and Pelegrí C (2021) Corpora
Amylacea in the Human Brain
Exhibit Neopeptides of a
Carbohydrate Nature.
Front. Immunol. 12:618193.
doi: 10.3389/fimmu.2021.618193

Corpora amylacea (CA) in the human brain are polyglucosan bodies that accumulate residual substances originated from aging and both neurodegenerative and infectious processes. These structures, which act as waste containers, are released from the brain to the cerebrospinal fluid, reach the cervical lymph nodes *via* the meningeal lymphatic system and may be phagocytosed by macrophages. Recent studies indicate that CA present certain neopeptides (NEs) that can be recognized by natural antibodies of the IgM class, and although evidence of different kinds suggests that these NEs may be formed by carbohydrate structures, their precise nature is unknown. Here, we adapted standard techniques to examine this question. We observed that the preadsorption of IgMs with specific carbohydrates has inhibitory effects on the interaction between IgMs and CA, and found that the digestion of CA proteins had no effect on this interaction. These findings point to the carbohydrate nature of the NEs located in CA. Moreover, the present study indicates that, *in vitro*, the binding between certain natural IgMs and certain epitopes may be disrupted by certain monosaccharides. We wonder, therefore, whether these inhibitions may also occur *in vivo*. Further studies should now be carried out to assess the possible *in vivo* effect of glycemia on the reactivity of natural IgMs and, by extension, on natural immunity.

Keywords: neoantigen, neopeptide, immunoglobulin M, natural antibodies, corpora amylacea, brain aging, hyperglycemia, diabetes

INTRODUCTION

Corpora amylacea (CA) in the human brain are polyglucosan aggregates that were first described by J.E. Purkinje in 1837 (1). They are intracellular astrocytic bodies that accumulate mainly in the periventricular and subpial regions of the aged brain (2–4), but are also present in large numbers in specific areas of the brain in neurodegenerative conditions (5–8). Different studies postulate that the function of CA is to entrap residual products derived from aging or degenerative processes (2, 4, 9–12). Accordingly, while essentially constituted of polymerized hexoses (2, 3),

with glucose the predominant one (3), a wide range of components have been attributed to CA. These products are mainly derived from neurons, astrocytes, oligodendrocytes or the blood (8, 12–17), or even related to viral, fungal or microbial infections (18–20). However, the presence of some of these components remain controversial (10, 21). In 2017, we reported that some positive immunostainings described in CA may have been induced by contaminant immunoglobulins M (IgMs) present in commercial antibodies, giving rise to false positive results (10). Later, in 2018, we reviewed and ruled out some of the components that have been reported to occur in CA. We observed that CA contain glycogen synthase (GS), which is presumed to take part in the formation of the polyglucosan structure, as well as ubiquitin and p62 proteins, which are both involved in the processing of waste products (21). Recently, an immunofluorescence study, which excluded the possible false positive staining caused by IgMs, reported that CA contain tau protein (22). The possible role of CA in trapping residual products is also supported by electron microscopy studies, which have described some cell debris inside the CA, including impaired mitochondria and lysosome-like vesicles, originating from degenerative processes (9, 12, 23). Moreover, we recently revealed that CA are released from the brain into the cerebrospinal fluid (CSF), reaching the cervical lymph nodes *via* the meningeal lymphatic system, and we observed that CA can be phagocytosed by macrophages *in vitro*. All these findings indicate that CA can act as containers that remove waste products from the brain (24).

CA share some features with a type of polyglucosan bodies, referred to as PAS granules, which appear in the mouse brain. Both, PAS granules and CA, are round or oval shaped and have a high polysaccharide content, and therefore become positively stained with periodic acid-Schiff (PAS). Both structures are age-related deposits that entrap residual products and present some neoantigens, or more specifically neopeptides (NEs), which can be recognized by natural antibodies of the IgM isotype (9, 10, 21, 24–30). NEs are epitopes that originate *de novo* in physiological conditions and also in pathological situations such as ischemia, diabetes, atherosclerosis, cancer and inflammatory events, as well as in aging (31–35). For its part, natural antibodies are generated throughout a lifetime, even during fetal development and before external antigen exposure (36–39). Their repertoire and reactivity pattern have been determined throughout evolution and are remarkably stable within species and even between species (40, 41), explaining their presence as contaminants in a wide range of commercial antibodies. They constitute a first line of immune defense, but also have important functions in the physiology of the organism (42). Some of these natural antibodies are able to recognize the NEs that occur in, for example, cell remnants and senescent or apoptotic cells, taking part in their controlled elimination and, thus, contributing to the maintenance of tissue homeostasis (31, 37, 38, 41–45). Therefore, the presence of NEs in both CA and PAS granules and the existence of natural IgMs that target them reinforce the idea that CA and PAS granules are involved in brain cleaning or in protective processes.

The nature of the NEs present in CA and recognized by natural IgMs remains unknown but several observations suggest that they can be of a carbohydrate nature. For instance, the NEs contained in PAS granules of the mouse brain, recognized by natural IgMs, have a carbohydrate nature (27, 30). In addition, natural IgM antibodies have been described to recognize some carbohydrates, such as advanced glycation end products, whose production is increased with aging (37, 44–48). In fact, many α -glycan antibodies present in human sera belong to the IgM class and are natural antibodies (49). In any case, IgMs often recognize epitopes that act as markers of own residual structures (42) and, as mentioned previously, CA contain some of these residual structures. Therefore, it seemed appropriate to explore whether the NEs of CA do have a carbohydrate nature. However, it has to be taken into account that in living beings glycans show great complexity, greater than that of proteins, nucleic acids and lipids, and currently there are few or at least insufficient tools to study glycans with the same ease and precision as that associated with the study of proteins (50). Thus, in this first attempt we adapted standard techniques to determine the nature of NEs of CA.

Two different approaches were used. First, IgM preadsorptions with increasing concentrations of specific carbohydrates were performed to ascertain if the preadsorption produced a partial or total inhibition of CA staining with the IgMs. As a control, the same preadsorption studies were undertaken by staining the CA with concanavalin A (ConA). ConA staining of CA has been previously described in the literature (24, 51). ConA is a plant lectin that binds to hexoses in which the d-pyranose ring system presents hydroxyl groups at C-3 and C-4 in the equatorial plane, as well as a hydroxyl group at C-6. These types of hexoses include d-mannose (Man) and d-glucose (Glc), but not d-galactose (Gal), in which the hydroxyl group at C-4 is in the axial plane. ConA also binds to certain sugars with a five-membered furanoid ring form, such as ketohexose d-fructose, in which the hydroxyl groups at C-3, C-4 and C-6 are oriented similarly to those in the mannopyranosyl ring, and aldopentose d-arabinose, in which the hydroxyl groups at C-2, C-3 and C-5 show a similar orientation (52–54). Thus, if carbohydrate preadsorption works well, CA staining with fluorochrome-labeled ConA will be blocked by Glc, Man, d-fructose (Fru) and N-acetyl-d-glucosamine (GlcNAc), but not by Gal or N-acetyl-d-galactosamine (GalNAc). Another control of the preadsorption with sugars was based on the staining of CA with an α -p62 antibody. As p62 is a protein, the preadsorption of the α -p62 antibody with the different sugars should not interfere with the staining of CA. This control was used to demonstrate that the preadsorption with the sugars did not block the antibodies directed against the proteins in the CA.

The second approach to study the interaction of the IgMs with CA involved staining the CA after digestion with the peptidic enzyme pepsin. If IgM recognizes glycosides that are not linked to proteins, the staining should be maintained after the digestion. As control experiments, AF555 NHS ester probe, α -p62 antibody and fluorescein-labeled ConA were used to stain CA. The AF555 NHS ester probe labels primary amines (R-NH₂) of proteins, amine-modified oligonucleotides, and other amine-containing molecules. On the one hand, since AF555 NHS ester probe and α -p62 bind to proteins, pepsin digestion might

prevent the staining of CA with them; on the other hand, the staining with ConA should not be affected since ConA binds to carbohydrate structures.

MATERIAL AND METHODS

Preadsorption Studies

Human Brain Samples

Post-mortem brain samples were obtained from the Banc de Teixits Neurològics (Biobanc-Hospital Clínic-IDIBAPS, Barcelona). Frozen hippocampal sections (6 μm -thick; stored at -80°C) were obtained from three cases of neuropathologically confirmed Alzheimer's disease, two cases of subcortical vascular encephalopathy and one case of Lewy body dementia. Medical data of these cases are detailed in **Table S1 (Supplementary Material)**. All procedures involving human samples were performed in accordance with appropriate guidelines and regulations. All experiments involving human tissue were approved by the Bioethical Committee of the Universitat de Barcelona.

Immunofluorescence and ConA Staining

Frozen hippocampal sections were air dried for 10 min and then fixed with acetone for 10 min at 4°C . After 2 h of drying, sections were rehydrated in phosphate-buffered saline (PBS) and then blocked and permeabilized with 1% bovine serum albumin in PBS (Sigma-Aldrich) (blocking buffer, BB) with 0.1% Triton X-100 (Sigma-Aldrich) for 20 min. They were then washed with PBS and incubated with the primary antibody overnight at 4°C . The slides were then washed and incubated for 1 h at room temperature with the secondary antibody. Nuclear staining was performed with Hoechst (2 $\mu\text{g}/\text{mL}$, H-33258, Fluka, Madrid, Spain) and the slides were washed and coverslipped with Fluoromount (Electron Microscopy Sciences, Hatfield, PA, USA). Staining controls were performed by incubating with BB instead of the primary antibody before incubation with the secondary antibody.

The following were used as primary antibodies: mouse monoclonal IgG_{2a} against p62 (diluted 1:200; Abcam, ab56416), human IgMs purified from myeloma serum (MS-IgMs) (1:10; AbD Serotec, OBT1524) and human IgMs purified from normal serum (NS-IgMs) (1:25; Sigma, I8260). Previous studies indicated that both pools of IgMs contain IgMs that bind to CA. The following were used as the secondary antibodies: Alexa Fluor (AF) 488 goat α -mouse IgG_{2a} (1:250; Life Technologies, A-21131) and AF488 goat α -human IgM (heavy chain) (1:200; Life Technologies, A-21215).

In some of the experiments, samples were incubated overnight with fluorescein-labeled ConA (1:250; Vector Laboratories) instead of the primary antibody and, as incubation with the secondary antibody was not needed, the slides were immediately washed and coverslipped with Fluoromount.

Preadsorption With Carbohydrates

Primary antibodies and ConA were preadsorbed in different assays with the monosaccharides Glc (Scharlab, GL01271000), Man (Sigma Aldrich, M2D69), Fru (Sigma Aldrich, F0127), Gal

(Sigma Aldrich, G0750), GlcNAc (Sigma Aldrich, A8625) and GalNAc (Sigma Aldrich, A2795). For each monosaccharide, we first prepared sugar dilutions of 0 (control), 50, 100, 200 and 400 mM in PBS, as well as 800 mM in some of the indicated cases. The preadsorption was then performed by using these sugar solutions to dilute the primary antibodies or ConA at the indicated concentrations, and the mixtures were maintained overnight at 4°C with agitation. The different hippocampal sections were incubated with each mixture instead of the primary antibody. Some preadsorption series of different sugars were performed at the same time and the 0 mM tissue section was shared. Thus, these series show the same fluorescence values and images at 0 mM. To reduce variability, consecutive hippocampal sections were used in each assay, i.e., in the study of the preadsorption of an antibody (or ConA) with a determinate sugar.

Image Acquisition

Images were captured with a fluorescence laser and optical microscope (BX41, Olympus, Germany) and saved in tiff format. All the images for each combination of antibody (or ConA) and sugar were taken using the same microscope, laser and software settings. The time of capture was adapted to each staining, but the control or reference images were acquired with the same time of capture as that of the respective set of images.

Image Processing and Fluorescence Intensity Measurements

The merging of the images from the different fluorescence channels was performed using the FIJI program (National Institutes of Health, USA). Image analysis and quantifications were also performed with the FIJI program, not using the composite image, but the original image in the appropriate color. All CA of each hippocampal section were analyzed. The degree of staining of each CA was quantified as described below. For each CA, we first defined the region of interest (ROI) manually by tracing the outline of the CA using the elliptical selection tool of the FIJI program. We then obtained the mean gray value of the ROI, which corresponded to the mean fluorescence intensity (in arbitrary units) of the outlined CA. To minimize possible differences in the basal intensity of each image, for each CA, we moved the ROI to an area next to the CA and obtained the mean fluorescence intensity of the background. Thereafter, we obtained the relative intensity (RI) for each CA, which was defined as the difference between the mean fluorescence intensity of the CA and the mean fluorescence intensity of the respective background. To standardize the data obtained from the different preadsorption studies, for each combination of antibody and sugar, we defined the mean value of all the RIs obtained with 0 mM of the monosaccharide as the reference value (RV). The intensity of each CA was expressed as a percentage with respect to the reference value (RI%), i.e., $100 \cdot \text{RI}/\text{RV}$. It should be noted that in all the cases, the mean RI% value will be 100% for 0 mM. If the carbohydrate preadsorption interferes with the CA staining, this percentage will decrease with increasing carbohydrate concentrations. The original data of the fluorescence intensities of the CA and their corresponding backgrounds are included in the **Supplementary Materials**.

Statistical Analysis

Statistical analysis was performed with the ANOVA module of SPSS Statistics (IBM). For each study, to determine if the sugar concentration influences the RI%, the variable sugar concentration has been defined as the independent variable and the RI% variable as the dependent one. When the ANOVA indicates that the variable sugar concentration influences the RI%, the Scheffe test was used for *post hoc* comparisons in order to compare the values obtained at each sugar concentration to the values obtained at 0 mM. Differences were considered significant when $p < 0.01$. However, as commented in the Editorial of Nature dated 20th March 2019 (55), using only p values to determine significance can also lead to some analyses being biased, some false positives being overhyped and some genuine effects being overlooked. Logic, background knowledge and experimental design should be considered alongside p values and similar metrics to reach a conclusion and decide on its certainty. Accordingly, in the present study, p values were used alongside other findings to reach conclusions based on a general view.

Digestion Studies

Human CSF Samples Used to Obtain CA

Post-mortem ventricular CSF samples were obtained from three cases of neuropathologically affected patients and one non-neuropathologically affected patient. When extracted, the CSF samples were centrifuged at 4,000 g at 4°C for 10 min and the pellets obtained were stored at -80°C until use. All these procedures were performed at the Banc de Teixits Neurològics (Biobanc-Hospital Clínic-IDIBAPS, Barcelona). Medical data about these cases are detailed in **Table S2 (Supplementary Material)**.

CA Extraction and Pepsin Digestion

CSF pellets were re-suspended in PBS and filtered through a 35- μ m porous filter (Fisher Scientific, 12934257). The samples were then centrifuged at 700 g for 10 min. The supernatants were then rejected and pellets were re-suspended in PBS to obtain 500- μ L aliquots. Another centrifugation at 700 g for 10 min was performed, and the pellet was re-suspended in 500 μ L of a solution of 4 mg/mL of pepsin (Merck, P6887) in 10 mM HCl (pH 2). The suspension was maintained under agitation overnight at 37°C. Control experiments were performed by incubating the samples overnight with PBS instead of the pepsin solution.

Immunofluorescence, AF555 NHS Ester Staining, and ConA Staining

After pepsin digestion, samples were washed 3 times by centrifugation at 700 g for 10 min and the pellet was re-suspended in 1,000 μ L of PBS. The samples were then incubated with the primary antibody overnight at 4°C. Thereafter, samples were washed 3 times by centrifugation and incubated for 1 h at room temperature with the secondary antibody. Samples were then washed twice and centrifuged again at 700 g for 10 min to obtain pellets that were then re-suspended in 40 μ L of PBS. These 40- μ L samples were spread on to slides, air dried and coverslipped with Fluoromount. Staining controls were performed by incubating with PBS instead of the primary antibody.

The following were used as the primary antibodies: mouse monoclonal IgG_{2a} against p62 (diluted 1:200; Abcam, ab56416)

and NS-IgMs (1:25; Sigma, I8260). The following were used as the secondary antibodies: AF555 goat α -mouse IgG_{2a} (1:250; Life Technologies, A-21131) and AF488 goat α -human IgM (heavy chain) (1:200; Life Technologies, A-21215).

In some of the immunofluorescence experiments, samples were incubated with fluorescein-labeled ConA (1:250; Vector Laboratories, FL-1001-25) overnight or with AF555 NHS ester probe (1 mg/mL; ThermoFisher Scientific, A37571) 1 h at room temperature with agitation, instead of the primary antibodies.

In some cases, sequential double staining was performed with the α -p62 antibody and ConA and with the α -p62 antibody and NS-IgMs. The α -p62 antibody and ConA double staining was carried out in the same way as the simple immunofluorescence procedure, but adding an overnight incubation at 4°C with ConA after the incubation with the secondary antibody. Regarding the α -p62 antibody and NS-IgM double immunostaining, the samples were incubated with the α -p62 antibody overnight at 4°C first and then with NS-IgMs overnight at 4°C, before being incubated with the secondary antibodies simultaneously for 1 h at room temperature.

Image Acquisition and Processing

Image acquisition and processing were performed as described above for the sugar preadsorption studies.

RESULTS

Sugar Preadsorption Studies

Effects of Sugar Preadsorption on ConA Staining of CA

As mentioned before, it is well established that ConA binds to CA and that fluorochrome-labeled ConA can be used to stain CA (24, 51). Thus, we performed the preadsorption studies with the different sugars using fluorochrome-labeled ConA. As shown in the upper row of **Figure 1**, preadsorption with glucose interfered with the staining. While ConA staining of the CA can be clearly observed when the Glc concentration is 0 mM (i.e., positive control), the staining is practically absent in the presence of glucose at all the tested concentrations. The same pattern was observed when the preadsorption was performed with Man, Fru or GlcNAc. However, when the preadsorption was performed with Gal or GalNAc, the staining with ConA was maintained, even at the highest concentration of sugar.

Table 1 presents the mean RI% values for each carbohydrate experiment and each carbohydrate concentration. This table contains the summary of all the results of the section to allow and facilitate the comparison between them. As can be observed, in the case of ConA staining, statistical analysis of the data from the Glc experiments indicated that the RI% decreased with the preadsorption, being significantly lower than 100% for all the tested concentrations ($p < 0.01$), i.e., lower than that of the reference value at 0 mM. This indicates that Glc significantly interfered with the ConA staining of CA. For Man, Fru and GlcNAc, there was also a significant decrease in the staining with increasing sugar concentrations. This was not the case for Gal and GalNAc, which did not reduce the staining. There were no significant differences with respect to their controls, except for

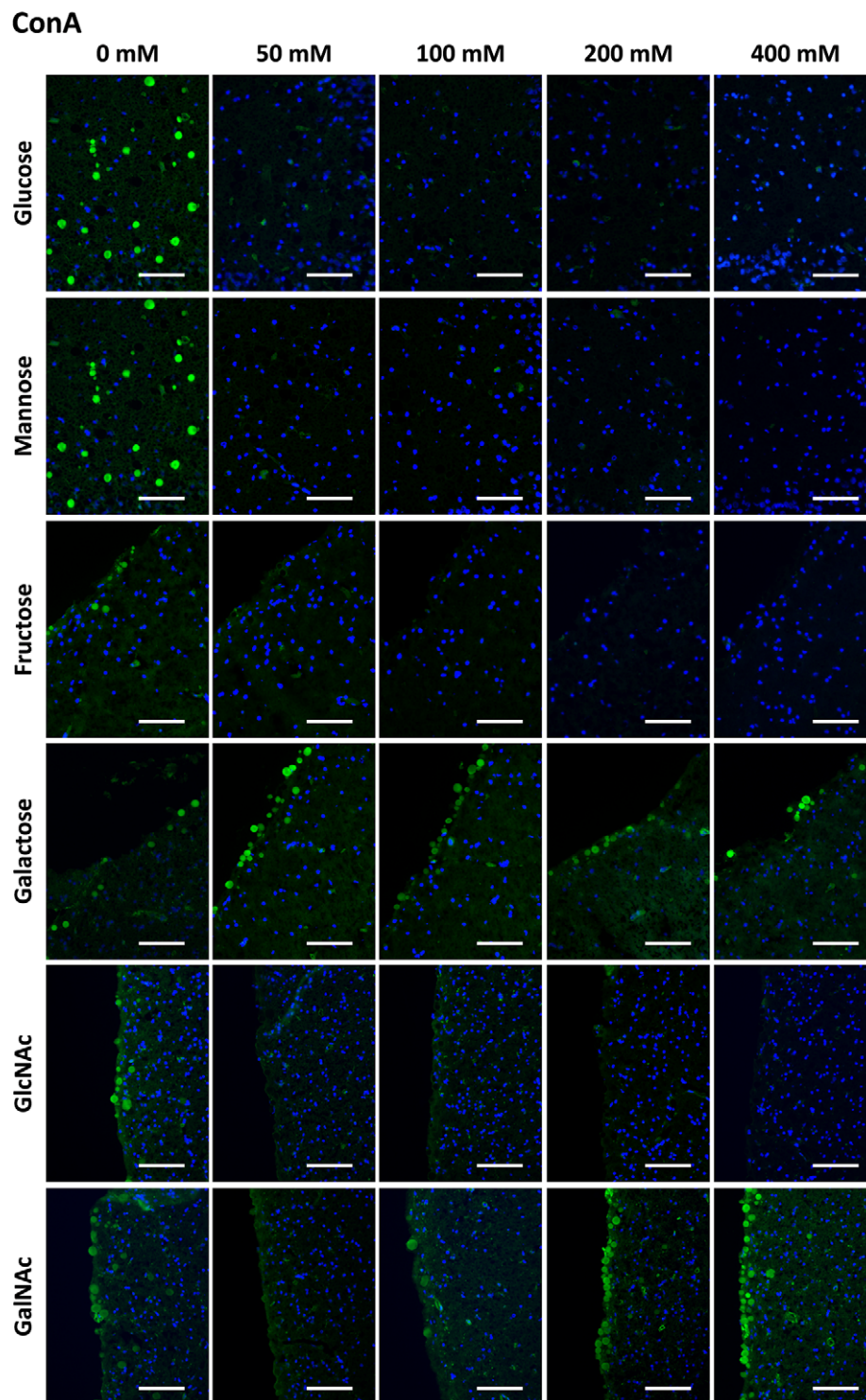


FIGURE 1 | Representative images of hippocampal sections stained with ConA (green) and Hoechst (blue). Each row corresponds to a preadsorption study performed with the indicated carbohydrate. Sugar concentrations are indicated above. The staining of CA (green) disappeared or decreased when the preadsorption was performed with Glc, Man, Fru or GlcNAc, but was not affected by Gal or GalNAc. Some discrepancies in the basal staining can be appreciated between the different preadsorption experiments (see, for example, the first column corresponding to the positive controls); for the statistical analysis, these discrepancies have been corrected in basis of the background intensity, as indicated in the Methods section. Scale bar: 100 μ m.

GalNAc at 800 mM, which resulted in a mean RI% of 168.49 that was higher than the value at 0 mM. This was considered an outlier because of the absence of any clear trend at the other concentrations (see below). In any case, GalNAc did not decrease the staining when used to preadsorb ConA.

Figure 7A presents a graphical view of these data, showing the different dynamics for Gal and GalNAc with respect to the other sugars. These results were expected according to the carbohydrate-binding domain of ConA, indicating that sugar preadsorption could be an optimal method for studying the nature of the interaction. This figure contains the summary of all the results of the section, and is located at the end of the section.

Effects of Sugar Preadsorption on α -p62 Staining of CA

Before using the preadsorption with sugars to study the interaction between IgMs and CA, we applied the preadsorption method to analyze the interaction between the α -p62 antibody and CA. As the α -p62 antibody stains the protein p62, it was expected that preadsorption with the different sugars would not interfere with

this immunostaining and, thus, α -p62 antibody staining would be used as a negative control to validate the sugar preadsorption method.

Figure 2 shows representative images of CA stained with the α -p62 antibody, previously preadsorbed with Glc, Man, Fru, Gal, GlcNAc and GalNAc at different concentrations ranging from 0 mM to 800 mM. As can be observed, the staining was maintained at all the sugar concentrations tested, indicating that the presence of the different sugars did not affect the α -p62 antibody staining.

Table 1 presents the mean RI% values obtained from the different p62 assays. The values ranged from 53.63% to 127%, with no significant differences compared to the values obtained at 0 mM ($p < 0.01$ in all cases). Moreover, the graphical view of these data (**Figure 7B**) shows no downward trends in relation to the sugar concentration for any of the four sugars tested.

Effects of Sugar Preadsorption on IgMs Staining of CA

As the preadsorption method used was reliable in describing the sugar-based interaction between ConA and CA and given that the staining of CA with antibodies directed against proteins was

TABLE 1 | Fluorescence intensity of CA staining expressed as mean RI% (\pm s.e.m.; N).

		0 mM	50 mM	100 mM	200 mM	400 mM	800 mM
ConA	Glc	100,00 (\pm 2,94; 20)	0,11 (\pm 0,11; 24)*	0,00 (\pm 0; 14)*	0,04 (\pm 0,04; 16)*	0,00 (\pm 0; 19)*	—
	Fru	100,00 (\pm 6,02; 7)	0,00 (\pm 0; 5)*	0,00 (\pm 0; 5)*	0,00 (\pm 0; 6)*	0,00 (\pm 0; 10)*	—
	Man	100,00 (\pm 2,94; 20)	0,01 (\pm 0,01; 29)*	0,00 (\pm 0; 17)*	0,00 (\pm 0; 13)*	0,00 (\pm 0; 20)*	—
	GlcNAc	100,00 (\pm 5,14; 8)	0,00 (\pm 0; 9)*	0,00 (\pm 0; 10)*	0,00 (\pm 0; 7)*	0,00 (\pm 0; 8)*	—
	Gal	100,00 (\pm 5,02; 20)	113,84 (\pm 7,5; 33)	114,29 (\pm 15,18; 12)	124,53 (\pm 12,1; 10)	85,61 (\pm 5,37; 18)	—
	GalNAc	100,00 (\pm 5,29; 19)	95,68 (\pm 7,8; 15)	135,36 (\pm 7,19; 33)	98,31 (\pm 10,56; 12)	168,49 (\pm 5,87; 57)**	—
p62	Glc	100,00 (\pm 5,43; 54)	112,71 (\pm 6,86; 57)	106,29 (\pm 6,04; 48)	110,03 (\pm 6,33; 49)	113,09 (\pm 8,77; 46)	110,43 (\pm 7,79; 47)
	Fru	100,00 (\pm 6,99; 64)	97,17 (\pm 7,76; 59)	83,91 (\pm 5,24; 56)	110,83 (\pm 7,33; 77)	90,7 (\pm 6,06; 54)	73,80 (\pm 5,10; 63)
	Man	100,00 (\pm 6,99; 64)	88,48 (\pm 6,62; 56)	108,27 (\pm 10,24; 36)	74,06 (\pm 5,47; 57)	92,53 (\pm 7,03; 68)	80,05 (6,76; 43)
	GlcNAc	100,00 (\pm 25; 12)	114,79 (\pm 34,35; 11)	54,88 (\pm 9,95; 16)	73,42 (\pm 14,22; 24)	126,59 (\pm 21,72; 14)	69,38 (\pm 10,03; 32)
	Gal	100,00 (\pm 8,06; 61)	65,22 (\pm 5,88; 32)	117,3 (\pm 7,51; 55)	123,98 (\pm 8,55; 55)	53,63 (\pm 11,47; 14)	80,99 (\pm 9,53; 34)
	GalNAc	100,00 (\pm 25; 12)	61,71 (\pm 5,46; 31)	81,42 (\pm 28,07; 11)	80,39 (\pm 17,28; 13)	57,94 (\pm 7,51; 24)	64,16 (\pm 9,74; 12)
MS-IgM (S1)	Glc	100,00 (\pm 7,66; 29)	80,28 (\pm 7,65; 20)	46,97 (\pm 3,64; 34)*	14,39 (\pm 1,68; 21)*	0,33 (\pm 0,23; 9)*	—
	Fru	100,00 (\pm 8,9; 19)	78,02 (\pm 15,23; 7)	69,59 (\pm 5,67; 6)	37,15 (\pm 5,17; 5)*	5,15 (\pm 1,21; 7)*	—
	Man	100,00 (\pm 7,66; 29)	69,57 (\pm 6,04; 30)*	27,45 (\pm 3,18; 14)*	25,32 (\pm 3,04; 13)*	0,65 (\pm 0,2; 7)*	—
	Gal	100,00 (\pm 8,9; 19)	66,21 (\pm 4,92; 8)	44,15 (\pm 2,9; 12)*	0,6 (\pm 0,47; 13)*	0,78 (\pm 0,36; 13)*	—
MS-IgM (S2)	Glc	100,00 (\pm 4,54; 26)	91,14 (\pm 4,81; 11)	41,77 (\pm 4,01; 9)*	35,61 (\pm 9,67; 2)*	4,3 (\pm 2,45; 10)*	—
	Fru	100,00 (\pm 3,14; 79)	48,69 (\pm 5,13; 27)*	37,08 (\pm 3,81; 34)*	28,51 (\pm 2,38; 31)*	0,41 (\pm 0,21; 28)*	—
	Man	100,00 (\pm 8,42; 39)	95,45 (\pm 6,98; 34)	90,21 (\pm 9,23; 15)	31,73 (\pm 8,21; 16)*	4,17 (\pm 1,36; 10)*	—
	Gal	100,00 (\pm 3,55; 66)	59,79 (\pm 3,24; 43)*	43,12 (\pm 2,15; 33)*	7,7 (\pm 0,7; 24)*	0,19 (\pm 0,12; 7)*	—
NS-IgM (S1)	Glc	100,00 (\pm 8,14; 53)	0,26 (\pm 0,26; 18)*	0,00 (\pm 0; 36)*	0,00 (\pm 0; 36)*	0,00 (\pm 0; 32)*	—
	Fru	100,00 (\pm 9,31; 9)	84,46 (\pm 7,61; 37)	65,51 (\pm 9,14; 11)	43,83 (\pm 2,39; 60)*	35,72 (\pm 4,95; 20)*	—
	Man	100,00 (\pm 9,31; 9)	63,4 (\pm 2,78; 21)*	57,41 (\pm 3,44; 43)*	44,69 (\pm 2,96; 17)*	42,07 (\pm 2,93; 22)*	—
	GlcNAc	100,00 (\pm 8,14; 53)	50,43 (\pm 6,85; 37)*	53,23 (\pm 6,97; 40)*	45,88 (\pm 7,42; 35)*	32,62 (\pm 4,86; 39)*	—
	Gal	100,00 (\pm 6,04; 36)	108,54 (\pm 5,23; 30)	134,42 (\pm 8,75; 16)*	61,68 (\pm 3,46; 9)*	93,08 (\pm 7,95; 15)	—
	GalNAc	100,00 (\pm 6,04; 36)	91,01 (\pm 5,12; 24)	87,39 (\pm 5,05; 13)	120,64 (\pm 12,25; 15)	80,13 (\pm 3,41; 29)	—
NS-IgM (S2)	Glc	100,00 (\pm 4,6; 67)	—	—	26,16 (\pm 5,28; 31)*	0,52 (\pm 0,28; 30)*	0,00 (\pm 0; 31)*
	Fru	100,00 (\pm 4,87; 42)	—	—	63,71 (\pm 4,89; 30)*	62,85 (\pm 3,29; 29)*	19,28 (\pm 4,25; 23)*
	Man	100,00 (\pm 5,57; 44)	—	—	91,43 (\pm 3,76; 46)	46,98 (\pm 3,79; 36)*	13,63 (\pm 1,42; 58)*
	GlcNAc	100,00 (\pm 4,6; 67)	—	—	61,76 (\pm 4,89; 25)*	48,41 (\pm 2,47; 25)*	28,41 (\pm 4,9; 18)*
	Gal	100,00 (\pm 4,59; 86)	—	—	85,13 (\pm 3,71; 64)	84,09 (\pm 3,07; 52)	58,62 (\pm 2,78; 56)*
	GalNAc	100,00 (\pm 4,59; 86)	—	—	92,33 (\pm 4,94; 77)	86,33 (\pm 5,03; 55)	68,45 (\pm 4,8; 58)*

Table 1. Mean values of CA fluorescence when stained with ConA, α -p62, MS-IgM and NS-IgM and previously preadsorbed with the indicated sugars at the indicated concentrations. For each sugar assay, the values are expressed as RI%, i.e. percentage respect to the mean value of fluorescence obtained in 0 mM, (\pm s.e.m.; N). * indicates significant differences respect to 0 mM ($p < 0,01$). ** indicates a significant value considered outlier (see text). — indicates not tested. **S1** and **S2** indicate different series. Note that in the case of ConA, all sugars produce a decrease of the CA staining, except Gal and GalNAc. For α -p62, none of the tested sugars interfere with the staining, indicating that the staining of this protein is not affected by the sugar preadsorption. Contrarily, all tested sugars interfere with the staining with the MS-IgM, reaching the mean RI% values near to 0% at 400 mM. In the case of NS-IgM, Glc is the sugar that produces the highest decrease, while Gal and GalNAc only produce a significant decrease at 800 mM, producing a lower than 42% reduction in RI%. Bold values are the significant ones, to improve visualization.

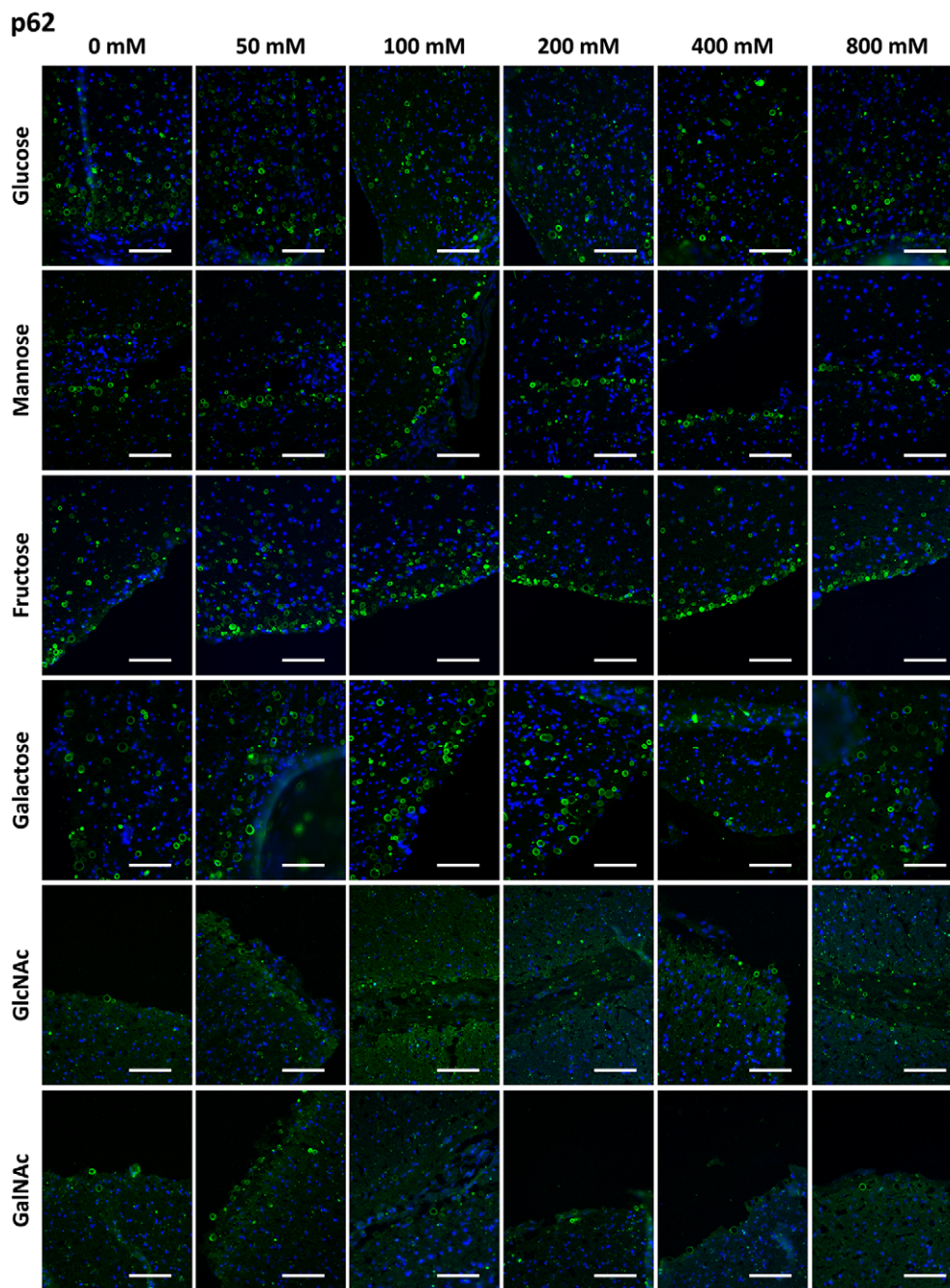


FIGURE 2 | Representative images of hippocampal sections stained with the α -p62 antibody (green) and Hoechst (blue). Each row corresponds to a preadsorption study performed with the indicated carbohydrate. Sugar concentrations are indicated above. The staining of CA (green) is always present for all the sugars tested and at all the sugar concentrations. Scale bar: 100 μ m.

not affected by the sugar preadsorption, we applied the preadsorption method to analyze if sugars interfered with the interaction between IgMs and CA. We used two different sources of IgMs: those obtained from myeloma serum (MS-IgMs) and those obtained from normal human serum (NS-IgMs).

In the case of MS-IgMs, we tested the preadsorption of IgMs with Glc, Gal, Fru and Man at concentrations ranging from 0

mM to 400 mM. As it was necessary to replicate the assay with the NS-IgMs (see below), the experiment with MS-IgMs was also replicated in order to analyze the robustness of the results. Thus, the preadsorption of MS-IgMs included two series, **S1** and **S2**.

Figures 3 and **4** show representative images of the staining of CA with MS-IgMs for each sugar at each concentration, corresponding to **S1** and **S2**, respectively. In the absence of

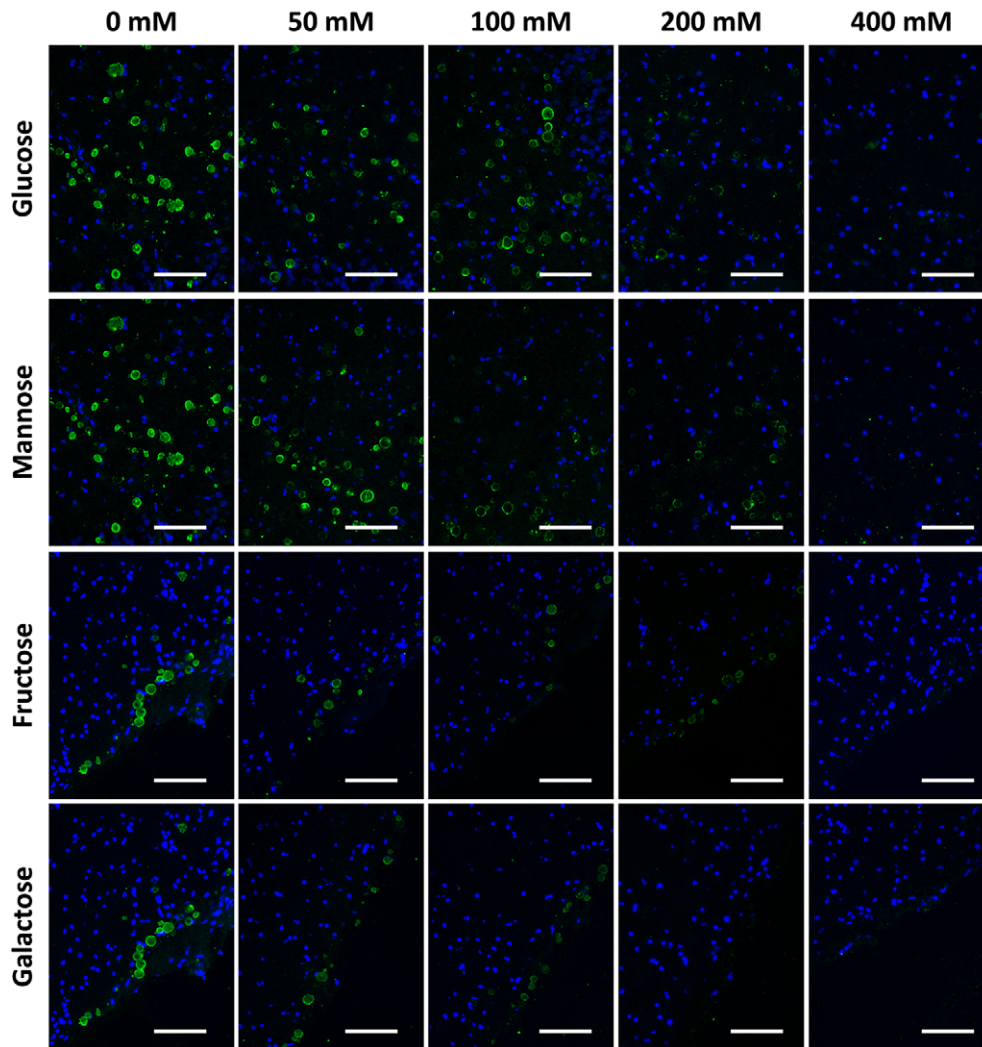
MS-IgM S1

FIGURE 3 | Representative images of hippocampal sections stained with MS-IgMs and Hoechst (blue) obtained in the first series (**S1**). Each row corresponds to a preadsorption study performed with the indicated carbohydrate. Sugar concentrations are indicated above. Note that the staining of CA becomes weaker with increasing sugar concentrations and even disappears. Scale bar: 100 μ m.

sugars, i.e. the positive controls of the staining, the staining of CA can be appreciated. When increasing the sugar concentration, the staining becomes weaker or even disappears.

Table 1 shows the mean RI% values for each experimental condition, including the results from **S1** and **S2**. Statistical significances with respect to the values obtained at 0 mM are indicated. As can be observed, all the sugars interfered with the staining, with the sugar concentrations of 200 mM and 400 mM producing a significant decrease. Moreover, as can be observed in the graphical view of these data (**Figures 7C, D** corresponding to **S1** and **S2**, respectively), there was a gradual decrease in staining when the sugar concentration increased. Although there were some discrepancies when comparing **S1** and **S2** (see, for example, Man at 50 and 100 mM), the general trends observed in **S1** were

the same as those observed in **S2**. Furthermore, the downward trends were similar for the different sugars, with the RI% values at 400 mM close to 0%. Thus, the results obtained with MS-IgMs indicated that the interaction between the MS-IgMs and CA was affected by all the sugars tested.

In the case of NS-IgMs, we first tested the preadsorption with Glc, Gal, Fru, Man, GlcNAc and GalNAc at concentrations ranging from 0 mM to 400 mM (**S1**). After considering the need to include the concentration of 800 mM, we performed a second series (**S2**) with all the sugars at concentrations of 0, 200, 400 and 800 mM. Representative images corresponding to **S1** and **S2** can be found in **Figures 5** and **6**.

Table 1 presents the mean RI% values from **S1** and **S2** and the statistical significances with respect to the values obtained at

MS-IgM S2

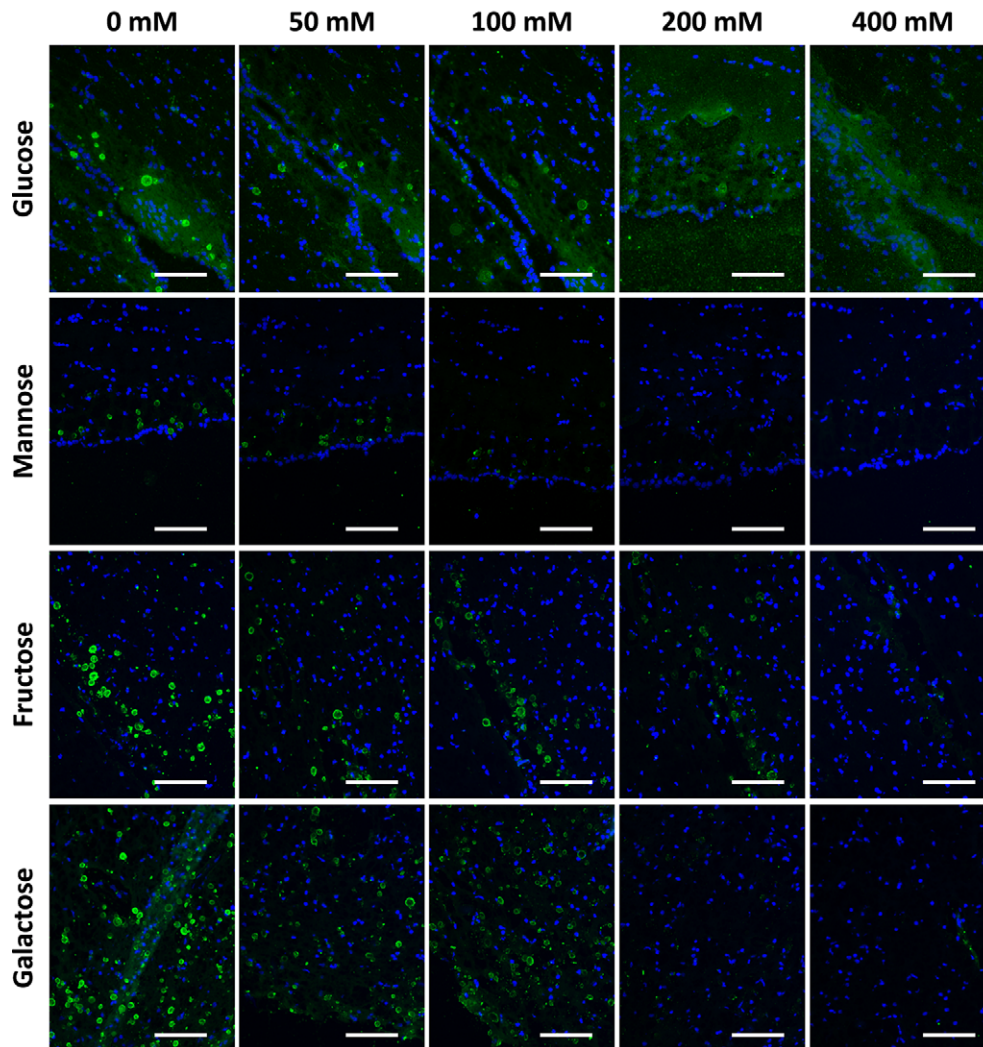


FIGURE 4 | Representative images of hippocampal sections stained with MS-IgMs and Hoechst (blue) obtained in the second series (**S2**). Each row corresponds to a preadsorption study performed with the indicated carbohydrate. Sugar concentrations are indicated above. As observed in **Figure S3**, the staining of CA becomes weaker with increasing sugar concentrations and even disappears. Scale bar: 100 μ m.

0 mM. The graphical view of these data is presented in **Figures 7E, F**. As can be observed, the results from **S1** and **S2** were very similar. The different sugars seem to interfere in different ways with the staining of CA with NS-IgM. Glc had the largest effect on the staining, with the RI% close to 0% for practically all the tested concentrations, being significantly lower than the control values. Man, Fru and GlcNAc also decreased the RI%. However, this decrease seems to be not as pronounced as that produced by Glc, with values at 800 mM being around 20%. The results from the experiments with Gal and GalNAc appear to be different to those with the other sugars, with no clear trend observed. **Table 1** shows that significant differences compared to the control values were observed only for 800 mM of Gal or GalNAc. At this concentration, the RI% values were 58.62 for Gal

and 68.45 for GalNAc, i.e., far from 0% and far from the values obtained with the other sugars at 800 mM. Thus, Glc showed the largest effect on the interaction between the NS-IgMs and CA, while Fru, Man and GlcNAc had an intermediate effect, and Gal and GalNAc had a minor effect. This indicates that there are some differences in the way in which MS-IgMs and NS-IgMs interact with CA, in terms of immunoreactivity. However, generally, the interaction between IgMs and CA seems to involve carbohydrates, suggesting that the NEs have a carbohydrate nature.

Digestion Studies

As explained before, to exclude the possible peptidic composition of the NEs recognized by the IgMs, we checked the IgM staining

of CA obtained from the CSF after their digestion with the peptidic enzyme pepsin. Staining with AF555 NHS ester probe, α -p62 antibody and fluorescein-labeled ConA were used as controls. After the digestion with pepsin, the AF555 NHS ester and α -p62 staining should not appear if the proteins have been digested, but the staining with ConA should not be affected, as ConA binds to carbohydrate structures.

First of all, we performed single staining of CA with NHS ester probe, α -p62, ConA and NS-IgM (**Figure 8A**). For each product, we used matching aliquots, one of them digested with pepsin and the other simply diluted in PBS. As expected, CA were stained with the NHS ester probe in the absence of pepsin digestion, but not when CA have been previously digested with pepsin, indicating that the digestion with pepsin, eliminated all the peptidic components of the CA. Accordingly, CA were stained with the α -p62 in absence of pepsin digestion, but not when CA have been previously digested. Staining with ConA was not affected by the pepsin digestion, indicating that the glucidic structure recognized by ConA was not affected by the peptidic enzyme. Finally, staining with NS-IgMs occurred with and without the pepsin digestion, indicating that the targets of the IgMs were not affected by this digestion and, thus, they do not have a peptidic nature.

Two double staining procedures were performed, using ConA and the α -p62 antibody in one case and NS-IgMs and α -p62 antibodies in the other. In the first case, CA were stained with both ConA and the α -p62 antibody in the absence of the pepsin digestion, while after the pepsin digestion the ConA staining can be observed but not that of p62 (**Figure 8B**). Similarly, pepsin digestion led to the disappearance of the α -p62 antibody staining, but did not affect NS-IgM staining in the double immunostaining with the α -p62 antibody and NS-IgMs (**Figure 8C**), indicating that the NEs recognized by the IgMs are not of a peptidic nature.

DISCUSSION

In previous studies, we had determined that CA in the human brain exhibit NEs that are recognized by plasma IgMs, which are in fact natural IgMs (10). The present study aimed to clarify the nature of these NEs, and we adapted standard techniques to this purpose.

Since the preadsorption of ConA with specific sugars interferes with the interaction between ConA and CA, and given that the sugar preadsorption of antibodies directed against proteins do not disrupt their interaction with CA, we used this strategy to study the interaction between IgMs and CA. We observed that the preadsorption of IgMs with specific carbohydrates had inhibitory effects. On the other hand, we found that the digestion of CA with pepsin, that eliminates their proteinaceous components, removes the staining with NHS ester probe and α -p62 while that of ConA is maintained, indicating that the sugar target of ConA has not been altered. We also observed that the pepsin digestion has no effect on IgM staining, thus excluding the peptidic nature of the NEs. Altogether, all

these results strongly support that the NEs contained in CA have a carbohydrate nature.

Glycans have multiple complex functions, including acting as “eat-me” signals to induce phagocytosis by macrophages or dendritic cells, either directly or indirectly, for example, *via* opsonization with natural IgMs (46, 50). Recently, Xia and Gildersleeve, analyzing α -glycan IgM repertoires in newborn human cord blood, reported that many α -glycan antibodies present in human sera belong to the IgM class and are natural antibodies (49), with natural IgMs estimated to constitute between 80% and 90% of natural antibodies (46). Membrane-derived epitopes are among the NEs recognized by these antibodies (56). Such epitopes include carbohydrate determinants generally anchored to intracellular membranes that act as “eat-me” signals when exposed to the outside of the cell, for example, when apoptosis occurs or in cell debris (56). In fact, under physiological conditions, there are multiple elements inside cells that can act as “eat-me” signals when externalized. This is an energy-saving process for the body because in the case of functional or structural alterations, it is not necessary to generate these signals *de novo*, but it is enough to relocate them to the outside of the cell (56). For all these reasons, given that CA accumulate different residual elements and that they can act as waste containers that are part of the brain cleaning system, it would not be surprising that different species of NEs with a carbohydrate nature occur in CA. Some of these could participate in the phagocytosis of CA by macrophages, a process that has been observed in nerve tissue samples from cases of neuromyelitis optica (17) and in *in vitro* studies (24).

In the present study, we used two different pools of IgMs (NS-IgMs and MS-IgMs). The binding of the NS-IgMs to CA was affected to varying levels by the different sugars, with Glc having the largest effect, reducing the RI% to 0% at a concentration of 50 mM. Gal and GalNAc had the smallest effects, producing a slight decrease in staining only at the highest concentration tested (800 mM), when the RI% value was around 60%. This suggests that the equatorial arrangement of the hydroxyl group at C-4 in the monosaccharide is critical for its interaction with IgMs. Moreover, the equatorial or axial arrangement of the hydroxyl group at C-2 might also have some importance. This is illustrated by the lower inhibition exerted by Man compared to Glc and also in the comparison of the inhibitions produced by Glc and GlcNAc, in which the hydroxyl group at C-2 is substituted with NAc. The effects of the changes at C-2, however, are not as strong as those at C-4.

The four monosaccharides tested interfered with the binding of the MS-IgMs to CA, with no significant differences observed among the sugars. This different behavior of MS-IgMs compared to NS-IgMs could be due to the fact that the former come from an extract of myeloma serum and, therefore, this pool of IgMs is restricted and possibly altered with respect to the pool of IgMs found in normal serum (NS-IgMs). However, it should be noted that in both cases, the interaction between the IgMs and CA was inhibited by the sugars, further supporting the carbohydrate nature of the NEs of CA that were recognized by these IgMs. We do not know whether there is only one type of NE in CA or whether there is a collection of different NEs. In any case, the

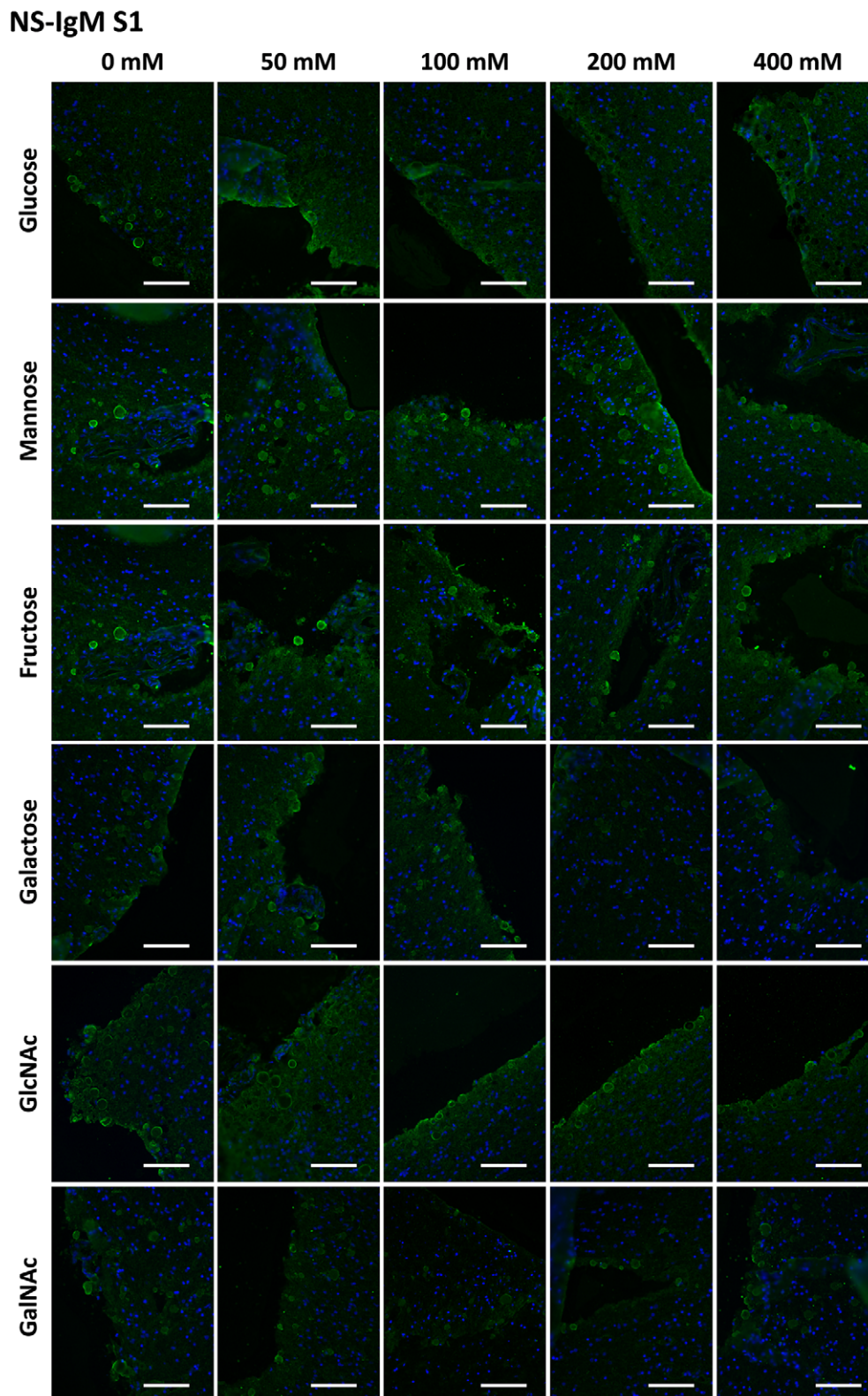


FIGURE 5 | Representative images of hippocampal sections stained with NS-IgMs and Hoechst (blue) obtained in the first series (**S1**). Each row corresponds to a preadsorption study performed with the indicated carbohydrate. Sugar concentrations are indicated above. Scale bar: 100 μ m.

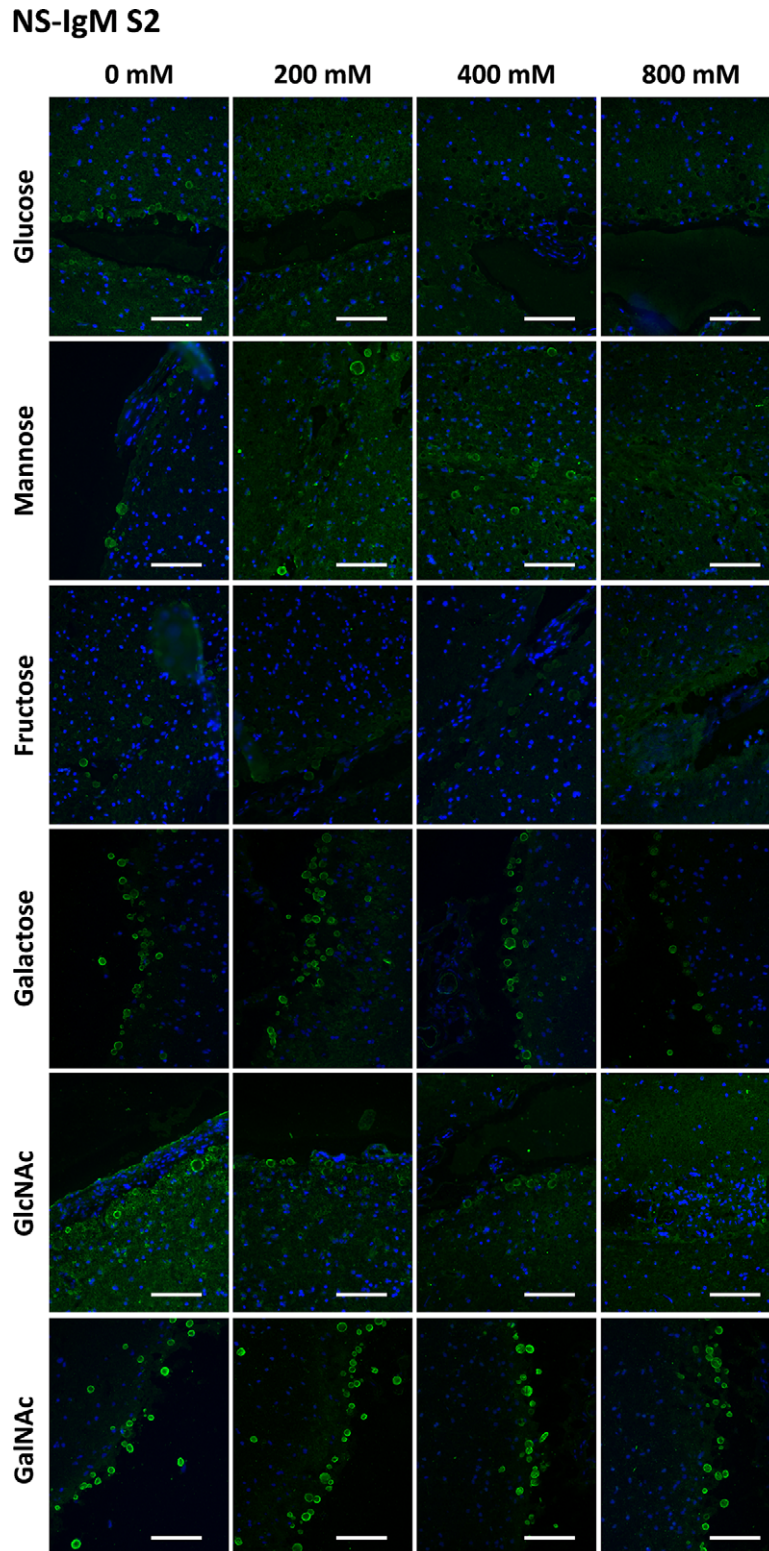


FIGURE 6 | Representative images of hippocampal sections stained with NS-IgMs and Hoechst (blue) obtained in the second series (**S2**). Each row corresponds to a preadsorption study performed with the indicated carbohydrate. Sugar concentrations are indicated above. Scale bar: 100 μ m.

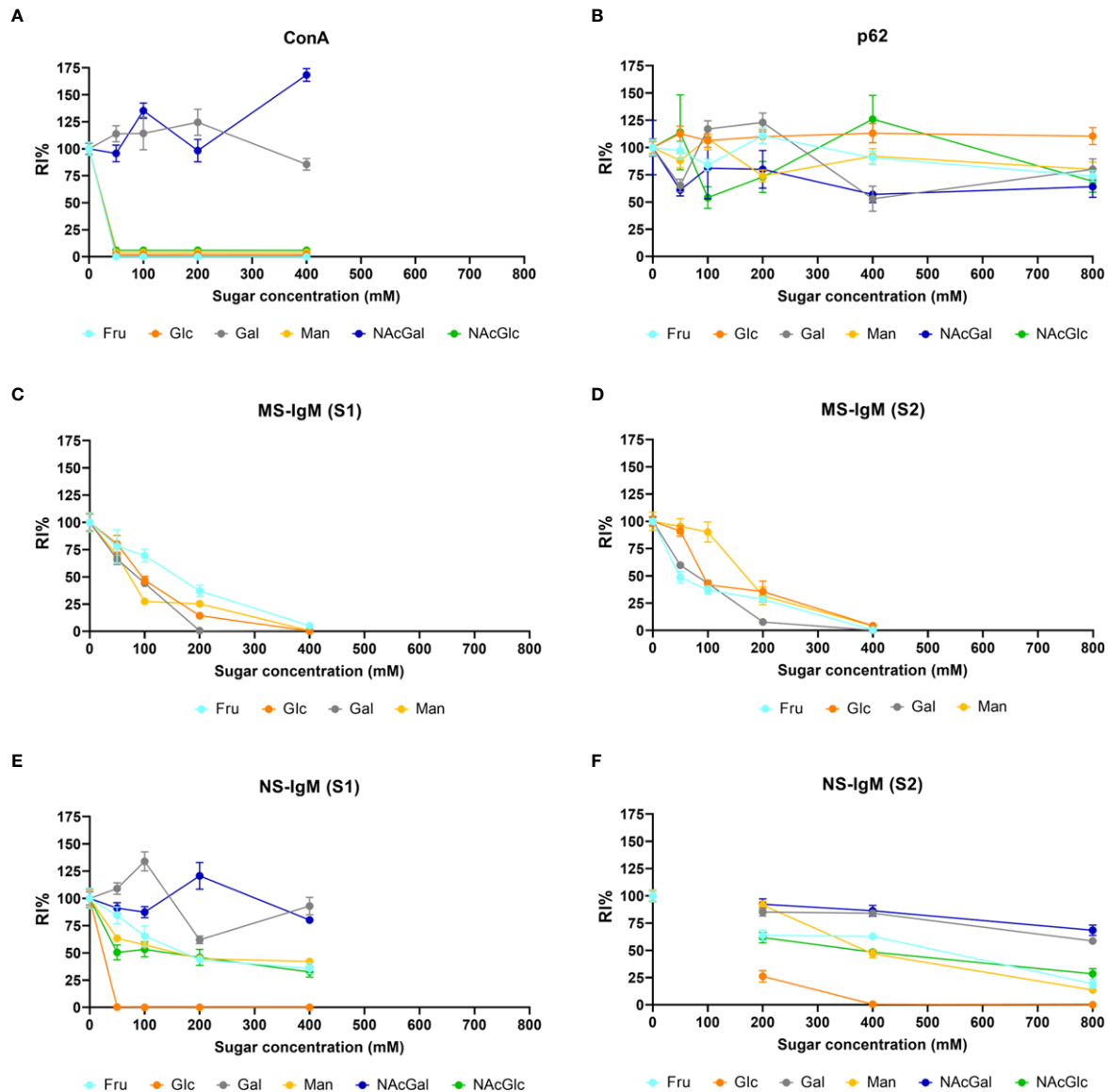


FIGURE 7 | Graphical view of the RI% mean values (\pm s.e.m.) of fluorescence resulting from the staining of CA with ConA, α -p62 antibody, MS-IgM or NS-IgM that have been preadsorbed with the indicated sugars at the indicated concentrations. **S1** and **S2** correspond to data from the different series. The data and significant differences are detailed in **Table 1**. Note in **(A)** the decrease produced by Glc, Fru, Man and GlcNAc, but not by Gal and GalNAc, in the ConA staining of CA. In **(B)** (corresponding to α -p62 antibody staining), note that the lines do not show the downward trend in relation to the sugar concentration for any of the four sugars tested. On the contrary, **(C, D)** show that staining with MS-IgMs (**S1** and **S2**) is affected by the presence of the sugars. Staining with NS-IgMs **(E, F)** is also affected by the presence of the sugars. See text for details.

binding of the IgMs to these NEs of CA can be completely blocked by certain monosaccharides.

The present work indicates that the binding between certain human IgMs and certain antigens or epitopes present in human structures can be inhibited *in vitro* by certain monosaccharides, especially glucose. Therefore, we wondered whether these inhibitions also occur *in vivo*. In human sera, the IgM concentration in early adulthood is 1.46 ± 0.12 mg/ml (57), while the normal plasma glucose two hours after eating is about 7.8 mM (58). In our study, the NS-IgM concentration was 0.044

mg/ml, while the lowest glucose concentration used to preadsorb the NS-IgM was 50 mM or, more precisely, 48.1 mM if we take into account the addition of the antibody during the antibody dilution. Therefore, the Glc/IgM ratio in our experimental conditions was about 205 times higher than that in physiological conditions. In any case, taking into account that in our experimental conditions the RI% decreases to about 0% at 48.1 mM of Glc concentration, we may consider that physiological levels of Glc could also induce some inhibitory effects on IgM. In this sense, it must be pointed that short-term

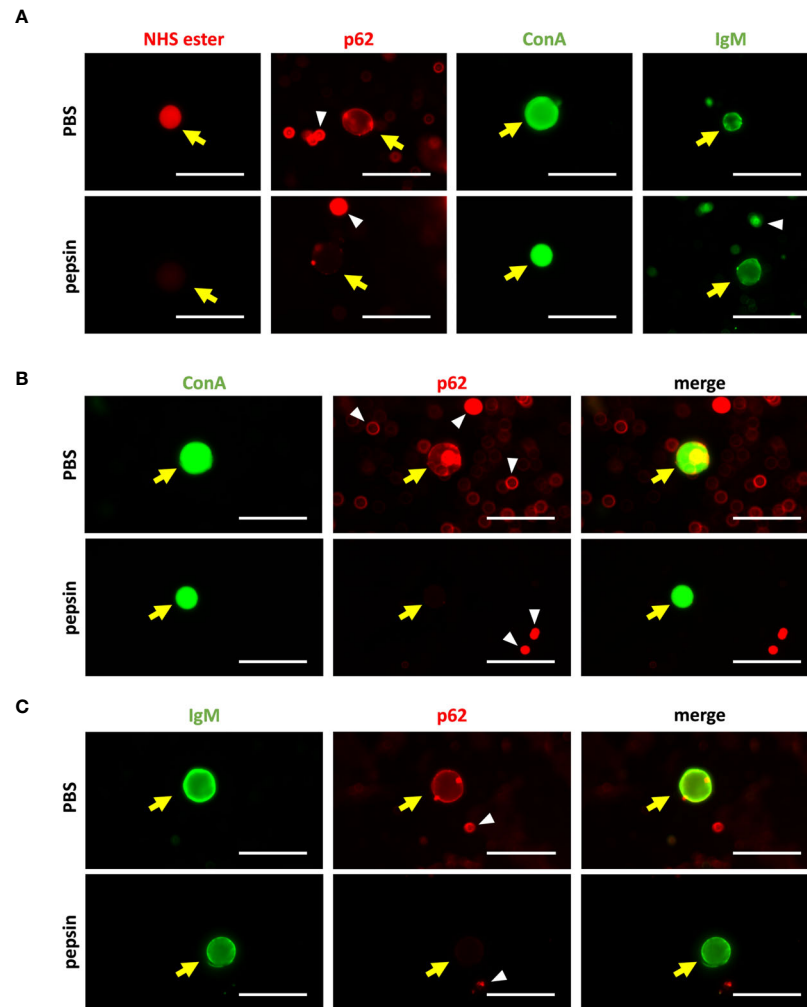


FIGURE 8 | (A) Representative images of single staining of CA from CSF with AF555 NHS ester probe, α -p62 antibody, ConA or NS-IgM (left to right). The staining has been performed after the incubation with pepsin (upper row), or after the incubation with PBS (lower row; controls). The digestion prevented the staining with the AF555 NHS ester probe and the α -p62 antibody, but not the staining with ConA or NS-IgM. CA are indicated by yellow arrows, while some artifacts or cell debris are pointed with white arrowheads. **(B)** Double staining of CA with ConA and the α -p62 antibody. The staining has been performed after the incubation with pepsin (upper row), or after the incubation with PBS (lower row; controls). Left: green channel (ConA); center: red channel (p62); right: merged images. Pepsin eliminated the staining of CA with the α -p62 antibody, but not that with ConA. **(C)**: Double staining of CA with NS-IgM and the α -p62 antibody, without and with the pepsin digestion (upper and lower rows, respectively). Left: green channel (IgM); center: red channel (p62); right: merged images. Pepsin eliminated the staining of CA with the α -p62 antibody, but not that with NS-IgM. Scale bar: 50 μ m.

hyperglycemia influence the innate immune system (59). Furthermore, diabetes mellitus increases susceptibility to viral, bacterial and fungal infections through modulating the immune system (59–61). Although different mechanisms have been described to explain this, including the activation of protein kinase C and the glycosylation of some proteins (59), the possible inhibition of IgM reactivity by glucose or other sugars has not been investigated to date. Thus, the present work introduces a new focus of interest.

In summary, the present work indicates that the NEs in CA have a carbohydrate nature. Furthermore, it indicates that the natural IgMs that recognize these NEs can be blocked *in vitro* by

preadsorption with different sugars, particularly glucose. Finally, our findings reveal the need to study the effects that glycemia produce *in vivo* on the reactivity of natural IgMs and, consequently, on natural immunity.

DATA AVAILABILITY STATEMENT

The original contributions presented in the study are included in the article/**Supplementary Material**. Further inquiries can be directed to the corresponding author.

ETHICS STATEMENT

The studies involving human samples were reviewed and approved by Bioethical Committee of the Universitat de Barcelona. The ethics committee waived the requirement of written informed consent for participation.

AUTHOR CONTRIBUTIONS

MR, EA, CP, and JV designed research. MR, EA, IT, JDV, LM-P, TX, CP, and JV performed research. MR, EA, JDV, CP, and JV analyzed data. MR, EA, JDV, CP, and JV wrote the paper. All authors contributed to the article and approved the submitted version.

ACKNOWLEDGMENTS

This study was funded by grant BFU2016-78398-P awarded by the Spanish Ministerio de Economía y Competitividad, by Agencia

Estat de Investigación, and by Fondo Europeo de Desarrollo Regional. We thank the Generalitat de Catalunya for funding our research group (2017/SGR625). We are sincerely grateful to the Spanish Ministerio de Ciencia, Innovación y Universidades for awarding a predoctoral fellowship to MR (Formación de Profesorado Universitario, 2018). We are indebted to the Biobanc-Hospital Clinic-Institut d'Investigacions Biomèdiques August Pi i Sunyer (IDIBAPS), integrated in the Spanish National Biobank Network, for samples and data procurement. We are sincerely grateful to Michael Maudsley for correcting the English version of the manuscript.

SUPPLEMENTARY MATERIAL

The Supplementary Material for this article can be found online at: <https://www.frontiersin.org/articles/10.3389/fimmu.2021.618193/full#supplementary-material>

REFERENCES

- Catola G, Achúcarro N. Über Die Entstehung De Amyloidkörperchen in Zentralnervensystem. *Virchows Arch f Path Anat (1906)* (1906) 184:454–69. doi: 10.1007/BF01999854
- Cavanagh JB. Corpora-Amylacea and the Family of Polyglucosan Diseases. *Brain Res Rev* (1999) 29:265–95. doi: 10.1016/S0165-0173(99)00003-X
- Sakai M, Austin J, Witmer F, Trueb L. Studies of Corpora Amylacea. *Arch Neurol* (1969) 21:526–44. doi: 10.1001/archneur.1969.00480170098011
- Sbarbati A, Carner M, Colletti V, Osculati F. Extrusion of Corpora Amylacea From the Marginal Glia at the Vestibular Root Entry Zone. *J Neuropathol Exp Neurol* (1996) 55:196–201. doi: 10.1097/00005072-199602000-00008
- Pirici D, Margaritescu C. Corpora Amylacea in Aging Brain and Age-Related Brain Disorders. *J Aging Gerontol* (2014) 2:33–57.
- Radhakrishnan A, Radhakrishnan K, Radhakrishnan VV, Mary PR, Kesavadas C, Alexander A, et al. Corpora Amylacea in Mesial Temporal Lobe Epilepsy: Clinico-Pathological Correlations. *Epilepsy Res* (2007) 74:81–90. doi: 10.1016/j.eplepsyres.2007.01.003
- Rohn TT. Corpora Amylacea in Neurodegenerative Diseases: Cause or Effect? *Int J Neurol Neurother* (2015) 2:031. doi: 10.23937/2378-3001/2/2/1031
- Singhrao SK, Neal JW, Piddlesden SJ, Newman GR. New Immunocytochemical Evidence for a Neuronal/Oligodendroglial Origin for Corpora Amylacea. *Neuropathol Appl Neurobiol* (1994) 20:66–73. doi: 10.1111/j.1365-2990.1994.tb00958.x
- Augé E, Bechmann I, Llor N, Vilaplana J, Krueger M, Pelegrí C. Corpora Amylacea in Human Hippocampal Brain Tissue Are Intracellular Bodies That Exhibit a Homogeneous Distribution of Neo-Epitopes. *Sci Rep* (2019) 9:2063. doi: 10.1038/s41598-018-38010-7
- Augé E, Cabezón I, Pelegrí C, Vilaplana J. New Perspectives on Corpora Amylacea in the Human Brain. *Sci Rep* (2017) 7:41807. doi: 10.1038/srep41807
- Schipper HM, Cissé S. Mitochondrial Constituents of Corpora Amylacea and Autofluorescent Astrocytic Inclusions in Senescent Human Brain. *Glia* (1995) 14:55–64. doi: 10.1002/glia.440140108
- Selmaj K, Pawłowska Z, Walczak A, Koziolkiewicz W, Raine CS, Cierniewski CS. Corpora Amylacea From Multiple Sclerosis Brain Tissue Consists of Aggregated Neuronal Cells. *Acta Biochim Pol* (2008) 55:43–9. doi: 10.18388/abp.2008_3199
- Ferraro A, Damon LA. The Histogenesis of Amyloid Bodies in the Central Nervous System. *Arch Pathol* (1931) 12:229–44.
- Meng H, Zhang X, Blaivas M, Wang MM. Localization of Blood Proteins Thrombospondin1 and ADAMTS13 to Cerebral Corpora Amylacea. *Neuropathology* (2009) 29:664–71. doi: 10.1111/j.1440-1789.2009.01024.x
- Martin JE, Mather K, Swash M, Garofalo O, Leigh PN, Anderton BH. Heat Shock Protein Expression in Corpora Amylacea in the Central Nervous System: Clues to Their Origin. *Neuropathol Appl Neurobiol* (1991) 17:113–9. doi: 10.1111/j.1365-2990.1991.tb00702.x
- Gáti I, Leel-Ossi L. Heat Shock Protein 60 in Corpora Amylacea. *Pathol Oncol Res* (2001) 7:140–4. doi: 10.1007/BF03032581
- Suzuki A, Yokoo H, Kakita A, Takahashi H, Harigaya Y, Ikota H, et al. Phagocytized Corpora Amylacea as a Histological Hallmark of Astrocytic Injury in Neuromyelitis Optica. *Neuropathology* (2012) 32:587–94. doi: 10.1111/j.1440-1789.2012.01299.x
- Libard S, Popova SN, Amini RM, Kärjä V, Pietiläinen T, Hämäläinen KM, et al. Human Cytomegalovirus Tegument Protein pp65 is Detected in All Intra- and Extra-Axial Brain Tumours Independent of the Tumour Type or Grade. *PLoS One* (2014) 9:e108861. doi: 10.1371/journal.pone.0108861
- Pisa D, Alonso R, Rábano A, Carrasco L. Corpora Amylacea of Brain Tissue From Neurodegenerative Diseases Are Stained With Specific Antifungal Antibodies. *Front Neurosci* (2016) 10:86. doi: 10.3389/fnins.2016.00086
- Pisa D, Alonso R, Marina AI, Rábano A, Carrasco L. Human and Microbial Proteins From Corpora Amylacea of Alzheimer's Disease. *Sci Rep* (2018) 8:9880. doi: 10.1038/s41598-018-28231-1
- Augé E, Duran J, Guinovart JJ, Pelegrí C, Vilaplana J. Exploring the Elusive Composition of Corpora Amylacea of Human Brain. *Sci Rep* (2018) 8:13525. doi: 10.1038/s41598-018-31766-y
- Wander CM, Tseng J, Song S, Al Housseiny HA, Tart DS, Ajit A, et al. The Accumulation of Tau-Immunoreactive Hippocampal Granules and Corpora Amylacea Implicates Reactive Glia in Tau Pathogenesis During Aging. *iScience* (2020) 23:101255. doi: 10.1016/j.isci.2020.101255
- Navarro PP, Genoud C, Castaño-Díez D, Graff-Meyer A, Lewis AJ, de Gier Y, et al. Cerebral Corpora Amylacea Are Dense Membranous Labyrinths Containing Structurally Preserved Cell Organelles. *Sci Rep* (2018) 8:18046. doi: 10.1038/s41598-018-36223-4
- Riba M, Augé E, Campo-Sabariz J, Moral-Anter D, Molina-Porcel L, Ximelis T, et al. Corpora Amylacea Act as Containers That Remove Waste Products From the Brain. *Proc Natl Acad Sci USA* (2019) 116:26038–48. doi: 10.1073/pnas.1913741116
- Jucker M, Walker LC, Schwarz P, Hengemihle J, Kuo H, Snow AD, et al. Age-Related Deposition of Glia-Associated Fibrillar Material in Brains of C57BL/6 Mice. *Neuroscience* (1994) 60:875–89. doi: 10.1016/0306-4522(94)90269-0
- Lamar CH, Hinsman EJ, Henrikson CK. Alterations in the Hippocampus of Aged Mice. *Acta Neuropathol* (1976) 36:387–91. doi: 10.1007/BF00699644
- Manich G, Cabezón I, Augé E, Pelegrí C, Vilaplana J. Periodic acid-Schiff Granules in the Brain of Aged Mice: From Amyloid Aggregates to Degenerative Structures Containing Neo-Epitopes. *Ageing Res Rev* (2016) 27:42–55. doi: 10.1016/j.arr.2016.03.001
- Manich G, Cabezón I, Camins A, Pallás M, Liberski PP, Vilaplana J, et al. Clustered Granules Present in the Hippocampus of Aged Mice Result From a

- Degenerative Process Affecting Astrocytes and Their Surrounding Neuropil. *Age* (2014) 36:9690. doi: 10.1007/s11357-014-9690-8
29. Augé A, Pelegrí C, Manich G, Cabezón I, Guinovart JJ, Duran J, et al. Astrocytes and Neurons Produce Distinct Types of Polyglucosan Bodies in Lafora Disease. *Glia* (2018) 66:2094–107. doi: 10.1002/glia.23463
 30. Manich G, del Valle J, Cabezón I, Camins A, Pallàs M, Pelegrí C, et al. Presence of a Neo-Epitope and Absence of Amyloid Beta and Tau Protein in Degenerative Hippocampal Granules of Aged Mice. *Age* (2014) 36:151–65. doi: 10.1007/s11357-013-9560-9
 31. Chou MY, Fogelstrand L, Hartvigsen K, Hansen LF, Woelkers D, Shaw PX, et al. Oxidation-Specific Epitopes Are Dominant Targets of Innate Natural Antibodies in Mice and Humans. *J Clin Invest* (2009) 119:1335–49. doi: 10.1172/JCI36800
 32. Kay M. Physiologic Autoantibody and Immunoglobulin Interventions During Aging. *Curr Aging Sci* (2013) 6:56–62. doi: 10.2174/1874609811306010008
 33. Pawelec G. Immunosenescence and Cancer. *Biogerontology* (2017) 18:717–21. doi: 10.1007/s10522-017-9682-z
 34. Singh R, Barden A, Mori T, Beilin L. Advanced Glycation End-Products: A Review. *Diabetologia* (2001) 44:129–46. doi: 10.1007/s001250051591
 35. Vollmers HP, Brändlein S. Natural Antibodies and Cancer. *N Biotechnol* (2009) 25:294–8. doi: 10.1016/j.nbt.2009.03.016
 36. Ehrenstein MR, Notley CA. The Importance of Natural IgM: Scavenger, Protector and Regulator. *Nat Rev Immunol* (2010) 10:778–86. doi: 10.1038/nri2849
 37. Grönwall C, Vas J, Silverman GJ. Protective Roles of Natural IgM Antibodies. *Front Immunol* (2012) 3:66. doi: 10.3389/fimmu.2012.00066
 38. Holodick NE, Rodríguez-Zhurbenko N, Hernández AM. Defining Natural Antibodies. *Front Immunol* (2017) 8:872. doi: 10.3389/fimmu.2017.00872
 39. Mannoor K, Xu Y, Chen C. Natural Autoantibodies and Associated B Cells in Immunity and Autoimmunity. *Autoimmunity* (2013) 46:138–47. doi: 10.3109/08916934.2012.748753
 40. Avrameas S. Natural Autoantibodies: From “Horror Autotoxicus” to “Gnothi Seauton”. *Immunol Today* (1991) 12:154–9. doi: 10.1016/0167-5699(91)90080-D
 41. Baumgarth N, Tung JW, Herzenberg LA. Inherent Specificities in Natural Antibodies: A Key to Immune Defense Against Pathogen Invasion. *Springer Semin Immunopathol* (2005) 26:347–62. doi: 10.1007/s00281-004-0182-2
 42. Reyneveld GI, Savelkoul HFJ, Parmentier HK. Current Understanding of Natural Antibodies and Exploring the Possibilities of Modulation Using Veterinary Models. A Review. *Front Immunol* (2020) 11:2139. doi: 10.3389/fimmu.2020.02139
 43. Chen Y, Park YB, Patel E, Silverman GJ. Igm Antibodies to Apoptosis-Associated Determinants Recruit C1q and Enhance Dendritic Cell Phagocytosis of Apoptotic Cells. *J Immunol* (2009) 9 182:6031–43. doi: 10.4049/jimmunol.0804191
 44. Lutz HU, Binder CJ, Kaveri S. Naturally Occurring Auto-Antibodies in Homeostasis and Disease. *Trends Immunol* (2009) 30:43–51. doi: 10.1016/j.it.2008.10.002
 45. Maddur MS, Lacroix-Desmazes S, Dimitrov JD, Kazatchkine MD, Bayry J, Kaveri SV. Natural Antibodies: From First-Line Defense Against Pathogens to Perpetual Immune Homeostasis. *Clin Rev Allergy Immunol* (2020) 58:213–28. doi: 10.1007/s12016-019-08746-9
 46. Bovin NV. Natural Antibodies to Glycans. *Biochemistry* (2013) 78:786–97. doi: 10.1134/S0006297913070109
 47. Haji-Ghassemi O, Blackler RJ, Young NM, Evans SV. Antibody Recognition of Carbohydrate Epitopes. *Glycobiology* (2015) 25:920–52. doi: 10.1093/glycob/cwv037
 48. Goldin A, Beckman JA, Schmidt AM, Creager MA. Advanced Glycation End Products: Sparking the Development of Diabetic Vascular Injury. *Circulation* (2006) 114:597–605. doi: 10.1161/CIRCULATIONAHA.106.621854
 49. Xia L, Gildersleeve JC. Anti-Glycan IgM Repertoires in Newborn Human Cord Blood. *PLoS One* (2019) 14:e0218575. doi: 10.1371/journal.pone.0218575
 50. Varki A. Biological Roles of Glycans. *Glycobiology* (2017) 27:3–49. doi: 10.1093/glycob/cww086
 51. Liu HM, Anderson K, Catterson B. Demonstration of a Keratan Sulfate Proteoglycan and a Mannose-Rich Glycoconjugate in Corpora Amylacea of the Brain by Immunocytochemical and Lectin-Binding Methods. *J Neuroimmunol* (1987) 14:49–60. doi: 10.1016/0165-5728(87)90100-7
 52. Coulbaly FS, Youan BB. Concanavalin A–Polysaccharides Binding Affinity Analysis Using a Quartz Crystal Microbalance. *Biosens Bioelectron* (2014) 59:404–11. doi: 10.1016/j.bios.2014.03.040
 53. Goldstein IJ, Hayes CE. The Lectins: Carbohydrate-Binding Proteins of Plants and Animals. *Adv Carbohydr Chem Biochem* (1978) 35:127–340. doi: 10.1016/S0065-2318(08)60220-6
 54. Goldstein IJ, Reichert CM, Misaki A. Interaction of Concanavalin A With Model Substrates. *Ann N Y Acad Sci* (1974) 234:283–96. doi: 10.1111/j.1749-6632.1974.tb53040.x
 55. Nature Editorial. It’s Time to Talk About Ditching Statistical Significance. *Nature* (2019) 567:283. doi: 10.1038/d41586-019-00874-8
 56. Franz S, Herrmann K, Führnrohr B, Sheriff A, Frey B, Gaipf US, et al. After Shrinkage Apoptotic Cells Expose Internal Membrane-Derived Epitopes on Their Plasma Membranes. *Cell Death Differ* (2007) 14:733–42. doi: 10.1038/sj.cdd.4402066
 57. Gonzalez-Quintela A, Alende R, Gude F, Campos J, Rey J, Meijide LM, et al. Serum Levels of Immunoglobulins (Igg, IgA, IgM) in a General Adult Population and Their Relationship With Alcohol Consumption, Smoking and Common Metabolic Abnormalities. *Clin Exp Immunol* (2008) 151:42–50. doi: 10.1111/j.1365-2249.2007.03545.x
 58. American Diabetes Association. 2. Classification and Diagnosis of Diabetes: Standards of Medical Care in Diabetes-2020. *Diabetes Care* (2020) 43(Suppl. 1):S14–31. doi: 10.2337/dc20-S002
 59. Jafar N, Edriss H, Nugent K. The Effect of Short-Term Hyperglycemia on the Innate Immune System. *Am J Med Sci* (2016) 351:201–11. doi: 10.1016/j.amjms.2015.11.011
 60. Dana TG, Rayyan AK. Diabetic Complications and Dysregulated Innate Immunity. *Front Biosci* (2008) 13:1227–39. doi: 10.2741/2757
 61. Juliana C, Janine C, Cresio A. Infections in Patients With Diabetes Mellitus: A Review of Pathogenesis. *Indian J Endocrinol Metab* (2012) 16:27–36. doi: 10.4103/2230-8210.94253

Conflict of Interest: The authors declare that the research was conducted in the absence of any commercial or financial relationships that could be construed as a potential conflict of interest.

Copyright © 2021 Riba, Augé, Tena, del Valle, Molina-Porcel, Ximelis, Vilaplana and Pelegrí. This is an open-access article distributed under the terms of the Creative Commons Attribution License (CC BY). The use, distribution or reproduction in other forums is permitted, provided the original author(s) and the copyright owner(s) are credited and that the original publication in this journal is cited, in accordance with accepted academic practice. No use, distribution or reproduction is permitted which does not comply with these terms.

3. ARTICLE 3

FROM *CORPORA AMYLACEA* TO WASTEOSOMES: HISTORY AND PERSPECTIVES

Marta Riba, Jaume del Valle, Elisabet Augé, Jordi Vilaplana, Carme Pelegrí

Ageing Research Reviews 2021, 72, 101484

DOI: [10.1016/j.arr.2021.101484](https://doi.org/10.1016/j.arr.2021.101484)

JCR 2020 IF: 10,895

RESUM

Antecedents: Els estudis previs realitzats en els CA del SNC han posat de manifest la seva funció com a estructures que capturen i acumulen productes de rebuig del cervell, i que són posteriorment fagocitades per macròfags constituint un sistema d'eliminació de substàncies de rebuig cerebrals.

Objectiu: Identificar similituds i divergències entre els CA dels diferents òrgans del cos humà, per tal d'establir una hipòtesi global i integradora envers la funció i la significança dels CA en l'organisme.

Material i mètodes: Es va realitzar una cerca i una recopilació exhaustiva dels articles relacionats amb els CA humans i es va procedir a determinar les característiques descrites dels CA en diferents òrgans en termes de composició, aparença i funció plantejada. Per tal de determinar-ne les característiques descrites, es va tenir en compte que el terme amilaci i amiloide s'estan utilitzant actualment de forma indistinta per anomenar estructures de poliglucosà semblants al midó i per anomenar proteïnes fibril·lars amb tendència a l'agregació, i que aquest fet dona lloc a interpretacions errònies a l'hora d'establir la composició dels CA. D'acord amb això, en el treball, s'han utilitzat els termes *amyloacea(p)* i *amiloid(p)* per fer referència a les estructures proteïnàcies i *amyloacea(s)* i *amiloid(s)* per referir-se a les estructures glucídiques similars al midó. Un cop feta la recopilació i anàlisi de la informació referent als CA dels diferents òrgans, el conjunt de resultats extrets van ser integrats per generar una hipòtesi conjunta referent a la funció dels CA del l'organisme humà.

Resultats: En la revisió cronològica dels diferents estudis sobre CA en diferents òrgans i estructures es va observar la presència d'alguns resultats contradictoris. No obstant això, algunes característiques es van mostrar recurrents, fet que va permetre obtenir una interpretació global i inclusiva sobre els CA. Una d'aquestes característiques recurrents va ser que en totes les localitzacions i/o teixits s'havia descrit que els CA acumulen substàncies de rebuig i/o productes potencialment tòxics, derivats per exemple de l'edat o de condicions fisiopatològiques. D'altra banda, en tots els teixits els CA han estat caracteritzats com a PAS positius, cosa que indica un elevat contingut en polisacàrids. Pel que fa al contingut proteic, els resultats publicats posen de manifest certa controvèrsia. Tot i això, la gran diversitat de components descrits en els CA dels diferents òrgans semblava indicar que la composició dels CA varia segons la seva ubicació i l'ambient on són generats. Aquest fet recolza la hipòtesi que els CA són estructures acumuladores de substàncies de rebuig generades allà on es localitzen. Tot i aquestes diferències de composició, els CA en els diferents teixits mostren una ultraestructura similar. Addicionalment, diversos estudis apunten una relació entre els CA i macròfags i la possible fagocitosis dels CA per part d'aquests. Aquesta relació ha estat observada, concretament, en CA del nervi òptic, en teixit pulmonar, en pròstata i en cultius cel·lulars amb macròfags THP-1. Cal remarcar que, malgrat aquestes característiques

comunes, en alguns teixits els CA han estat descrits com a intracel·lulars i en altres com a extracel·lulars.

Conclusions: Els resultats i conclusions observats en els estudis revisats permeten definir els CA com a estructures generades per cèl·lules astrocítiques, en el cervell, o per cèl·lules epitelials o glandulars específiques, en els altres teixits, que segresten i acumulen substàncies de rebuig i altres productes de diferents orígens en un esquelet glucídic. Posteriorment, els CA són extruïts al medi extern o a espais intersticials on, en aquest segon cas, són fagocitats per macròfags. Tot això fa que els CA formin part d'un sistema d'eliminació de productes de rebuig. A més a més, el fet que els CA siguin generats per cèl·lules i seguidament, siguin extruïts, permet explicar perquè en determinades circumstàncies i localitzacions alguns CA es troben intracel·lulars i en d'altres extracel·lulars. Finalment, i per tal d'evitar interpretacions errònies derivades de l'ús del terme *amyloidea*, es proposa reanomenar els CA (*corpora amyloidea*) com a *wasteosomes*, mot que inclou el terme en *waste* (producte de rebuig) i *soma* (cos en llatí), de manera que s'emfatitza l'acumulació de substàncies de rebuig en aquestes estructures més que no pas la seva confusa propietat amilàcia.

Contents lists available at [ScienceDirect](https://www.sciencedirect.com)

Ageing Research Reviews

journal homepage: www.elsevier.com/locate/arrFrom *corpora amylacea* to wasteosomes: History and perspectivesMarta Riba^{a,b,c}, Jaume del Valle^{a,b,c}, Elisabet Augé^{a,b,c}, Jordi Vilaplana^{a,b,c,*}, Carme Pelegrí^{a,b,c,1}^a Secció de Fisiologia, Departament de Bioquímica i Fisiologia, Facultat de Farmàcia i Ciències de l'Alimentació, Universitat de Barcelona, 08028 Barcelona, Spain^b Institut de Neurociències, Universitat de Barcelona, 08035 Barcelona, Spain^c Centros de Biomedicina en Red de Enfermedades Neurodegenerativas (CIBERNED), 28031 Madrid, Spain

ARTICLE INFO

Keywords:

corpora amylacea
Amyloid
Polyglucosan
Ageing
Hyaline bodies
Lafora disease

ABSTRACT

Corpora amylacea (CA) have been described in several human organs and have been associated with ageing and several pathological conditions. Although they were first discovered two centuries ago, their function and significance have not yet been identified. Here, we provide a chronological summary of the findings on CA in various organs and identify their similarities. After collecting and integrating these findings, we propose to consider CA as waste containers created by specific cells, which sequester waste products and foreign products, and assemble them within a glycan structure. The containers are then secreted into the external medium or interstitial spaces, in this latter case subsequently being phagocytosed by macrophages. This proposal explains, among others, why CA are so varied in content, why only some of them contain fibrillary amyloid proteins, why all of them contain glycan structures, why some of them contain neo-epitopes and are phagocytosed, and why they can be intracellular or extracellular structures. Lastly, in order to avoid the ambiguity of the term amyloid (which can indicate starch-like structures but also insoluble fibrillary proteins), we propose renaming CA as “wasteosomes”, emphasising the waste products they entrap rather than their misleading amyloid properties.

1. Introduction

The presence of ageing-related granular structures has long been known in several human tissues, and was first described in histopathology reports. “*That is to say, in the prostate gland, which was enlarged, and, in its external circumference, of a red color inclining to brown, I found within the remaining part of its substance; which was in other respects in a natural state; granules of tobacco as it were, of a yellowish colour inclining to blackness; and those in several places. (...) But of what nature are these granules? For I have found them in many bodies, and not then for the first time*”. This description was given by Morgagni in 1779 (Morgagni, 1779), and seems to be the first recorded observation indicating the presence of granules in the prostate gland (Prather and Skinner, 1956).

Similar granular bodies were also described by Purkinje in 1837, in the brain of elderly patients (Catola and Achúcarro, 1906), while Virchow found them in brain, spinal cord, at the neck of the bladder and in the so-called female prostate (Eastman, 1897). In 1854, Virchow noted that the granules shared some similarities with starch, and called

them *corpora amylacea* (CA), i.e., starch bodies in Latin (Virchow, 1854). Since then, these bodies have commonly been referred to as CA. Friedreich described them in the respiratory organs (Friedreich, 1856), Hildebrand in a sarcoma of the sternum, in 1895, and Lubarsch in a tumour of the suprarenal capsule (Eastman, 1897).

In 1897, Eastman wrote “*Widely varying hypotheses concerning the histogenesis of these bodies have been proposed by those whose attention they have attracted, the same after painstaking investigations, but none has led to an agreement as to the meaning of the observations made*”. Today, more than two centuries later, his words remain true, as the meaning of these granular structures has not yet been clarified.

To date, the CA in each organ or tissue have been analysed or interpreted almost exclusively in terms of the organ or tissue in which they occur, without taking into account what is known about CA in other organs or structures and thus without adopting a broader perspective. In this review, we provide an extensive review of the findings on CA in the various human tissues and identify their similarities and differences in terms of composition, appearance and hypothesised function. As neither

* Correspondence to: Secció de Fisiologia, Departament de Bioquímica i Fisiologia, Facultat de Farmàcia i Ciències de l'Alimentació, Universitat de Barcelona. Avda Joan XXIII 27-31, 08028 Barcelona, Spain

E-mail address: vilaplana@ub.edu (J. Vilaplana).

¹ Jordi Vilaplana and Carme Pelegrí contributed equally to this work.

<https://doi.org/10.1016/j.arr.2021.101484>

Received 16 July 2021; Received in revised form 1 October 2021; Accepted 5 October 2021

Available online 9 October 2021

1568-1637/© 2021 The Author(s).

Published by Elsevier B.V. This is an open access article under the CC BY-NC-ND license

(<http://creativecommons.org/licenses/by-nc-nd/4.0/>).

the function nor the pathophysiological significance of CA has yet been identified, two centuries after they were first described, our overview of CA will help to clarify these aspects.

Before starting, it should be noted that the term amyloid (i.e., starch-like in Latin) is currently used to describe two different kinds of structure: polyglucosan structures similar to starch, but also some types of fibrillary proteins that tend to aggregate, such as β -amyloid in Alzheimer's disease or synuclein in Parkinson's disease. Use of the term amyloid to describe these proteins reflects the original erroneous identification of these proteinaceous substances as starch because they stain with iodine, considered a marker of starch-like structures. In the literature, the concept of amyloid bodies frequently refers to proteinaceous amyloid bodies, whereas amyloids or corpora amyloidea usually refer to polyglucosan amyloid bodies. However, these terms are sometimes used interchangeably, generating confusion and misinterpretation. In order to differentiate between the two structures, it should be borne in mind that polyglucosan amyloid structures stain with Periodic acid-Schiff (PAS), whereas the proteinaceous structures stain with either Congo red or thioflavin. In order to avoid confusion, here we will use the terms amyloidea(p) and amyloid(p) to refer to the proteinaceous structures, and amyloidea(s) and amyloid(s) to refer to starch or carbohydrate structures. The term amyloidosis will be reserved for the abnormal build-up of amyloid(p) in tissues or organs.

2. Chronological review

2.1. Corpora amyloidea in the central nervous system

Since CA were first described in the brain by Purkinje and Virchow, many studies have examined these structures in the central nervous system (CNS). Robertson (1900) argued that CA were the product of cell degeneration, while Ellis (1920) described them as being generally associated with normal ageing. In a book on nervous system pathology published in 1923, Buzzard and Greenfield ruled out the idea that these bodies had any pathological significance, and this opinion endured for many years (Buzzard and Greenfield, 1923). Ferraro and Damon (1931) published an article reviewing the findings to date on the origin of these bodies in several tissues and claimed that they were merely "post-mortem" artefacts formed by protein precipitates. In 1933, large numbers of CA stained by haematoxylin and eosin were described in the *filum terminale* from several cases irrespective of age, sex or cause of death (Harmer, 1933). They were located beneath the pia mater but also formed masses scattered throughout the tissue, in which large numbers of glial cells, including astrocytes, were also found (Tarlov, 1938). However, no study reported the possible function or meaning of these bodies at the end of the spinal cord.

In 1953, Alder conducted a detailed study of CA in the CNS, and described them as amyloid(s) structures that were abundant in the subpial and subependymal regions (Alder, 1953). He observed that their presence constituted one of the typical changes that occurred in senile and senescent brains, although they were also encountered under a variety of conditions in widely varying amounts and at different sites in the CNS. Subsequent studies indicated that brain CA were located within the processes of astrocytes (Ramsey, 1965), but others found them in neurons (Anzil et al., 1974). Several attempts were made at the time to elucidate the composition of CA. Some studies demonstrated that brain CA were not amyloid(p) deposits because they did not stain with Congo red or possess the typical rigid fibrillary structure, but instead contained a glycogen-like substance to which phosphate and sulphate were bound (Ramsey, 1965; Stam and Roukema, 1973). In 1969, Sakai and co-workers developed the first method to isolate CA, and observed that samples from patients aged over 70 years old were strongly stained with both iodine and PAS-dimideone. They determined that CA were formed mainly by glucose polymers and did not contain fucose or mannose. No evidence was obtained of significant quantities of mucopolysaccharides, mucoproteins or glycoproteins, but small amounts of protein and

phosphate were detected. The amount of hexoses was estimated at about 68.4% (by weight), that of proteins 8.1% and the remaining 23.5% was unidentified (Sakai et al., 1969a, 1969b). They concluded that CA were round bodies lying inside the cytoplasm of fibrillary astrocytes and the result of a defect in glycogen metabolism. They found CA in the hippocampus, subependymal zones of the ventricles and beneath the pia, and indicated that proximity to cerebrospinal fluid (CSF) was a prominent feature of their distribution.

In 1980, Avendano et al. examined one hundred autopsy eyes and found CA in 93% of cases, either in the optic nerve or the inner retinal layers, being more common in older individuals. CA were round or oval and measured 2–20 μ m in diameter, with those in the retina being smaller than those in the optic nerve. CA were usually present as intracellular structures containing randomly oriented, elongated and straight 6–7 nm thick filaments, were PAS positive and were composed of sulphated polysaccharides. In some cases, CA were surrounded by myelin, which led the authors to suggest that these structures contained degenerated products of axons rather than of glial cells, although they did not rule out an association with the degeneration of glial cells. Kubota et al. (1993) also studied the presence of CA in sections of the retina and the optic nerve from patients with malignant melanoma of the choroid, patients with glaucoma and control patients. The count of CA in sections from non-glaucomatous subjects increased significantly with advancing age and CA were more abundant in eyes with melanoma than in eyes with glaucoma. The authors concluded that CA represent intraneuronal ageing products that are diminished in eyes with end-stage glaucoma due to neuronal loss.

Research interest in these bodies in the nervous system increased when they were described to accumulate in the human brain in the course of normal ageing (Mrak et al., 1997), and to a much larger extent in Alzheimer's disease (Cissé et al., 1993; Inoue et al., 1996) and other neurodegenerative conditions (Chung and Horoupian, 1996; Robitaille et al., 1980). In 1994, Singhrao and colleagues published an article about the origin of these bodies and proposed that they were accumulations of waste products from neurons and oligodendrocytes (Singhrao et al., 1994). In 1995, Schipper and Cissé determined that CA progressively accumulated in periventricular regions with advancing age, were astrocytic in origin and contained various heat shock proteins and ubiquitin (Schipper and Cissé, 1995). In biopsied material from the vestibular root entry zone in cases of Meniere's disease, Sbarbati et al. (1996) observed at ultrastructural level that CA were sited in astroglial processes and mainly located in the *glia limitans*, near the pial region. In some CA, the astrocytic cytoplasmic membrane presented folds that created fissures which, according to these authors, could split the CA apart, allowing them to escape into the pial connective tissue or subpial space. In these cases, CA could be observed without the cytoplasmic membrane, i.e., in an extracellular location. Moreover, Schipper and Cissé (1995) suggested that CA were derived from autofluorescent Gomori-positive astrocytic granules which reside in periventricular regions of the senescent CNS. They proposed that, in the ageing human brain, degenerating mitochondria within periventricular astrocytes gave rise to autofluorescent cytoplasmic granules and CA.

In order to provide an insight into the composition of CA, Steyaert et al. (1990) purified and analysed CA from elderly individuals without neurological disease. Most CA showed a spherical shape but some of them displayed an ovoid or even an elongated shape and they presented a wide range of sizes. In phase-contrast microscopy, isolated CA showed a dense core surrounded by a rim of lighter material, while by scanning electron microscopy (SEM), they appeared to possess a lumpy surface. The amount of protein in the isolated CA was about 3.6% of the total dry weight. With respect to identification of the proteins contained in CA, different studies have been performed, mainly based on immunohistochemical procedures. Loeffler et al. (1993) described the presence of tau protein in CA from human retina and optic nerve. Amyloid precursor protein (Tate-Ostroff et al., 1989) and proteins specifically involved in ageing or stress, such as heat shock proteins (Iwaki et al., 1996),

ubiquitin (Kawashima et al., 1999) and advanced glycation end products (Iwaki et al., 1996; Kimura et al., 1998), have also been identified in brain CA. Hoyaux et al. (2000) studied the presence of S100 proteins in brain CA, which are calcium-binding proteins that have been described as being involved in neurodegenerative diseases (Li et al., 1998; Mrak et al., 1996). They detected the presence of S100 A1, A2, A3, A4, A5, A6, A8, A9 and A12, but not S100B, which is abundant in astrocytes and to a lesser extent in neurons from normal brain. The authors suggested that S100B could be rapidly degraded by the normal cell machinery and did not accumulate in CA, which may host substances escaping normal cell catabolism. A1, A8 and A9 were the most frequent S100 proteins found in CA, with A8 and A9 being highly expressed in activated granulocytes and found in serum from patients with chronic inflammatory disorders (Kerckhoff et al., 1998).

Chung and Horoupian (1996) considered CA a marker for mesial temporal sclerosis, the most frequent abnormality in temporal lobectomies performed for medically intractable seizure disorders. In mild cases, moderate to abundant numbers of CA were present in extra-hippocampal tissues, showing a predilection for the white matter parenchyma, but in the most severe cases, massive deposits of CA were seen in the pyramidal layer, endfolium and dentate fascia of hippocampus, in a distribution paralleling the neuronal loss that characterises mesial temporal sclerosis. These bodies were PAS positive and associated with some scattered reactive astrocytes (GFAP-positive), and thus an astrocytic role in the mechanisms underlying mesial temporal sclerosis was proposed.

Cavanagh (1998) supported the neuronal origin of brain CA, as he observed that the number of CA decreased in the spinal cord with the loss of neurons in motor neuron degeneration. Moreover, he hypothesised that CA may contribute to the removal of waste materials of highly metabolically active cells, as an analogy to the lysosome-lipofuscin system. In 1999, Cavanagh wrote an extensive review of CA and concluded that they may exert an important role in collecting products from cell metabolism, mainly during ageing but also in diseases in which many potentially toxic waste products are produced (Cavanagh, 1999). He suggested that age-related products of the glycation process of long-lived proteins become incorporated into a glucose polymer mass, which may grow in size over time and eventually be retained intracellularly, for example in cardiac myocytes and some axons, or transported by astrocytes to various brain surfaces. However, he also acknowledged that their exact function was not known yet.

Several studies continued to provide evidence that CA are a product of neurons. CA were observed in patients with pharmaco-resistant epilepsy, especially in areas of neuronal loss (Nishio et al., 2001). In a 2008 article about CA in the brain of patients with multiple sclerosis, Selmaj et al. (2008) reported that these structures accumulated remnants of neurons that were degenerating. A year later, Meng and co-workers concluded in their study that CA were conglomerates of proteins from neurons that were degenerating and blood elements that had entered the brain when the blood-brain barrier had been broken (Meng et al., 2009).

However, in a study of neuromyelitis optica (NMO), Suzuki et al. (2012) strongly supported the hypothesis that CA were a signal of astrocyte rather than neuron destruction. In fact, some authors consider that NMO is an astrocytopathy provoked by an autoantibody against aquaporin-4 (Lennon et al., 2005; Roemer et al., 2007; Suzuki et al., 2012). Suzuki et al. (2012) reported that CA were expelled from astrocyte processes and phagocytised by macrophages in early phase lesions of NMO in the optic nerve, the spinal cord or the *medulla oblongata*. In the lesions, the phagocytised CA were significantly smaller than intact CA and both were PAS positive. A subsequent study of the same disease also found numerous phagocytosed CA within the infiltrating macrophages in the necrotic lesion (Ohara et al., 2019).

Following another line of research, the olfactory tract of patients with Alzheimer's disease and controls was analysed because olfaction declines with ageing and appears to be a prodromal sign of cognitive impairment in progressive neurodegenerative diseases (Bathini et al.,

2019). This study revealed an abundance of CA in control subjects but a decline in their density in the first stages of the disease, which appeared to persist over the course of the disease. Moreover, a gradual shift was observed in cytoskeletal proteins with increasing severity of dementia. These bodies were round, with a diameter greater than 10 μm , and extracellular. They showed negative staining for myelin, thus ruling out any oligodendrocyte-derived content. After performing staining for Jagged 1, MAP2, GAD67, PDS95 and synaptophysin, the authors concluded that CA from the olfactory tract were of neuronal origin and contained synaptic markers, neurosignalling molecules and cytoskeletal proteins with an ensheathing glial layer.

Meanwhile, a recent study using label-free multiphoton microscopy found that CA are composed of polyglucosans with an unusual, abnormally branched amylopectin-like structure. Moreover, the study proved that CA are not located within axons (Galli et al., 2018). With respect to CA composition, several fungal and bacterial proteins have recently been described in brain CA, contributing to the complexity of the proteins that form part of these structures (Pisa et al., 2016, 2018). Mold et al. (2018) found mineralised deposits in CA from the hippocampus of a multiple sclerosis patient, and again, a role for CA in collecting the remnants of cell death was suggested. Den Haan et al. (2018) reported the presence of amyloid- β in CA from the retina of patients with Alzheimer's disease and controls, identified by Klüber-PAS staining. These CA were described as rounded extracellular deposits and were positive for 6E10 (amyloid- β 1–16) and 12F4 (amyloid- β 1–42) antibodies but negative for 4G8 (amyloid- β 17–24) and an APP c-terminal antibody.

In 2017, our group described the presence of neo-epitopes in CA from the hippocampus of patients with Alzheimer's disease, and the existence of plasmatic IgM natural antibodies that recognise these neo-epitopes (Augé et al., 2017). It should be noted that neo-epitopes are epitopes associated with the elimination of residual products and are commonly recognised by natural antibodies of the IgM isotype. Given that plasmatic IgMs do not cross the blood-brain barrier, natural IgMs do not have access to CA unless the blood-brain barrier is injured or CA are extruded out of the brain. Our findings supported the idea that CA, with their neo-epitopes as targets for the immune system, are waste containers involved in protective or cleaning mechanisms. Moreover, we reported that some positive immunostaining results described in several reports analysing CA might have been induced by contaminant IgMs present in commercial antibodies, giving rise to false positive results and indicating the need to revise the immunohistochemistry studies performed on CA. In 2018, we ruled out the presence of tau protein and β -amyloid peptides in CA, at least at immunofluorescence detection levels, but detected the presence of ubiquitin and p62 proteins, both associated with waste substance elimination processes, and glycogen synthase, an indispensable enzyme for polyglucosan formation (Augé et al., 2018a). A recent study by Wander et al. (2020) described the presence of tau protein in some, but not all, CA from control subjects and Alzheimer's disease patients, and also found astrocytes associated with them. They reported a potential negative correlation between tau-positive CA and the severity of Braak staging, and suggested that CA could be a mean for astrocytes to clean neuronal debris, including those induced by age-related stress.

Based on correlative serial block-face scanning electron microscopy (SBF-SEM) and transmission electron microscopy (TEM), Navarro et al. (2018) concluded that brain hippocampal CA are primarily composed of densely packed, aggregated lipid membrane fragments and disrupted cellular organelles, such as mitochondria and lysosomes, together with glycogen granules and digestive vesicles. They suggested that CA originated from aggregated cell components that formed when intracellular biochemical properties were perturbed, and that the bulk of membranous and glycosylated cellular material was of lysosomal origin. In 2019, we showed that CA were intracellular astrocytic structures, as they were surrounded by a plasma membrane and included intermediate filaments compatible with GFAP (Augé et al., 2019). This was the first study to show the ultrastructure of immature CA, which present distinctive

characteristics with respect to mature CA. These latter contain an external region which accumulates residual products, such as degenerating mitochondria and membrane fragments, and an inner region with fibrillary material. Meanwhile, immature CA contain an inner region that is less structured and less compact than that of mature CA and also contain mitochondria, cellular debris and membranous blebs located inside and surrounding the inner structure. In the same study, we also showed that the neo-epitopes present in CA were uniformly localised throughout the entire structure.

Also in 2019, we demonstrated that CA are released from the brain to the CSF and are present in the deep cervical lymph nodes (DCLNs), into which the CSF drains through the meningeal lymphatic system (Riba et al., 2019). Moreover, we showed that CA can be phagocytosed by macrophages. Accordingly, we postulated that CA from human brain act as containers that collect waste products and participate in a mechanism to clean the brain. Moreover, we hypothesised that CA may contribute in some autoimmune brain diseases, exporting brain substances that interact with the immune system, and suggested that CA may contain biomarkers that could aid in the diagnosis of certain brain diseases.

2.2. Corpora amylacea in peripheral nerves

CA have also been found outside the CNS, in peripheral nerves (reviewed in Cenacchi et al., 2019). They have been described as a hallmark of chronic vestibular nerve impairment in patients with intractable Meniere's disease (Wang et al., 2019). The pathological changes reported in this study demonstrated that CA formation is highly correlated with the degree of central vestibular nerve impairment, and the authors suggested that CA assist in the clean-up of abnormal materials such as cell debris or lipofuscin. In these cases, no positive correlation was observed between CA density and ageing. From a broader perspective, it has been estimated that CA are present in sural peripheral nerves in up to 8.5% of the general population, almost always associated with polyneuropathies, and showing an increasing prevalence with age (Busard et al., 1990). However, as the sural nerve is a sensory nerve and CA seem more prone to accumulate in motor nerves (Cavanagh, 1999), the incidence of CA in nerves in the general population may be higher than 8.5%. Other studies have indicated the presence of CA in peripheral nerves, and most have described them as intraneuronal or intra-axonal deposits (Yagishita et al., 1977; Komure et al., 1985; Yoshikawa et al., 1990; Matsumuro et al., 1993; Lu et al., 2016). However, Wang et al. (2019) observed CA within the axonal area, but also found them in the endoneurium and epineurium.

2.3. Corpora amylacea in the prostate

Morgagni observed granular concretions in the prostate gland in 1779 and regarded them as a pathological product of precipitation in prostatic secretion (Morgagni, 1779). Later, Paulitzki found two different types of concretions: those that contained starch, as they stained with iodine and were degraded by saliva (supposedly due to their amylase content), and those which did not (Eastman, 1897). Posner also studied prostatic concretions but did not observe any staining with iodine, and thus concluded that prostatic concretions did not contain vegetable starch. He suggested instead that they contained lecithin, and classified these structures as calculus (Eastman, 1897). Seigert contended that these structures in the prostate resulted from the union of cell products, gland secretions and tissue fluids, and indicated that they frequently calcified. He attributed two principal qualities to these structures: a strong light-reflecting power and high resistance to the strongest chemical reagents (Eastman, 1897). After examining several prostates, Eastman (1897) reported that prostatic CA were related to degeneration of the epithelium, contained amyloid(s) material and exhibited broad concentric laminations. From that time, prostatic CA are usually considered as lamellated structures. In addition, Marx et al. (1965) indicated that prostatic CA were related to epithelial cell desquamation

and degeneration.

Smith (1966) observed that many studies concerning prostatic CA, concretions and calculi had been published and that the data were confusing. According to Röcken et al. (1996), prostatic CA could contain different types of endogenous and exogenous stones, the latter being formed in the bladder or the urinary system. Furthermore, endogenous stones could be divided into two entities: concretions, which consisted mainly of salt precipitates with apatite and whitlockite, had little protein content, were calcified, were mainly found in atrophic glands, did not stain with Congo red and were not deposits of amyloid(p) (Fox, 1963; Torres Ramirez et al., 1980; Sutor and Wooley, 1974); and prostatic CA, which have been described as a proteinaceous matrix which stained with Congo red, showed an X-ray diffraction pattern consistent with amyloid (p) and had a fibrillar ultrastructure (Schrodt and Murray, 1966; Gueft, 1972; Cross et al., 1992). All this evidence suggested that they were amyloid(p) deposits. Moreover, prostatic CA contain mucopolysaccharides, a characteristic of all amyloid(p) deposits (Pasqualucci and Macha, 1968).

An immunohistochemical study of the prostate in people aged over 85 years old revealed hyperplasia in every studied prostate, and CA were localised exclusively within the zones of hyperplasia (Röcken et al., 1996). The CA showed a polymorphic shape with an irregular inner structure and an eosinophilic appearance when stained with haematoxylin and eosin. Their size varied from as small as a single epithelial cell to as large as the entire lumen of a hyperplastic gland duct. These CA were homogeneously immunostained with anti-amyloid $\beta 2$ microglobulin ($A\beta 2M$) and intense immunostaining with anti- $A\beta 2M$ was also observed of the hyperplastic epithelium surrounding CA (Röcken et al., 1996). $\beta 2$ microglobulin is known to be the precursor protein of amyloid deposits associated with long-term haemodialysis (Gejyo et al., 1985), which relates CA to amyloid(p) deposits. However, according to Cohen et al. (2000), the staining with anti- $A\beta 2M$ was merely a false staining produced by endogenous biotin reactivity.

A study by Cohen et al. (2000) of the differences between benign and malignant prostatic secretions revealed that benign glands contained CA while cancerous ones did not, but did contain crystalloids and mucin accumulations. In benign glands, CA were present in the lumen of large ducts, with eosinophilic bodies (EB) attached to their surface. Biochemical analysis of CA showed that glycosaminoglycans were the main constituent. Moreover, prostatic secretory cells in benign glands were filled with 1 μm -diameter prostatic secretory granules (PSG). These PSG originated from the Golgi apparatus and contained many of the secreted cell constituents, including enzymes such as prostatic-specific antigen (PSA) and prostatic acid phosphatase (PAP) (Cohen et al., 1998). In cancerous glands, these PSG were almost completely absent, and PSA and PAP were dispersed in the cytoplasm of the secretory cells. Together, these findings revealed a dramatic change in the nature of the secretory process in malignant glands. Prostatic PSG, EB and CA are both Congo red and PAS positive structures. Prostatic CA contained glucosamine, galactose and sulphur, and the monosaccharide/protein ratio was 2:1, while this ratio was 30:1 in PSG (Cohen et al., 2000). The notion that prostatic CA arise from urinary proteins (Cross et al., 1992) was discarded, and histological findings as well as the composition suggested that PSG contributed to the formation of CA. In prostatic adenocarcinomas, the inability to form CA seems to stem from the fact that the entire secretory apparatus is absent (Cohen et al., 2000). This suggests that prostatic CA are the final consequence of the apocrine prostatic secretion and the accumulation of cellular remains (Cohen et al., 2000). Milord et al. (2000) found CA in benign reactive prostatic glands adjacent to infarcts. Although CA have frequently been described in benign prostatic acini and rarely observed in adenocarcinoma, Christian et al. (2005) contended that the presence of such inclusions cannot be used to rule out malignancy, as some cancerous acini did contain CA.

The presence of CA in normal and hyperplastic prostatic glands was further studied by Morales et al. (2005). They found that these structures were larger and more numerous in hyperplastic than in normal glands.

In normal glands CA were moderately stained with PAS, while in hyperplastic glands CA were moderately or strongly stained. The study of the expression of glycoconjugates in CA revealed the presence of fucose, mannose, sialic acid, N-acetyl-galactosamine and N-acetyl-glucosamine residues in both normal and hyperplastic glands, with an increase in the four former components in the hyperplastic ones. As these components are also expressed in the glandular epithelium, their results suggested that prostatic CA originate, at least in part, from prostatic secretion.

In 2011, Hammar found CA in prostate gland lumens and highlighted the absence of macrophages around them (Hammar, 2011). Sfanos et al. (2013) reviewed the relationship between infection, inflammation and prostate cancer and stated that CA were remnants of previous prostatic infections and presumably the precursors of calcified stones or prostatic calculi. In fact, an outstanding study by the same authors using high-performance liquid chromatography combined with tandem mass spectrometry demonstrated that the predominant protein components of both prostatic CA and calculi were proteins involved in acute inflammation and, in particular, proteins contained in neutrophil granules. The most prevalent protein was lactoferrin, an iron-binding protein traditionally recognised as bacteriostatic in innate immunity, and other proteins identified were S100 A8 and A9, myeloperoxidase and α -defensins (Sfanos et al., 2009). Moreover, they observed CA engulfed by macrophages and multinucleated giant cells (Sfanos et al., 2009).

Fritz et al. (2010) quantified the components of CA from prostate cancer patients. These structures were found in inflamed glands and the authors suggested that they were associated with age-related prostate tissue remodelling. With respect to their composition, 30–40% consisted of proteinaceous compounds (including mainly S100 A8 and A9), whereas the remainder corresponded to inorganic components comprising hydroxylapatite and whitlockite with high concentrations of Zn^{2+} ions. They reported that Ca^{2+} and Zn^{2+} played a critical role in promoting amyloid(p) assembly of S100 A8 and A9 proteins and formation of amyloid(p) fibrils. Other studies have also reported the presence of S100 A8 and S100 A9 in CA, as well as DNA and proteins from *E. coli* (Yanamandra et al., 2009), and the presence of bacterial “imprints” in prostatic calculi using SEM (Dessombz et al., 2012).

Badea et al. (2015) performed a histochemical and ultrastructural study of the intraluminal content of benign and malignant prostatic tissue. In this study, CA from some patients stained brown with von Kossa staining, indicating the presence of calcium or calcium salts, and some structures were interpreted as transitional forms from CA to prostatic calculi. Furthermore, some CA also stained with autometallography, which labels free or loosely bound heavy metal ions, and with antibodies against PSA. The authors found heterogeneous patterns of intraluminal structures in prostatic acini from the different patients and suggested that this heterogeneity might represent developmental stages of the same type of inclusion, CA or prostatic calculi. Their study also showed the ultrastructure of prostate CA, with fibrillar elements similar to amyloid(p). Kodaka et al. (2008) have also reported that primary prostatic calculi I to III begin from mineralisation of CA as a core, while organic substances that form stone IV might be derived from simple precipitation of prostatic secretions.

A huge study of 355 men with prostate cancer found CA in 84% of cases, in adjacent normal tissue, and this presence was strongly associated with pro-inflammatory factors and with some markers of less aggressive prostate cancer (DuPre et al., 2018). The authors suggested that CA formation might be a normal response to early cancers and could serve to consolidate inflammatory debris and thus prevent more aggressive or mutated tumours. Palangmonthip et al. (2020) also found an association between CA and both concurrent cancer and chronic inflammation. In their study, 75% of all studied prostatic samples showed CA in benign acini, but cancer specimens had a higher incidence of CA in benign acini compared to benign specimens. They concluded that CA was a marker for benign glands but also an indicator that might suggest increased suspicion of concurrent cancer.

A recent study confirmed that prostate CA contained amyloid(p)

deposits, as they were stained with Congo red, and the following proteins were identified by mass spectrometric analysis in prostate CA from 46 post-mortem samples: lactoferrin, β 2 microglobulin, S100 A9, Ig kappa chain and transgelin (Kanenawa et al., 2019).

2.4. Corpora amylacea in the respiratory system

Friedreich was the first to describe intra-alveolar CA in lung, in 1856. He suggested that CA were the product of haemorrhage or exudation into lung tissue, and were composed of a carbohydrate developed by chemical metamorphosis of proteins from extravasated blood (Friedreich, 1856). Later, in 1878, Zahn also noticed CA in the lung, exhibiting a concentric arrangement of layers and a regular, symmetric radial structure (Eastman, 1897). He found various forms of corpora, including round, oval and triangular with rounded corners, and frequently observed a black nucleus, which he took to be a foreign body. He also found bodies in the form of drops which resembled degenerated epithelium and had no detectable radial marking. Zahn proposed that CA were either a product of extravasated blood, as suggested by Friedreich, or of degenerated epithelium. According to Favre, one of Zahn's pupils, the CA could nearly always be found in adults, were formed by the degeneration of mucous membrane epithelium and increased in certain constitutional diseases (Eastman, 1897).

In 1893, Seigert postulated that CA in lung was the product of degenerated epithelium around any possible nucleus (Eastman, 1897). Lubarsch and Plenge (1931) described CA in cases of emphysema, chronic bronchitis, congestion, infarction, atelectasis and pneumonia. Michaels and Levene (1957) studied CA in lungs from 1070 autopsies, and found CA in 3.8% of them. However, CA were not found in samples from people younger than 20 years old, occurred in limited numbers and frequency between ages 20 and 60 and were more frequent after 60 years of age. CA usually ranged from 60 to 100 μ m, were found as PAS positive structures and frequently showed alveolar macrophages on their surface.

A rare disorder called CA *pulmonum* was described by Dobashi et al. (1989). In this disease, a solitary mass appeared as an abnormal focus in the lung. In this region, CA were free-floating in the alveolar space and surrounded by exudate alveolar macrophages or multinuclear giant cells. These CA found in lungs appeared as concentrically laminated acellular bodies with a diameter of about 40–80 μ m, and were fundamentally composed of fibrillary elements, similar to amyloid(p) fibrils. Moreover, they showed an affinity for Congo red and partial birefringence as well as a strong positivity for PAS reaction. The reactivity for PAS staining was also displayed by the alveolar macrophages and the multinuclear giant cells, which in addition exhibited amyloid(p)-like fibrils in their cytoplasm. This observation led the authors to suggest that CA might be formed by sequential aggregation and compaction of degenerated alveolar macrophages.

Another study found CA in the alveolar spaces of the lung (Röcken et al., 1996). These had a consistently round or ovoid shape with a concentric stratified structure, and most of them showed a rhomboid eosinophilic nucleus. The nuclei were partly black and interpreted to be carbon pigment. Moreover, most of them showed diffuse or ring-shaped staining with anti- $A\beta$ 2M antibodies. They were not associated with any other histopathological change in the lung, such as oedema or inflammation. These results suggested that some particles can serve as niduses for the formation of pulmonary CA.

Ohori and Hoff (2008) also indicated that CA in the lungs appeared to be free-floating in the alveoli, showed a Maltese cross pattern with polarisation and presented inclusions in the centre. Some of these inclusions might represent carbon fragments, and the authors concluded that many of these concretions in the lungs formed around small, inhaled particles or other foci of irritation to the alveoli or macrophages. CA have also been described in lung from patients with mesothelioma (Hammar, 2011). These were also found in the alveolar spaces, showing no specific location with respect to the lobe or region of the lung, and

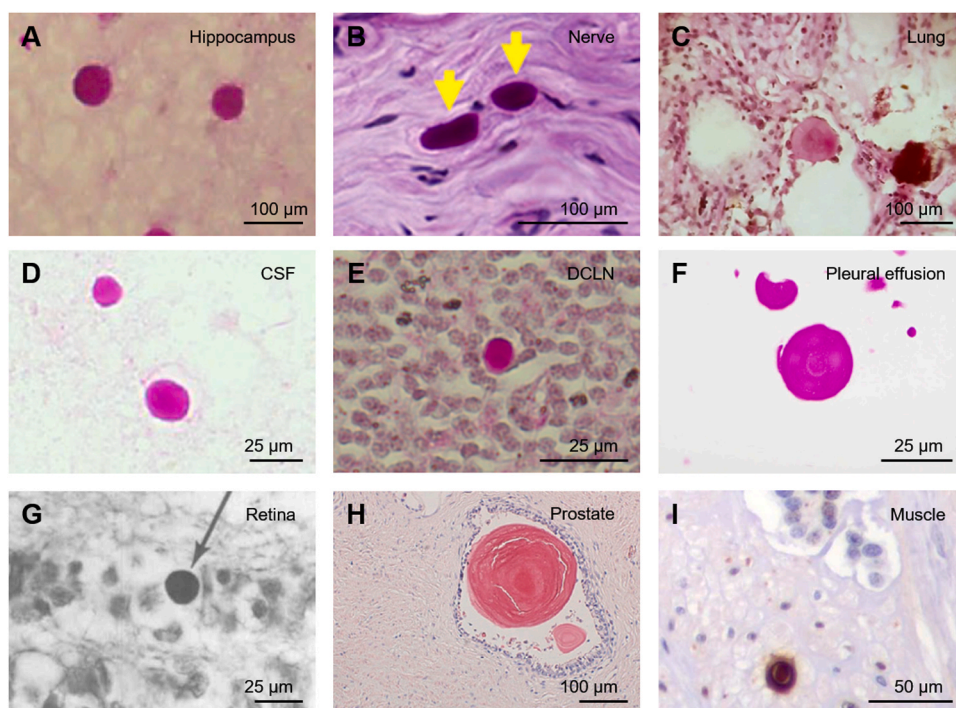


Fig. 1. CA from several human organs and tissues stained with PAS or other stains. A) CA from brain hippocampus stained by PAS (Augé et al., 2017). B) CA from peripheral nerve (intermuscular nerve from quadriceps muscle) stained by PAS-diastase (reprinted from Lu et al., 2016; with permission of Elsevier). C) CA from lung stained by PAS (Gupta et al., 2018). D) CA from CSF stained by PAS (Riba et al., 2019). E) CA from DCLNs stained by PAS (Riba et al., 2019). F) CA from pleural effusion stained by PAS (reprinted from Mani and Wang, 2021; with permission of Wiley Periodicals LLC). G) CA from retina stained by iron staining (reprinted from Avendano et al., 1980; with permission of Association for Research of Vision and Ophthalmology). H) CA from prostate stained by Congo red (reprinted from Kane-nawa et al., 2019; with permission of Taylor & Francis Ltd.). I) Intramuscular CA labelled by immunohistochemistry with an anti-ubiquitin monoclonal antibody (reprinted from Hechtman et al., 2013; with permission from BMJ Publishing Group Ltd.).

were surrounded by macrophages. They showed radiating fibrillary lines with delicate circumferential lines under light microscopy, were PAS positive, contained glycoproteins and were free of lipids, calcium and iron. With respect to their shape, they were spherical, elliptical or even rectangular. There were frequent inclusions in the centre of these bodies, such as asbestos bodies or fibres, iron and other particulates and were mostly surrounded by macrophages. The author concluded that CA rid the lung of foreign material.

Numerous CA have also been described in pleural effusion from a patient with systemic lupus erythematosus (SLE) (Mani and Wang, 2021). These bodies ranged between 10 and 92 µm in diameter and were positively stained by PAS, Diff-Quick and Papanicolaou staining as well as by haematoxylin-eosin, where they appeared as eosinophilic structures. They were negative for Congo red stain for amyloid(p) and did not contain ubiquitin.

A recent study searched for CA in sputum smears for the first time (Martínez-Girón and Pantanowitz, 2021). They studied 6898 sputum smears from 1075 patients with a range of respiratory diseases, including acute bronchitis, adenocarcinoma, aspergillosis and asthma. Some 1.91% of these smears contained CA, corresponding to 9.7% of the patients. These CA comprised round to oval structures, ranging from 80 to 160 µm in diameter, with a concentric lamellar pattern but no reported nucleus. They were much more frequent in older people and were associated with benign lung diseases. The most frequently observed diseases in the group of patients with CA in their sputum were chronic obstructive pulmonary disease, asthma and congestive heart failure. In contrast, the number of cases of lung cancer with CA in the sputum was very low, leading the authors to conclude that CA are related to non-neoplastic lung diseases.

2.5. Corpora amylacea in other organs

CA have also been described in breast, in a primary low-grade marginal zone B lymphoma from a woman with Sjögren's syndrome. These were Congo red and PAS positive and were associated with mammary ductular amyloidosis (Kambouchner et al., 2003). An ultrastructural examination of these CA showed sharply delineated round structures with fibrillary material displaying radial organisation. In any

case, CA have only been observed in marginal zone B lymphoma, not in healthy breast, and are thus unusual findings.

Hechtman et al. (2013) described the presence of intramuscular CA adjacent to ileal low-grade neuroendocrine tumours, with a prevalence directly related to tumour size and the presence of carcinoid syndrome. These CA were intracytoplasmic and positive for PAS staining after diastase digestion. They showed the presence of ubiquitin, and a slight positive staining on the periphery for desmin and smooth muscle actin. They measured approximately 7 µm and an ultrastructural analysis revealed a peripheral rim consisting of condensed filaments and a heterogeneous core containing amorphous particles, but the analysis performed by mass spectrometry gave no signals for calcium, iron or other inorganic metals. The authors suggested that CA were the result of a degenerative process, possibly due to chronic myocyte stress caused by the infiltrating, slow growing mass or local hormonal effects.

CA were also found in the gastrointestinal tract, in the lining of cystic spaces of parotid Warthin's tumours (slow growing neoplasms) and were described as a degenerative feature of the tissue together with squamous metaplasia (Webb and Eveson, 2002).

Some uteri from women aged over 84 years old exhibited CA. They were localised in dilated glands of atrophic endometrium and had a slight eosinophilic appearance when stained with haematoxylin-eosin. No nuclei were observed in these CA. They were negative to immunohistochemistry with several anti-amyloid(p) antibodies. In the uterus, CA appeared exclusively in atrophic glands and showed no relationship with amyloid(p) syndromes (Röcken et al., 1996). CA were also found in cervicovaginal smears from healthy fertile women free from any relevant disease, although this finding is not common (Martínez Girón, 2004), and in a woman with *Moluscum contagiosum* (Buckley and Li, 2017). In this latter case, the CA were found physically isolated from the surrounding squamous cells and presented concentric rings arranged in a radial peripheral striation. Although the tissue did not show signs of inflammation, probably due to the patient's history of steroid treatment, the authors suggested that CA might constitute a cervical response to the *Moluscum contagiosum* infection.

Sun (1983) described the presence of CA, as large cytoplasmic inclusions, in the follicular epithelial cells of a thyroid gland with medullary carcinoma, from an old patient. The CA were positive to Congo

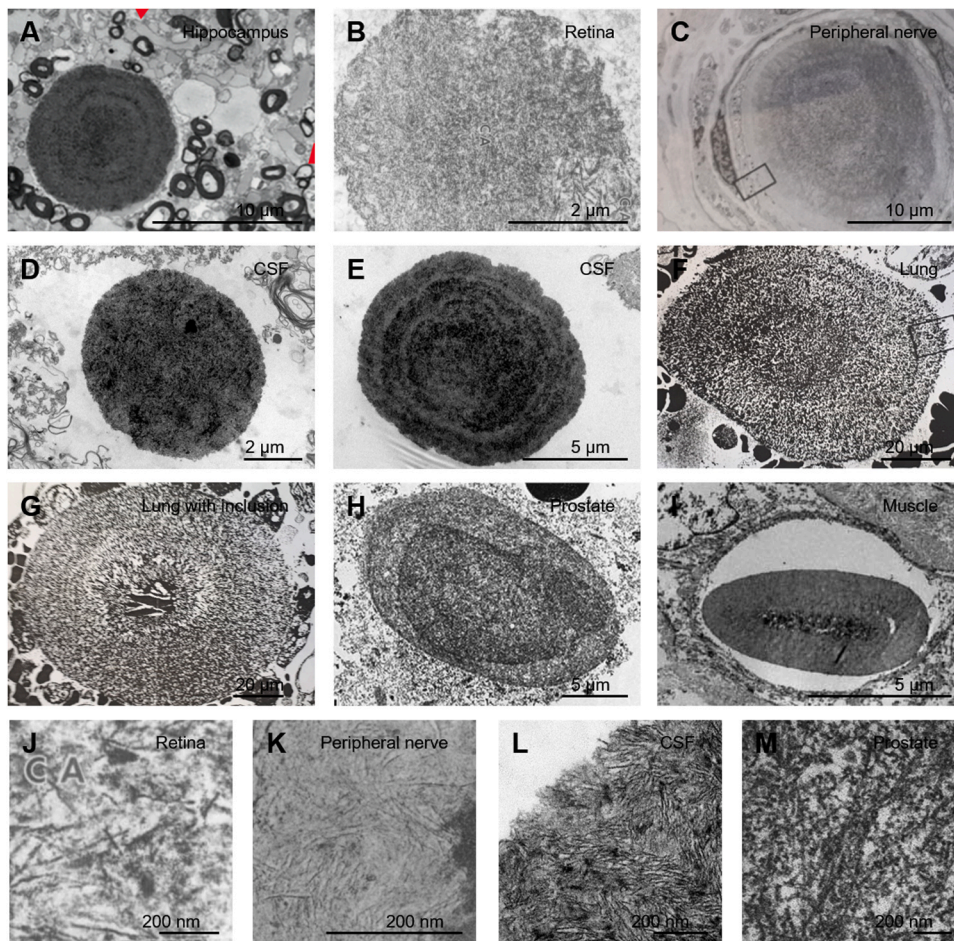


Fig. 2. Ultrastructural images of CA from several human organs and tissues. A) CA from hippocampus (Navarro et al., 2018). B) CA from retina (reprinted from Avendano et al., 1980; with permission of Association for Research of Vision and Ophthalmology). C) CA from a peripheral nerve (sural nerve) (reprinted from Matsumuro et al., 1993; with permission of Springer). D-E) CA from CSF, without (D) and with (E) concentric layers (Riba et al., 2019). F-G) CA from lung, without (F) and with (G) an inclusion in the centre (Dobashi et al., 1989). H) CA from prostate (reprinted from Badea et al., 2015; with permission of Cambridge University Press). I) Intramuscular CA (reprinted from Hechtman et al., 2013; with permission from BMJ Publishing Group Ltd.). J) Inset from B. K) Inset from C. L) Inset from D. M) Higher magnification of a prostate CA (reprinted from Badea et al., 2015; with permission of Cambridge University Press).

red staining, their size varied from 1.5 to 10 μm and their shapes from fusiform to irregular. In addition, fine fibrils were randomly arranged within these inclusions, some of them with poorly defined double strands and rough transverse granularity.

As noted earlier, we also encountered CA in both CSF and DCLNs (Riba et al., 2019). These were PAS positive and contained ubiquitin, p62 and NE that were recognised by natural IgMs. We interpreted them as CA extruded from brain to the CSF, from where some of them reached the DCLNs via the lymphatic system of the meninges. In the case of DCLNs, the CA were attached to a kind of cell which, given their location and form, were probably macrophages.

3. General concerns about CA: discussion and perspectives

As shown in the chronological review, numerous and varied studies have been conducted about CA in different organs and structures, and some of the results appear to be contradictory. However, several features of CA recur in different studies, rendering it possible to obtain a global and inclusive interpretation of these bodies.

Undoubtedly, and as will be discussed below, the most notable feature is that CA have repeatedly been described in every location as accumulating waste products and/or potentially toxic products derived from ageing, pathophysiological conditions, the entry of external material or infectious elements.

However, other features also appear repeatedly. For instance, in all locations, CA have been reported to be PAS positive. Fig. 1 shows representative images of CA stained with PAS from some of these organs. In some structures, such as the prostate, several authors indicated that CA stained with PAS but no images were shown. In these cases, in order

to illustrate these bodies in as many organs as possible, Fig. 1 includes images of CA stained with other stains. The fact that CA are positive for PAS staining in all tissues indicates a high polysaccharide content. As shown in the chronological review, early studies of CA in the CNS postulated a high presence of hexoses, predominantly glucose, and related CA to carbohydrate metabolism disruptions (Sakai et al., 1969a, 1969b). However, later studies indicated that brain CA are much more complex than a simple accumulation of glucose polymers resulting from metabolism alterations (Augé et al., 2018a; Riba et al., 2019). In the case of lung, the carbohydrates present in CA have been attributed to the presence of glycoproteins, some of which would have an epithelial origin (Eastman, 1897; Friedreich, 1856; Hammar, 2011). CA observed in peripheral nerve, CSF, DCLNs, breast, muscle and prostate are also PAS positive. In the case of the prostate, it has been observed that sugars can double the amount of proteins, and that this carbohydrate content may include mucopolysaccharides and glucosaminoglycans. Moreover, various monosaccharides have been described in prostate CA, such as mannose, galactose, N-acetyl-glucose and N-acetyl-galactose (Cohen et al., 2000; Morales et al., 2005).

Based on PAS staining, it can be assumed that the CA in different organs and tissues are all amyloid(s) bodies, although it should be noted that this amyloid(s) would reflect the generic presence of carbohydrates rather than starch, and therefore it would be truer to say that CA are glycan rather than starch-like bodies. In the case of the prostate, it is well documented that CA also stain with Congo red, indicating that they contain amyloid(p) proteins as well. Consequently, these CA can be simultaneously considered amyloid(s) and amyloid(p) bodies. Note that most studies of prostate CA use the term amyloid to refer to amyloid(p) content. Meanwhile, although there is little information about them, CA

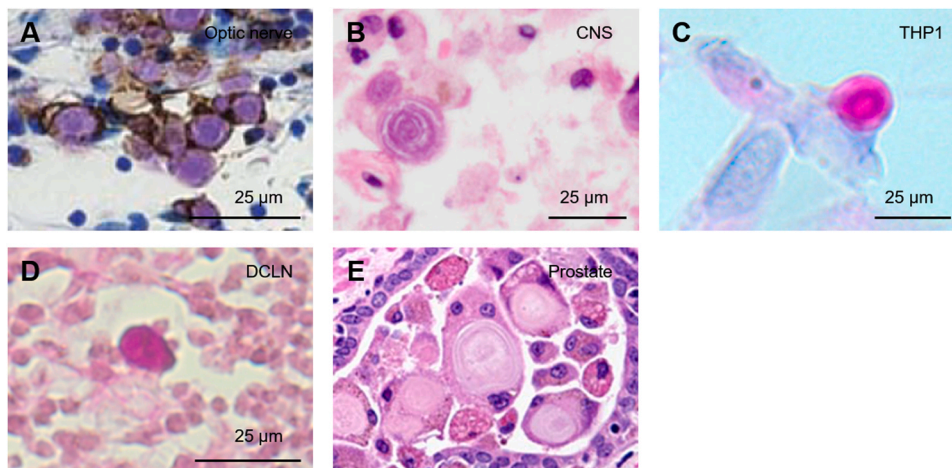


Fig. 3. CA from several organs phagocytosed by macrophages. A) CA from the optic nerve in a NMO-affected region, CA are stained by PAS, and macrophages by an anti-CD68 antibody (reprinted from Suzuki et al., 2012; with permission of Wiley Periodicals LLC). B) CA from basal ganglia stained by hematoxylin-eosin, and macrophages stained by an anti-CD68 antibody (Ohara et al., 2019). C) CA from CSF phagocytosed by THP-1-derived macrophages, PAS staining (Riba et al., 2019). D) CA from DCLNs stained by PAS and surrounded by macrophages (Riba et al., 2019). E) CA from prostate engulfed by macrophages and multinucleated giant cells, hematoxylin staining (Sfanos et al., 2009). Scale bar in E is not provided in the original source.

from breast and in some cases from lung are also described as refringent once stained with Congo red, and therefore may also contain amyloid (p).

Concerning the protein content of CA, the published results seem to be disparate and contradictory. This is partly due to the problem of false positive stainings obtained in immunofluorescence studies. In the case of the CNS, commercial antibodies used in immunofluorescence studies often contain contaminating IgMs that bind to CA. IgMs are recognised by most secondary antibodies, including many that target IgGs, generating false positives that are then reported in articles and give rise to discrepancies (Augé et al., 2017). The problem of false positive immunostaining results has also been observed in studies of prostate CA, such as those on the presence of A β 2M, which seems to be produced by endogenous biotin reactivity (Cohen et al., 2000). However, other techniques have been used to study CA, such as MALDI-TOF and high-performance liquid chromatography combined with tandem mass spectrometry, and the results confirm that the components of CA are numerous and of varied origin. As detailed in the chronological review, in the case of CA from CNS, proteins of neuronal origin but also substances of astrocytic origin have been repeatedly described, as well as proteins of haematological origin or related to infections. In the case of the prostate, PSA and PAP proteins as well as glycoproteins and aminoglycans have been described in CA, and could be responsible for the amyloidosis observed there (Badea et al., 2015; Cohen et al., 1998). In CA from lung, proteins are mainly part of glycoprotein accumulations, and in those from skeletal muscle, fragments of actin and desmin have been described (Hechtman et al., 2013). Therefore, in view of this disparity of components, it can be concluded that CA are not identical but vary depending on the environment in which they are generated. Consequently, these findings support the notion that CA are structures in which various products derived from different situations are accumulated. Such products may be mainly waste elements, as supported by the fact that CA from CNS, CSF, DCLNs and skeletal muscle contain ubiquitin and p62 proteins, both related to waste substance processing and elimination, and by TEM studies of the ultrastructure of CA.

TEM in human tissue is complex and caution should be observed when interpreting the images obtained because the self-digestion or autolysis of tissue that occurs during post-mortem delay alters its characteristics. Nevertheless, as can be seen in Fig. 2, CA from different tissues exhibit some common features. In general, the ultrastructure of CA shows a dense mass of structures arranged randomly, or in some cases, forming concentric rings, with successive regions of higher and lower densities. The presence or not of concentric rings is not a characteristic feature of a particular organ or tissue, because both configurations are present, for example, in the CSF (Figs. 2D and E). In addition, in some cases, such as lung, a central nucleus interpreted as a foreign

body can be seen inside the CA (Fig. 2G). If CA are visualised at higher magnification (Figs. 2J–M), it can be seen that this dense mass often contains fibrillary structures that are tens of nanometres long and a few nanometres thick. Interpretations of these fibrillary structures vary: in some cases, they have been attributed to the carbohydrate component, and in others to fibrillary amyloid(p) protein. In CA from CNS, these fibrillary structures cannot be attributed to amyloid protein because these CA do not stain with Congo red, but in other organs, such as the prostate, some of these fibrils may be amyloid(p). In some of the ultrastructural studies, membranous remains and remnants from cell organelles have been observed close to CA. The presence of cellular debris and the possibility of particles included inside CA further supports the idea that these accumulate waste elements. In addition, the presence of concentric rings has been attributed to different phases or stages of CA growth (Cavanagh, 1999; Dobashi et al., 1989), which could vary according to the rate of waste accumulation and/or the kind of waste products generated.

The idea that CA accumulate waste substances and participate in cleaning processes is also corroborated by the presence, at least in CA from CNS, CSF and DCLN, of NES that are recognised by natural plasma IgMs. As discussed above, natural IgMs often recognise epitopes that act as markers of residual structures (Reyneveld et al., 2020), and IgM antibodies have been reported to recognise some carbohydrates, such as advanced glycation end products, the production of which increases with ageing (Bovin, 2013; Goldin et al., 2006; Grönwall et al., 2012; Haji-Ghassemi et al., 2015; Lutz et al., 2009; Maddur et al., 2020). Furthermore, our recent studies (Riba et al., 2021) indicate that the NES present in CA are of a carbohydrate nature. Thus, the presence of NES in CA may be related to the alterations that occur when waste elements are generated, and NES may contribute to phagocytosis and elimination of CA. In this regard, CA have often been related to phagocytosis by macrophages. For example, our previous studies have reported that CA in DCLNs are connected to cells whose appearance suggests that they are most probably macrophages (Riba et al., 2019). In addition, in vitro studies have shown that CA isolated from CSF are phagocytosed by macrophages derived from the human THP-1 cell line (Riba et al., 2019). Macrophages have also been found phagocytosing CA in optic nerve from patients with NMO (Suzuki et al., 2012), lung tissue from patients with mesothelioma (Hammar, 2011) and CA from prostate (Sfanos et al., 2009). Fig. 3 shows representative images of CA from different tissues being phagocytosed by or in contact with macrophages.

Despite all these convergent features, other aspects of CA appear to be inconsistent. For example, they can be intracellular or extracellular. In the CNS, there is no doubt that some CA are intracellular. TEM images have shown cell organelles such as mitochondria or vacuolar structures in their vicinity, all surrounded by the cell membrane. In order to detect

the cell membrane surrounding the CA and organelles, the tissue must be especially well preserved and obtained preferably from biopsies or resections, thus avoiding post-mortem delay and tissue self-digestion. In the CNS, the cells that contain CA have sometimes been identified as astrocytes, and it has also been reported that astrocytes can expel CA into the CSF, in an extrusion process that resembles an apocrine secretion (Sbarbati et al., 1996; Riba et al., 2019). In this respect, the presence of matrix metalloproteinase 2 (MMP2) found in the proximity of CA in the CNS could be related to the extracellular remodelling necessary for their extrusion (Augé et al., 2018a). Nevertheless, CA located in the CSF are mainly extracellular. Extracellular CA have also been observed in the alveoli or pulmonary ducts, in pleural effusion, in sputum smears and in the ductular lumen of the breast. It has been proposed that CA from lung derive from epithelial lung cells, and an epithelial origin is also possible in some other tissues or organs. It should be borne in mind that the prostate and the breast, and in general the glandular tissues, contain secretory cells that are of an epithelial nature. Given all this, it is perhaps conceivable that extracellular CA are the result of an apocrine extrusion or secretion of CA formed in certain cells of the surrounding tissues.

At the beginning of Section 3 it was noted that in light of the high carbohydrate content of CA, some authors have suggested that they are products generated simply as a consequence of altered glycogen metabolism (Sakai et al., 1969a, 1969b). However, if this were the case, it would raise questions with no global explanation, and the answers would be inconsistent and unconvincing. For example, if CA were formed as a result of altered glycosidic metabolism, it would be difficult to explain why such a wide variety of products (essentially waste products) have been described in CA. It would also be difficult to explain the presence, at least in some CA, of high amounts of ubiquitin and p62, the former acting as a marker of waste products and the latter as an adaptor for waste processing. In the case of ubiquitin, it should be borne in mind that malin, an E3 ubiquitin ligase, modulates glycogen metabolism in multiple cellular compartments (Gentry et al., 2020). However, in the context of CA it seems difficult to associate ubiquitin solely with glycogen metabolism and not with waste elements. On the other hand, glycogen synthase (GYS) and p62 have mainly been found on the periphery of the CA, whereas ubiquitin is found in peripheral but also central areas, indicating a level of internal organisation of CA. It would also be difficult to explain why CA are generally found in the border areas of the organs or tissues which contain them, and are sometimes found outside these structures. Neither does the metabolic theory explain why some CA are intracellular and others extracellular. Necrosis of CA-containing cells does not appear to explain extracellular CA, as these would be accompanied by significant levels of tissue inflammation and this is not usually the case. Furthermore, the metabolic theory cannot explain the presence of NE in CA (at least in those in CNS, CSF and DCLNs) or the presence of natural IgMs directed against these NE, or why extracellular CA are phagocytosed by macrophages.

Having observed the inconsistencies and weakness of the metabolic theory, it is time to seek another explanation and provide an integrative, all-encompassing hypothesis capable of answering all these questions.

4. Integrative hypothesis regarding CA

Collecting and integrating the results and conclusions given in the studies reviewed above, we propose considering CA in human organs and tissues as waste containers. These waste containers, which are actively created by specific cells, sequester or retain waste products or foreign products, and are then secreted into the external medium or interstitial spaces, in this latter case subsequently being phagocytosed by macrophages. Moreover, as previously posited for CA from brain (Cavanagh, 1999; Riba et al., 2019), we propose that the glycan structure (or part of the glycan structure) is necessary to generate the container skeleton.

In light of this integrated perspective, the time may have come to redefine CA. As noted earlier, the ambiguity of term amyloid, which

includes amyloid(p) and amyloid(s), has repeatedly given rise to misinterpretations in studies on CA. Likewise, the concept of CA (corpora “amylacea”) has also generated misunderstanding. Consequently, it would perhaps be appropriate to rename CA, and a term such as “wasteosome” (a new term for a body containing waste products) would be more descriptive and would define them more satisfactorily, placing the emphasis on the waste products they entrap, rather than on their amyloid (s and/or p) content.

Wasteosome generation would be intracellular, and would involve the capture of waste elements that may have originated inside or outside the cell, some of which can be marked with ubiquitin and sequestered by p62. Their genesis would also involve the cell machinery necessary for formation of the glycan component that forms the container skeleton. Since the polyglucosan structure containing the wasteosomes or CA from CNS is formed by modified glycogen which resembles that of the polyglucosan bodies found in diseases such as adult polyglucosan body disease and Lafora disease, the machinery involved in their formation might be similar. The aetiology of these diseases includes genetic defects affecting the enzymes that participate in glycogen metabolism, including malin, laforin, glycogen branching enzyme (GBE), glycogen debranching enzyme (GDE) and protein targeting to glycogen (PTG). Thus, these enzymes could be involved in the genesis of the polyglucosan structure that constitutes the CA skeleton. The machinery to form this kind of glycan structure would be physiologically active in cells in which CA are produced, but also in other cells in the case of specific diseases. In such diseases, polyglucosan bodies are found in locations with high glycogen metabolism, such as skeletal muscle and myocardium, and in structures where glycogen metabolism has differential characteristics, as is the case of neurons and retina. It is of interest to note that waste products and the collection of waste elements have not been described in the polyglucosan bodies formed in these diseases, and that we did not find NE in these bodies in a rodent model of Lafora disease (Augé et al., 2018b). Thus, the polyglucosan bodies found in these diseases must be equivalent to the glycan skeleton of CA, and their formation explains the presence of CA-like bodies described in neurons, muscle and other structures. In these diseases, alteration of the glycan metabolism could induce the formation of this kind of glycan skeleton in particular cells. However, alteration of glycan metabolism is not a prerequisite for CA formation. The rate of CA formation may be related to the production of waste elements, which increases with ageing, but also in conditions such as those that involve high levels of oxidative stress. Intracellular waste elements are usually eliminated by specific mechanisms, including the ubiquitin proteasome system and the phagosome/lysosome pathway, but in some cases they may be eliminated through wasteosomes. All the evidence suggests that glycogen or glycogen-like structures can perform the well-known functions of carbon and energy storage and the recently described function of NAcGlc reservoir as a source for N-glycans (Sun et al., 2021), but also the function of coating structures, as in the case of the wasteosome skeleton proposed here.

In addition, we hypothesise that the machinery of wasteosomes would be particularly active in epithelial structures, such as lung epithelial cells and glandular structures (e.g. prostate and breast), in which secretory cells also have an epithelial origin. It would also be active in astrocytes sited near the periventricular margins and in the subpial layer or *glia limitans* of the CNS. Subsequently, wasteosomes would be expelled outside the body or into interstitial areas for their elimination. For example, prostatic CA could be eliminated through the renal system, and CA which are expelled to the CSF or pulmonary ducts could be eliminated through phagocytosis and digestion by macrophages.

Our proposal endows explanations and answers to the previous questions with overall consistency. Because it is based on the presence of waste elements, our theory explains why such a wide variety of products have been described in CA. It also explains why all CA are PAS positive but only some of them are Congo red positive: all CA are PAS positive

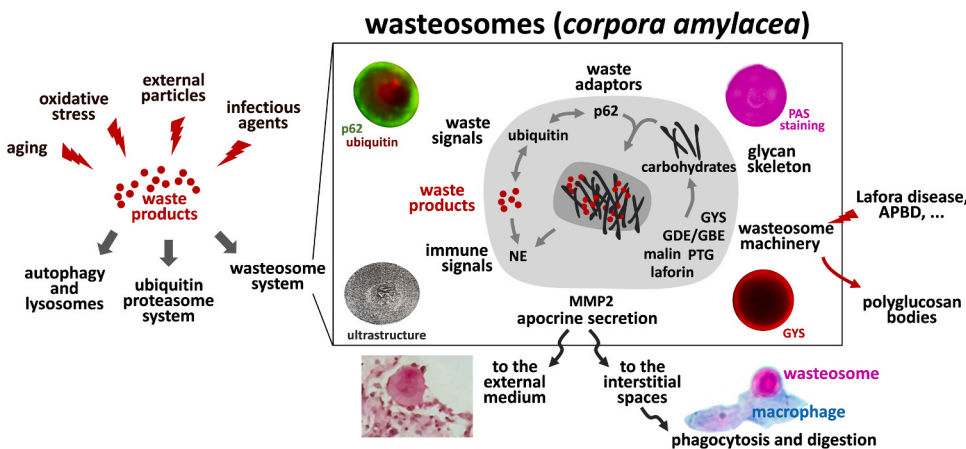


Fig. 4. Wasteosome system: Scheme of the processes involved in the generation and elimination of wasteosomes or CA. Waste products, the production of which increases with age and other circumstances such as those generating an increase in oxidative damage, are usually eliminated via intracellular mechanisms, including the ubiquitin proteasome system and autophagy. In some places, waste elements accumulate to form specific structures known as CA and here renamed as wasteosomes. The genesis of wasteosomes involves the capture of waste elements that may have originated inside or outside the cell, some of which are marked with ubiquitin and sequestered by p62. Their genesis would also involve the cell machinery necessary for the formation of the glycan component that forms the skeleton. This machinery includes malin, laforin, GBE, GDE and PTG. Wasteosomes can be secreted to an external or internal medium, where they are

phagocytosed by macrophages. The NE present in wasteosomes might facilitate this process. The aberrant, delocalised activation of the machinery participating in the formation of the skeleton could lead to the formation of particular polyglucosan bodies in other structures, such as those formed in Lafora disease or adult polyglucosan body disease (APBD). See text for details.

because there is a glycan structure, corresponding to the amyloid(s), present in all CA, but only some CA are Congo red positive because only some contain amyloid(p) protein, which accumulates as a waste product. A waste element-based understanding also explains why substances related to infectious processes have sometimes been observed, as well as central nuclei. In addition, our theory explains the reason for the presence and non-random distribution of p62, ubiquitin and GYS. The central part of the CA (containing ubiquitin) would contain an accumulation of waste products, while in the outer part (containing GYS, p62 and ubiquitin), the structure would still be growing and adding new waste products. Concentric rings would be due to non-uniform growth of the CA. Our proposal would also explain why some CA are intracellular and others are extracellular, and why they are mainly found in border areas. Lastly, it also explains why they have been mainly related to ageing, which could be associated with an increase in waste elements.

As a summary of this theory, the processes involved in wasteosome generation and elimination are shown in Fig. 4. A re-reading of the chronological review taking into account this scheme will demonstrate that a high number of observations are coherent with the proposed hypothesis.

CRediT authorship contribution statement

Marta Riba: Conceptualization, Investigation, Writing – original draft, Writing – review & editing. **Jaume del Valle:** Conceptualization, Investigation, Writing – original draft, Writing – review & editing. **Elisabet Augé:** Conceptualization, Investigation. **Jordi Vilaplana:** Conceptualization, Writing – original draft, Writing – review & editing, Supervision, Funding acquisition, Project administration. **Carne Pelegrí:** Conceptualization, Writing – original draft, Writing – review & editing, Supervision, Funding acquisition, Project administration.

Acknowledgements

This study was funded by grants from the Spanish Ministerio de Economía y Competitividad (BFU2013-47382-P, BFU2016-78398-P), Spanish Ministerio de Ciencia e Innovación (PID2020-115475GB-I00 / AEI / 10.13039/501100011033) and by the Centros de Investigación Biomédica en Red (CIBER) at the *Instituto de Salud Carlos III*. We thank the Generalitat de Catalunya for funding our research group [2017/SGR625]. M. Riba received the predoctoral fellowship *Formación de*

Profesorado Universitario (2018) from the Ministerio de Ciencia, Innovación y Universidades. The authors are grateful to Iraida Tena for technical assistance and Michael Maudsley and Denise Phelps for revising the English text.

Declarations of Interest

None.

References

- Alder, N., 1953. On the nature, origin and distribution of the corpora amylacea of the brain with observations on some new staining reactions. *J. Ment. Sci.* 99, 689–697. <https://doi.org/10.1192/bjp.99.417.689>.
- Anzil, A.P., Herrlinger, H., Blinzinger, K., Kronska, D., 1974. Intraneuritic corpora amylacea - demonstration in orbital cortex of elderly subjects by means of early postmortem brain sampling and electron microscopy. *Virchows Arch. A Pathol. Anat. Histol.* 364, 297–301. <https://doi.org/10.1007/BF00432727>.
- Augé, E., Bechmann, I., Llor, N., Vilaplana, J., Krueger, M., Pelegrí, C., 2019. Corpora amylacea in human hippocampal brain tissue are intracellular bodies that exhibit homogeneous distribution of neo-epitopes. *Sci. Rep.* 9. <https://doi.org/10.1038/s41598-018-38010-7>.
- Augé, E., Cabezón, I., Pelegrí, C., Vilaplana, J., 2017. New perspectives on corpora amylacea in the human brain. *Sci. Rep.* 7. <https://doi.org/10.1038/srep41807>.
- Augé, E., Duran, J., Guinovart, J.J., Pelegrí, C., Vilaplana, J., 2018a. Exploring the elusive composition of corpora amylacea of human brain. *Sci. Rep.* 8. <https://doi.org/10.1038/s41598-018-31766-y>.
- Augé, E., Pelegrí, C., Manich, G., Cabezón, I., Guinovart, J.J., Duran, J., Vilaplana, J., 2018b. Astrocytes and neurons produce distinct types of polyglucosan bodies in Lafora disease. *Glia* 66, 2094–2107. <https://doi.org/10.1002/glia.23463>.
- Avendano, J., Rodrigues, M.M., Hackett, J.J., Gaskins, R., 1980. Corpora amylacea of the optic nerve and retina: a form of neuronal degeneration. *Invest. Ophthalmol. Vis. Sci.* 19, 550–555.
- Badea, P., Petrescu, A., Moldovan, L., Zarnescu, O., 2015. Structural heterogeneity of intraluminal content of the prostate: a histochemical and ultrastructural study. *Microsc. Microanal.* 21, 368–376. <https://doi.org/10.1017/S1431927615000197>.
- Bathini, P., Mottas, A., Jaquet, M., Brai, E., Alberi, L., 2019. Progressive signaling changes in the olfactory nerve of patients with Alzheimer's disease. *Neurobiol. Aging* 76, 80–95. <https://doi.org/10.1016/j.neurobiolaging.2018.12.006>.
- Bovin, N.V., 2013. Natural antibodies to glycans. *Biochemistry*. <https://doi.org/10.1134/S0006297913070109>.
- Buckley, K., Li, Z., 2017. Corpora amylacea and molluscum contagiosum on a cervical pap smear. *Diagn. Cytopathol.* 45, 179–181. <https://doi.org/10.1002/dc.23630>.
- Busard, H., Gabreëls-Festen, A., Van't Hof, M., Renier, W., Gabreëls, F.J.M., 1990. Polyglucosan bodies in sural nerve biopsies. *Acta Neuropathol.* 80, 554–557.
- Buzzard, E.F., Greenfield, J.G., 1923. Pathology of the nervous system, PB Hoeber.
- Catola, G., Achúcarro, N., 1906. Über die Entstehung der Amyloidkörperchen im Zentralnervensystem. *Virchows Arch. Pathol. Anat. Physiol. Klin. Med.* 184, 454–469. <https://doi.org/10.1007/BF01999854>.
- Cavanagh, J.B., 1998. Spinal corpora amylacea and motor neuron disease: a quantitative study. *J. Neurol. Neurosurg. Psychiatry* 65, 488–491. <https://doi.org/10.1136/jnnp.65.4.488>.

4. ARTICLE 4

**WASTEOSOMES (*CORPORA AMYLACEA*) OF HUMAN BRAIN ARE
PHAGOCYTOSED BY NON-INFLAMMATORY MACROPHAGES**

Marta Riba, Joan Campo-Sabariz, Iraida Tena, Laura Molina-Porcel, Teresa Ximelis,
Maria Calvo, Ruth Ferrer, Raquel Martín-Venegas, Jaume del Valle, Jordi Vilaplana,
Carme Pelegrí

Journal of Neuroinflammation 2022, sotmès per a la seva publicació

JCR 2020 IF: 8,322

RESUM

Antecedents: D'acord amb l'Article 3, en aquest treball, els CA seran referits com a *wasteosomes*. Els estudis previs indiquen que els CA poden ser fagocitats per macròfags, però no es coneixen els mecanismes desencadenants de la fagocitosi ni el processament d'aquestes estructures una vegada fagocitades, fet que aportaria més detalls pel que fa a la funció dels CA a l'organisme.

Objectiu: Analitzar el procés de fagocitosi dels CA per part de macròfags i determinar els mecanismes involucrats en aquest procés.

Material i mètodes: Es van utilitzar mostres *post-mortem* de LCR ventricular de 7 casos afectats de malaltia d'Alzheimer, malaltia de Parkinson o esclerosi lateral amiotròfica (66-87 anys) i seccions criostàtiques d'hipocamp humà de 2 casos de malaltia d'Alzheimer (86 i 89 anys) i 2 casos d'encefalopatia vascular (70 i 80 anys). Per a l'anàlisi del procés de fagocitosi, es van purificar *wasteosomes* del LCR i es van marcar amb ConA o NHS ester, ambdós conjugats amb fluorescència, o amb tinció de PAS, i seguidament els *wasteosomes* marcats es van afegir a cultius de macròfags THP-1 tenyits amb el colorant vital Vybrant CFDA i es van dur a terme estudis de *time-lapse*. D'altra banda, per tal de determinar els possibles mecanismes implicats en el procés de fagocitosi, i es van marcar *wasteosomes* procedents del LCR amb ConA conjugada amb fluorescència o amb IgM, es van afegir els *wasteosomes* ja marcats a cultius de macròfags THP-1, i posteriorment es van realitzar immunomarcatges específics de receptors de macròfags per tal de veure les característiques dels macròfags que interaccionaven amb els *wasteosomes*. Concretament, es van utilitzar anticossos dirigits contra el receptor CD68, contra el receptor de la Man CD206, contra el receptor de la proteïna C3b del complement conegut com a CD35 (també anomenat CR1), i contra el receptor de la cadena μ de les IgM conegut com a Fc μ R o FAIM3. Així mateix, es van realitzar estudis d'immunofluorescència en els *wasteosomes* del LCR per determinar si aquests es troben opsonitzats per la lectina d'unió a Man (*mannose binding lectin*, MBL) i/o per la proteïna del sistema de complement C3b, i així poder analitzar la contribució d'aquestes proteïnes a la fagocitosi dels *wasteosomes*. Els marcatges d'MBL i C3b es van estudiar també en seccions d'hipocamp humà per determinar si la opsonització amb aquestes proteïnes es produïa ja en els *wasteosomes* del parènquima cerebral. A més a més, en les seccions d'hipocamp humà es van realitzar marcatges de p62, per localitzar els *wasteosomes* en els talls, i simultàniament marcatges dels receptors CD206, CD35, Fc μ R i CD68, per determinar la possible presència de cèl·lules fagocítiques amb aquests receptors interaccionant amb els *wasteosomes* en el teixit cerebral.

Resultats: Els estudis de *time-lapse* van confirmar que els *wasteosomes* eren fagocitats pels macròfags THP-1. Els *wasteosomes* més petits van ser interioritzats i degradats i alguns dels fragments resultants van ser exposats a la membrana de la cèl·lula. En canvi, els

wasteosomes de mida superior no van ser totalment fagocitats per un determinat macròfag, sinó que es van observar diferents macròfags establint contacte simultàniament amb un mateix CA, el qual acabava sent degradat parcialment. Els assaigs d'immunofluorescència van identificar els receptors CD68, CD206 i CD35 en els macròfags THP-1, però no el receptor Fc μ R, i van confirmar la presència d'MBL i C3b opsonitzant els *wasteosomes* del LCR. Així doncs, aquests marcatges van suggerir que els *wasteosomes* podrien ser fagocitats mitjançant el receptor CD206, el qual podria reconèixer les Man dels *wasteosomes*, o mitjançant el sistema del complement per la via de la lectina mediada per l'MBL o per la via espontània, ambdues vies donant lloc a una opsonització amb C3b, el qual seria reconegut pel receptor CD35. L'absència del receptor Fc μ R en macròfags THP-1 va excloure el mecanisme de fagocitosi mediat per les IgM i aquest receptor en aquesta línia cel·lular. De totes maneres, no es descarta que aquest mecanisme tingui lloc *in vivo* en altres tipus de cèl·lules. Cal remarcar que les proteïnes MBL i C3b no van ser detectades en els *wasteosomes* de les seccions d'hipocamp, el que va indicar que els *wasteosomes* són opsonitzats per l'MBL o C3b una vegada extruïts del teixit cap al LCR. Pel que fa als marcatges dels receptors CD206, CD35, Fc μ R i CD68 en les seccions d'hipocamp, i) es van identificar macròfags CD206 positius en les interfícies del cervell, fora del parènquima, en contacte amb *wasteosomes* que havien estat alliberats del teixit cap al ventricle o l'espai subaracnoidal, ii) es va identificar que els astròcits situats a les zones limítrofes dels SNC, i que són els formadors de *wasteosomes*, són CD35 positius, iii) no es va observar marcatge de Fc μ R en cap tipus cel·lular, i iv) es va observar amb CD68 el marcatge de micròglia, però aquesta no estableix cap contacte amb els *wasteosomes*.

Conclusions: Aquest treball conclou que els CA són fagocitats i degradats per macròfags i alguns dels fragments derivats de la degradació són exposats a la membrana dels macròfags. A més a més, corrobora que hi ha diferents mecanismes involucrats en la fagocitosi dels *wasteosomes* una vegada aquests són extruïts del teixit cerebral. El mecanisme principal de fagocitosi seria mediat pel receptor CD206, el qual desencadena aquest procés sense produir una resposta inflamatòria i per tant, evitant dany tissular, cosa que dona lloc a una eliminació silenciosa dels *wasteosomes*. Altres possibles mecanismes de fagocitosi són els mediats pel receptor CD35 o l'Fc μ R, el primer derivat de l'opsonització dels *wasteosomes* amb C3b i el segon per l'opsonització dels *wasteosomes* amb IgM, el qual no tindria lloc per part dels macròfags THP-1 però no es descarta en altres circumstàncies. Aquests mecanismes, en conjunt, assegurarien la fagocitosi i l'eliminació dels *wasteosomes*, sigui a nivell de les regions limitants del SNC o bé en altres òrgans com els ganglis limfàtics, i recolzen el paper dels *wasteosomes* com a estructures involucrades en l'eliminació de substàncies de rebuig proveïdes amb suficients marcadors que garanteixin la seva eliminació.

Journal of Neuroinflammation

Wasteosomes (corpora amylacea) of human brain are phagocytosed by non-inflammatory macrophages --Manuscript Draft--

Manuscript Number:	JNEU-D-21-01037	
Full Title:	Wasteosomes (corpora amylacea) of human brain are phagocytosed by non-inflammatory macrophages	
Article Type:	Research	
Funding Information:	Ministerio de Economía y Competitividad (BFU2016-78398-P)	Dr. Jordi Vilaplana
	Agencia Estatal de Investigación (PID2020-115475GB-I00/AEI/10.13039/501100011033)	Dr. Jordi Vilaplana
	Ministerio de Ciencia, Innovación y Universidades (FPU)	Ms. Marta Riba
Abstract:	<p>Background</p> <p>Corpora amylacea of human brain, recently renamed as wasteosomes, are granular structures that appear during aging and also accumulate in specific areas of the brain in neurodegenerative conditions. Acting as waste containers, wasteosomes are formed by polyglucosan aggregates that entrap waste substances of different origins, are expelled from the brain to the cerebrospinal fluid (CSF) and are thereafter phagocytosed by macrophages. In the present study, we analyze the phagocytosis of wasteosomes and the mechanisms involved in this process.</p> <p>Methods</p> <p>We purified wasteosomes from human CSF and incubated them with THP-1 macrophages. Immunofluorescence staining and time-lapse recording techniques were performed to evaluate the phagocytosis. We also immunostained human hippocampal sections to study the interactions between wasteosomes and macrophages at central nervous system interfaces.</p> <p>Results</p> <p>We show that wasteosomes are phagocytosed by THP-1 macrophages. Once phagocytosed, they are degraded and some of their fractions are later exposed on the surface of macrophages and interchanged between different macrophages. The phagocytosis by THP-1 macrophages can be triggered through the CD206 and the CD35 receptors, but not the FAIM3 receptor, whereas all these receptors may be involved, <i>in vivo</i>, in the phagocytosis of wasteosomes. Moreover, we observed that the wasteosomes obtained from the CSF are opsonized by MBL and the complement protein C3b, and can also contain mannose or other targets of CD206.</p> <p>Conclusions</p> <p>Our findings indicate that, <i>in vivo</i>, different mechanisms can be involved in the phagocytosis of wasteosomes, some of them triggering non-inflammatory responses and avoiding tissue damage. However, as wasteosomes export brain substances eluding the blood brain barrier, it is necessary to elucidate if some of the macrophages that phagocytose the wasteosomes participate in the induction of immunological tolerance and of adaptive immunological responses in the central nervous system, and may also play significant roles in some brain autoimmune diseases.</p>	
Corresponding Author:	Jordi Vilaplana Universitat de Barcelona Barcelona, Catalunya SPAIN	

Corresponding Author E-Mail:	vilaplana@ub.edu
Corresponding Author Secondary Information:	
Corresponding Author's Institution:	Universitat de Barcelona
Corresponding Author's Secondary Institution:	
First Author:	Marta Riba
First Author Secondary Information:	
Order of Authors:	Marta Riba
	Joan Campo-Sabariz
	Iraida Tena
	Laura Molina-Porcel
	Teresa Ximelis
	Maria Calvo
	Ruth Ferrer
	Raquel Martín-Venegas
	Jaume del Valle
	Jordi Vilaplana
	Carme Pelegrí
Order of Authors Secondary Information:	
Additional Information:	
Question	Response
Is this study a clinical trial?<hr><i>A clinical trial is defined by the World Health Organisation as 'any research study that prospectively assigns human participants or groups of humans to one or more health-related interventions to evaluate the effects on health outcomes'.</i>	No



Secció de Fisiologia
Departament de Bioquímica i Fisiologia
Facultat de Farmàcia i Ciències de l'Alimentació

Edifici B, escala A, 3a planta
Av. Joan XXIII, 27-31
08028 Barcelona

Dear Editor,

We are pleased to submit the manuscript entitled "**Wasteosomes (corpora amylacea) of human brain are phagocytosed by non-inflammatory macrophages**" for consideration by the Editorial Board of Journal of Neuroinflammation.

We are at your disposal for any questions or comments.

Thanking you in advance for your attention,

Yours sincerely,

Dr. Jordi Vilaplana
Secció de Fisiologia
Departament de Bioquímica i Fisiologia
Facultat de Farmàcia i Ciències de l'Alimentació
Universitat de Barcelona

Barcelona, 04/11/2021

[Click here to view linked References](#)**Title**

Wasteosomes (*corpora amylacea*) of human brain are phagocytosed by non-inflammatory macrophages

Authors:

Marta Riba^{1,2,3}, Joan Campo-Sabariz^{1,4}, Iraidia Tena¹, Laura Molina-Porcel^{5,6}, Teresa Ximelis^{5,6}, Maria Calvo⁷, Ruth Ferrer^{1,4}, Raquel Martín-Venegas^{1,4}, Jaume del Valle^{1,2,3}, Jordi Vilaplana^{1,2,3,*} and Carme Pelegrí^{1,2,3,*}

* These authors contributed equally to this study

Affiliations:

¹Secció de Fisiologia, Departament de Bioquímica i Fisiologia, Universitat de Barcelona, Barcelona, Spain.

²Institut de Neurociències, Universitat de Barcelona, Barcelona, Spain.

³Centros de Biomedicina en Red de Enfermedades Neurodegenerativas (CIBERNED), Madrid, Spain.

⁴Institut de Recerca en Nutrició i Seguretat Alimentàries (INSA-UB), Universitat de Barcelona, Barcelona, Spain.

⁵Alzheimer's Disease and Other Cognitive Disorders Unit, Neurology Service, Hospital Clinic, Institut d'Investigacions Biomèdiques August Pi i Sunyer (IDIBAPS), Universitat de Barcelona, Barcelona, Spain.

⁶Neurological Tissue Bank of the Biobanc-Hospital Clinic-IDIBAPS, Barcelona, Spain.

⁷Unitat de Microscòpia Òptica Avançada - Campus Clínic, Facultat de Medicina, Centres Científics i Tecnològics - Universitat de Barcelona.

Corresponding author:

Dr. Jordi Vilaplana, Secció de Fisiologia, Departament de Bioquímica i Fisiologia, Universitat de Barcelona, Av. Joan XXIII 27-31, 08028 Barcelona, Spain. Tel.: +34 934024505. E-mail: vilaplana@ub.edu.

ABSTRACT

Background: *Corpora amylacea* of human brain, recently renamed as wasteosomes, are granular structures that appear during aging and also accumulate in specific areas of the brain in neurodegenerative conditions. Acting as waste containers, wasteosomes are formed by polyglucosan aggregates that entrap waste substances of different origins, are expelled from the brain to the cerebrospinal fluid (CSF) and are thereafter phagocytosed by macrophages. In the present study, we analyze the phagocytosis of wasteosomes and the mechanisms involved in this process.

Methods: We purified wasteosomes from human CSF and incubated them with THP-1 macrophages. Immunofluorescence staining and time-lapse recording techniques were performed to evaluate the phagocytosis. We also immunostained human hippocampal sections to study the interactions between wasteosomes and macrophages at central nervous system interfaces.

Results: We show that wasteosomes are phagocytosed by THP-1 macrophages. Once phagocytosed, they are degraded and some of their fractions are later exposed on the surface of macrophages and interchanged between different macrophages. The phagocytosis by THP-1 macrophages can be triggered through the CD206 and the CD35 receptors, but not the FAIM3 receptor, whereas all these receptors may be involved, *in vivo*, in the phagocytosis of wasteosomes. Moreover, we observed that the wasteosomes obtained from the CSF are opsonized by MBL and the complement protein C3b, and can also contain mannose or other targets of CD206.

Conclusions: Our findings indicate that, *in vivo*, different mechanisms can be involved in the phagocytosis of wasteosomes, some of them triggering non-inflammatory responses and avoiding tissue damage. However, as wasteosomes export brain substances eluding the blood brain barrier, it is necessary to elucidate if some of the macrophages that phagocytose the wasteosomes participate in the induction of immunological tolerance and of adaptive immunological responses in the central nervous system, and may also play significant roles in some brain autoimmune diseases.

KEYWORDS

Corpora amylacea; Wasteosome; Brain; Phagocytosis; M2 macrophage; natural immunity; IgM; CD206; CD35; C3b.

BACKGROUND

1 *Corpora amylacea* of the human brain are polyglucosan aggregates that appear mainly in the
2 periventricular, perivascular and subpial regions of the human brain during aging [1–3] and they
3 also accumulate in specific areas of the brain in neurodegenerative conditions [4–7]. For a long
4 time, they have been thought to entrap residual or waste products, including those derived from
5 aging or degenerative processes [2, 3, 8–12], and they have recently been renamed as
6 wasteosomes [13]. Although essentially composed of glucose polymers, wasteosomes can
7 contain products derived from neurons, astrocytes, oligodendrocytes and the blood [4, 9, 14–
8 19] or even related to viral, fungal or microbial infections [20–22]. Wasteosomes also contain
9 ubiquitin and p62 proteins, which are both involved in the processing and collecting of waste
10 products, as well as glycogen synthase (GS), which takes part in the formation of their
11 polyglucosan structure [23]. Moreover, wasteosomes exhibit some neoantigens, more
12 specifically neoepitopes (NEs), which are recognized by natural antibodies of the IgM isotype
13 [10] and are of a carbohydrate nature [24]. NEs originate *de novo* and appear in both
14 physiological and pathological conditions as well as in aging [25–29]. On the other hand, natural
15 antibodies (including natural IgMs) are generated throughout a lifetime, even during fetal
16 development and before external antigen exposure. They have been determined throughout
17 evolution and are remarkably stable within species and even between species [30–35]. Natural
18 antibodies are involved in the first line of immune defense against foreign microbes and also
19 have important physiological functions [36]. Some of these natural antibodies are able to
20 recognize some NEs that are present in, for example, cell remnants and senescent or apoptotic
21 cells, participating in their controlled elimination and contributing to the maintenance of tissue
22 homeostasis [26, 31, 33, 35–39]. The presence of NEs in wasteosomes and the existence of
23 natural IgMs that target them reinforce the idea that wasteosomes are involved in brain cleaning
24 or in protective processes [10]. Our group previously revealed that wasteosomes are released
25 from the brain into the cerebrospinal fluid (CSF), some of them reaching the cervical lymph
26 nodes via the meningeal lymphatic system. We also noticed that wasteosomes are
27 phagocytosed *in vitro* by macrophages. All these findings indicated that wasteosomes not only
28 entrap residual products, but they can also act as containers that participate in removing waste
29 products from the brain [40].
30
31
32
33
34
35
36
37
38
39
40
41
42
43
44
45
46
47
48
49
50
51

52
53 Concerning the phagocytosis of wasteosomes, we previously observed that the wasteosomes
54 obtained from the CSF and opsonized by IgMs are phagocytosed *in vitro* by macrophages derived
55 from THP-1 cells (THP-1 macrophages). We also noticed that non-opsonized wasteosomes are
56 phagocytosed as well, suggesting that the opsonization with IgMs is not required for the
57
58
59
60
61
62
63
64
65

1 phagocytosis of wasteosomes [40]. Moreover, we detected the presence of the mannose
2 receptor CD206 in THP-1 macrophages [40]. Liu et al. (1987) suggested the presence of mannose
3 in wasteosomes, as these structures are marked by concanavalin A (ConA), a plant lectin that
4 recognizes certain carbohydrates, with a special affinity for mannose oligomers [41]. Although
5 the presence of mannose in wasteosomes needs to be verified, since ConA can bind to sugars
6 other than mannose, this finding suggested that the phagocytosis of wasteosomes by THP-1
7 macrophages could involve the mannose receptor [40].
8
9

10
11 In this study, we aimed to shed light on the interactions between wasteosomes and THP-1
12 macrophages and to clarify the processes that trigger the phagocytosis of wasteosomes.
13 Previous results have indicated that there may be redundant mechanisms that lead to the
14 phagocytosis of wasteosomes [40]. Thus, we considered: (1) the possibility of the
15 abovementioned mannose receptor pathway, in which THP-1 macrophages recognize the
16 presence of mannose components in wasteosomes, (2) the process involving the opsonization
17 of wasteosomes by IgMs combined with the presence of IgM receptors like FAIM3 (also known
18 as FC μ R) in THP-1 macrophages, and (3) the process involving the opsonization of wasteosomes
19 with complement proteins (like the C3b protein) combined with the presence of complement
20 protein receptors (like CD35) in THP-1 cells [42]. The activation of the complement system can
21 occur via (a) the classical pathway, triggered by antibody-antigen interactions such as the
22 interaction between IgMs and the NEs present in wasteosomes, (b) the lectin pathway, triggered
23 by lectin-sugar interactions such as the interaction between mannose and mannose-binding
24 lectin (MBL), and (c) the alternative pathway, in which complement proteins become activated
25 directly upon contact with the particle to be engulfed.
26
27
28
29
30
31
32
33
34
35
36
37
38
39

40 In the present study, we also examined the responses generated by the phagocytosis of
41 wasteosomes by macrophages. Once phagocytosed, wasteosomes might simply undergo a
42 process of biochemical degradation, but it could also be possible that some of their components
43 are exposed on the surfaces of macrophages, which would then act as antigen-presenting cells
44 (APCs).
45
46
47
48
49

50 Besides *in vitro* studies, it is also of interest to elucidate the responses that are generated *in vivo*.
51 The interaction between macrophages and wasteosomes cannot occur within the brain
52 parenchyma in physiological circumstances as wasteosomes are intracytoplasmic astrocytic
53 bodies and are therefore unreachable by infiltrating macrophages or even by microglia.
54 However, this interaction could be possible in pathological conditions or inflammatory processes
55 that induce tissue damage. In this sense, the phagocytosis of wasteosomes by macrophages has
56
57
58
59
60
61
62
63
64
65

1
2
3
4
5
6
7
8
9
10
11
12
13
14
15
16
17
18
19
20
21
22
23
24
25
26
27
28
29
30
31
32
33
34
35
36
37
38
39
40
41
42
43
44
45
46
47
48
49
50
51
52
53
54
55
56
57
58
59
60
61
62
63
64
65

been described in the affected areas of tissue samples of the optic nerve and spinal cord in neuromyelitis optica [18]. Furthermore, given that wasteosomes are generally found in the perivascular, periventricular, or subpial regions of the brain and since they are released into the CSF and Virchow-Robin perivascular spaces [11, 40], it is conceivable that wasteosomes could be phagocytosed in these regions by meningeal macrophages, choroid plexus macrophages or perivascular macrophages [43]. This has not been previously examined and is also addressed in the present study.

For all these reasons, the objectives of the present work were to ascertain the mechanisms that trigger the phagocytosis of wasteosomes by THP-1 macrophages, find out how the wasteosomes are processed following phagocytosis by THP-1 macrophages and, finally, determine if macrophages located in the border areas or in the perivascular regions of the brain can interact with wasteosomes.

METHODS

1. Studies on wasteosomes from human CSF samples

Human CSF samples

Post-mortem ventricular CSF samples were obtained from 7 neuropathologically affected patients (66 to 87 years old). When extracted, CSF samples were centrifuged at 4,000 x *g* at 4 °C for 10 min and the pellets obtained were stored at -80 °C until use. All these procedures were performed at the Banc de Teixits Neurològics (Biobanc-Hospital Clínic-IDIBAPS, Barcelona). Medical data on these cases are detailed in Table 1.

All procedures involving human samples were performed in accordance with appropriate guidelines and regulations. All experiments involving human tissue were approved by the Bioethics Committee of the Universitat de Barcelona.

Wasteosomes obtaining and purification

Frozen pellets of CSF were defrosted and resuspended in 5 mL of phosphate-buffered saline (PBS) and divided into 500- μ L aliquots in Eppendorf tubes. These aliquots were centrifuged at 700 x *g* for 10 min, the supernatants were ruled out and the pellets obtained were resuspended in 1,000 μ L of PBS. This process was repeated five times to separate the wasteosomes from CSF

1
2
3
4
5
6
7
8
9
10
11
12
13
14
15
16
17
18
19
20
21
22
23
24
25
26
27
28
29
30
31
32
33
34
35
36
37
38
39
40
41
42
43
44
45
46
47
48
49
50
51
52
53
54
55
56
57
58
59
60
61
62
63
64
65

cell debris and other remnants. Thereafter, another centrifugation at $700 \times g$ for 10 min was performed. The supernatants were ruled out and the wasteosomes were concentrated in the pellet for subsequent opsonization or staining.

ConA staining, AF555 NHS ester staining and IgM opsonization of wasteosomes

Purified wasteosomes for ConA staining or opsonization with IgMs were resuspended in 500 μL of Rhodamine-labeled ConA (ConA-Rhod; 1:250; RL-1002-25; Vector Laboratories), Fluorescein-labeled ConA (ConA-FI; 1:250; FL-1001-25; Vector Laboratories) or purified human IgMs (1:10 dilution; OBT1524; AbD Serotec). Samples were maintained for 21 h at 4°C with agitation. Purified wasteosomes for staining with Alexa Fluor (AF) 555 NHS ester (AF555-NHS; A37571; Thermo Fisher Scientific) were resuspended in 500 μL of 0.1 M sodium bicarbonate buffer (pH 8.3), while, in parallel, 100 μg of the amine-reactive dye AF555-NHS were dissolved in 10 μL of DMSO. Next, 10 μL of the AF555-NHS solution were slowly added to the sample. The mixture was then maintained for 1 hour at room temperature under continuous stirring. After incubation with ConA, IgMs or AF555-NHS, samples were washed by centrifugation at $700 \times g$ for 10 min, the resulting supernatants were ruled out and the pellets resuspended in 1,000 μL of PBS. This washing process was repeated three times. Another centrifugation at $700 \times g$ for 10 min was performed and the supernatants were removed. The resulting pellets were then resuspended in supplemented RPMI 1640 media (Sigma-Aldrich) and added to the cell culture.

Periodic acid-Schiff (PAS) staining of wasteosomes

Purified wasteosomes were resuspended in 1,000 μL of PBS and transferred to Pyrex glass tubes. Samples were centrifuged at $700 \times g$ for 10 min and the pellets obtained were resuspended in 1,000 μL of periodic acid (0.25%; 9324-50; Electron Microscopy Sciences) and stirred for 5 min. Samples were centrifuged at $700 \times g$ for 10 min, the resulting supernatants were removed and the pellets resuspended in 1,000 μL of PBS. This washing process was repeated three times. Samples were centrifuged at $700 \times g$ for 10 min and the pellets obtained were resuspended in 1,000 μL of the Schiff reagent (26052-06; Electron Microscopy Sciences) and stirred for 5 min. Another centrifugation at $700 \times g$ for 10 min was performed, the resulting supernatants were ruled out, and the pellets resuspended in 1,000 μL of PBS. This three-step process was repeated three times. Finally, another centrifugation at $700 \times g$ for 10 min was performed and the supernatants were removed. The pellets were resuspended in supplemented RPMI and added to the cell culture.

Cell culture and differentiation

1 THP-1 cells provided by the American Type Culture Collection (ATCC) were subcultured at a
2 density of 5×10^4 cells/cm² in 24-well plates with 12-mm round coverslips for the
3 immunofluorescence studies and in 8-well chambered slides (μ -Slide 8 Well, Ibidi) for the time-
4 lapse assays. Cells were differentiated into macrophages (THP-1 macrophages) with phorbol 12-
5 myristate 13-acetate (PMA; Sigma-Aldrich) at a concentration of 100 nmol/L in RPMI
6 supplemented with 10% heat-inactivated Fetal Bovine Serum (FBS) (GE Healthcare Life
7 Sciences), 50 μ M β -mercaptoethanol (Sigma-Aldrich), and penicillin (100 U/mL)/streptomycin
8 (100 μ g/mL) (Life Technologies) for 3 days. Differentiation of PMA-treated cells was enhanced
9 after the initial 3-day stimulus by removing the PMA-containing media and incubating the cells
10 in fresh supplemented RPMI for a further 3 days.
11
12
13
14
15
16
17
18
19
20

Phagocytosis studies: time-lapse assays

21 THP-1 macrophages were washed twice using supplemented RPMI without FBS. The cells were
22 then stained for 30 min at 37 °C with 300 μ L of the Vybrant® CFDA-SE Cell Tracer Kit (1:2,000;
23 V12883; Thermo Fisher Scientific) in supplemented RPMI without FBS. Next, the cells were
24 washed with PBS and incubated in 300 μ L of RPMI with all the supplements. Before starting the
25 time-lapse study, the stained macrophages were washed with supplemented RPMI three times
26 before replacing the media with 300 μ L of supplemented RPMI containing the wasteosomes
27 stained with ConA-Rhod, AF555-NHS or PAS. The regions of interest (ROIs) were selected
28 following specific criteria based on the presence and aspect of the wasteosomes and the
29 closeness of the macrophages in relation to the chosen wasteosomes. By selecting the ROIs, only
30 the X and Y coordinates were established. Three Z sections were appointed for each ROI. After
31 selecting all the coordinates, the number of cycles was defined. A cycle consisted of the process
32 of capturing every picture defined by the X, Y and Z coordinates. Thus, in each cycle, the number
33 of pictures captured equaled the number of ROIs multiplied by the amount of Z coordinates
34 selected for each field. In this study, the microscope took nearly 2 minutes to complete each
35 cycle, which means that the frame rate of the definitive recording was 0.5 frames per minute
36 (fpm). Once the sample was placed and the parameters established, the recording process was
37 started and the microscope was left to record overnight for a minimum of 15 hours. Automated
38 multi-position live cell imaging was carried out using a Leica TCS SP5 (Leica Microsystems) or a
39 Zeiss LSM 880 (Zeiss) confocal microscopes, both equipped with an Adaptive Focus Control
40 system to keep the specimen in focus and an incubation system with controlled temperature
41 (37 °C) and CO₂ as well as a humidified atmosphere. Images of CFDA-SE (green channel) and
42
43
44
45
46
47
48
49
50
51
52
53
54
55
56
57
58
59
60
61
62
63
64
65

1
2
3
4
5
6
7
8
9
10
11
12
13
14
15
16
17
18
19
20
21
22
23
24
25
26
27
28
29
30
31
32
33
34
35
36
37
38
39
40
41
42
43
44
45
46
47
48
49
50
51
52
53
54
55
56
57
58
59
60
61
62
63
64
65

ConA-Rhod, AF555-NHS or PAS staining (red channel) were acquired sequentially line by line using the 488 and 561 laser lines and detection ranges of 500-550 and 570-650 nm, respectively. All images were acquired using a Plan Apo 40x oil immersion objective lens (NA 1.1) and a pinhole set at 1.5 Airy units. Simultaneously, bright-field images were acquired. The footage obtained was later processed using the software FIJI (National Institutes of Health, USA).

Phagocytosis studies: immunofluorescence assays

Purified and stained/opsonized wasteosomes obtained from the CSF and resuspended in 1,000 μ L of supplemented RPMI were added to the wells containing THP-1 macrophages. After 2 h, the macrophages were washed with Dulbecco's PBS (DPBS; GIBCO) and fixed in 4% paraformaldehyde in PBS for 15 min. Samples were rehydrated with PBS and then blocked and permeabilized with 1% bovine serum albumin (BSA) in PBS (Sigma-Aldrich) (blocking buffer, BB) containing 0.1% Triton X-100 (Sigma-Aldrich) for 20 min. They were then washed with PBS and incubated for 21 h at 4 °C with one of the following primary antibodies: mouse monoclonal IgG₁ against the mannose receptor CD206 (1:100; ab64693; Abcam), mouse monoclonal IgG₁ against CD35 (1:40; MA5-13122; Thermo Fisher Scientific), mouse monoclonal IgG₁ against CD68 (1:200; ab955; Abcam) or mouse monoclonal IgG₁ against Fc μ R (1:150; MA5-13122; Thermo Fisher Scientific). Next, the samples were washed and incubated for 1 h at room temperature with the AF555 goat anti-mouse IgG₁ secondary antibody (1:250; A-21127; Life Technologies) and the AF488 goat anti-human IgM heavy chain secondary antibody (1:200; A-21215; Life Technologies) if the wasteosomes were opsonized with human IgM. Nuclear staining was performed by incubating the samples with the Hoechst stain (2 μ g/mL; H-33258; Fluka) for 5 min before washing and coverslipping them in ProLong Gold (Thermo Fisher Scientific). Staining controls were performed by incubating with the BB instead of the primary antibody.

MBL and C3b opsonization of wasteosomes and immunofluorescence assays

To opsonize wasteosomes with MBL and C3b, purified wasteosomes were resuspended in 500 μ L of human plasma obtained from healthy donors from the Banc de Sang i Teixits de Barcelona and were maintained for 21 h at 37 °C under continuous stirring. Controls were resuspended in 500 μ L of PBS instead of human plasma and maintained under the same conditions. Samples were washed by centrifugation at 700 \times *g* for 10 min, the resulting supernatants were ruled out and the pellets resuspended in 1,000 μ L of PBS. This washing process was repeated three times. Then, to evaluate the MBL or C3b attachment to the wasteosomes, samples were processed for immunofluorescence assays. Samples were centrifuged at 700 \times *g* for 10 min and the

1 supernatants were removed. The resulting pellets containing the wasteosomes were incubated
2 with 500 μ L of the primary antibody, which was either the mouse monoclonal IgG_{2b} primary
3 antibody against C3/C3b (anti-C3b; 1:100; ab11871; Abcam) or the FITC-conjugated rabbit
4 polyclonal IgG antibody directed against MBL (anti-MBL; 1:100; orb463830; Biorbyt). Incubation
5 with the primary antibody was maintained for 21 h at 4 °C with agitation. Staining controls were
6 performed by incubating with 500 μ L of PBS instead of the primary antibody under the same
7 conditions. Once the incubations ended, the samples were washed by centrifugation at 700 \times *g*
8 for 10 min, the resulting supernatants were ruled out and the pellets resuspended in 1,000 μ L
9 of PBS. This washing process was repeated three times. Samples were centrifuged at 700 \times *g* for
10 10 min and the supernatants were removed. When using the unlabeled primary antibody against
11 C3/C3b, the pellets were resuspended in 500 μ L of the secondary antibody AF555 goat anti-
12 mouse IgG_{2b} (1:250; A-21147; Life Technologies). The incubation was maintained for 1 h at room
13 temperature with agitation. The samples were then washed by centrifugation at 700 \times *g* for 10
14 min, the resulting supernatants removed and the pellets resuspended in 1,000 μ L of PBS. This
15 process was repeated three times. The samples were then centrifuged at 700 *g* for 10 min and
16 the supernatants were removed. Afterwards, the pellets obtained were resuspended in 40 μ L of
17 PBS, spread onto a microscope slide, air-dried and coverslipped with Fluoromount (Electron
18 Microscopy Sciences) for microscope observation.
19
20
21
22
23
24
25
26
27
28
29
30

31 **2. Studies on wasteosomes from brain hippocampal sections**

32 **Human brain samples**

33
34
35
36
37
38
39 Post-mortem brain samples were obtained from the Banc de Teixits Neurològics (Biobanc-
40 Hospital Clínic-IDIBAPS, Barcelona). Frozen hippocampal sections (6 μ m thick; stored at -80 °C)
41 were obtained from two cases of neuropathologically confirmed Alzheimer's disease and two
42 cases of vascular encephalopathy. Medical data on these cases are detailed in Table 2.
43
44
45
46

47 All procedures involving human samples were performed in accordance with appropriate
48 guidelines and regulations. All experiments involving human tissue were approved by the
49 Bioethics Committee of the Universitat de Barcelona.
50
51
52

53 **Immunofluorescence studies of the hippocampal sections**

54
55
56
57
58 Frozen hippocampal sections were left to defrost and air dry for 10 min at room temperature
59 and then fixed with acetone at 4 °C for 10 min. After 2 h of further drying, the sections were
60
61
62
63
64
65

1 rehydrated in PBS and then blocked and permeabilized with the BB containing 0.1% Triton X-
2 100 (Sigma-Aldrich) for 20 min. They were then washed with PBS and incubated for 21 h at 4 °C
3 with two primary antibodies for double staining. The primary antibodies used were: chicken
4 polyclonal IgY against glial fibrillary acidic protein (GFAP) (1:300; AB5541; Merck), mouse
5 monoclonal IgG₁ against the mannose receptor CD206 (1:100; ab64693; Abcam), mouse
6 monoclonal IgG₁ against CD35 (1:40; MA5-13122; Thermo Fisher Scientific), mouse monoclonal
7 IgG₁ against CD68 (1:200; ab955; Abcam), mouse monoclonal IgG₁ against FcμR (1:150; MA5-
8 26353; Thermo Fisher Scientific), mouse monoclonal IgG_{2a} against p62 (1:400; ab56416; Abcam),
9 mouse monoclonal IgG_{2b} against C3/C3b (1:100; ab11871; Abcam), FITC-conjugated rabbit
10 polyclonal IgG antibody directed against MBL (1:100; orb463830; Biorbyt) and rabbit
11 monoclonal IgG against GS (1:100; 15B1; Cell Signaling, Leiden, Netherlands). The slides were
12 then washed and incubated for 1 h at room temperature with the corresponding secondary
13 antibodies: AF488 goat anti-chicken IgY (H + L) (1:250; A-11039; Thermo Fisher Scientific), AF488
14 goat anti-mouse IgG₁ (1:250; A-21121; Life Technologies), AF555 goat anti-mouse IgG₁ (1:250;
15 A-21127; Life Technologies), AF555 goat anti-mouse IgG_{2a} (1:250; A-21137; Life Technologies),
16 AF555 goat anti-mouse IgG_{2b} (1:250; A-21147; Life Technologies) and AF488 donkey anti-rabbit
17 IgG directed against both their heavy and their light chains (1:250; A-21206; Life Technologies).
18 Nuclear staining was performed by incubation with the Hoechst stain (2 μg/mL; H-33258; Fluka)
19 for 5 min and the slides were washed and coverslipped with Fluoromount (Electron Microscopy
20 Sciences). Staining controls were performed by incubating with the BB instead of the primary
21 antibody before incubation with the secondary antibody.
22
23
24
25
26
27
28
29
30
31
32
33
34
35
36

37 **Image acquisition and processing**

38
39
40 Hippocampal images were taken with a fluorescence laser and optical microscope (BX41,
41 Olympus) and stored as tiff files. All the images were acquired using the same microscope, laser,
42 and software settings. The exposure time was adapted to each staining, but the respective
43 control images were acquired with the same exposure time. Image treatment and analysis were
44 performed with ImageJ (NIH). Images that were modified for contrast and brightness to enhance
45 their visualization were processed in the same way as those of their respective controls.
46
47
48
49
50
51
52

53 **RESULTS**

54 **1. Time-lapse study of the phagocytosis of wasteosomes by THP-1 macrophages**

55
56
57
58
59
60
61
62
63
64
65

To study the phagocytosis of wasteosomes by THP-1 macrophages, different sets of experiments were performed using time-lapse imaging.

In the first set of experiments, wasteosomes obtained from the CSF were stained with ConA-Rhod and added to a culture of THP-1 macrophages that had been previously stained with the vital tracer CFDA-SE. From that point on and for each ROI (i.e., regions that contain wasteosomes), an image was taken every 2 minutes over a period of a minimum of 15 hours. The sequence of images was then put into a video format to see the interaction between the macrophages and wasteosomes at each ROI during this period.

In all the ROIs, we observed that the macrophages did interact with wasteosomes. Video 1A, summarized in Figure 1A, shows the encounter of one macrophage with a wasteosome as well as several steps of phagocytosis. Firstly, a lamellipodium extends from the macrophage until it reaches the wasteosome. Once the lamellipodium has attached to the wasteosome, it pulls it towards the body of the macrophage and the macrophage completely engulfs the wasteosome. Once the wasteosome has been phagocytosed, the red fluorescence signal progressively spreads inside the macrophage, indicating that the wasteosome (or its ConA-Rhod protein fraction) has been digested. After the engulfment and digestion, some of the fluorescence appears on the surface of the macrophage. This process was corroborated by the 3D reconstructions from the confocal images obtained in the last moment of some sequences (Figure 1B, Video 1B). This suggests that parts of the stained wasteosome were exposed on the surfaces of THP-1 macrophages. Thus, THP-1 macrophages could act as APCs.

In other cases, the wasteosomes were too big to be engulfed by the macrophages, but an interaction between the wasteosomes and macrophages could be observed. Figure 2A and Video 2A show different macrophages making contact with a large wasteosome. The wasteosome is eroded by these macrophages and a gradual increase in the red fluorescence signal can be seen inside the macrophages. Moreover, some spots of fluorescence are also present on the surface of the macrophages and some interchanges of these spots of fluorescence between the different macrophages can be appreciated. Video 2B and Figure 2B show three different wasteosomes, of which two are just eroded by the macrophages and the remaining one is not just eroded but fragmented, with the resulting fragments digested by several macrophages.

From the results of this first set of experiments, we deduced that THP-1 macrophages can engulf and digest wasteosomes when these are opsonized by ConA-Rhod. Moreover, these

macrophages might act as APCs by presenting the fluorescent component (i.e., ConA-Rhod or some of its fragments containing Rhod) on their surface.

In the second set of experiments, wasteosomes obtained from the CSF were stained with AF555-NHS and added to a culture of THP-1 macrophages that had been stained with CFDA-SE. In contrast to the first set of experiments, where we used an external protein (ConA-Rhod) that binds to the sugar components of wasteosomes, in this second set of experiments we used the AF555-NHS probe, which directly stains the proteins contained in the wasteosomes, thus enabling the determination of whether these proteins were also digested and presented on the surface of macrophages.

In this second set of experiments, we also observed that some macrophages interacted with the wasteosomes stained with the AF555-NHS dye. Video 3A and Figure 3A show a macrophage making contact with a wasteosome at different times. Although the wasteosome is not entirely phagocytosed, some spots of red fluorescence are translocated from the wasteosome to the macrophage. When the macrophage detach from the wasteosome, the spots of fluorescence remain at the macrophage, indicating that the fluorescence signal from the wasteosome has been incorporated into the macrophage. The same process can be seen in Video 3B and Figure 3B. In this case, some spots of fluorescence can be observed on the surface of the macrophage, indicating possible antigen presentation. Thus, this second set of experiments indicated that the proteins contained in the wasteosomes can be phagocytosed by macrophages and that these proteins can later be presented on the surface of macrophages.

In the third set of experiments, wasteosomes obtained from the CSF were stained with the PAS technique and added to a culture of THP-1 macrophages that had been stained with CFDA-SE. In contrast to the first and second set of experiments, the fluorescence was generated here by the PAS staining, specifically related to the carbohydrate constituents of wasteosomes. This protocol allowed to determine if the carbohydrate components of wasteosomes are also digested and/or presented on the macrophage surface.

In this case, we observed that macrophages also interacted with wasteosomes. A representative sequence of images is presented in Video 4A and Figure 4A. Initially, a lamellipodium from a distant macrophage making contact with the wasteosome can be observed. Thereafter, the macrophage shrinks over the wasteosome and both structures displace together. However, unlike in the previous sets of experiments, digestion of the wasteosomes could not be observed in most of these experiments. In only a few cases, as that shown in Figure 4B and Video 4B, small

amounts of fluorescence were observed to detach from the wasteosomes and spread inside the macrophages. In any case, the processes of phagocytosis, digestion and antigen presentation seemed to be reduced in this set of experiments, which indicates that the processing of the polyglucosan structure of wasteosomes differs from that of the protein fraction.

2. Identification of phagocytic receptors on THP-1 macrophages that interact with wasteosomes

Since the time-lapse studies demonstrated that THP-1 macrophages interact with wasteosomes and can phagocytose them, the next step was to shed light on the mechanisms triggering this phagocytosis. In this regard, the study of the phenotype or, more specifically, of the phagocytic receptors expressed by THP-1 macrophages was determining. We postulated that the phagocytosis of wasteosomes could be mediated by CD206, CD35 and/or FAIM3. Thus, we isolated wasteosomes from the CSF and stained them with ConA-FI or opsonized them with IgM before adding them to THP-1 macrophage cultures. The cultures were then fixed and processed for immunofluorescence analysis using anti-CD68, anti-CD206, anti-CD35 and anti-Fc μ R (directed against FAIM3) antibodies, and adding the AF488 anti-IgM antibody in the cases of wasteosomes that had been opsonized with IgM. This protocol allowed not only the detection of the abovementioned markers in THP-1 macrophages, but also the detection of these markers in wasteosomes-interacting macrophages. CD68 is a transmembrane glycoprotein that is highly expressed by human monocytes and macrophages [44]. It was used here to identify macrophages in the cultures, observe the interactions between macrophages and wasteosomes, and validate the effectiveness of the immunofluorescence method. As shown in Figure 5a, THP-1 macrophages stained with the anti-CD68 antibody were observed to make contact with ConA-FI-stained wasteosomes. Using the same protocol, we searched for the presence of the other indicated markers on macrophages that made contact with wasteosomes. CD206, also known as the mannose receptor, is a C-lectin that recognizes mannose residues, as well as N-acetylglucosamine and fucose residues [45]. It is normally expressed on M2, but not on M1 macrophages [46]. Figure 5b shows a representative image of CD206-positive THP-1 macrophage encircling and making contact with a ConA-FI-stained wasteosome. These results, which are consistent with those obtained previously [40], suggest that macrophages that phagocytose wasteosomes are non-inflammatory or of the M2 subtype. Regarding the possible CD35-mediated phagocytosis, we stained THP-1 macrophages with the anti-CD35 antibody. CD35, also known as Complement Receptor type 1 (CR1), is a protein that binds to C3b/C4b-opsonized substances that are tagged for phagocytosis [47]. Figure 5c and 5d indicate that THP-1 macrophages that phagocytose wasteosomes express CD35, suggesting that these

1
2
3
4
5
6
7
8
9
10
11
12
13
14
15
16
17
18
19
20
21
22
23
24
25
26
27
28
29
30
31
32
33
34
35
36
37
38
39
40
41
42
43
44
45
46
47
48
49
50
51
52
53
54
55
56
57
58
59
60
61
62
63
64
65

macrophages might also recognize some complement proteins in wasteosomes. Since wasteosomes are recognized by natural IgMs [10], complement activation could be triggered through the classical complement pathway, which would lead to wasteosomes opsonization by C3b and the induction of their CD35-mediated phagocytosis. However, as IgMs do not cross the blood-brain barrier, this process might occur in the lymphatic system or beyond, but not inside the brain. Since wasteosomes may contain mannose and N-acetylglucosamine, which are both targets of MBL [48], wasteosomes could also activate the complement system through the lectin pathway. The alternative pathway is the third biochemical pathway of the complement cascade and should also be considered. This pathway is based on the spontaneous hydrolysis of C3 into C3b. It has been reported that C3b binds to glucose oligomers [49, 50]. Since glucose has been described to be the main component of wasteosomes, C3b could probably bind to this carbohydrate. Given that natural IgMs recognize wasteosomes, we also considered FAIM3-mediated phagocytosis as well. FAIM3, also known as FcμR, is an IgM receptor found in some macrophages and dendritic cells that are associated with phagocytic processes [51–53]. Accordingly, we stained THP-1 macrophages with the anti-FcμR antibody, but these cells did not stain with this antibody, thus ruling out this pathway in the phagocytosis of wasteosomes by THP-1 macrophages.

3. The presence of opsonins on the wasteosomes surface

Wasteosomes have a polyglucosan structure based on polymerized hexoses, which are mainly glucose [1] although not exclusively. As previously mentioned, MBL binds to several hexoses such as mannose and N-acetylglucosamine, while C3b can bind to glucose [48–50]. Accordingly, we explored the CD35- or complement-mediated phagocytosis and analyzed if the wasteosomes from the CSF could be opsonized by MBL or C3b. After incubating the wasteosomes with human plasma, some aliquots were immunostained with the anti-C3b antibody (directed against C3b) while others were immunostained with the anti-MBL antibody. As shown in Figure 6A, wasteosomes were stained by both the anti-C3b and anti-MBL antibodies, indicating that wasteosomes are opsonized by MBL and C3b. However, and surprisingly, wasteosomes from the control samples (where the wasteosomes were incubated with PBS instead of human plasma) were also stained with the anti-C3b or anti-MBL antibody, indicating that wasteosomes from the CSF are opsonized by MBL and C3b. It is of interest that wasteosomes located in the brain parenchyma are not opsonized by these proteins (Figure 6B), indicating that the opsonization with MBL and C3b is produced when wasteosomes attain the CSF. Regardless, these results support the complement-mediated phagocytosis of wasteosomes once these bodies are extruded out of the brain.

4. Wasteosomes and macrophage interactions at central nervous system interfaces

1
2
3 After observing that different mechanisms might be involved in the phagocytosis of
4 wasteosomes by THP-1 macrophages *in vitro*, we ascertained whether this phagocytosis also
5 happens *in vivo* when wasteosomes are released from the brain parenchyma into the CSF. As
6 mentioned above, wasteosomes accumulate mainly in the perivascular, periventricular and
7 subpial regions of the brain. When they are expelled from these regions, they may encounter
8 perivascular macrophages, choroid plexus macrophages and meningeal macrophages.
9 Therefore, double immunostaining of human hippocampal sections was performed with the
10 anti-p62 antibody, a protein marker that allows the localization of wasteosomes, together with
11 the anti-CD206, anti-CD35, anti-FAIM3 or anti-CD68 antibody, which are associated with
12 phagocytosis or phagocytic cells. Immunostaining with the anti-CD206 antibody revealed some
13 CD206-positive macrophages that were in contact with wasteosomes. Figure 7a1, exhibiting a
14 section including a part of the hippocampus and the lateral ventricle, shows a CD206-positive
15 choroid plexus macrophage making contact with a wasteosome that has been released from the
16 brain tissue into the CSF in the lateral ventricle. The choroid plexus macrophage attached to the
17 wasteosome can be clearly observed in the magnification of this image shown in Figure 7a2.
18 Figure 7a3 and 7a4 show several wasteosomes that have been released from the bordering
19 regions of the hippocampus into the subarachnoid space making contact with CD206-positive
20 meningeal macrophages. A magnification of Figure 7a4 is shown in Figure 7a5, where the
21 staining of wasteosome is digitally intensified to illustrate the presence of a wasteosome with
22 two encircling meningeal macrophages. Staining with the anti-CD35 antibody also revealed
23 some positive cells located at the border of the brain parenchyma surrounding several
24 wasteosomes (Figure 7b). As astrocytes in the *glia limitans* of brain cavities can be positive for
25 CD35, we tested the possible colocalization of CD35 with GFAP, which is a specific marker of
26 astrocytes. As shown in Figure 7c, CD35 staining colocalized with GFAP staining, indicating that
27 the cells containing the wasteosomes are not macrophages in this case, but astrocytes that are
28 probably generating the wasteosomes. The staining with the anti-FAIM3 antibody did not show
29 any positive cells in the hippocampal sections (Figure 7d). Finally, the staining with the anti-CD68
30 antibody stained some cells located in the brain parenchyma. For their localization, these cells
31 are presumably microglial cells, although it cannot be discarded possible infiltrating
32 macrophages. In any case, these CD68 positive cells do not contact with wasteosomes (Figure
33 7e). As expected, microglia or macrophages did not reach the wasteosomes within the brain
34 parenchyma since in this region wasteosomes are intracellular astrocytic structures.
35
36
37
38
39
40
41
42
43
44
45
46
47
48
49
50
51
52
53
54
55
56
57
58
59
60
61
62
63
64
65

DISCUSSION

1 The study of wasteosomes has been intriguing since its inception, mainly due to the enormous
2 variety in the results that have been obtained and the difficulty of fitting them all into a
3 consistent and coherent theory. From this perspective, it is not surprising that the present study,
4 which initiates a new line of research focused on the interaction of wasteosomes with
5 macrophages, also leads to diverse findings and leaves open different possibilities. However,
6 and as will be developed below, all these possibilities are consistent with the recent hypothesis
7 formulated about wasteosomes and their function [10, 40]. Briefly, this hypothesis considers
8 that (a) wasteosomes act as waste containers, (b) these containers are formed by a polyglucosan
9 structure that surround or entraps waste substances of different origins, (c) the containers are
10 expelled from the central nervous system towards the CSF for its subsequent elimination, and
11 (d) the natural immune system can participate in this elimination.
12
13
14
15
16
17
18
19
20
21

22 In the first part of the present study involving time-lapse assays, we were able to observe that
23 THP-1 macrophages phagocytose and process wasteosomes. This is, to our knowledge, the first
24 time in which the phagocytosis of wasteosomes has been recorded. In our point of view, this
25 was a starting point towards subsequent studies about wasteosomes, particularly the
26 mechanisms implicated in the phagocytosis of waste elements generated in the organism. Under
27 all the experimental conditions (i.e., ConA-, AF555-NHS- and PAS-labeled wasteosomes), the
28 time-lapse studies revealed that macrophages phagocytose or interact with wasteosomes. We
29 also observed that once phagocytosed, ConA-labeled and AF555-NHS-labeled wasteosomes
30 were digested or fragmented and (at least) the fluorescent protein fraction was exposed on the
31 surface of macrophages as well as transferred from one macrophage to another. We observed
32 a lower reactivity of macrophages towards PAS-stained wasteosomes. Although macrophages
33 also contacted with wasteosomes, we did not observe the fluorescent fraction (in this case, the
34 glycan component) spreading throughout the cytoplasm of the macrophages. This could be
35 attributed to a different processing inside the macrophages of the protein fraction of the
36 wasteosomes with respect to the carbohydrate one. Alternatively, it could be due to the changes
37 generated by the PAS staining in the carbohydrate skeleton of the wasteosomes, which would
38 make the wasteosomes less susceptible to the activities of lysosomal amylases or enzymes. In
39 any case, the reactivity of macrophages to wasteosomes was observed in every set of
40 experiments, and supports the role of the immune system in the elimination of wasteosomes.
41
42
43
44
45
46
47
48
49
50
51
52
53
54
55
56

57 The results obtained about the phagocytic markers present in macrophages and about opsonins
58 present in wasteosomes leave many possibilities open, reinforcing the idea already pointed out
59
60
61
62
63
64
65

1
2
3
4
5
6
7
8
9
10
11
12
13
14
15
16
17
18
19
20
21
22
23
24
25
26
27
28
29
30
31
32
33
34
35
36
37
38
39
40
41
42
43
44
45
46
47
48
49
50
51
52
53
54
55
56
57
58
59
60
61
62
63
64
65

in Riba et al. (2019) that there may be redundant mechanisms underlying the phagocytosis of wasteosomes and their elimination [40]. Figure 8 shows an integrative scheme of the results obtained, providing a broad view of them. We observed that THP-1 macrophages express CD206 and CD35, but not FAIM3. The absence of FAIM3 in THP-1 macrophages indicates that in this cell type, phagocytosis does not occur directly through the interaction of IgMs with this specific IgM membrane receptor. However, phagocytosis could occur through CD206 and CD35, which are both present in THP-1 macrophages.

As commented before, CD206, also known as the mannose receptor, is a C-lectin that recognizes mannose residues, as well as N-acetylglucosamine and fucose residues [45]. It is normally expressed on M2, but not on M1 subtype of macrophages [46]. Although the classification of macrophages as M1 or M2 subtypes is not clear or binary [54, 55], it is of interest that M2 macrophages, such as those of the M2a or M2c subsets that contain the CD206 receptors, are considered to be anti-inflammatory, with M2a macrophages involved in tissue remodeling and M2c macrophages associated with the phagocytosis of apoptotic cells [56–58]. From this point of view and bearing in mind that wasteosomes include waste elements that would need to be removed without triggering unnecessary inflammatory responses, it seems conceivable that wasteosomes contain elements that can be recognized by the CD206 receptor of these macrophages. The presence of these target elements of the CD206 receptor in the wasteosomes has not been studied yet, but since wasteosomes are recognized by ConA, it is possible that wasteosomes may contain mannose or N-acetylglucosamine, which are targets of both ConA [59–61] and CD206 proteins [45]. These sugars might form part of the wasteosomes polyglucosan structure or be a part of the waste substances that accumulate in these bodies. Based on current evidence and given that non-inflammatory responses are expected under physiological conditions, the first option is more likely.

We also observed that THP-1 macrophages express CD35. CD35, also known as the C3b receptor and CR1 receptor, recognizes the C3b opsonizing protein. This receptor is found, among other locations, on the membrane of certain macrophages and triggers the phagocytosis of C3b-opsonized substances [62, 63]. As wasteosomes from the CSF are opsonized by C3b, the presence of CD35 in THP-1 macrophages may also explain the phagocytosis of wasteosomes. The presence of C3b in wasteosomes can be explained by the lectin pathway, since wasteosomes from the CSF are opsonized by MBL. The presence of C3b and MBL in the wasteosomes from the CSF may be due to the presence of C3 and MBL in the CSF [64-68]. In addition, from a theoretical point of view, we cannot rule out the possibility that the opsonization of wasteosomes with C3b

also occurs in the CSF by the alternative route or that it may occur at other locations in the case of wasteosomes making contact with plasma natural IgMs.

The fact that wasteosomes might already become opsonized by C3b when entering the CSF indicates that they could be phagocytosed at central nervous system interfaces through CD35- or complement-mediated phagocytosis by perivascular macrophages, meningeal macrophages or choroid plexus macrophages. In the present study, we did not observe the presence of CD35-positive macrophages at these interfaces, although the large presence of CD35-positive astrocytes could have masked them. We also did not observe FAIM3-positive macrophages at these interfaces, but we did observe CD206-positive macrophages interacting with wasteosomes. Interestingly and coincidentally, in previous studies, we observed that the wasteosomes that reach the cervical lymph nodes bind to macrophages that do not express CD35 or FAIM3 receptors [40]. This suggests that the mannose receptor could be involved in *in vivo* phagocytosis of wasteosomes, as observed *in vitro* with the THP-1 macrophages.

CONCLUSIONS

The present study indicates that, *in vivo*, there may be redundant mechanisms that trigger the phagocytosis of wasteosomes after their extrusion from the nervous system. The main mechanism involves the CD206 receptor, which triggers the phagocytosis without leading to inflammatory responses, and thus avoiding tissue damage. CD35 and FAIM3 receptors constitute other possible mechanisms, in the first case due to the C3b opsonization of the wasteosomes in the CSF, and in the second case due to the possible opsonization of wasteosomes by natural IgMs. These redundant mechanisms would ensure the elimination of wasteosomes by macrophages located in the border areas of the nervous system or beyond, and reinforce the role of wasteosomes as waste containers equipped with sufficient markers to ensure their elimination. However, as wasteosomes export brain substances avoiding the blood brain barrier, it is necessary to elucidate if some of the macrophages that phagocytose the wasteosomes participate in the induction of immunological tolerance and of adaptive immunological responses in the central nervous system, and may also play significant roles in some brain autoimmune diseases.

ABBREVIATIONS

AF: Alexa Fluor; APCs: Antigen-presenting cells; BB: Blocking buffer; BSA: Bovine serum albumin; ConA: Concanavalin A; CR1: Complement receptor type 1; CSF: Cerebrospinal fluid; DPBS:

1
2
3
4
5
6
7
8
9
10
11
12
13
14
15
16
17
18
19
20
21
22
23
24
25
26
27
28
29
30
31
32
33
34
35
36
37
38
39
40
41
42
43
44
45
46
47
48
49
50
51
52
53
54
55
56
57
58
59
60
61
62
63
64
65

Dulbecco's PBS; FBS: Fetal bovine serum; FI: Fluorescein; fpm: Frames per minute; GFAP: Glial fibrillary acidic protein; GS: Glycogen synthase; MBL: Mannose-binding lectin; NEs: Neoepitopes; PAS: Periodic acid-Schiff; PBS: Phosphate-buffered saline; PMA: Phorbol 12-myristate 13-acetate; Rhod: Rhodamine; ROIs: Regions of interest; THP-1 macrophages: Macrophages derived from THP-1 cells.

DECLARATIONS

Ethics approval and consent to participate

All procedures involving human samples were performed in accordance with appropriate guidelines and regulations. All experiments involving human tissue were approved by the Bioethics Committee of the Universitat de Barcelona.

Consent for publication

Not applicable.

Availability of data and materials

The data sets and materials are available on request to the corresponding author.

Competing interests

The authors declare that they have no competing interests.

Funding

This study was funded by the Spanish Ministerio de Economía y Competitividad (BFU2016-78398-P) and by Agencia Estatal de Investigación (PID2020-115475GB-I00/AEI/10.13039/501100011033). MR is a recipient of a predoctoral fellowship from the Spanish Ministerio de Ciencia, Innovación y Universidades (Formación de Profesorado Universitario, 2018).

Authors' contributions

MR, JdV, JV and CP designed and conceptualized the study, performed the experiments, analyzed the data and prepared the manuscript. IT provided technical support. LM-P and TX contributed to the obtention and processing of human samples. MC contributed to experiments

with confocal microscopy and time-lapse experiments. JC-S, RF and RM-V prepared and provided the cultures of THP-1 monocytes. JV and CP directed the study.

Acknowledgements

We are sincerely grateful to Elisenda Coll and Gemma Martin from the Servei de Microscòpia Òptica Avançada (Centres Científics i Tecnològics, Universitat de Barcelona) for their help and availability. We are indebted to the Biobanc-Hospital Clinic-Institut d'Investigacions Biomèdiques August Pi i Sunyer (IDIBAPS), integrated in the Spanish National Biobank Network, for the samples and data procurement. We are sincerely grateful to Tasneem Ahmed and Michael Maudsley for correcting the English version of the manuscript.

REFERENCES

1. Sakai M, Austin J, Witmer F, Trueb L. Studies of Corpora Amylacea. *Arch Neurol.* 1969;21:526–44. <https://doi.org/10.1001/archneur.1969.00480170098011>.
2. Sbarbati A, Carner M, Colletti V, Osculati F. Extrusion of Corpora Amylacea From the Marginal Glia at the Vestibular Root Entry Zone. *J Neuropathol Exp Neurol.* 1996;55:196–201. <https://doi.org/10.1097/00005072-199602000-00008>.
3. Cavanagh JB. Corpora-Amylacea and the Family of Polyglucosan Diseases. *Brain Res Rev.* 1999;29:265–95. [https://doi.org/10.1016/S0165-0173\(99\)00003-X](https://doi.org/10.1016/S0165-0173(99)00003-X).
4. Singhrao SK, Neal JW, Piddlesden SJ, Newman GR. New Immunocytochemical Evidence for a Neuronal/Oligodendroglial Origin for Corpora Amylacea. *Neuropathol Appl Neurobiol.* 1994;20:66–73. <https://doi.org/10.1111/j.1365-2990.1994.tb00958.x>.
5. Radhakrishnan A, Radhakrishnan K, Radhakrishnan VV, Mary PR, Kesavadas C, Alexander A, et al. Corpora Amylacea in Mesial Temporal Lobe Epilepsy: Clinico-Pathological Correlations. *Epilepsy Res.* 2007;74:81–90. <https://doi.org/10.1016/j.eplepsyres.2007.01.003>.
6. Pirici D, Margaritescu C. Corpora Amylacea in Aging Brain and Age-Related Brain Disorders. *J Aging Gerontol.* 2014;2:33–57. <http://dx.doi.org/10.12974/2309-6128.2014.02.01.6>.
7. Rohn TT. Corpora Amylacea in Neurodegenerative Diseases: Cause or Effect? *Int J Neurol Neurother.* 2015;2:031. <https://doi.org/10.23937/2378-3001/2/2/1031>.
8. Schipper HM, Cissé S. Mitochondrial Constituents of Corpora Amylacea and Autofluorescent Astrocytic Inclusions in Senescent Human Brain. *Glia.* 1995;14:55–64. <https://doi.org/10.1002/glia.440140108>.
9. Selmaj K, Pawłowska Z, Walczak A, Koziółkiewicz W, Raine CS, Cierniewski CS. Corpora Amylacea From Multiple Sclerosis Brain Tissue Consists of Aggregated Neuronal Cells. *Acta Biochim Pol.* 2008;55:43–9. https://doi.org/10.18388/abp.2008_3199.
10. Augé E, Cabezón I, Pelegrí C, Vilaplana J. New Perspectives on Corpora Amylacea in the Human Brain. *Sci Rep.* 2017;7:41807. <https://doi.org/10.1038/srep41807>.
11. Navarro PP, Genoud C, Castaño-Díez D, Graff-Meyer A, Lewis AJ, de Gier Y, et al. Cerebral Corpora Amylacea Are Dense Membranous Labyrinths Containing Structurally Preserved Cell Organelles. *Sci Rep.* 2018;8:18046. <https://doi.org/10.1038/s41598-018-36223-4>.
12. Augé E, Bechmann I, Llor N, Vilaplana J, Krueger M, Pelegrí C. Corpora Amylacea in Human Hippocampal Brain Tissue Are Intracellular Bodies That Exhibit a Homogeneous Distribution of Neo-Epitopes. *Sci Rep.* 2019;9:2063. <https://doi.org/10.1038/s41598-018-38010-7>.

13. Riba M, Del Valle J, Augé E, Vilaplana J, Pelegrí C. From corpora amylacea to wasteosomes: History and perspectives. *Ageing Res Rev.* 2021; 72:101484. <https://doi.org/10.1016/j.arr.2021.101484>.
14. Ferraro A, Damon LA. The Histogenesis of Amyloid Bodies in the Central Nervous System. *Arch Pathol.* 1931;12:229–44.
15. Martin JE, Mather K, Swash M, Garofalo O, Leigh PN, Anderton BH. Heat Shock Protein Expression in Corpora Amylacea in the Central Nervous System: Clues to Their Origin. *Neuropathol Appl Neurobiol.* 1991;17:113–9. <https://doi.org/10.1111/j.1365-2990.1991.tb00702.x>.
16. Gáti I, Leel-Ossi L. Heat Shock Protein 60 in Corpora Amylacea. *Pathol Oncol Res.* 2001;7:140–4. <https://doi.org/10.1007/BF03032581>.
17. Meng H, Zhang X, Blaivas M, Wang MM. Localization of Blood Proteins Thrombospondin1 and ADAMTS13 to Cerebral Corpora Amylacea. *Neuropathology.* 2009;29:664–71. <https://doi.org/10.1111/j.1440-1789.2009.01024.x>.
18. Suzuki A, Yokoo H, Kakita A, Takahashi H, Harigaya Y, Ikota H, et al. Phagocytized Corpora Amylacea as a Histological Hallmark of Astrocytic Injury in Neuromyelitis Optica. *Neuropathology.* 2012;32:587–94. <https://doi.org/10.1111/j.1440-1789.2012.01299.x>.
19. Wander CM, Tseng J, Song S, Al Housseiny HA, Tart DS, Ajit A, et al. The Accumulation of Tau-Immunoreactive Hippocampal Granules and Corpora Amylacea Implicates Reactive Glia in Tau Pathogenesis During Aging. *iScience.* 2020;23:101255. <https://doi.org/10.1016/j.isci.2020.101255>.
20. Libard S, Popova SN, Amini RM, Kärjä V, Pietiläinen T, Hämäläinen KM, et al. Human Cytomegalovirus Tegument Protein pp65 is Detected in All Intra- and Extra-Axial Brain Tumours Independent of the Tumour Type or Grade. *PloS One.* 2014;9:e108861. <https://doi.org/10.1371/journal.pone.0108861>.
21. Pisa D, Alonso R, Rábano A, Carrasco L. Corpora Amylacea of Brain Tissue From Neurodegenerative Diseases Are Stained With Specific Antifungal Antibodies. *Front Neurosci.* 2016;10:86. <https://doi.org/10.3389/fnins.2016.00086>.
22. Pisa D, Alonso R, Marina AI, Rábano A, Carrasco L. Human and Microbial Proteins From Corpora Amylacea of Alzheimer’s Disease. *Sci Rep.* 2018;8:9880. <https://doi.org/10.1038/s41598-018-28231-1>.
23. Augé E, Duran J, Guinovart JJ, Pelegrí C, Vilaplana J. Exploring the Elusive Composition of Corpora Amylacea of Human Brain. *Sci Rep.* 2018;8:13525. <https://doi.org/10.1038/s41598-018-31766-y>.
24. Riba M, Augé E, Tena I, del Valle J, Molina-Porcel L, Ximelis T, et al. Corpora amylacea in the human brain exhibit neoepitopes of a carbohydrate nature. *Front Immunol.* 2021;12:618193. <https://doi.org/10.3389/fimmu.2021.618193>.
25. Singh R, Barden A, Mori T, Beilin L. Advanced Glycation End-Products: A Review. *Diabetologia.* 2001;44:129–46. <https://doi.org/10.1007/s001250051591>.
26. Chou MY, Fogelstrand L, Hartvigsen K, Hansen LF, Woelkers D, Shaw PX, et al. Oxidation-Specific Epitopes Are Dominant Targets of Innate Natural Antibodies in Mice and Humans. *J Clin Invest.* 2009;119:1335–49. <https://doi.org/10.1172/JCI36800>.
27. Vollmers HP, Brändlein S. Natural Antibodies and Cancer. *N Biotechnol.* 2009;25:294–8. <https://doi.org/10.1016/j.nbt.2009.03.016>.
28. Kay M. Physiologic Autoantibody and Immunoglobulin Interventions During Aging. *Curr Aging Sci.* 2013;6:56–62. <https://doi.org/10.2174/1874609811306010008>.
29. Pawelec G. Immunosenescence and Cancer. *Biogerontology.* 2017;18:717–21. <https://doi.org/10.1007/s10522-017-9682-z>.

30. Avrameas S. Natural Autoantibodies: From “Horror Autotoxicus” to “Gnothi Seauton”. *Immunol Today*. 1991;12:154–9. [https://doi.org/10.1016/0167-5699\(91\)90080-D](https://doi.org/10.1016/0167-5699(91)90080-D).
31. Baumgarth N, Tung JW, Herzenberg LA. Inherent Specificities in Natural Antibodies: A Key to Immune Defense against Pathogen Invasion. *Springer Semin Immunopathol*. 2005;26:347–62. <https://doi.org/10.1007/s00281-004-0182-2>.
32. Ehrenstein MR, Notley wasteosomes. The Importance of Natural IgM: Scavenger, Protector and Regulator. *Nat Rev Immunol*. 2010;10:778–86. <https://doi.org/10.1038/nri2849>.
33. Grönwall C, Vas J, Silverman GJ. Protective Roles of Natural IgM Antibodies. *Front Immunol*. 2012;3:66. <https://doi.org/10.3389/fimmu.2012.00066>.
34. Mannoor K, Xu Y, Chen C. Natural Autoantibodies and Associated B Cells in Immunity and Autoimmunity. *Autoimmunity*. 2013;46:138–47. <https://doi.org/10.3109/08916934.2012.748753>.
35. Holodick NE, Rodríguez-Zhurbenko N, Hernández AM. Defining Natural Antibodies. *Front Immunol*. 2017;8:872. <https://doi.org/10.3389/fimmu.2017.00872>.
36. Reyneveld GI, Savelkoul HFJ, Parmentier HK. Current Understanding of Natural Antibodies and Exploring the Possibilities of Modulation Using Veterinary Models. A Review. *Front Immunol*. 2020;11:2139. <https://doi.org/10.3389/fimmu.2020.02139>.
37. Chen Y, Park YB, Patel E, Silverman GJ. IgM Antibodies to Apoptosis-Associated Determinants Recruit C1q and Enhance Dendritic Cell Phagocytosis of Apoptotic Cells. *J Immunol*. 2009;182:6031–43. <https://doi.org/10.4049/jimmunol.0804191>.
38. Lutz HU, Binder CJ, Kaveri S. Naturally Occurring Auto-Antibodies in Homeostasis and Disease. *Trends Immunol*. 2009;30:43–51. <https://doi.org/10.1016/j.it.2008.10.002>.
39. Maddur MS, Lacroix-Desmazes S, Dimitrov JD, Kazatchkine MD, Bayry J, Kaveri SV. Natural Antibodies: From First-Line Defense Against Pathogens to Perpetual Immune Homeostasis. *Clin Rev Allergy Immunol*. 2020;58:213–28. <https://doi.org/10.1007/s12016-019-08746-9>.
40. Riba M, Augé E, Campo-Sabariz J, Moral-Anter D, Molina-Porcel L, Ximelis T, et al. Corpora Amylacea Act as Containers That Remove Waste Products From the Brain. *Proc Natl Acad Sci USA*. 2019;116:26038–48. <https://doi.org/10.1073/pnas.1913741116>.
41. Liu HM, Anderson K, Caterson B. Demonstration of a keratan sulfate proteoglycan and a mannose-rich glycoconjugate in corpora amylacea of the brain by immunocytochemical and lectin-binding methods. *J Neuroimmunol*. 1987;14:49–60. [https://doi.org/10.1016/0165-5728\(87\)90100-7](https://doi.org/10.1016/0165-5728(87)90100-7).
42. Aderem A, Underhill DM. Mechanisms of phagocytosis in macrophages. *Annu Rev Immunol*. 1999;17:593–623. <https://doi.org/10.1146/annurev.immunol.17.1.593>.
43. Kierdorf K, Masuda T, Jordão MJC, Prinz M. Macrophages at CNS interfaces: ontogeny and function in health and disease. *Nat Rev Neurosci*. 2019;20:547–62. <https://doi.org/10.1038/s41583-019-0201-x>.
44. Holness CL, Simmons DL. Molecular cloning of CD68, a human macrophage marker related to lysosomal glycoproteins. *Blood*. 1993;81:1607–13. <https://doi.org/10.1182/blood.V81.6.1607.1607>.
45. Feinberg H, Jégouzo SAF, Lasanajak Y, Smith DF, Drickamer K, Weis WI, et al. Structural analysis of carbohydrate binding by the macrophage mannose receptor CD206. *J Biol Chem*. 2021;296:100368. <https://doi.org/10.1016/j.jbc.2021.100368>.
46. Mantovani A, Sica A, Sozzani S, Allavena P, Vecchi A, Locati M. The chemokine system in diverse forms of macrophage activation and polarization. *Trends Immunol*. 2004;25:677–86. <https://doi.org/10.1016/j.it.2004.09.015>.
47. Smith BO, Mallin RL, Krych-Goldberg M, Wang X, Hauhart RE, Bromek K, et al. Structure of the C3b binding site of CR1 (CD35), the immune adherence receptor. *Cell*. 2002;108:769–80. [https://doi.org/10.1016/s0092-8674\(02\)00672-4](https://doi.org/10.1016/s0092-8674(02)00672-4).

- 1
2
3
4
5
6
7
8
9
10
11
12
13
14
15
16
17
18
19
20
21
22
23
24
25
26
27
28
29
30
31
32
33
34
35
36
37
38
39
40
41
42
43
44
45
46
47
48
49
50
51
52
53
54
55
56
57
58
59
60
61
62
63
64
65
48. Ip WK, Takahashi K, Ezekowitz RA, Stuart LM. Mannose-binding lectin and innate immunity. *Immunol Rev.* 2009;230:9–21. <https://doi.org/10.1111/j.1600-065X.2009.00789.x>.
 49. Pangburn MK. Analysis of recognition in the alternative pathway of complement. Effect of polysaccharide size. *J Immunol.* 1989;142:2766–70.
 50. Hostetter MK. Handicaps to host defense. Effects of hyperglycemia on C3 and *Candida albicans*. *Diabetes.* 1990;39:271–5. <https://doi.org/10.2337/diab.39.3.271>.
 51. Shibuya A, Sakamoto N, Shimizu Y, Shibuya K, Osawa M, Hiroyama T, et al. Fc alpha/mu receptor mediates endocytosis of IgM-coated microbes. *Nat Immunol.* 2000;1:441–6. <https://doi.org/10.1038/80886>.
 52. Sakamoto N, Shibuya K, Shimizu Y, Yotsumoto K, Miyabayashi T, Sakano S, et al. A novel Fc receptor for IgA and IgM is expressed on both hematopoietic and non-hematopoietic tissues. *Eur J Immunol.* 2001;31:1310–6. [https://doi.org/10.1002/1521-4141\(200105\)31:5<1310::AID-IMMU1310>3.0.CO;2-N](https://doi.org/10.1002/1521-4141(200105)31:5<1310::AID-IMMU1310>3.0.CO;2-N).
 53. Kikuno K, Kang DW, Tahara K, Torii I, Kubagawa HM, Ho KJ, et al. Unusual biochemical features and follicular dendritic cell expression of human Fc alpha/mu receptor. *Eur J Immunol.* 2007;37:3540–50. <https://doi.org/10.1002/eji.200737655>.
 54. Martinez FO, Gordon S. The M1 and M2 paradigm of macrophage activation: time for reassessment. *F1000Prime Rep.* 2014;6:13. <https://doi.org/10.12703/P6-13>.
 55. Chávez-Galán L, Olleros ML, Vesin D, Garcia I. Much More than M1 and M2 Macrophages, There are also CD169(+) and TCR(+) Macrophages. *Front Immunol.* 2015;6:263. <https://doi.org/10.3389/fimmu.2015.00263>.
 56. Murray PJ, Wynn TA. Protective and pathogenic functions of macrophage subsets. *Nature Rev.* 2011;11:723–37. <https://doi.org/10.1038/nri3073>.
 57. Ley K. M1 means kill; M2 means heal. *J Immunol.* 2017;199:2191–3. <https://doi.org/10.4049/jimmunol.1701135>.
 58. Shapouri-Moghaddam A, Mohammadian S, Vazini H, Taghadosi M, Esmaeili SA, Mardani F, et al. Macrophage plasticity, polarization and function in health and disease. *J Cell Physiol.* 2018;233:6425–40. <https://doi.org/10.1002/jcp.26429>.
 59. Goldstein IJ, Reichert CM, Misaki A. Interaction of Concanavallin A With Model Substrates. *Ann N Y Acad Sci.* 1974;234:283–96. <https://doi.org/10.1111/j.1749-6632.1974.tb53040.x>.
 60. Goldstein IJ, Hayes CE. The Lectins: Carbohydrate-Binding Proteins of Plants and Animals. *Adv Carbohydr Chem Biochem.* 1978;35:127–340. [https://doi.org/10.1016/S0065-2318\(08\)60220-6](https://doi.org/10.1016/S0065-2318(08)60220-6).
 61. Coulibaly FS, Youan BB. Concanavalin A–Polysaccharides Binding Affinity Analysis Using a Quartz Crystal Microbalance. *Biosens Bioelectron.* 2014;59:404–11. <https://doi.org/10.1016/j.bios.2014.03.040>.
 62. Huber H, Polley MJ, Linscott WD, Fudenberg HH, Muller-Eberhard HJ. Human monocytes: distinct receptor sites for the third component of complement and for immunoglobulin. *G Sci.* 1968;162:1281–3. <https://doi.org/10.1126/science.162.3859.1281>.
 63. Lay WH, Nussenzweig V. Receptors for complement of leukocytes. *J Exp Med.* 1968;128:991–1009. <https://doi.org/10.1084/jem.128.5.991>.
 64. Lanzrein AS, Jobst KA, Thiel S, Jensenius JC, Sim RB, Perry VH, et al. Mannan-binding lectin in human serum, cerebrospinal fluid and brain tissue and its role in Alzheimer's disease. *Neuroreport.* 1998;9:1491–5. <https://doi.org/10.1097/00001756-199805110-00045>.
 65. Reiber H, Padilla-Docal B, Jensenius JC, Dorta-Contreras AJ. Mannan-binding lectin in cerebrospinal fluid: a leptomeningeal protein. *Fluids Barriers CNS.* 2012;9:17. <https://doi.org/10.1186/2045-8118-9-17>.

- 1
2
3
4
5
6
7
8
9
10
11
12
13
14
15
16
17
18
19
20
21
22
23
24
25
26
27
28
29
30
31
32
33
34
35
36
37
38
39
40
41
42
43
44
45
46
47
48
49
50
51
52
53
54
55
56
57
58
59
60
61
62
63
64
65
66. Stephan AH, Barres BA, Stevens B. The complement system: an unexpected role in synaptic pruning during development and disease. *Annu Rev Neurosci.* 2012;35:369–89. <https://doi.org/10.1146/annurev-neuro-061010-113810>.
 67. Tatomir A, Talpos-Caia A, Anselmo F, Kruszewski AM, Boodhoo D, Rus V, et al. The complement system as a biomarker of disease activity and response to treatment in multiple sclerosis. *Immunol Res.* 2017;65:1103–09. <https://doi.org/10.1007/s12026-017-8961-8>.
 68. Wu T, Dejanovic B, Gandham VD, Gogineni A, Edmonds R, Schauer S, et al. Complement C3 Is Activated in Human AD Brain and Is Required for Neurodegeneration in Mouse Models of Amyloidosis and Tauopathy. *Cell Rep.* 2019;28:2111–23.e6. <https://doi.org/10.1016/j.celrep.2019.07.060>.

FIGURE LEGENDS

1 **Figure 1: (A)** Sequence of images from a time-lapse recording showing how a THP-1 macrophage
2 (green arrow) extends a lamellipodium (empty green arrow) to a wasteosome opsonized with
3 ConA (red arrow) and pulls it towards the body of the macrophage, triggering the engulfment of
4 the wasteosome. The phagocytosed wasteosome become later digested and fragmented
5 (yellow arrows). Empty yellow arrow: wasteosome is out of the focus plane. See video for details.
6
7 At 1202 minutes, confocal images were taken and the 3D reconstruction was made. (B)
8 Sequence of images showing the 360° rotation of the 3D reconstruction. Images permit to
9 observe the location of the remains of the wasteosomes (red and yellow) at the macrophage.
10 Some dots of red or yellow fluorescence appear on the surface of the macrophage, suggesting
11 antigen presentation. The big green spot in the lower region corresponds to a macrophage that
12 is in contact with the one that has phagocytosed and digested the wasteosome.
13
14
15
16
17
18
19
20
21
22

23 **Figure 2: (A)** Sequence of images from a time-lapse recording showing two THP-1 macrophages
24 (green arrows) eroding a wasteosome opsonized with ConA (red arrow). Some spots of red
25 fluorescence become incorporated into the macrophages. In some cases, the fluorescence is
26 transferred from one macrophage to another one (empty green arrow). See video for details.
27
28 **(B)** Sequence of images showing different macrophages interacting with three different
29 wasteosomes (arrows). One of the wasteosomes (yellow arrow) become digested and
30 fragmented. Empty arrows indicate that the wasteosome is out of the focus plane.
31
32
33
34
35
36

37 **Figure 3: (A)** Sequence of images showing a THP-1 macrophage (green arrow) eroding a
38 wasteosome opsonized with AF555-NHS (red arrow). Note that the spots of red fluorescence,
39 corresponding to stained proteins, become incorporated into the macrophage. A similar process
40 can be observed in **(B)**. See the corresponding videos for details.
41
42
43
44
45

46 **Figure 4: (A)** Sequence of images showing a THP-1 macrophage (green) contacting a
47 wasteosome stained with PAS (red). Initially, a lamellipodium from a distant macrophage making
48 contact with the wasteosome can be observed. Thereafter, the macrophage shrinks over the
49 wasteosome and both structures displace together. However, unlike in the previous sets of
50 experiments, the digestion of the PAS stained wasteosomes could not be observed in most of
51 the experiments. **(B)** In only a few cases, as the one shown here, small amounts of fluorescence
52 were observed to detach from the wasteosomes and spread inside the macrophages. See videos
53 for details.
54
55
56
57
58
59
60
61
62
63
64
65

1
2
3
4
5
6
7
8
9
10
11
12
13
14
15
16
17
18
19
20
21
22
23
24
25
26
27
28
29
30
31
32
33
34
35
36
37
38
39
40
41
42
43
44
45
46
47
48
49
50
51
52
53
54
55
56
57
58
59
60
61
62
63
64
65

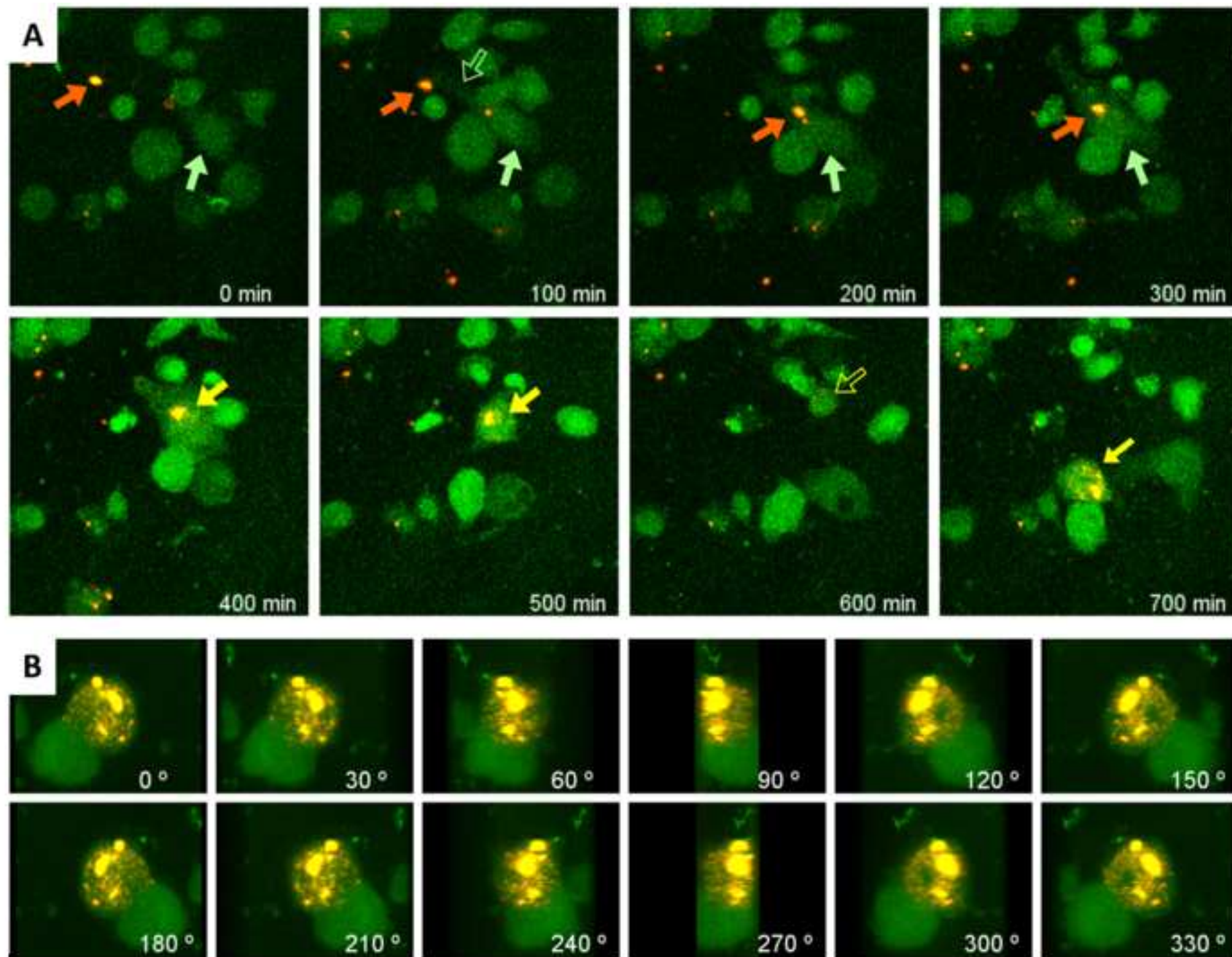
Figure 5: THP-1 macrophages which make contact with wasteosomes are CD68+, CD206+ and CD35+. **(a)** A CD68+ THP-1 macrophage (red) in contact with a wasteosome stained with ConA (green). **(b)** A CD206+ THP-1 macrophage (red) attached to a wasteosome (ConA, green). **(c)** A CD35+ THP-1 macrophage (red) encircling a wasteosome stained with ConA (green). **(d)** A CD35+ THP-1 macrophage (red) encircling a wasteosome immunostained with IgM (green). Nuclei are stained with Hoechst (blue). Scale bar: 25 μ m.

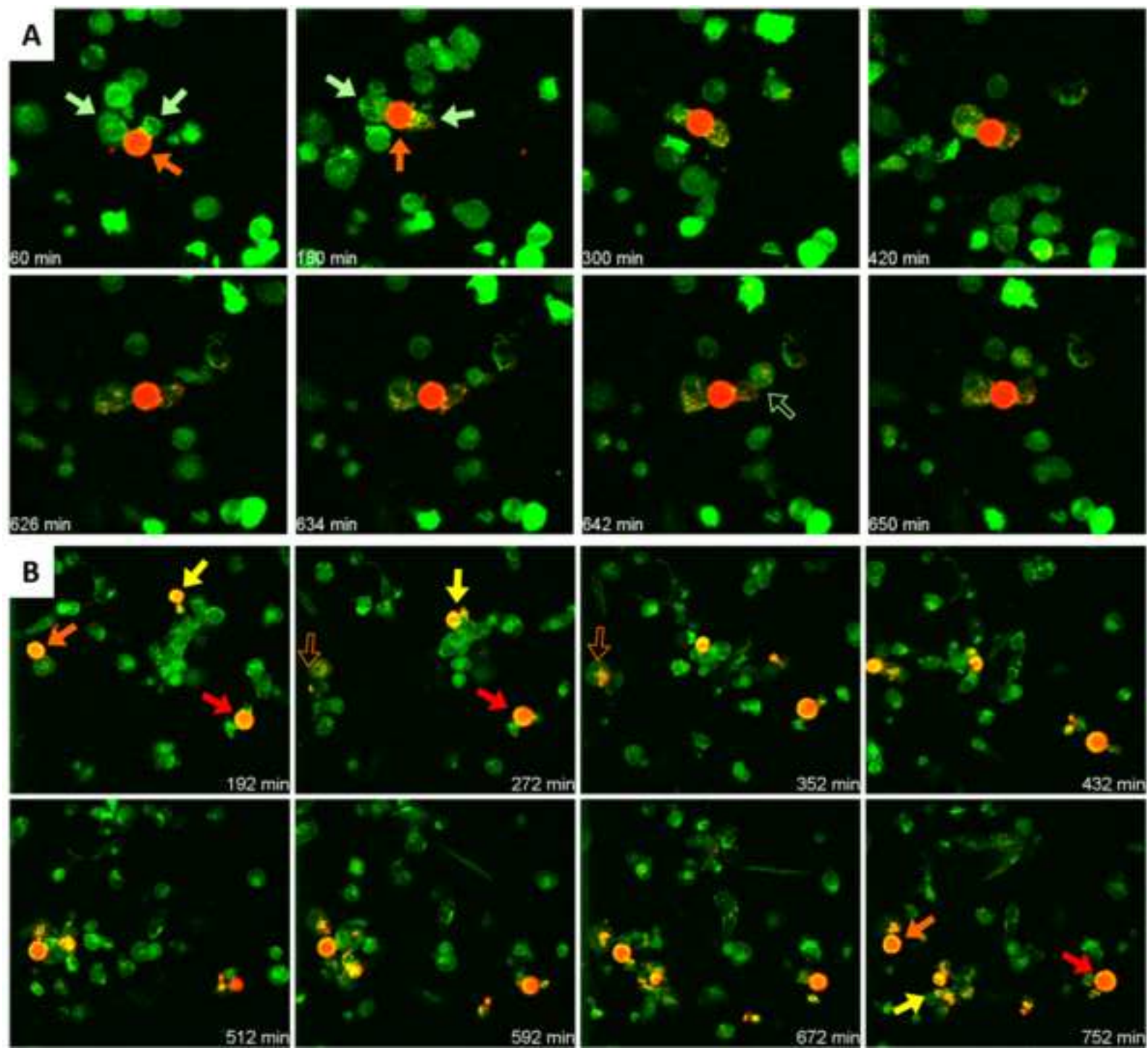
Figure 6: (A) Wasteosomes from CSF have opsonins on their surface. **(a)** wasteosomes purified from CSF and incubated with human plasma become stained with anti-MBL (green). **(b)** wasteosomes from CSF and incubated with human plasma become immunostained with anti-C3b (red). **(c)** wasteosomes purified from CSF and incubated with PBS instead of human plasma also become immunostained with anti-MBL (green). **(d)** wasteosomes purified from CSF and incubated with PBS instead of human plasma also become immunostained with anti-C3b (red). **(B)** Hippocampal wasteosomes do not have the opsonins on their surface. **(a)** When the hippocampal tissue is double-immunostained with anti-MBL (green) and anti-C3b (red), the wasteosomes do not become immunostained and are observed as a black circle. In this case, one wasteosome can be observed in the center of the image. **(b)** When the hippocampal tissue is immunostained with anti-GS and anti-C3b, wasteosomes become stained with anti-GS (green) but not by anti-C3b (red). Scale bars: 25 μ m.

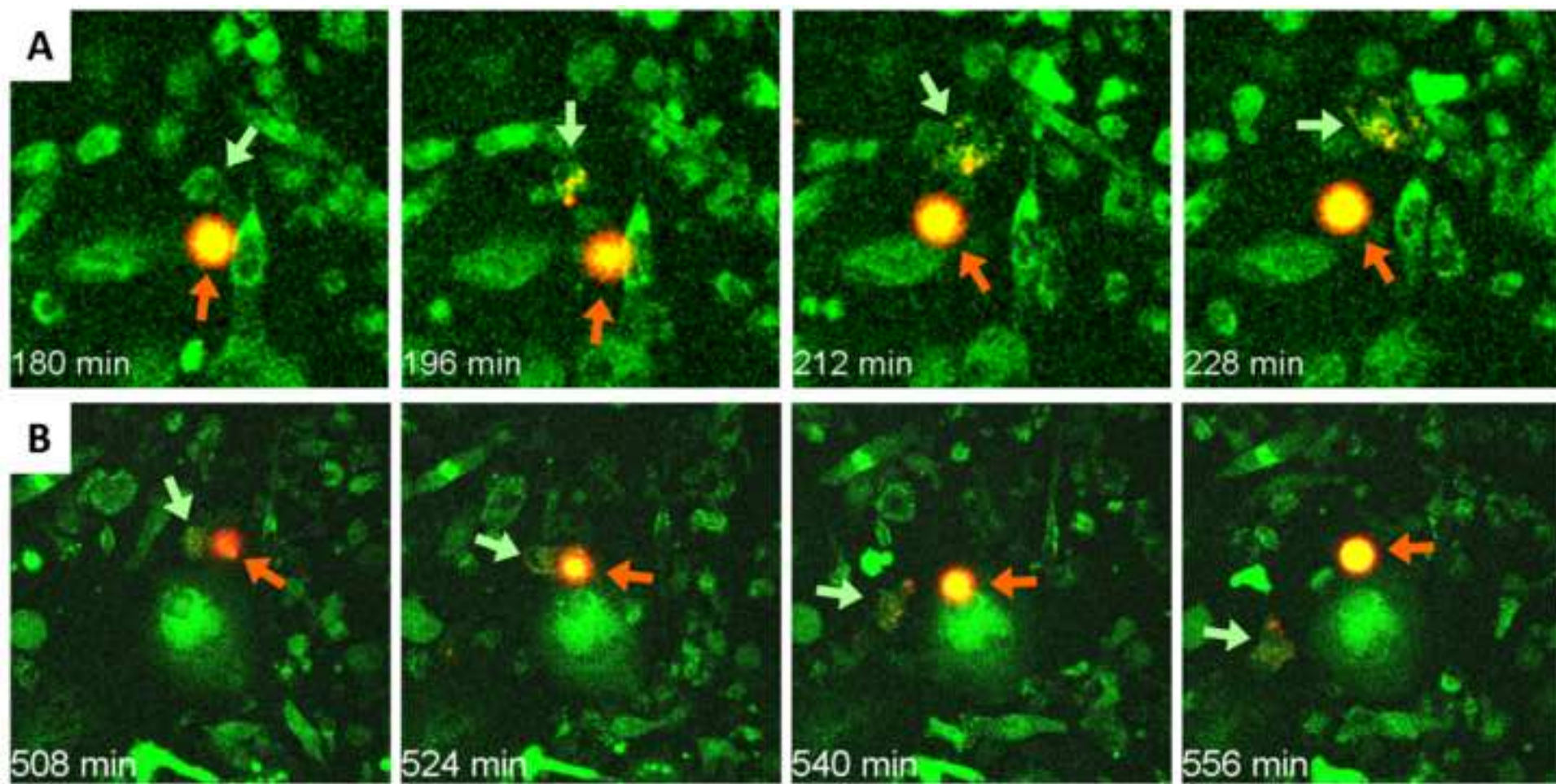
Figure 7: Some macrophages at central nervous system interfaces interact with wasteosomes. **(a1, a2, a3, a4 and a5)** wasteosomes from human hippocampal sections immunostained with anti-p62 (red) and interface macrophages immunostained with anti-CD206 (green). **(a1)** A choroid plexus macrophage in contact with a wasteosome released from the brain tissue to the ventricular CSF. **(a2)** inset of **a1**, where the macrophage attached to the wasteosome is magnified. **(a3 and a4)** wasteosomes released from hippocampus to the subarachnoid space in contact with meningeal macrophages. **(a5)** inset of **a4**, where the red staining is digitally intensified to evidence the presence of a wasteosome, in this case surrounded by two macrophages (white arrowheads). **(b)** within the brain parenchyma, wasteosomes become immunostained with anti-p62 (red) and are surrounded by CD35+ cells (green). **(c)** CD35 staining (red) colocalize with GFAP staining (green, white arrowheads), indicating that cells that surround wasteosomes are CD35+ astrocytes. **(d)** wasteosomes from human hippocampus immunostained with anti-p62. FAIM3 positive cells are not found in the hippocampal sections (green). **(e)** wasteosomes from human hippocampal tissue immunostained with IgMs (green) are not contacted by CD68+ cells (red, marked with white arrowheads). For their localization, these CD68+ cells are presumably microglial cells, although possible infiltrating macrophages

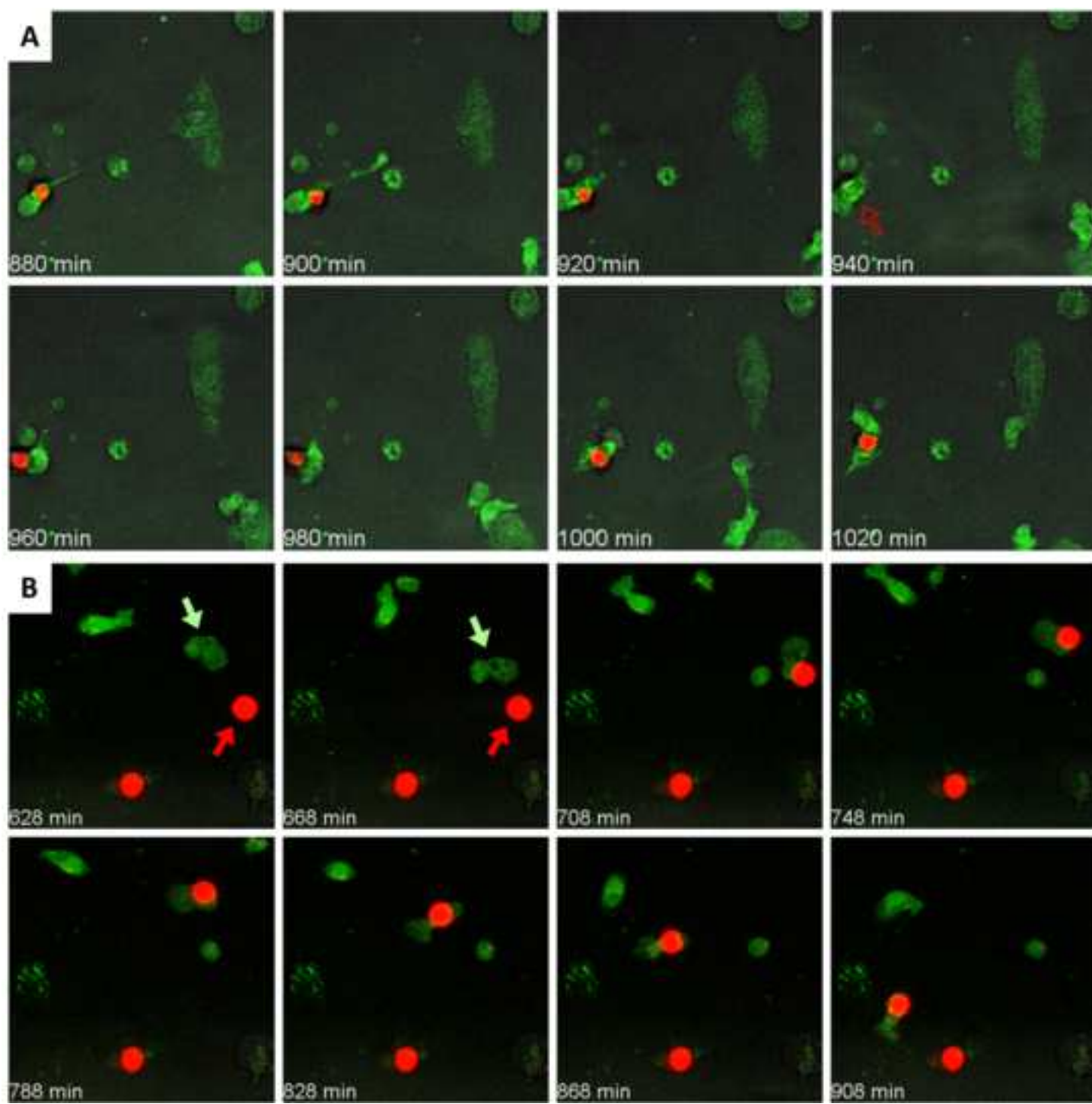
cannot be discarded. In any case, and as expected, microglia or macrophages did not reach the wasteosomes within the brain parenchyma since in this region wasteosomes are intracellular astrocytic structures. Scale bar in **a1**: 200 μm ; scale bars in **a2**, **a3** and **a4**: 25 μm ; other scale bars: 50 μm . Hoechst (blue) was used for nuclear staining.

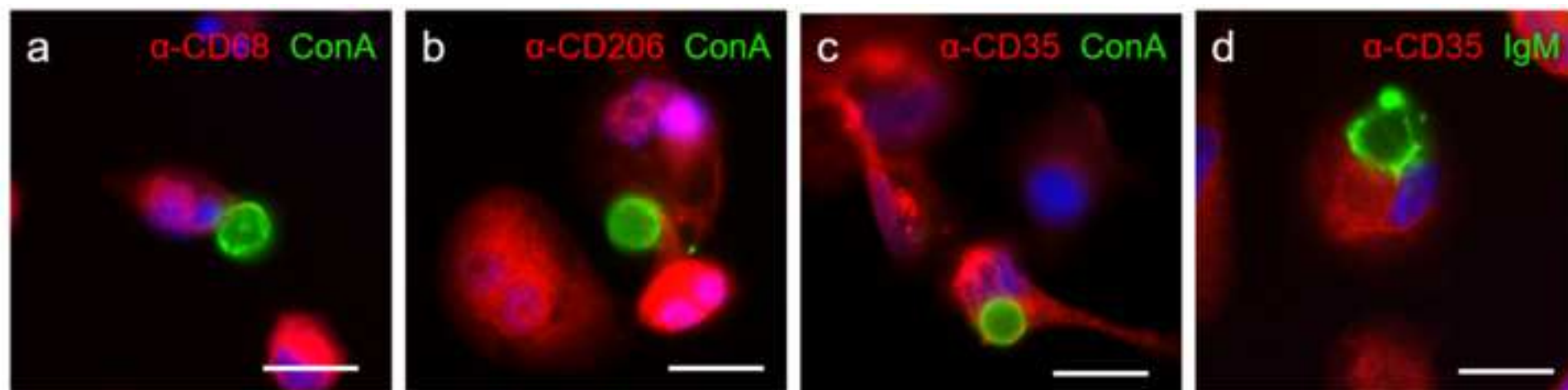
Figure 8: Integrative scheme of the mechanisms involved in the phagocytosis of CSF wasteosomes by THP-1 macrophages. The absence of FAIM3 in THP-1 macrophages and the absence of IgM opsonizing the CSF wasteosomes (binding to their NEs) indicate that the phagocytosis by THP-1 macrophages does not occur through the IgM-FAIM3 interaction. However, phagocytosis could occur through CD206 and CD35 receptors, which are both present in THP-1 macrophages. In the first case, the CD206 receptor can interact with mannose or other carbohydrates located in the wasteosomes. In the second one, the CD35 receptor can recognize the C3b that opsonizes wasteosomes once they arrive at the CSF. The opsonization with C3b in the CSF can be produced through the lectin pathway (L), triggered by the binding of MBL with the wasteosomes, and through the alternative pathway (A), triggered by the contact between C3 and wasteosomes, but not through the complement pathway (C), because IgM do not opsonize wasteosomes in the CSF. At central nervous system interfaces, we observed CD206+ macrophages, but not CD35+ or FAIM3+ macrophages.

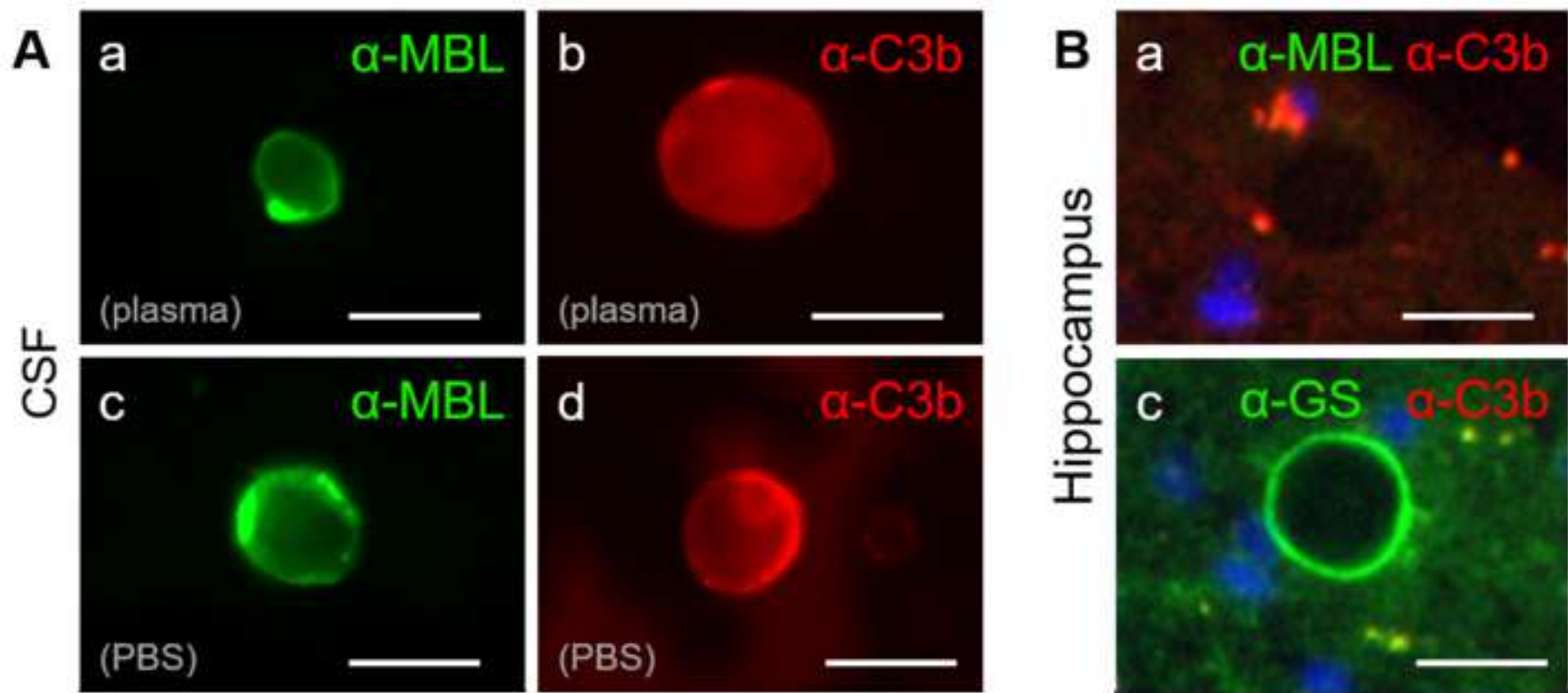


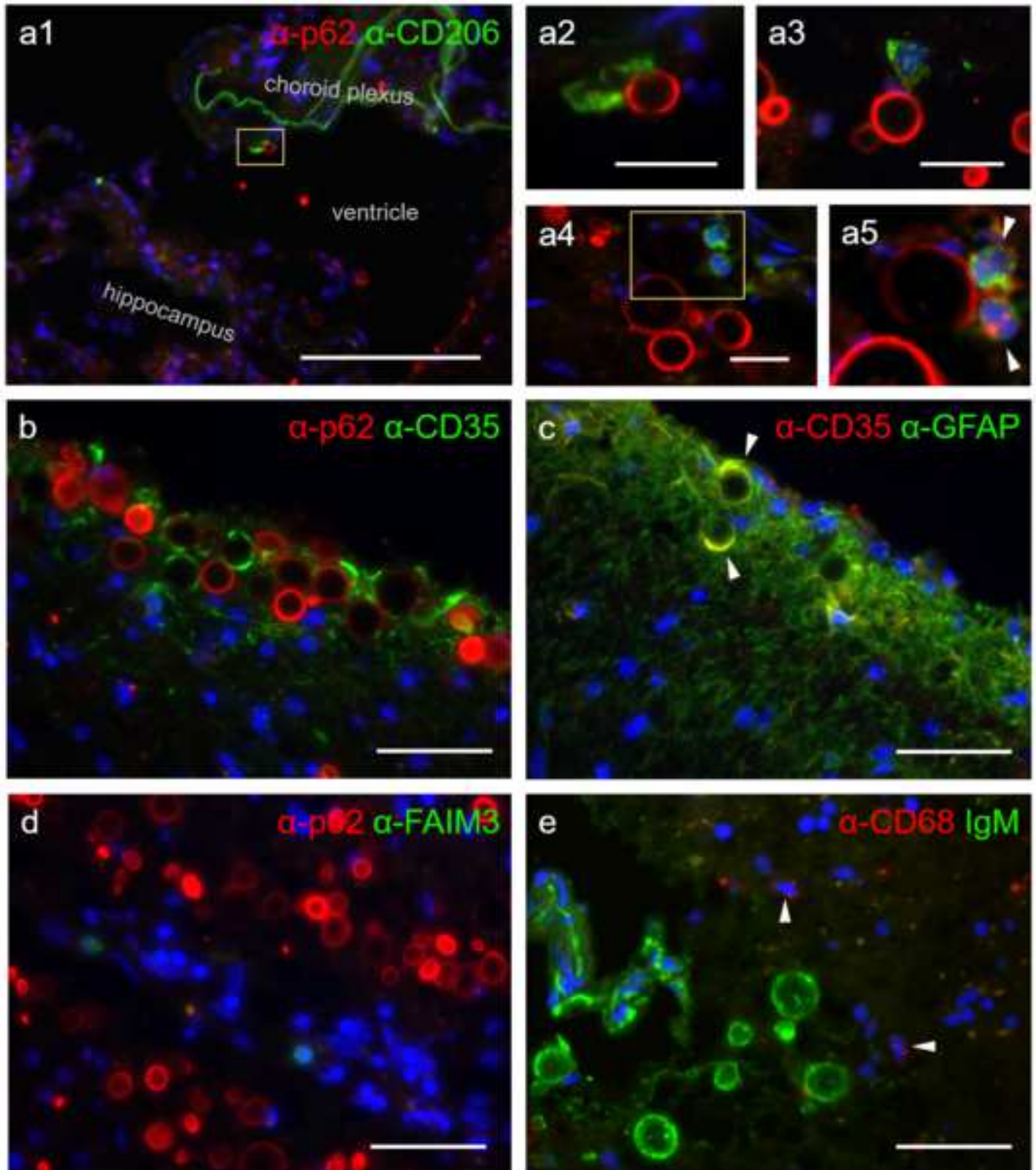












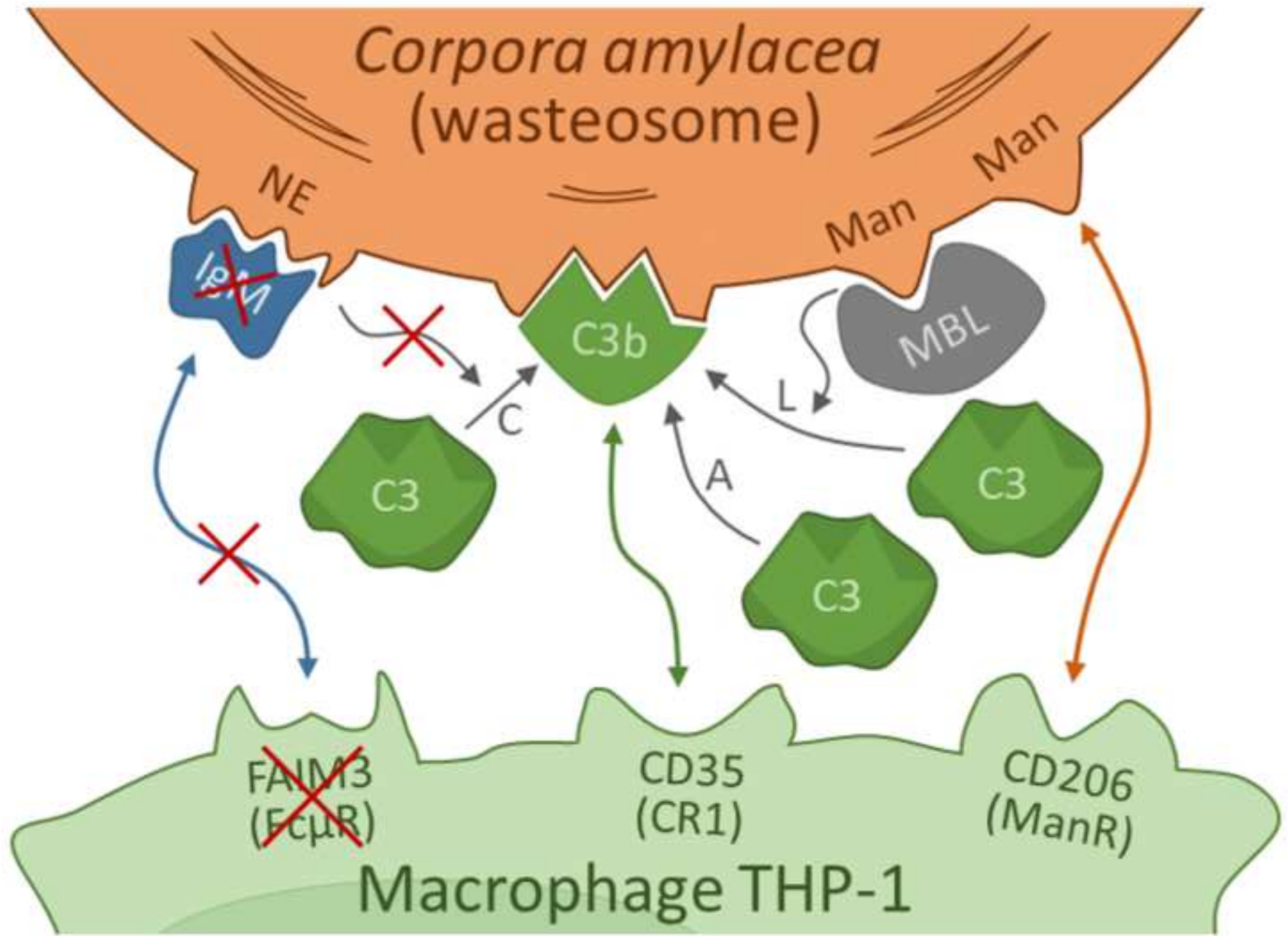


Table 1. Medical data about the CSF donors. S: subject. G: gender (F: female, M: male). A: age at death (years); PMD: post-mortem delay (in hh:mm). ^aAD: Alzheimer's Disease; ALS: Amyotrophic Lateral Sclerosis; LBD: Lewy Body Dementia; MSA: Multiple System Atrophy; PD: Parkinson's Disease.

S	G	A	PMD	Clinical diagnosis ^a
1	M	66	08:00	Presenile AD
2	F	68	10:20	Presenile AD
3	F	69	07:08	ALS
4	M	71	12:00	AD VS LBD
5	M	74	06:40	MSA with Parkinsonism
6	F	87	07:10	PD


Table 2. Medical data about the brain donors. S: subject. G: gender (F: female, M: male). A: age at death (years). PMD: post-mortem delay (in hh:mm). ^aAD: Alzheimer's Disease; LBD: Lewy Body Dementia.

S	G	A	PMD	Neuropathological diagnosis ^a
7	M	70	04:30	Atherosclerotic vascular encephalopathy
8	M	80	10:00	Vascular encephalopathy
9	M	86	07:15	AD (A2B1C1, Braak II, Thal 3, CERAD B) + LBD (Braak I, Brainstem)
10	M	89	12:00	AD (A3B3C3, Braak VI, Thal 5, CERAD frequent, severe CAA)

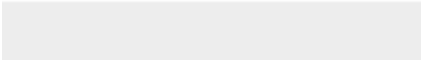



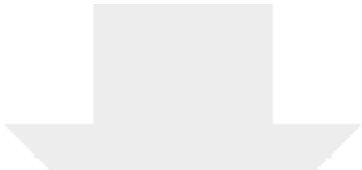
Click here to access/download
Supplementary Material
Video 1A.avi







Click here to access/download
Supplementary Material
Video 1B.avi



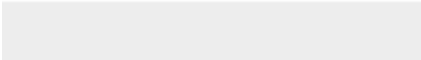




Click here to access/download
Supplementary Material
Video 2A.avi



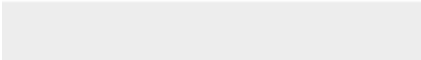




Click here to access/download
Supplementary Material
Video 2B.avi



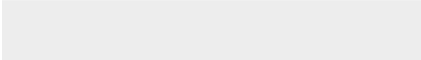



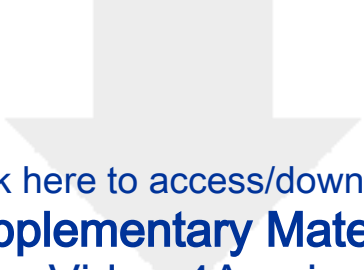
Click here to access/download
Supplementary Material
Video 3A.avi



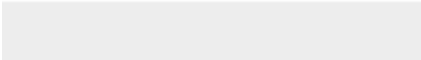



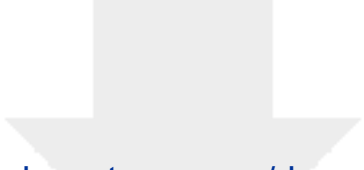
Click here to access/download
Supplementary Material
Video 3B.avi






Click here to access/download
Supplementary Material
Video 4A.avi





Click here to access/download
Supplementary Material
Video 4B.avi



IV. DISCUSSIÓ

En les últimes dècades, s'han realitzat nombrosos estudis enfocats a establir la composició i caracterització dels *wasteosomes*, o CA com han estat coneguts en treballs previs, en diferents òrgans i teixits de l'organisme humà, els quals han atribuït a aquestes estructures funcions molt diverses. De fet, l'estudi dels *wasteosomes* ha estat complex des del seu descobriment, principalment, per l'enorme varietat de resultats que s'han obtingut i la dificultat d'integrar-los en una teoria coherent i consistent.

Pel que fa a l'estudi dels *wasteosomes* del SNC, s'ha descrit que són unes estructures formades per un esquelet de poliglucosà el qual recull i integra productes de rebuig i/o potencialment tòxics derivats de l'envelliment i de condicions fisiopatològiques (Cavanagh, 1999; Augé *et al.*, 2018). Fins al moment, tots els estudis partien de *wasteosomes* provinents del teixit cerebral, però la presència de *wasteosomes* en el LCR i en els ganglis limfàtics cervicals aporta noves evidències envers la seva funció. En efecte, la presència de *wasteosomes* en el LCR recolza que aquestes estructures podrien actuar com a contenidors de substàncies de rebuig que traslladen els productes de rebuig del cervell cap al LCR. Tanmateix, la presència de *wasteosomes* en els ganglis limfàtics cervicals suggereix que una vegada al LCR, aquests accedeixen al sistema limfàtic de les meninges i arriben als ganglis. Cal destacar que les característiques histològiques dels *wasteosomes* dels ganglis són compatibles amb les dels *wasteosomes* del teixit cerebral i, a més a més, la seva localització en els sins trabeculars i no en el teixit ganglionar indica que aquestes estructures no són generades en els propis ganglis limfàtics. Així mateix, el gradient en el nombre de *wasteosomes* observats en els ganglis relacionat amb la seva localització propera al cervell apunta que aquestes estructures provenen del LCR. Considerant que altres òrgans i teixits de l'organisme, a banda del cervell, generen *wasteosomes*, cal contemplar la possibilitat que els *wasteosomes* dels ganglis podrien provenir d'aquestes altres estructures. No obstant això, en aquest cas, aquests òrgans o teixits haurien de generar *wasteosomes* que es tenyissin amb PAS i fossin reconeguts per IgM naturals, els *wasteosomes* haurien de ser extruïts directament o indirectament cap a la limfa i la limfa hauria de drenar cap als ganglis limfàtics situats en les regions cervicals I, II, III i IV. D'acord amb aquestes aproximacions, el cervell és l'única estructura que compleix amb aquestes premisses. Altres òrgans com la glàndula mamària, múscul cardíac o pròstata serien descartats ja que la limfa d'aquestes estructures no flueix cap als ganglis limfàtics cervicals. D'altra banda, els *wasteosomes* originats a la glàndula tiroide i la pròstata són estructures calcificades (Sfanos *et al.*, 2009; Sun, 1983), cosa que no coincideix amb les característiques dels *wasteosomes* en els ganglis limfàtics cervicals.

Aquest conjunt d'evidències, juntament amb altres característiques descrites en els *wasteosomes* del SNC, suggereixen que aquest procés de formació i extrusió dels *wasteosomes* podria tractar-se d'un mecanisme fisiològic. Pel que fa a la localització, la distribució dels *wasteosomes* en les regions periventriculars, perivasculars i subpials del cervell humà, zones molt properes al LCR (Cavanagh, 1999; Sakai *et al.*, 1969), sembla no ser

casual. De fet, en estudis realitzats en mostres de nervi vestibular, es descriu l'extrusió dels *wasteosomes* presents en els astròcits fibrosos del nervi cap al teixit connectiu de la piamàter, creuant la làmina basal de la *glia limitans*, com a un procés actiu (Sbarbati *et al.*, 1996). D'acord amb això, la presència d'MMP2 en la proximitat dels *wasteosomes* del SNC podria estar relacionada amb la remodelació de la matriu extracel·lular necessària per l'extrusió (Augé *et al.*, 2018). En referència a l'estructura i composició, els *wasteosomes*, a banda de l'esquelet glucídic, presenten un nucli central compacte amb presència d'Ubi i a les regions perifèriques s'hi localitzen GS, p62 i Ubi. Aquest nivell d'organització apunta que els *wasteosomes* contenen un nucli central on s'acumulen diferents substàncies de rebuig ubiquitinades i una regió perifèrica que es correspon a una zona activa de recollida de productes de rebuig recollits per la p62 i empaquetats per la GS, la qual genera l'esquelet del poliglucosà del *wasteosome* (Augé *et al.*, 2018). A més a més, la presència de NE en els *wasteosomes* que són reconeguts per IgM naturals indica que aquestes estructures són capaces d'interaccionar amb el sistema immunitari i ser fagocitades per macròfags o altres cèl·lules immunitàries una vegada són alliberades del cervell (Augé *et al.*, 2017; Augé *et al.*, 2019). En aquest sentit, els *wasteosomes* dels ganglis limfàtics cervicals s'han localitzat adherits a cèl·lules que per mida i forma són compatibles amb macròfags. Conjuntament, aquests resultats estenen la hipòtesi ja plantejada en l'estudi d'Augé *et al.* (2017), la qual postula que els *wasteosomes* recullen substàncies de rebuig i són extruïts del cervell i eliminats per part del sistema immunitari. Cal destacar que, anteriorment, els estudis de Sbarbati *et al.*, (1996), ja havien postulat que els *wasteosomes* formen part d'un sistema d'eliminació de substàncies, d'acord amb les observacions de transferència dels *wasteosomes* des dels astròcits cap la piamàter del nervi vestibular. Fins i tot, al ser els *wasteosomes* transferits cap a una zona d'elevada densitat de capil·lars sanguinis i estructures microvasculars, es va plantejar que aquestes estructures vasculars estarien implicades en l'eliminació dels *wasteosomes* (Sbarbati *et al.*, 1996). Malgrat tot, caldria considerar l'obstaculització d'aquesta via a causa de la BHE. Addicionalment, es va especular que les cèl·lules fagocítiques de la piamàter o l'aracnoide podrien tenir un paper en l'eliminació i el processament dels *wasteosomes*, de manera que tot el procés es veuria implicat en l'eliminació de substàncies de rebuig del nervi vestibular (Sbarbati *et al.*, 1996). No obstant això, en els treballs d'Augé *et al.* (2017) i Sbarbati *et al.*, (1996), tot i considerar l'extrusió dels *wasteosomes* del teixit cerebral i la seva possible implicació en l'eliminació de substàncies de rebuig, es va contemplar una expulsió directa dels *wasteosomes* del SNC cap a la sang, i no al LCR. En canvi, Cavanagh (1999), va assenyalar que els CA, un cop extruïts del teixit, podrien ser transferits cap al LCR de l'espai subaracnoidal. Aquest autor però, va obviar l'existència del sistema limfàtic de les meninges a l'espai subaracnoidal, de manera que va plantejar que els *wasteosomes* podrien escapar del SNC travessant les vellositats aracnoidals, arribant a la sang. La present tesi posa en dubte l'eliminació dels *wasteosomes* mitjançant una extrusió directa des del parènquima cerebral cap a la sang per la presència de la BHE, la

qual impediria el pas dels *wasteosomes* principalment per la seva mida micromètrica. Es podria considerar l'accés directe dels *wasteosomes* del teixit cap la sang en determinades zones del cervell sense BHE, com ara els òrgans circumventriculars, però els *wasteosomes* no han estat descrits en aquestes regions. Pel que fa a l'accés dels *wasteosomes* a la sang de manera indirecta, és a dir, tenint en compte prèviament l'extrusió dels *wasteosomes* del teixit cap al LCR i l'arribada a la sang mitjançant les vellositats aracnoidals, cal considerar que tot i que aquestes vellositats no presenten BHE, els *wasteosomes* haurien de ser capaços de travessar el teixit aracnoidal i l'endoteli continu que separa el LCR de la llum dels sinus venosos (Fricke *et al.*, 2001; Pollay, 2010; Proulx, 2021). Malgrat que hi ha certes discrepàncies entre diferents autors, s'ha descrit un possible mecanisme de vàlvules en les vellositats aracnoidals les quals podrien permetre la sortida de partícules de fins a 7,5 µm del LCR cap a la sang (Welch i Friedman, 1960). No obstant això, la mida mitjana dels *wasteosomes* és lleugerament superior, d'entre 10-12 µm (Cavanagh, 1999), i a més a més, l'obertura de les vàlvules tindria lloc en cas d'un increment de la pressió intracranial. Altres autors han descrit un mecanisme de transport de substàncies a través de les vellositats aracnoidals mitjançant canals transcel·lulars vacuolars en primats (Tripathi i Tripathi, 1974). De totes maneres, la mida d'aquests canals és de fins a 2,3 µm, inferior a la mida freqüent d'un *wasteosome*. Per tant, tot i que sembla que els *wasteosomes* més petits podrien desplaçar-se del LCR cap a la sang a través de les vellositats aracnoidals per algun mecanisme encara no clarament descrit en humans, aquesta via de sortida dels *wasteosomes* del SNC no seria la més habitual. De totes maneres, aquest recorregut alternatiu seria una via més de sortida i eliminació dels *wasteosomes* del SNC que recolzaria el seu paper com a part d'un mecanisme d'eliminació de substàncies de rebuig cerebrals. En tot cas, tal com s'ha comentat anteriorment, els resultats d'aquesta tesi posen de manifest l'extrusió dels *wasteosomes* del parènquima cerebral cap al LCR i la seva sortida del SNC mitjançant el sistema limfàtic de les meninges. El recorregut realitzat pels *wasteosomes*, des de la seva formació en el parènquima cerebral fins a la seva eliminació en els ganglis limfàtics cervicals es mostra resumit en la Figura 8.

Tot i que puntualment s'ha observat la presència de *wasteosomes* en alguns axons neuronals (Anzil *et al.*, 1974), la majoria d'estudis descriu la formació dels *wasteosomes* a l'interior dels astròcits, concretament en els processos astrocítics, dins el parènquima cerebral (Leel-Össy, 2001; Navarro *et al.*, 2019; Ramsey, 1965; Palmucci *et al.*, 1982; Sbarbati *et al.*, 1996). Aquestes estructures agrupen substàncies de rebuig provinents no només dels propis astròcits sinó també d'altres tipus cel·lulars (Augé *et al.*, 2017; Augé *et al.*, 2018; Navarro *et al.*, 2019; Pirici *et al.*, 2014; Sbarbati *et al.*, 1996; Suzuki *et al.*, 2012). Cal remarcar que el sistema glimfàtic podria intervenir en el transport de substàncies de rebuig d'origens diversos cap als astròcits (Navarro *et al.*, 2019). S'ha descrit que aquest sistema implica el moviment del líquid intersticial des de les zones periarterials cap a les zones perivenoses (Jessen *et al.*, 2015), fet que provoca el desplaçament de productes de rebuig que podrien

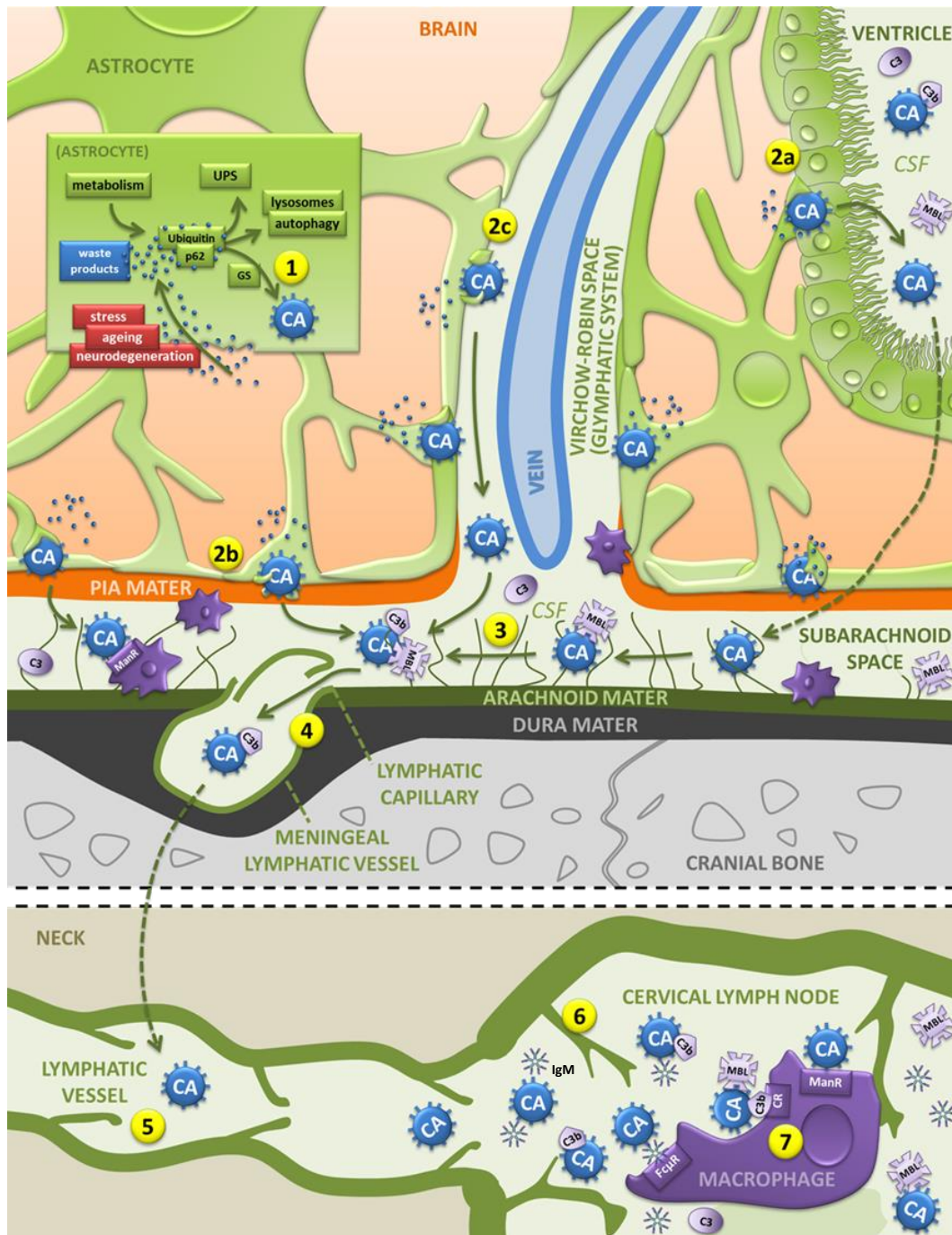


Figura 8. Via proposada d'eliminació de substàncies de rebuig del cervell basada en el sistema *wasteosome*. La via s'inicia als astròcits, els quals generen els *wasteosomes* (CA) on s'hi recullen substàncies de rebuig de diferents orígens (1). Els *wasteosomes* s'alliberen al LCR del ventricle (2a), de l'espai subaracnoide (2b) o a l'espai perivascular (2c). Al LCR, alguns *wasteosomes* són opsonitzats amb C3b i/o MBL, i poden ser eliminats pels macròfags de les meninges o macròfags perivasculars mitjançant el ManR (3). Des del LCR, els *wasteosomes* poden accedir al sistema limfàtic de les meninges (4), passant dels capil·lars limfàtics als vasos limfàtics subseqüents (5), i arribar als ganglis limfàtics cervicals (6). Allà, els macròfags poden fagocitar els *wasteosomes* per diferents mecanismes com ara els mediats pel ManR, per la interacció IgM-Fc μ R o per les diferents vies del sistema del complement (la via clàssica induïda per les IgM, la via de la lectina induïda per l'MBL i la via espontània produïda per una escissió espontània de C3) (7). C3, component C3 del sistema del complement; C3b, fragment C3b derivat de l'escissió de C3; CA, *corpora amylacea*; CR, receptor del C3b; CSF, *cerebrospinal fluid*, líquid cefalorraquídic; Fc μ R, receptor de la fracció constant μ de les IgM; GS, glicogen sintasa; ManR, receptor de mannan; MBL, *mannose binding lectin*, lectina d'unió a la mannan; UPS, sistema Ubi-proteosoma. Veure el text per més detalls.

ser absorbits o fagocitats pels astròcits de les zones limítrofes, i acumulats a l'interior dels *wasteosomes* (Navarro *et al.*, 2019). Seguidament, els *wasteosomes* s'alliberen al LCR per la seva subseqüent eliminació, en la qual hi participa el sistema immunitari. De fet, els resultats obtinguts en la present tesi mostren que els *wasteosomes*, una vegada alliberats del teixit, en el LCR, es troben opsonitzats amb la partícula C3b del sistema del complement. La presència de C3b pot ser explicada pel desencadenament de la via de la lectina del sistema del complement ja que també s'observen *wasteosomes* del LCR opsonitzats amb MBL, proteïna la qual inicia aquesta via i provoca una opsonització amb C3b. Tot i això, no es descarta l'escissió espontània de la partícula C3 en C3b i la conseqüent opsonització dels *wasteosomes*. Cal destacar que no s'observa marcatge d'MBL o C3b en els *wasteosomes* del parènquima cerebral, aquest fet s'explica per la localització intracel·lular dels *wasteosomes* en el teixit (Augé *et al.*, 2019). En canvi, una vegada extruïts, els *wasteosomes* entren en contacte amb l'MBL i C3b presents en el LCR (Lanzrein *et al.*, 1998; Reiber *et al.*, 2012; Stephan *et al.*, 2012; Tatomir *et al.*, 2017; Wu *et al.*, 2019). El fet que els *wasteosomes* del LCR estiguin opsonitzats amb C3b indica que ja podrien ser fagocitats a les interfícies del cervell per part de macròfags perivasculars, de les meninges o del plexe coroide mitjançant el receptor de la proteïna C3b o CD35. Malgrat tot, en les seccions d'hipocamp estudiades, no s'observen macròfags marcats amb CD35 a les interfícies del cervell, però la gran presència d'astròcits marcats amb CD35 podria haver-los emmascarat. En referència a la presència del receptor CD35 en alguns astròcits formadors de CA, aquest receptor podria estar implicat en la captació i interiorització de substàncies de rebuig per part d'aquestes cèl·lules. D'altra banda, s'observen macròfags marcats amb el receptor de la Man o CD206 en les zones limitants del teixit hipocampal en contacte amb *wasteosomes* que han estat alliberats del parènquima. Això suggereix que el receptor de la Man podria estar implicat en la fagocitosi *in vivo* dels *wasteosomes*. Convé fer esment que no és la primera vegada que s'observen *wasteosomes* interaccionant amb macròfags al SNC, Suzuki *et al.* (2012) ja van observar *wasteosomes* sent fagocitats per macròfags infiltrants en mostres de bulb raquidi de casos de neuromielitis òptica. Aquest trastorn autoimmunitari cursa amb una desmielinització inflamatòria crònica focalitzada en el nervi òptic i la medul·la espinal. Principalment, la interacció entre els macròfags infiltrants i *wasteosomes* va ser descrita en lesions d'estadi inicial on encara es conservava la mielina. En les zones afectades per la desmielinització amb lesió crònica destructiva, no es van observar pràcticament *wasteosomes*, i els *wasteosomes* de les zones no afectades per lesió no establien contactes amb macròfags.

Atès que els resultats obtinguts mostren interaccions dels *wasteosomes* amb cèl·lules fagocítiques en el LCR, a nivell de les interfícies del cervell, i també en els ganglis limfàtics cervicals, es van realitzar estudis *in vitro* de *time-lapse* utilitzant *wasteosomes* purificats del LCR i macròfags THP-1 per aprofundir en el procés de fagocitosi d'aquestes estructures. Aquests estudis mostren macròfags THP-1 fagocitant i processant els *wasteosomes*, fet que

estableix un punt de partida per a l'estudi dels mecanismes implicats en la fagocitosis dels *wasteosomes* i, particularment, de substàncies de rebuig generades pel propi organisme. En aquests estudis s'observa que, sota totes les condicions experimentals estudiades, amb els *wasteosomes* opsonitzats amb ConA i marcats amb NHS ester i tinció de PAS, els macròfags fagociten o interaccionen amb aquestes estructures. En el cas dels *wasteosomes* marcats amb ConA i NHS ester, aquests són digerits o fragmentats i la fracció proteica fluorescent és exposada a la superfície dels macròfags i és transferida d'un macròfag a un altre. S'observa una reactivitat menor dels macròfags envers els *wasteosomes* marcats amb PAS. En el cas dels *wasteosomes* marcats amb PAS, tot i que els macròfags contacten amb aquestes estructures, la fracció fluorescent, en aquest cas derivada de la fracció glucídica, no es distribueix pel citoplasma dels macròfags. Això pot ser atribuït a un diferent processament a l'interior dels macròfags de la fracció proteica dels *wasteosomes* respecte a la fracció glucídica. Alternativament, aquestes diferències podrien derivar de canvis provocats per la tinció de PAS en l'esquelet glucídic dels *wasteosomes*, la qual cosa podria provocar que els *wasteosomes* fossin menys susceptibles a les activitats lisosomàtiques o enzims. En qualsevol cas, la reactivitat dels macròfags envers els *wasteosomes* va ser observada en tots els experiments, fet que dona suport al paper del sistema immunitari en l'eliminació d'aquestes estructures.

D'altra banda, es van realitzar estudis d'immunofluorescència utilitzant *wasteosomes* purificats del LCR i macròfags THP-1 per examinar quins mecanismes podrien estar implicats en aquest procés de fagocitosis. D'entre diversos mecanismes possibles, es van estudiar aquells mediats per IgM, el receptor de la proteïna C3b o CD35 del sistema del complement i el receptor de la Man o CD206. Els resultats obtinguts indiquen que els macròfags THP-1 expressen els receptors CD35 i CD206, però no el receptor de les IgM, també conegut com a Fc μ R o FAIM3. L'absència del receptor de les IgM en aquestes cèl·lules indica que en aquest tipus cel·lular, la fagocitosis no té lloc directament mitjançant la interacció entre les IgM i aquest receptor de membrana. Pel que fa al mecanisme de fagocitosis mediat pel receptor de la partícula C3b o CD35, aquest podria tenir lloc per part dels macròfags THP-1 ja que, tal i com s'ha esmentat, aquest receptor està present en la membrana d'aquestes cèl·lules i els *wasteosomes* del LCR es troben opsonitzats amb C3b. Pel que fa al mecanisme mediat pel receptor de la Man o CD206, s'observa la presència d'aquest receptor en les cèl·lules THP-1, però encara no s'ha analitzat amb detall la presència dels elements diana d'aquest receptor en els *wasteosomes*. Tot i això, cal destacar que el receptor CD206 és una lectina que no només reconeix residus de Man, sinó que també s'ha descrit que reconeix GlcNAc i fucosa (Feinberg *et al.*, 2021) i s'ha descrit que els *wasteosomes* són reconeguts per ConA, per la qual cosa podrien contenir Man o GlcNAc, els dos diana de la ConA (Goldstein *et al.*, 1974; Goldstein *et al.*, 1978; Coulibaly *et al.*, 2014) i del receptor CD206 (Feinberg *et al.*, 2021). Aquests sucres podrien formar part de l'esquelet glucídic dels *wasteosomes* o bé part de les substàncies de rebuig acumulades en aquests *wasteosomes*. No obstant, considerant el nivell

d'organització dels *wasteosomes*, és probable que aquests sucres formin part de l'esquelet glucídic dels *wasteosomes* i alhora actuïn com a marcador per a la fagocitosi i l'eliminació d'aquestes estructures. Addicionalment, cal tenir en compte que, normalment, el receptor CD206 s'expressa en macròfags del subtipus M2 i no en el subtipus M1 (Mantovani *et al.*, 2004). Encara que la classificació M1 i M2 no és del tot clara (Chávez-Galán, *et al.*, 2015), els M2, en particular els M2a i M2c que presenten el receptor CD206, són considerats no inflamatoris. Concretament, els M2a estan involucrats en remodelació tissular i M2c estan associats amb la fagocitosi de cèl·lules apoptòtiques (Ley, 2017; Murray i Wynn, 2011; Shapouri-Moghaddam *et al.*, 2018). Globalment, el fet que els *wasteosomes* inclouen substàncies de rebuig que en condicions fisiològiques haurien de ser eliminades sense desencadenar respostes inflamatòries concorda amb que aquestes estructures continguin elements que puguin ser reconeguts per macròfags que expressen CD206. En definitiva, aquest conjunt d'evidències referents als receptors fagocítics presents en els macròfags i les opsonines presents en els *wasteosomes* fonamenta que hi hauria diversos mecanismes redundants que donarien lloc a la fagocitosi dels *wasteosomes* i n'assegurarien la seva eliminació sense desencadenar processos inflamatoris, la qual cosa proporciona un argument més que recolza la participació d'aquestes estructures en un mecanisme d'eliminació fisiològica de substàncies de rebuig cerebrals.

Reprement el mecanisme de fagocitosi mediat per IgM, tot i que els resultats mostren que els macròfags THP-1 no expressen el receptor que reconeix aquestes IgM, Fc μ R o FAIM3, i per tant, es descarta que al fagocitosi dels *wasteosomes* sigui mediada per aquest mecanisme en aquest tipus de cèl·lules, cal considerar que aquest mecanisme podria tenir lloc *in vivo* o mitjançant altres línies cel·lulars. Val la pena recordar que aquestes IgM reconeixen uns NE en els *wasteosomes* d'origen fins ara desconegut (Augé *et al.*, 2017). En la present tesi, s'ha intentat clarificar la naturalesa d'aquests NE.

Considerant que la preadsorció de la ConA amb monosacàrids específics va mostrar que aquests monosacàrids interfereixen en la interacció entre la ConA i els *wasteosomes*, i atès que la preadsorció amb sucres no afecta a la interacció entre anticossos dirigits contra proteïnes i el seu corresponent epítot, es va utilitzar l'estratègia de preadsorció per avaluar la interacció entre les IgM i els NE dels *wasteosomes*. Efectivament, els resultats obtinguts de la preadsorció de les IgM amb sucres específics mostren efectes inhibitoris en el marcatge dels NE. D'altra banda la digestió dels *wasteosomes* amb pepsina, la qual elimina els components proteics i, en conseqüència, evita els marcatges amb l'NHS ester i l'anticòs dirigit contra la proteïna p62, no altera el marcatge de ConA, el que demostra no afecta la fracció glucídica dels *wasteosomes*. La pepsina tampoc afecta el marcatge d'IgM, fet que descarta la naturalesa peptídica o glucopeptídica dels NEs. Conjuntament, els resultats recolzen la naturalesa glucídica dels NEs. De fet, s'ha descrit que els glicans poden presentar múltiples funcions, entre les quals s'inclou la seva actuació com a senyals *eat-me* que indueixen

processos de fagocitosi per part de macròfags o cèl·lules dendrítiques, de manera directa o indirecta, per exemple, mitjançant la opsonització amb IgM naturals (Bovin, 2013; Varki, 2017). En l'estudi de Xia i Gildersleeve (2019), es van analitzar els diferents tipus d'IgM que reconeixen glicans en sang de cordó umbilical humana i es va posar de manifest la presència de diversos anticossos dirigits contra glicans en aquestes mostres, els quals eren majoritàriament IgM naturals. En efecte, s'ha descrit que les IgM naturals reconeixen epítops que actuen com a marcadors d'estructures residuals (Reyneveld *et al.*, 2020) i productes de glicació avançada, els quals s'ha demostrat que la seva producció incrementa amb l'edat (Bovin, 2013; Goldin *et al.*, 2006; Grönwall *et al.*, 2012; Haji-Ghassemi *et al.*, 2015; Lutz *et al.*, 2009; Maddur *et al.*, 2020). Cal destacar que hi ha epítops derivats de membranes que són reconeguts per aquests anticossos. Aquests epítops inclouen glicans generalment ancorats a membranes intracel·lulars que actuen com a senyal *eat-me* quan són exposats fora de la cèl·lula, per exemple en processos apoptòtics o en restes cel·lulars. Sota condicions fisiològiques, hi ha múltiples elements a l'interior de les cèl·lules que poden actuar com a senyals *eat-me* quan són externalitzats. Això representa un procés d'estalvi d'energia per l'organisme perquè en cas d'alteracions funcionals o estructurals, no és necessari generar aquestes senyals de *novo*, sinó que només cal reubicar-les fora de la cèl·lula (Franz *et al.*, 2017). En definitiva, aquestes premisses recolzen la naturalesa glucídica dels NE dels *wasteosomes* i el seu paper com a marcador de fagocitosi i eliminació dels *wasteosomes*.

D'altra banda, en l'estudi i la caracterització dels NE dels *wasteosomes*, es van utilitzar dos tipus d'IgM humanes. D'una banda, es van utilitzar IgM provinents de sèrum normal (*normal serum IgM*, NS-IgM) i, d'altra banda, es van utilitzar IgM provinents de sèrum de mieloma (*myeloma serum IgM*, MS-IgM). En els estudis de preadsorció de les IgM amb els diferents monosacàrids específics, s'observa que la unió de les NS-IgM als *wasteosomes* es veu afectada a diferents concentracions de diferents sucres, essent la Glc el monosacàrid amb un major efecte, reduint la intensitat de fluorescència dels marcatges al 0% a la concentració de 50 mM, la més baixa testada. En canvi, la Gal i l'NacGal van tenir el menor efecte reduint la intensitat de fluorescència només al 60% a la concentració més elevada de 800 mM de sucre. Això suggereix que el grup hidroxil en posició equatorial en el C-4 és crític per la interacció amb les IgM. A més a més, la disposició equatorial o axial del grup hidroxil en C-2 sembla també tenir certa importància, ja que la Man mostra una inhibició menor respecte la Glc i també la GlcNAc respecte la Glc on l'hidroxil és substituït pel grup N-acetil. Els canvis en C-2 però sembla que mostren menys efectes que aquells produïts en C-4. En el cas de les MS-IgM, els 4 monosacàrids testats interfereixen en la unió entre aquestes IgM i els *wasteosomes* sense observar diferències significatives entre els diferents sucres. Les diferències entre el comportament de les NS-IgM i les MS-IgM podria ser explicat pel fet que les NS-IgM són policlonals, mentre que les MS-IgM són monoclonals i per tant, probablement més restringides i alterades respecte les obtingudes del sèrum normal. En tot cas, la

interacció entre els dos tipus d'IgM i els *wasteosomes* és inhibida pels diferents sucres, cosa que recolza la naturalesa glucídica dels NE dels *wasteosomes* reconeguts per les IgM.

Es desconeix si només hi ha un únic tipus de NE en els *wasteosomes* o si es tracta de diferents tipus de NEs. En qualsevol cas, la unió de les IgM a aquests NE dels *wasteosomes* pot ser bloquejat totalment per determinats monosacàrids. Per consegüent, la unió entre algunes IgM i alguns antígens o epítops presents en estructures de l'organisme humà podria ser inhibida *in vitro* per determinats monosacàrids, especialment Glc. Aquesta consideració permet plantejar que aquestes inhibicions podrien tenir lloc *in vivo*. En el sèrum humà, la concentració d'IgM en joves adults és de $1,46 \pm 0,12$ mg/ml (Gonzalez-Quintela, *et al.* 2007), mentre que en plasma, la concentració de Glc dues hores després de menjar és al voltant de 7,8 mM (American Diabetes Association, 2020). En els experiments realitzats, la concentració d'IgM és de 0,044 mg/mL, mentre que la concentració de Glc més baixa utilitzada per la preadsorció és de 50 mM o, més acuradament 48,1 mM considerant l'addició de l'anticòs en la preparació de la dilució. En aquest sentit, la relació Glc/IgM en les condicions experimentals emprades és 205 vegades més elevada que en condicions fisiològiques. No obstant això, considerant que la intensitat de fluorescència disminueix fins al 0% a 48,1 mM de Glc, es podria considerar que a nivells fisiològics de Glc podria haver-hi efectes inhibitoris en les IgM. A més a més, s'haurien de considerar els possibles efectes d'una hiperglucèmia de curta durada en la immunitat innata (Jafar *et al.*, 2016). De fet, s'ha descrit que la diabetis mellitus incrementa la susceptibilitat de patir infeccions víriques, bacterianes o fúngiques (Dana *et al.*, 2008; Jafar *et al.*, 2016; Juliana *et al.*, 2012). Tot i això, existeixen diversos mecanismes que podrien explicar aquesta susceptibilitat, com ara l'activitat de la proteïna quinasa C i la glicosilació d'algunes proteïnes (Jafar *et al.*, 2016). Certament, la possible inhibició de la reactivitat de les IgM amb Glc o altres sucres no s'ha investigat fins al moment, de manera que s'introdueix un nova línia d'estudi d'interès per malalties que cursen amb una alteració del metabolisme de la Glc. Conjuntament, els resultats recolzen que els NE dels *wasteosomes* presenten naturalesa glucídica i posen de manifest la necessitat d'estudiar els efectes que la glicèmia produeix *in vivo* en la reactivitat de les IgM naturals i en la immunitat natural.

Aquestes IgM naturals, tot i reconèixer els NE dels *wasteosomes*, no són capaces de creuar la BHE en condicions fisiològiques. De fet, a causa de la BHE i la barrera entre el LCR i el cervell, el cervell s'ha considerat un òrgan immuno-privilegiat, fins al descobriment del sistema limfàtic de les meninges, el qual recull substàncies del cervell i les transporta cap a fora del SNC. A l'any 1869, Schwalbe va descriure que els vasos limfàtics cervicals es tenyien amb una solució de Prussian blue quan aquesta era injectada a l'espai subaracnoidal, demostrant per primera vegada una interconnexió entre l'espai subaracnoidal i els vasos limfàtics. No obstant, aquest autor no va establir l'origen dels vasos limfàtics descrits per ell mateix. Va ser Jacobi, a l'any 1924, el que va postular la presència de vasos limfàtics a la

duramàter mitjançant estudis macroscòpics, premissa que va ser confirmada per Ivanov i Romodanovsky (1928) amb estudis microscòpics pocs anys més tard. Földi *et al.* (1963), van aprofundir en l'estudi del sistema limfàtic del SNC i van demostrar l'arribada de substàncies del SNC als ganglis limfàtics cervicals mitjançant els vasos limfàtics ja descrits prèviament. Anys més tard, Bradbury *et al.* (1981), van descriure que podria haver-hi possibles implicacions immunològiques del drenatge del LCR mitjançant el sistema limfàtic de les meninges posant de manifest el possible desencadenament de malalties autoimmunitàries dirigides contra el sistema nerviós com l'esclerosi múltiple. Baxter, 2007 i Gold *et al.*, 2016 van plantejar també que la interacció de substàncies provinents del SNC amb el sistema immunitari podrien tenir conseqüències fatals. En aquest aspecte, estudis recents han confirmat que elements cel·lulars i solubles del LCR poden causar respostes en els ganglis limfàtics cervicals (Louveau *et al.*, 2015). De fet, Weller *et al.* (2010) ja havien apuntat que el drenatge limfàtic del líquid intersticial del cervell i el LCR cap als ganglis limfàtics cervicals juga un paper important en la inducció d'una tolerància immunitària i de respostes immunitàries adaptatives en el SNC. D'acord amb això, i atès que els resultats indiquen que els *wasteosomes* arriben als ganglis limfàtics cervicals, no es pot descartar que en determinades circumstàncies, les substàncies de rebuig contingudes en els *wasteosomes* puguin desencadenar certes respostes o intervenir en alteracions autoimmunitàries. Conseqüentment, i considerant les possibles implicacions clíniques, s'hauria d'aprofundir en l'estudi del paper dels *wasteosomes* en processos immunitaris o malalties autoimmunitàries en el SNC.

Els resultats obtinguts en la present tesi, no només obren la porta a l'estudi de la relació entre els *wasteosomes* i les malalties autoimmunitàries per la sortida d'aquestes estructures cerebrals fora del SNC i la seva interacció amb el sistema immunitari, sinó que la presència de *wasteosomes* en el LCR també representa un punt d'inici per a l'estudi de marcadors clínics de malalties cerebrals. Els *wasteosomes* contenen substàncies de rebuig produïdes en el cervell i algunes d'aquestes substàncies poden ser marcadors d'algunes malalties cerebrals, com ara malalties neurodegeneratives. En les últimes dècades, el LCR ha estat analitzat exhaustivament per a l'obtenció de biomarcadors de malalties neurodegeneratives. Per exemple, està ben establert que la proteïna fosfo-tau181, la tau total i l'A β són marcadors en LCR per la malaltia d'Alzheimer (Olsson *et al.*, 2016). S'estan estudiant també altres biomarcadors per monitoritzar la demència frontotemporal com ara la cadena lleugera de neurofilaments (NfL), un marcador de dany axonal (Meeter *et al.*, 2016; Meeter *et al.*, 2017). A més a més, l'anàlisi del LCR s'utilitza per excloure altres malalties en el diagnòstic diferencial de l'esclerosi múltiple (Stangel *et al.*, 2013). Els biomarcadors del LCR són també utilitzats en pacients de malaltia de Parkinson (Lleó *et al.*, 2015). No obstant això, els procediments establerts d'obtenció de mostres de LCR impliquen sistemàticament una centrifugació immediatament després de l'extracció del líquid per a l'eliminació de restes cel·lulars, de manera que el sediment obtingut d'aquesta centrifugació és sistemàticament

descartat, i la fracció del LCR que és estudiada és el sobrenedant. Així doncs, tots els biomarcadors examinats fins al moment són biomarcadors solubles de la fracció líquida del LCR. Cal remarcar però que els *wasteosomes* es troben en mostres de LCR no centrifugat i en els sediments de LCR centrifugat, per tant, l'eliminació del sediment del LCR, ha suposat una pèrdua d'informació dels possibles biomarcadors presents en els *wasteosomes* o altres biomarcadors insolubles. En definitiva, els nostres resultats donen suport a la necessitat d'estudiar no només els *wasteosomes* del LCR, sinó també la fracció sòlida del LCR, postulant que s'hi podrien trobar marcadors d'interès diagnòstic.

En conjunt, tot apunta que els *wasteosomes* del cervell són contenidors de substàncies de rebuig que permeten l'eliminació de productes de rebuig del SNC mitjançant diferents mecanismes redundants de fagocitosi, a nivell del LCR a les interfícies del cervell o als ganglis limfàtics cervicals. A més a més, sembla que aquests *wasteosomes* presenten una organització estructural específica per a l'empaquetament de substàncies en un esquelet glucídic que alhora constitueix els NE que actuen com a senyal per a la seva eliminació. Globalment, els resultats indiquen que els *wasteosomes* formen part d'un mecanisme fisiològic de neteja del cervell.

Observant les evidències referents als *wasteosomes* cerebrals i considerant la seva funció en el SNC, es va considerar d'interès analitzar les característiques dels *wasteosomes* d'altres òrgans del cos humà, per establir una hipòtesi entorn a una funció comuna d'aquestes estructures en els diferents teixits i determinar el seu significat fisiopatològic en l'organisme en general. D'acord amb això, es va realitzar un estudi de les característiques dels *wasteosomes* en diferents òrgans en termes de composició, aparença i funció postulada pels autors.

Convé recalcar que alguns dels resultats contrastats mostren certa discrepància, mentre que d'altres semblen recurrents en els diferents estudis. La característica més destacable és que els *wasteosomes* de les diferents localitzacions de l'organisme humà s'han definit com a estructures acumuladores de substàncies de rebuig i/o potencialment tòxiques com a resultat del procés d'envelliment i de determinades condicions fisiopatològiques, material extern i elements infecciosos. Una altra característica que es va repetint en els *wasteosomes* dels diferents teixits és el marcatge positiu amb la tinció de PAS, la qual cosa indica un elevat contingut en polisacàrids en aquestes estructures. En funció de la seva localització, en els *wasteosomes* s'ha descrit la presència de diferents tipus de monosacàrids i la relació entre glúcids i proteïnes és diversa. Tot i això, en qualsevol cas, en tots els òrgans, sembla que els glúcids en són l'element majoritari. Pel que fa al contingut proteic, els resultats confirmen components nombrosos i d'origen molt variat. Considerant la disparitat de components, sembla que els *wasteosomes* dels diferents teixits no són idèntics i podrien variar segons l'entorn en el qual són generats. De tota manera, tot concorda amb la hipòtesi que postula que els *wasteosomes* són estructures en les quals s'acumulen substàncies diverses de

diferents orígens. Pel que fa a la ultraestructura, els *wasteosomes* mostren una densa massa que sovint conté estructures fibril·lars disposades de manera aleatòria, les quals ocasionalment formen anells concèntrics, amb zones de menys i més densitat. La presència d'aquests anells s'atribueix a les diferents fases o estadis de creixement dels CA (Cavanagh, 1999; Dobashi et al., 1989). En alguns casos, com en el pulmó, s'observa un nucli central d'alguna partícula externa a l'interior dels *wasteosomes*. En alguns estudis també s'observen restes cel·lulars i membranoses i alguns orgànuls en els *wasteosomes* o molt propers a ells. La presència de restes cel·lulars i la possibilitat de partícules incloses dins els *wasteosomes* dona suport a la idea que acumulen substàncies de rebuig.

D'altra banda, i tal com s'ha comentat anteriorment, els resultats de la present tesi mostren que els *wasteosomes* del SNC poden ser fagocitats una vegada alliberats del parènquima cerebral per macròfags de les interfícies del cervell i per macròfags dels ganglis limfàtics cervicals, i també s'ha demostrat la seva fagocitosi *in vitro* per part de macròfags THP-1. A més a més, tal i com s'ha comentat prèviament, Suzuki *et al.* (2012) ja van observar interaccions entre *wasteosomes* i macròfags infiltrants en mostres de bulb raquidi i també en mostres de nervi òptic de casos de neuromielitis òptica. Aquest procés sembla no ser exclusiu del sistema nerviós, ja que també s'han trobat *wasteosomes* en contacte amb macròfags en el teixit pulmonar de pacients de mesotelioma (Hammar, 2011) i en la pròstata (Sfanos *et al.*, 2009). Amb tot això, la presència de substàncies de rebuig de diferents orígens en els *wasteosomes* de diferents localitzacions i la seva fagocitosi posen de manifest la participació d'aquestes estructures en l'eliminació de productes de rebuig a nivell global de l'organisme humà.

Malgrat tot, s'han determinat altres aspectes dels *wasteosomes* que semblen discordants, com ara la presència de *wasteosomes* intracel·lulars i extracel·lulars. En cervell, els *wasteosomes* són intracel·lulars, sovint identificats a l'interior d'astròcits (Augé *et al.*, 2019; Navarro *et al.* 2019; Sbarbati *et al.*, 1996; Suzuki *et al.* 2012). En canvi, els *wasteosomes* localitzats en el LCR són extracel·lulars, però aquest fet s'explica perquè aquests *wasteosomes* són resultat d'un procés d'extrusió des del teixit cerebral. També s'han observat *wasteosomes* extracel·lulars en alvèols i ductes pulmonars, en l'efusió pleural, i en saliva i en la llum dels conductes lactífers de la mama (Kambouchner *et al.*, 2003; Mani i Wang, 2021; Martínez-Girón i Pantanowitz, 2021; Otori i Hoff, 2008). S'ha proposat que els *wasteosomes* del pulmó deriven de cèl·lules epitelials del pulmó, i que l'origen epitelial és possible en altres teixits o òrgans. Cal destacar que la pròstata i la mama, i en general els teixits glandulars, contenen cèl·lules secretores que són de naturalesa epitelial. Per tant, sembla ser que els *wasteosomes* extracel·lulars són el resultat d'una extrusió o secreció apocrina dels *wasteosomes* formats en cèl·lules de determinats teixits, principalment cèl·lules de naturalesa epitelial.

Val la pena puntualitzar que alguns autors suggereixen que els *wasteosomes* són derivats d'una alteració del metabolisme del glicogen. Aquesta hipòtesi sorgeix de l'elevat contingut en polisacàrids descrit en aquestes estructures, fet que, les ha relacionat amb malalties com la malaltia de Lafora, una epilèpsia en la qual apareixen els cossos de Lafora que mostren certes similituds amb els *wasteosomes* (Sakai *et al.*, 1969). No obstant això, aquesta hipòtesi deixa moltes qüestions sense resoldre i no permet una integració global de tots els resultats descrits en els *wasteosomes*, com ara la presència d'una gran varietat de productes de rebuig d'origens molt diversos o la presència de les proteïnes Ubi i p62, implicades en el marcatge i processament de substàncies de rebuig. La hipòtesi metabòlica tampoc permet explicar que els *wasteosomes* puguin localitzar-se en el medi intracel·lular i extracel·lular. Un procés de necrosi de les cèl·lules que contenen *wasteosomes* podria explicar l'alliberament dels *wasteosomes* en el medi extracel·lular, però en aquest cas, el teixit mostraria nivells significatius d'inflamació, cosa que generalment no ha estat observada al voltant dels *wasteosomes*. A més a més, la teoria metabòlica no explica perquè hi ha NE en els *wasteosomes* ni la presència d'IgM naturals contra els NE o perquè els *wasteosomes* extracel·lulars són fagocitats per macròfags.

Així doncs, considerant el conjunt de resultats revisats, en aquesta tesi, es proposa considerar els *wasteosomes* com a contenidors de substàncies de rebuig els qual són generats activament per cèl·lules epitelials o glandulars que recullen i retenen productes de rebuig o estranys, els quals seguidament, són secretats al medi extern o a espais intersticials, essent en aquest últim cas, on són fagocitats per macròfags per ser eliminats. En definitiva, els *wasteosomes* de l'organisme humà formen part d'un sistema d'eliminació de productes de rebuig.

Tal i com es mostra a la Figura 9, la formació dels *wasteosomes* s'iniciaria a nivell intracel·lular amb la captura de productes de rebuig provinents de la pròpia cèl·lula o d'altres orígens els quals alguns d'ells haurien estat assenyalats amb Ubi i segrestats per la p62. La taxa de formació de *wasteosomes* estaria relacionada amb la producció d'elements de rebuig, la qual augmenta amb l'envelliment, però també en condicions com les que involucren alts nivells d'estrès oxidatiu. Cal considerar que els elements de rebuig intracel·lulars generalment s'eliminen mitjançant mecanismes específics com ara sistema Ubi-proteosoma o processos d'autofàgia via fagosoma/lisosoma, però en alguns casos, aquestes substàncies de rebuig poden eliminar-se a través dels *wasteosomes*. Al mateix temps, s'activaria la maquinària cel·lular involucrada en la generació de l'esquelet glucídic que constitueix l'estructura principal del *wasteosome*. Considerant que l'estructura de poliglucosà dels *wasteosomes* del SNC està constituïda per glicogen modificat el qual mostra certes similituds al dels cossos de poliglucosà que es desenvolupen en malalties com la malaltia de cossos de poliglucosà en adults (*adult polyglucosan body disease*) i la malaltia de Lafora, la maquinària involucrada en la seva formació podria ser semblant. L'etiologia d'aquestes malalties inclou defectes

genètics que afecten els enzims que participen en el metabolisme del glicogen. Alguns d'aquests enzims afectats són la malina i laforina, una ubiquitin-ligasa i una fosfatasa que conjuntament formen un complex i regulen l'acumulació de glicogen mitjançant el control dependent del proteosoma de proteïnes relacionades amb el glicogen com la proteïna dirigida a glicogen (*protein targeting to glycogen*, PTG), implicada en l'activació de la GS o l'enzim desramificant del glicogen (*glycogen debranching enzyme*, GDE) (Cheng *et al.*, 2007; Sharma *et al.*, 2011; Vilchez *et al.*, 2007; Worby *et al.*, 2008). Així doncs, es postula que aquests enzims podrien estar implicats en la gènesi de l'estructura de poliglucosà que constitueix l'esquelet dels *wasteosomes*. En efecte, es considera que la maquinària per formar aquest tipus d'estructura de glucídica seria fisiològicament activa en les cèl·lules en què es produeixen els *wasteosomes*. Aquest conjunt d'evidències suggereixen que el glicogen o estructures similars no només realitzen funcions d'emmagatzematge de carboni i energia sinó que també estarien implicats en la formació d'estructures de revestiment, com en el cas de l'esquelet dels *wasteosomes* proposat en aquest treball.

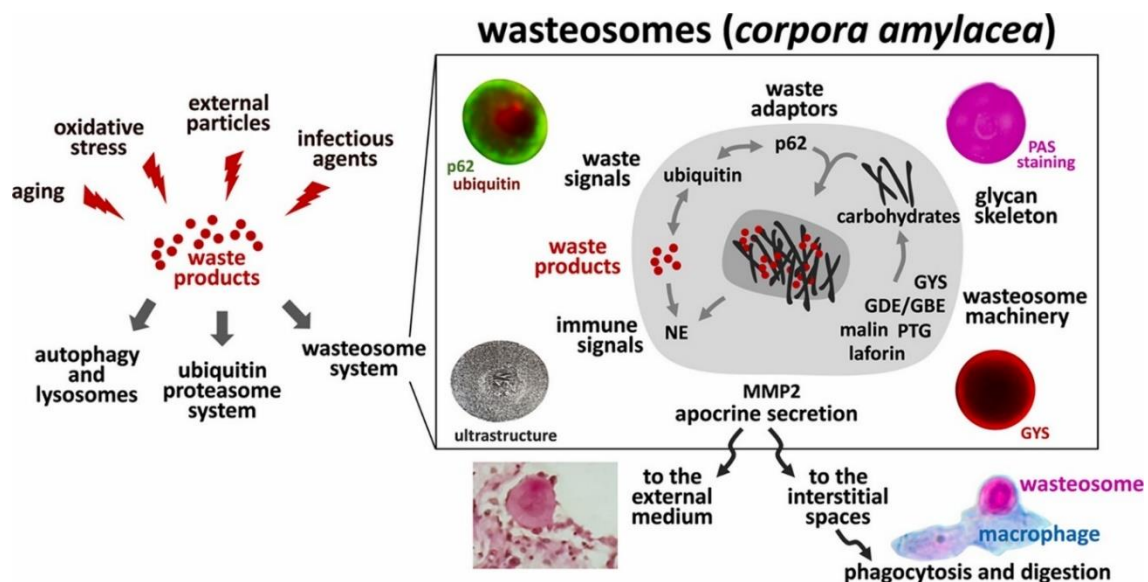


Figura 9. Sistema *wasteosome*: esquema del procés implicat en la generació i eliminació dels *wasteosomes*. La producció de substàncies de rebuig incrementa amb l'edat i altres circumstàncies com ara l'estrès oxidatiu, la presència d'alguns agents infecciosos o condicions patològiques. Aquestes substàncies poden ser processades i eliminades mitjançant mecanismes intracel·lulars com el sistema Ubi-proteosoma o processos d'autòfaga. No obstant això, en alguns casos, l'acumulació de substàncies de rebuig pot donar lloc a la formació dels *wasteosomes*. En la generació de *wasteosomes*, inicialment, es produeix un recull de substàncies de rebuig d'origens diversos, les quals són marcades amb Ubi i capturades per la p62. Paral·lelament, també es desencadena la formació de l'esquelet glucídica mitjançant la maquinària cel·lular que inclou proteïnes com la malina, la laforina, el GBE, el GDE i la PTG. Un cop formats, els *wasteosomes*, són secretats al medi extern o a espais intersticials, on podrien ser fagocitats per macròfags. Els NE presents en els *wasteosomes* i altres components podrien facilitar el procés de fagocitosis. GBE, *glycogen branching enzyme*, enzim ramificant del glicogen; GDE, *glycogen debranching enzyme*, enzim desramificant del glicogen; GYS, glicogen sintasa; MMP2, *matrix-metalloproteinase-2*, metal·loproteasa de matriu 2; NE, neo-epítip; PTG, *protein targeting to glycogen*, proteïna dirigida a glicogen (Article 3).

A partir dels estudis realitzats i presentats a la present tesi, s'han obert noves perspectives que han estat comentades a la discussió. Resumint, en aquest apartat, les perspectives que semblen més destacables i que es consideren més rellevants són:

- 1) La possibilitat d'utilitzar els *wasteosomes* del SNC com a eina de diagnòstic de malalties cerebrals. Tot i que els *wasteosomes*, fins al moment, han estat obtinguts de mostres de LCR intraventricular *post-mortem*, no es descarta que es puguin trobar *wasteosomes* en les mostres de LCR obtingut de punció lumbar els quals puguin ser utilitzats amb finalitats diagnòstiques. En aquesta línia, ja s'està treballant en una millora de la caracterització i l'aïllament d'aquestes estructures.
- 2) La possible implicació dels *wasteosomes* del SNC en el desenvolupament de malalties autoimmunitàries a l'exportar substàncies d'origen cerebral fora del sistema nerviós.
- 3) L'establiment d'una relació entre la glucèmia i els anticossos naturals, fet que assenyalava una possible alteració de la immunitat innata en condicions d'hiperglicèmia.

Es precisa de més estudis per abordar aquests nous enfocaments que han sorgit del present treball. En tot cas, aquesta tesi posa els *wasteosomes*, unes estructures ignorades durant dècades, en el punt de mira novament.

V. CONCLUSIONS

1. Human *post-mortem* ventricular cerebrospinal fluid contains *corpora amylacea*.
2. *Corpora amylacea* from the cerebrospinal fluid show the same features in terms of composition and ultrastructure as those from the hippocampus.
3. *Corpora amylacea* reach the cervical lymph nodes.
4. Lymph nodes located in the upper region of the neck contain higher numbers of *corpora amylacea* than those of the lower zone.
5. Lymph nodes retain or eliminate *corpora amylacea*.
6. In the lymph nodes, *corpora amylacea* are sited in regions through which lymph flows and make contact with specific cells that are identified as macrophages.
7. *In vitro*, THP-1 macrophages phagocytose and digest *corpora amylacea*.
8. IgM opsonization is not a requisite for *corpora amylacea* phagocytosis by THP-1 macrophages.
9. Mannose receptor CD206 may be involved in the phagocytosis of *corpora amylacea* by THP-1 macrophages.
10. *In vivo*, *corpora amylacea* can be phagocytosed through complement pathways or IgM receptor Fc μ R.
11. Redundant mechanisms lead to the phagocytosis of *corpora amylacea* and ensure their elimination.
12. Neo-epitopes of *corpora amylacea* that are recognised by natural IgM do not have a peptide nature.
13. Neo-epitopes of *corpora amylacea* that are recognised by natural IgM have a carbohydrate nature.
14. Phagocytosis of *corpora amylacea* by macrophages may be produced once they are extruded from brain parenchyma and are located in the central nervous system interfaces or beyond.

15. Phagocytosis of *corpora amylacea* can be carried out by non-inflammatory mechanisms, thus avoiding tissue damage.
16. *Corpora amylacea* act as waste containers that remove waste substances from the human brain.
17. *Corpora amylacea* of human brain act as waste containers that remove waste substances from the central nervous system.
18. *Corpora amylacea* in the human brain are generated by astrocytes, while those generated in other tissues are generated by specific epithelial or glandular cells.
19. In all tissues, *corpora amylacea* sequester and accumulate waste substances and other products of different origins in a carbohydrate skeleton.
20. The nature of the waste products accumulated in CA depends on the tissue where these structures are located and the possible local damage of the tissue.
21. *Corpora amylacea* are extruded in the external environment or in interstitial spaces.
22. When released to interstitial spaces, *corpora amylacea* are phagocytosed by macrophages.
23. *Corpora amylacea* are part of a system for the elimination of waste products.
24. To avoid the ambiguity of the term *amylacea*, we proposed renaming *corpora amylacea* as “wasteosomes”, emphasizing the waste products they entrap rather than their misleading amyloid properties.
25. The present work suggests that wasteosomes from cerebrospinal fluid may contain brain markers that may aid in the diagnosis of certain brain diseases.
26. The use of wasteosomes for diagnostic purposes may become a valuable new strategy.
27. Moreover, it is suggested that glycemia may affect the reactivity of some natural IgM and, by extension, the natural immunity.
28. Although *corpora amylacea* or wasteosomes have been ignored for almost two centuries, they are back in the spotlight once again.

VI. BIBLIOGRAFIA

A

- Absinta M, Ha SK, Nair G, Sati P, Luciano NJ, Palisoc M, Louveau A, Zaghoul KA, Pittaluga S, Kipnis J, Reich DS. Human and nonhuman primate meninges harbor lymphatic vessels that can be visualized noninvasively by MRI. *Elife*. 2017; 6:e29738.
- Anzil AP, Herrlinger H, Blinzinger K, Kronska D. Intraneuritic corpora amylacea. *Virchows Arch A Pathol Anat Histol*. 1974; 364:297–301.
- Augé E, Cabezón I, Pelegrí C, Vilaplana J. New perspectives on corpora amylacea in the human brain. *Sci Rep*. 2017; 7:41807.
- Augé E, Duran J, Guinovart JJ, Pelegrí C, Vilaplana J. Exploring the elusive composition of corpora amylacea of human brain. *Sci Rep*. 2018; 8:13525.
- Augé E, Bechmann I, Llor N, Vilaplana J, Krueger M, Pelegrí C. Corpora amylacea in human hippocampal brain tissue are intracellular bodies that exhibit a homogeneous distribution of neo-epitopes. *Sci Rep*. 2019; 9:2063.
- American Diabetes Association. 2. Classification and diagnosis of diabetes: standards of medical care in diabetes-2020. *Diabetes Care*. 2020; 43(Suppl. 1):S14–31.
- Averback P. Parasynaptic corpora amylacea in the striatum. *Arch Pathol*. 1981; 105:334–5.
- Alder N. On the nature, origin and distribution of the corpora amylacea of the brain with observations on some new staining reactions. *J Mental Sci*. 1953; 99:689–97.

B

- Bakić M, Jovanović I. Morphological features of corpora amylacea in human parahippocampal cortex during aging. *Acta Medica Int*. 2017; 4:25–31.
- Baxter AG. The origin and application of experimental autoimmune encephalomyelitis. *Nat Rev Immunol*. 2007; 7:904–12.
- Botez G, Rami A. Immunoreactivity for Bcl-2 and C-Jun/AP1 in hippocampal corpora amylacea after ischaemia in humans. *Neuropathol Appl Neurobiol*. 2001; 27:474–80.
- Bovin NV. Natural antibodies to glycans. *Biochemistry*. 2013; 78:786–97.
- Bradbury MV, Cserr HF, Westrop RJ. Drainage of cerebral interstitial fluid into deep cervical lymph of the rabbit. *Am J Physiol*. 1981; 240:F329–36.
- Buzzard EF, Greenfield JG. Pathology of the nervous system. Londres. 1921.

Buervenich S, Olson L, Galter D. Nestin-like immunoreactivity of corpora amylacea in aged human brain. *Brain Res Mol Brain Res*. 2001; 94:204–8.

Busard HL, Span JP, Renkawek K, Renier WO, Gabreëls FJ, Slooff JL, Van't Hof MA. Polyglucosan bodies in brain tissue: a systematic study. *Clin Neuropathol*. 1994; 13:60–3.

C

Catola G, Achúcarro N. Über die Entstehung de Amyloidkörperchen in Zentralnervensystem. *Virchows Arch f Path Anat*. 1906; 184:454–69.

Cavanagh JB. Corpora-amylacea and the family of polyglucosan diseases. *Brain Res Brain Res Rev*. 1999; 29:265–95.

Ceci A. Contribuzione allo studio della fibra nervosa midollata ed osservazioni sui corpuscoli amilacei dell'encefalo e midollo spinale. *Atti della Reale Accademia Nazionale dei Lincei*. 1881.

Chávez-Galán L, Olleros ML, Vesin D, Garcia I. Much more than M1 and M2 macrophages, there are also CD169(+) and TCR(+) macrophages. *Front Immunol*. 2015; 6:263.

Cheng A, Zhang M, Gentry MS, Worby CA, Dixon JE, Saltiel AR. A role for AGL ubiquitination in the glycogen storage disorders of Lafora and Cori's disease. *Genes Dev*. 2007; 21:2399–409.

Chung MH, Horoupian DS. Corpora amylacea: a marker for mesial temporal sclerosis. *J Neuropathol Exp Neurol*. 1996; 55:403–8.

Cissé S, Perry G, Lacoste-Royal G, Cabana T, Gauvreau D. Immunochemical identification of ubiquitin and heat-shock proteins in corpora amylacea from normal aged and Alzheimer's disease brains. *Acta Neuropathol*. 1993; 85:233–40.

Cissé S, Lacoste-Royal G, Laperriere J, Cabana T, Gavreau D. Ubiquitin is a component of polypeptides purified from corpora amylacea of aged human brain. *Neurochem Res*. 1991; 16:429–33.

Cissé S, Schipper HM. Experimental induction of corpora amylacea-like inclusions in rat astroglia. *Neuropathol Appl Neurobiol*. 1995; 21:423–31.

Coulibaly FS, Youan BB. Concanavalin A-polysaccharides binding affinity analysis using a quartz crystal microbalance. *Biosens Bioelectron*. 2014; 59:404–11.

D

Dana TG, Rayyan AK. Diabetic complications and dysregulated innate immunity. *Front Biosci.* 2008; 13:1227–39.

Day RJ, Mason MJ, Thomas C, Poon WW, Rohn TT. Caspase-cleaved tau co-localizes with early tangle markers in the human vascular dementia brain. *PLoS One.* 2015; 10:e0132637.

del Río-Hortega P. El "tercer elemento" de los centros nerviosos. Poder fagocitario y movilidad de la microglía. *Bol de la R Soc Esp de Hist Nat.* 1919; 13:154–66.

E

Ellis RS. Norms for some structural changes in the human cerebellum from birth to old age. *J. Comp. Neurol.* 1920; 32:1–33.

Erdamar S, Zhu ZQ, Hamilton WJ, Armstrong DL, Grossman RG. Corpora amylacea and heat shock protein 27 in Ammon's horn sclerosis. *J Neuropathol Exp Neurol.* 2000; 59:698–706.

E

Feinberg H, Jégouzo SAF, Lasanajak Y, Smith DF, Drickamer K, Weis WI, Taylor ME. Structural analysis of carbohydrate binding by the macrophage mannose receptor CD206. *J Biol Chem.* 2021; 296:100368.

Ferraro A, Damon LA. The histogenesis of amyloid bodies in the central nervous system. *Arch Pathol.* 1931; 12:229–44.

Fleming PD, Cordoza ME, Woods SG, Griesbach EJ, Worcester MA. Corpora amylacea increased in Alzheimer's disease. *Neurology.* 1987; 37:157.

Földi M, Csada E, Obál F, Madarász I, Szeghy G, Zoltán ÖT. Über Wirkungen der Unterbindung der Lymphgefäße und Lymphknoten des Hases auf das Zentralnervensystem im Tierversuch. *Z ges Exp Med.* 1963; 137: 484–510.

Franz S, Herrmann K, Fürnrohr BG, Sheriff A, Frey B, Gaipf US, Voll RE, Kalden JR, Jäck HM, Herrmann M. After shrinkage apoptotic cells expose internal membrane-derived epitopes on their plasma membranes. *Cell Death Differ.* 2007; 14:733–42.

Fricke B, Andres KH, Von Düring M. Nerve fibers innervating the cranial and spinal meninges: morphology of nerve fiber terminals and their structural integration. *Microsc Res Tech.* 2001; 53:96–105.

Fujii M, Goto N, Okada A, Kida A, Kikuchi K. Distribution of amyloid bodies in the aged human vestibulocochlear nerve. *Acta Oto-Laryngol.* 1996; 116:566–71.

G

Gáti I, Leel-Össy L. Heat shock protein 60 in corpora amylacea. *Pathol Oncol Res.* 2001; 7:140–4.

Gold R, Linington C, Lassmann H. Understanding pathogenesis and therapy of multiple sclerosis via animal models: 70 years of merits and culprits in experimental autoimmune encephalomyelitis research. *Brain.* 2006; 129:1953–71.

Goldin A, Beckman JA, Schmidt AM, Creager MA. Advanced glycation end products: sparking the development of diabetic vascular injury. *Circulation.* 2006; 114:597–605.

Goldstein IJ, Reichert CM, Misaki A. Interaction of concanavallin A with model substrates. *Ann N Y Acad Sci.* 1974; 234:283–96.

Goldstein IJ, Hayes CE. The lectins: carbohydrate-binding proteins of plants and animals. *Adv Carbohydr Chem Biochem.* 1978; 35:127–340.

Gonzalez-Quintela A, Alende R, Gude F, Campos J, Rey J, Meijide LM, et al. Serum levels of immunoglobulins (IgG, IgA, IgM) in a general adult population and their relationship with alcohol consumption, smoking and common metabolic abnormalities. *Clin Exp Immunol.* 2008; 151:42–50.

Grönwall C, Vas J, Silverman GJ. Protective roles of natural IgM antibodies. *Front Immunol.* 2012; 3:66.

H

Haji-Ghassemi O, Blackler RJ, Young NM, Evans SV. Antibody recognition of carbohydrate epitopes. *Glycobiology.* 2015; 25:920–52.

Hammar SP. Ultrastructural pathology of pulmonary corpora amylacea. Society for Ultrastructural Pathology. USCAP, San Antonio, TX, USA, 2011.

Hoyaux D, Decaestecker C, Heizmann CW, Vogl T, Schäfer BW, Salmon I, Kiss R, Pochet R. S100 proteins in corpora amylacea from normal human brain. *Brain Res.* 2000; 867:280–8.

I

Ivanov G, Romodanovsky K. Über den anatomischen Zusammenhang der cerebralen und spinalen submeningealen Räume mit dem Lymphsystem. *Z ges exp Med.* 1928; 60: 554.

Iwaki T, Hamada Y, Tateishi J. Advanced glycosylation end-products and heat shock proteins accumulate in the basophilic degeneration of the myocardium and the corpora amylacea of the glia. *Pathol Int.* 1996; 46:757–63.

J

Jacobi W. Das Spaltensystem der Dura. *Arch Psychiat Nervenkd.* 1924; 70:269–85.

Jafar N, Edriss H, Nugent K. The effect of short-term hyperglycemia on the innate immune system. *Am J Med Sci.* 2016; 351:201–11.

Jessen NA, Munk AS, Lundgaard I, Nedergaard M. The glymphatic system: a beginner's guide. *Neurochem Res.* 2015; 40:2583–99.

Juliana C, Janine C, Cresio A. Infections in patients with diabetes mellitus: a review of pathogenesis. *Indian J Endocrinol Metab.* 2012; 16:27–36.

K

Kambouchner M, Godmer P, Guillevin L, Raphaël M, Droz D, Martin A. Low grade marginal zone B cell lymphoma of the breast associated with localised amyloidosis and corpora amylacea in a woman with long standing primary Sjögren's syndrome. *J Clin Pathol.* 2003; 56:74–7.

Klebs. *Die allgemeine Pathologie.* Jena (Gustav Fischer). 1889; 2:628

Kimura T, Takamatsu J, Miyata T, Miyakawa T, Horiuchi S. Localization of identified advanced glycation end-product structures, N epsilon(carboxymethyl)lysine and pentosidine, in age-related inclusions in human brains. *Pathol Int.* 1998; 48:575–9.

Korzhevskii DE, Giliarov AV. Demonstration of nuclear protein neuron in the human brain corpora amylacea. *Morfologija.* 2007; 131:75–6.

L

Lanzrein AS, Jobst KA, Thiel S, Jensenius JC, Sim RB, Perry VH, Sim E. Mannan-binding lectin in human serum, cerebrospinal fluid and brain tissue and its role in Alzheimer's disease. *Neuroreport.* 1998; 9:1491–5.

Leel-Össy L. Corpora amylacea in hippocampal sclerosis. *J Neurol Neurosurg Psychiatry.* 1998; 65:614.

Leel-Össy L. New data on the ultrastructure of the corpus amylaceum (polyglucosan body). *Pathol Oncol Res.* 2001; 7:145–50.

- Loiseau H, Marchal C, Vital A, Vital C, Rougier A, Loiseau P. Occurrence of polyglucosan bodies in temporal lobe epilepsy. *J Neurol Neurosurg Psychiatry*. 1992; 55:1092–3.
- Leber T. *Handbuch der Augenheilkunde von Graefe und Saemisch*. 1875; 5.
- Lehesjoki AE, Koskiniemi M, Sistonen P, Miao J, Hästbacka J, Norio R, de la Chapelle A. Localization of a gene for progressive myoclonus epilepsy to chromosome 21q22. *Proc Natl Acad Sci U S A*. 1991; 88:3696–9.
- Ley K. M1 means kill; M2 means heal. *J Immunol*. 2017; 199:2191–3.
- Leyden E. *Zeitschrift für klinische Medizin*. 1880; 1.
- Liu HM, Anderson K, Caterson B. Demonstration of a keratin sulfate proteoglycan and a mannose-rich glycoconjugate in corpora amylacea of the brain by immunocytochemical and lectin-binding methods. *J Neuroimmunol*. 1987; 14:49–60.
- Loeffler KU, Edward DP, Tso MO. Tau-2 immunoreactivity of corpora amylacea in the human retina and optic nerve. *Invest Ophthalmol Vis Sci*. 1993; 34:2600–3.
- Louveau A, Plog BA, Antila S, Alitalo K, Nedergaard M, Kipnis J. Understanding the functions and relationships of the glymphatic system and meningeal lymphatics. *J Clin Invest*. 2017; 127:3210–9.
- Libard S, Popova SN, Amini RM, Kärjä V, Pietiläinen T, Hämäläinen KM, Sundström C, Hesselager G, Bergqvist M, Ekman S, Zetterling M, Smits A, Nilsson P, Pfeifer S, de Ståhl TD, Enblad G, Ponten F, Alafuzoff I. Human cytomegalovirus tegument protein pp65 is detected in all intra- and extra-axial brain tumours independent of the tumour type or grade. *PLoS One*. 2014; 9:e108861.
- Lleó A, Cavedo E, Parnetti L, Vanderstichele H, Herukka SK, Andreassen N, Ghidoni R, Lewczuk P, Jeromin A, Winblad B, Tsolaki M, Mroczko B, Visser PJ, Santana I, Svenningsson P, Blennow K, Aarsland D, Molinuevo JL, Zetterberg H, Mollenhauer B. Cerebrospinal fluid biomarkers in trials for Alzheimer and Parkinson diseases. *Nat Rev Neurol*. 2015; 11:41–55.
- Lutz HU, Binder CJ, Kaveri S. Naturally occurring auto-antibodies in homeostasis and disease. *Trends Immunol*. 2009; 30:43–51.

M

- Maddur MS, Lacroix-Desmazes S, Dimitrov JD, Kazatchkine MD, Bayry J, Kaveri SV. Natural antibodies: from first-line defense against pathogens to perpetual immune homeostasis. *Clin Rev Allergy Immunol*. 2020; 58:213–28.

- Mani H, Wang BG. Corpora amylacea in pleural effusion. *Diagn Cytopathol.* 2021; 49:E231–3.
- Manich G, Cabezón I, Camins A, Pallàs M, Liberski PP, Vilaplana J, Pelegrí C. Clustered granules present in the hippocampus of aged mice result from a degenerative process affecting astrocytes and their surrounding neuropil. *Age.* 2014a; 36:9690.
- Manich G, del Valle J, Cabezón I, Camins A, Pallàs M, Pelegrí C, Vilaplana J. Presence of a neo-epitope and absence of amyloid beta and tau protein in degenerative hippocampal granules of aged mice. *Age.* 2014b; 36:151–65.
- Manich G, Augé E, Cabezón I, Pallàs M, Vilaplana J, Pelegrí C. Neo-epitopes emerging in the degenerative hippocampal granules of aged mice can be recognized by natural IgM auto-antibodies. *Immun Ageing.* 2015; 12:23.
- Mantovani A, Sica A, Sozzani S, Allavena P, Vecchi A, Locati M. The chemokine system in diverse forms of macrophage activation and polarization. *Trends Immunol.* 2004; 25:677–86.
- Maqbool A, Tahir M. Corpora amylacea in human cadaveric brain age related differences. *Biomedica.* 2008; 24:92–5.
- Martin JE, Mather K, Swash M, Garafalo O, Leigh PN, Anderton BH. Heat shock protein expression in corpora amylacea in the central nervous system: clue to their origin. *Neuropathol Appl Neurobiol.* 1991; 17:113–9.
- Martínez-Girón R, Pantanowitz L. Corpora amylacea in sputum smears: Incidence and clinical significance. *Cytopathology.* 2021; 32:108–14.
- Meng H, Zhang X, Blaivas M, Wang MM. Localization of blood proteins thrombospondin1 and ADAMTS13 to cerebral corpora amylacea. *Neuropathology.* 2009; 29:664–71.
- Meeter LH, Doppert EG, Jiskoot LC, Sanchez-Valle R, Graff C, Benussi L, Ghidoni R, Pijnenburg YA, Borroni B, Galimberti D, Laforce RJ, Masellis M, Vandenberghe R, Ber IL, Otto M, van Minkelen R, Papma JM, Rombouts SA, Balasa M, Öijerstedt L, Jelic V, Dick KM, Cash DM, Harding SR, Jorge Cardoso M, Ourselin S, Rossor MN, Padovani A, Scarpini E, Fenoglio C, Tartaglia MC, Lamari F, Barro C, Kuhle J, Rohrer JD, Teunissen CE, van Swieten JC. Neurofilament light chain: a biomarker for genetic frontotemporal dementia. *Ann Clin Transl Neurol.* 2016; 3:623–36.
- Meeter LH, Kaat LD, Rohrer JD, van Swieten JC. Imaging and fluid biomarkers in frontotemporal dementia. *Nat Rev Neurol.* 2017; 13:406–19.

Mittal KR, Olszewski WA. Widening of inter-Purkinje cell distances in association with corpora amylacea. *J Gerontol.* 1985; 40:700–2.

Mizutani T, Satoh J, Morimatsu Y. Axonal polyglucosan body in the ventral posterolateral nucleus of the human thalamus in relation to aging. *Acta Neuropathol.* 1987; 74:9–12.

Morgagni JB. *Adversaria Anatomica Omnia.* Lug Bat. 1723; 4.

Murray PJ, Wynn TA. Protective and pathogenic functions of macrophage subsets. *Nature Rev.* 2011;11:723–37.

N

Nam IH, Kim DW, Song H, Kim S, Lee KS, Lee YH. Association of corpora amylacea formation with astrocytes and cerebrospinal fluid in the aged human brain. *Korean J Phys Anthropol.* 2012; 25:177–84.

Navarro PP, Genoud C, Castaño-Díez D, Graff-Meyer A, Lewis AJ, de Gier Y, Lauer ME, Britschgi M, Bohrmann B, Frank S, Hench J, Schweighauser G, Rozemuller AJM, van de Berg WDJ, Stahlberg H, Shahmoradian SH. Cerebral Corpora amylacea are dense membranous labyrinths containing structurally preserved cell organelles. *Sci Rep.* 2018; 8:18046.

Nishio S, Morioka T, Kawamura T, Fukui K, Nonaka H, Matsushima M. Corpora amylacea replace the hippocampal pyramidal cell layer in a patient with temporal lobe epilepsy. *Epilepsia.* 2001; 42:960–2.

Notter T, Knuesel I. Reelin immunoreactivity in neuritic varicosities in the human hippocampal formation of non-demented subjects and Alzheimer's disease patients. *Acta Neuropathol Commun.* 2013; 1:27.

O

Ohori NP, Hoff ER. *Cytopathology of pulmonary neoplasia.* A: Springer. Dail and Hammar's Pulmonary Pathology. Tercera Ed. Nova York, 2008. p. 767–806.

Olsson B, Lautner R, Andreasson U, Öhrfelt A, Portelius E, Bjerke M, Hölttä M, Rosén C, Olsson C, Strobel G, Wu E, Dakin K, Petzold M, Blennow K, Zetterberg H. CSF and blood biomarkers for the diagnosis of Alzheimer's disease: A systematic review and meta-analysis. *Lancet Neurol.* 2016; 15:673–84.

P

- Palmucci L, Anzil AP, Luh S. Intra-astrocytic glycogen granules and corpora amylacea stain positively for polyglucosans: a cytochemical contribution on the fine structural polymorphism of particulate polysaccharides. *Acta Neuropathol.* 1982; 57:99–102.
- Pirici D, Mărgăritescu C. Corpora amylacea in aging brain and age-related brain disorders. *J Aging Gerontol.* 2014; 2:33–57.
- Pirici I, Mărgăritescu C, Mogoantă L, Petrescu F, Simionescu CE, Popescu ES, Cecoltan S, Pirici D. Corpora amylacea in the brain form highly branched three dimensional lattices. *Rom J Morphol Embryol.* 2014; 55:1071–7.
- Pisa D, Alonso R, Rábano A, Carrasco L. Corpora amylacea of brain tissue from neurodegenerative diseases are stained with specific antifungal antibodies. *Front Neurosci.* 2016; 10:86.
- Pisa D, Alonso R, Marina AI, Rábano A, Carrasco L. Human and microbial proteins from corpora amylacea of Alzheimer's disease. *Sci Rep.* 2018; 8:9880.
- Pollay M. The function and structure of the cerebrospinal fluid outflow system. *Cerebrospinal Fluid Res.* 2010; 7:9.
- Proulx ST. Cerebrospinal fluid outflow: a review of the historical and contemporary evidence for arachnoid villi, perineural routes, and dural lymphatics. *Cell Mol Life Sci.* 2021; 78:2429–57.
- Purkinje JE. *Naturforscherversammlung.* Praga. 1837.

R

- Ramsey HI. Ultrastructure of corpora amylacea. *J Neuropathol Exp Neurol.* 1965; 24:25–39.
- Redlich E. Die Amyloidkörperchen im Nervensystem. *Jahrbücher für Psychiatrie.* 1891; 10.
- Reiber H, Padilla-Docal B, Jensenius JC, Dorta-Contreras AJ. Mannan-binding lectin in cerebrospinal fluid: a leptomeningeal protein. *Fluids Barriers CNS.* 2012; 9:17.
- Reyneveld GI, Savelkoul HFJ, Parmentier HK. Current Understanding of Natural Antibodies and Exploring the Possibilities of Modulation Using Veterinary Models. A Review. *Front Immunol.* 2020; 11:2139.
- Robertson WF. *A text-book of pathology in relation to mental diseases.* Clay R Coll Psychiatr. 1900.

S

- Sakai M, Austin J, Witmer F, Trueb L. Studies of corpora amylacea. I. Isolation and preliminary characterization by chemical and histochemical techniques. *Arch Neurol.* 1969; 21:526–44.
- Sbarbati A, Carner M, Colletti V, Osculati F. Extrusion of corpora amylacea from the marginal glia at the vestibular root entry zone. *J Neuropathol Exp Neurol.* 1996; 55:196–201.
- Schaffer K. Pathologie und Anatomie der Lyssa. *Zieglers Beitr Anat.* 1890; 7.
- Schipper HM, Cissé S. Mitochondrial constituents of corpora amylacea and autofluorescent astrocytic inclusions in senescent human brain. *Glia.* 1995; 14:55–64.
- Schipper HM. Brain iron deposition and the free radical-mitochondrial theory of ageing. *Ageing Res Rev.* 2004; 3:265–301.
- Schwalbe G. Der Archnoidealraum, ein Lymphraum und sein Zusammenhang mit dem Perichorioidealraum. *Zbl med Wiss.* 1869; 7:465.
- Selmaj K, Pawłowska Z, Walczak A, Koziółkiewicz W, Raine CS, Cierniewski CS. Corpora amylacea from multiple sclerosis brain tissue consists of aggregated neuronal cells. *Acta Biochim Pol.* 2008; 55:43–9.
- Sfanos KS, Wilson BA, De Marzo AM, Isaacs WB. Acute inflammatory proteins constitute the organic matrix of prostatic corpora amylacea and calculi in men with prostate cancer. *Proc Natl Acad Sci U S A.* 2009; 106:3443–8.
- Shapouri-Moghaddam A, Mohammadian S, Vazini H, Taghadosi M, Esmaili SA, Mardani F, et al. Macrophage plasticity, polarization and function in health and disease. *J Cell Physiol.* 2018; 233:6425–40.
- Sharma J, Rao SN, Shankar SK, Satishchandra P, Jana NR. Lafora disease ubiquitin ligase malin promotes proteasomal degradation of neuronatin and regulates glycogen synthesis. *Neurobiol Dis.* 2011; 44:133–41.
- Singhrao SK, Neal JW, Newman GR. Corpora amylacea could be an indicator of neurodegeneration. *Neuropathol Appl Neurobiol.* 1993; 19:269–76.
- Singhrao SK, Neal JW, Piddlesden SJ, Newman GR. New immunocytochemical evidence for a neuronal/oligodendroglial origin for corpora amylacea. *Neuropathol Appl Neurobiol.* 1994; 20:66–73.
- Singhrao SK, Morgan BP, Neal JW, Newman GR. A functional role for corpora amylacea based on evidence from complement studies. *Neurodegeneration.* 1995; 4:335–45.

- Stam FC, Roukema PA. Histochemical and biochemical aspects of corpora amylacea. *Acta Neuropathol.* 1973; 25:95–102.
- Stangel M, Fredrikson S, Meinl E, Petzold A, Stüve O, Tumani H. The utility of cerebrospinal fluid analysis in patients with multiple sclerosis. *Nat Rev Neurol.* 2013; 9:267–76.
- Stephan AH, Barres BA, Stevens B. The complement system: an unexpected role in synaptic pruning during development and disease. *Annu Rev Neurosci.* 2012; 35:369–89.
- Steyaert A, Cissé S, Merhi Y, Kalbakji A, Reid N, Gauvreau D, Lacoste-Royal G. Purification and polypeptide composition of corpora amylacea from aged human brain. *J Neurosci Methods.* 1990; 31:59–64.
- Sun CN. Ultrastructural study of corpora amylacea in human thyroid gland. *Exp Pathol.* 1983; 23:219–25.
- Suzuki A, Yokoo H, Kakita A, Takahashi H, Harigaya Y, Ikota H, Nakazato Y. Phagocytized corpora amylacea as a histological hallmark of astrocytic injury in neuromyelitis optica. *Neuropathology.* 2012; 32:587–94.
- Sweeney MD, Zlokovic BV. A lymphatic waste-disposal system implicated in Alzheimer's disease. *Nature.* 2018; 560(7717):172–4.

I

- Takahashi K, Agari M, Nakamura H. Intra-axonal corpora amylacea in ventral and lateral horns of the spinal cord. *Acta Neuropathol.* 1975; 11:151–8.
- Tate-Ostroff B, Majocha RE, Marotta CA. Identification of cellular and extracellular sites of amyloid precursor protein extracytoplasmic domain in normal and Alzheimer disease brains. *Proc Natl Acad Sci U S A.* 1989; 86:745–9.
- Tatomir A, Talpos-Caia A, Anselmo F, Kruszewski AM, Boodhoo D, Rus V, et al. The complement system as a biomarker of disease activity and response to treatment in multiple sclerosis. *Immunol Res.* 2017; 65:1103–9.
- Tokutake S, Nagase H, Morisaki S, Oyanagi S. X-ray microprobe analysis of corpora amylacea. *Neuropathol Appl Neurobiol.* 1995; 21:269–73.
- Treitel T. *Graefes Archiv für Ophtalmologie.* 1876; 22.
- Tripathi BJ, Tripathi RC: Tracing the bulk outflow route of cerebrospinal fluid by transmission and scanning electron microscopy. *Brain Res.* 1974; 80:503–6.

V

Varki A. Biological roles of glycans. *Glycobiology*. 2017; 27:3–49.

Vasaikar S, Tsiaras G, Landázuri N, Costa H, Wilhelmi V, Scicluna P, Cui HL, Mohammad AA, Davoudi B, Shang M, Ananthasethan S, Strååt K, Stragliotto G, Rahbar A, Wong KT, Tegner J, Yaiw KC, Söderberg-Naucler C. Overexpression of endothelin B receptor in glioblastoma: a prognostic marker and therapeutic target? *BMC Cancer*. 2018; 18:154.

Vilchez D, Ros S, Cifuentes D, Pujadas L, Vallès J, García-Fojeda B, Criado-García O, Fernández-Sánchez E, Medraño-Fernández I, Domínguez J, García-Rocha M, Soriano E, Rodríguez de Córdoba S, Guinovart JJ. Mechanism suppressing glycogen synthesis in neurons and its demise in progressive myoclonus epilepsy. *Nat Neurosci*. 2007; 10:1407–13.

Virchow R. Über eine Gehirn und Rückenmark des Menschen aufgefundenene Substanz mit der chemischen Reaction der Cellulose. *Arch Pathol Anat Physiol Klin Med*. 1854; 6:135–8.

Virchow R. Zur Cellulosefrage. *Virchow's Arch Pathol Anat Physiol*. 1855; 6–7.

Virchow R. Die Cellularpathologie in Ihrer Begründung auf physiologische und pathologische Gewebelehre. 1871.

W

Wander CM, Tseng JH, Song S, Al Housseiny HA, Tart DS, Ajit A, Ian Shih YY, Lobrovich R, Song J, Meeker RB, Irwin DJ, Cohen TJ. The accumulation of tau-immunoreactive hippocampal granules and corpora amylacea implicates reactive glia in tau pathogenesis during aging. *iScience*. 2020; 23:101255.

Weller RO, Galea I, Carare RO, Minagar A. Pathophysiology of the lymphatic drainage of the central nervous system: Implications for pathogenesis and therapy of multiple sclerosis. *Pathophysiology*. 2010; 17:295–306.

Wilhelmus MM, Verhaar R, Bol JG, van Dam AM, Hoozemans JJ, Rozemuller AJ, Drukarch B. Novel role of transglutaminase 1 in corpora amylacea formation? *Neurobiol Aging*. 2011; 32:845–56.

Wichmann. Die Amyloiderkrankung. *Zieglers Beitr*. 1893; 13:539.

Woodford B, Tso MO. An ultrastructural study of the corpora amylacea of the optic nerve head and retina. *Am J Ophthalmol*. 1980; 90:492–502.

Wolf P. Die Amyloidkörperchen des Nervensystems. Inaug.-Dissert. Múnic. 1901.

Worby CA, Gentry MS, Dixon JE. Malin decreases glycogen accumulation by promoting the degradation of protein targeting to glycogen (PTG). *J Biol Chem.* 2008; 283:4069–76.

Wu T, Dejanovic B, Gandham VD, Gogineni A, Edmonds R, Schauer S, et al. Complement C3 is activated in human AD brain and is required for neurodegeneration in mouse models of amyloidosis and tauopathy. *Cell Rep.* 2019;28:2111–23.e6.

X

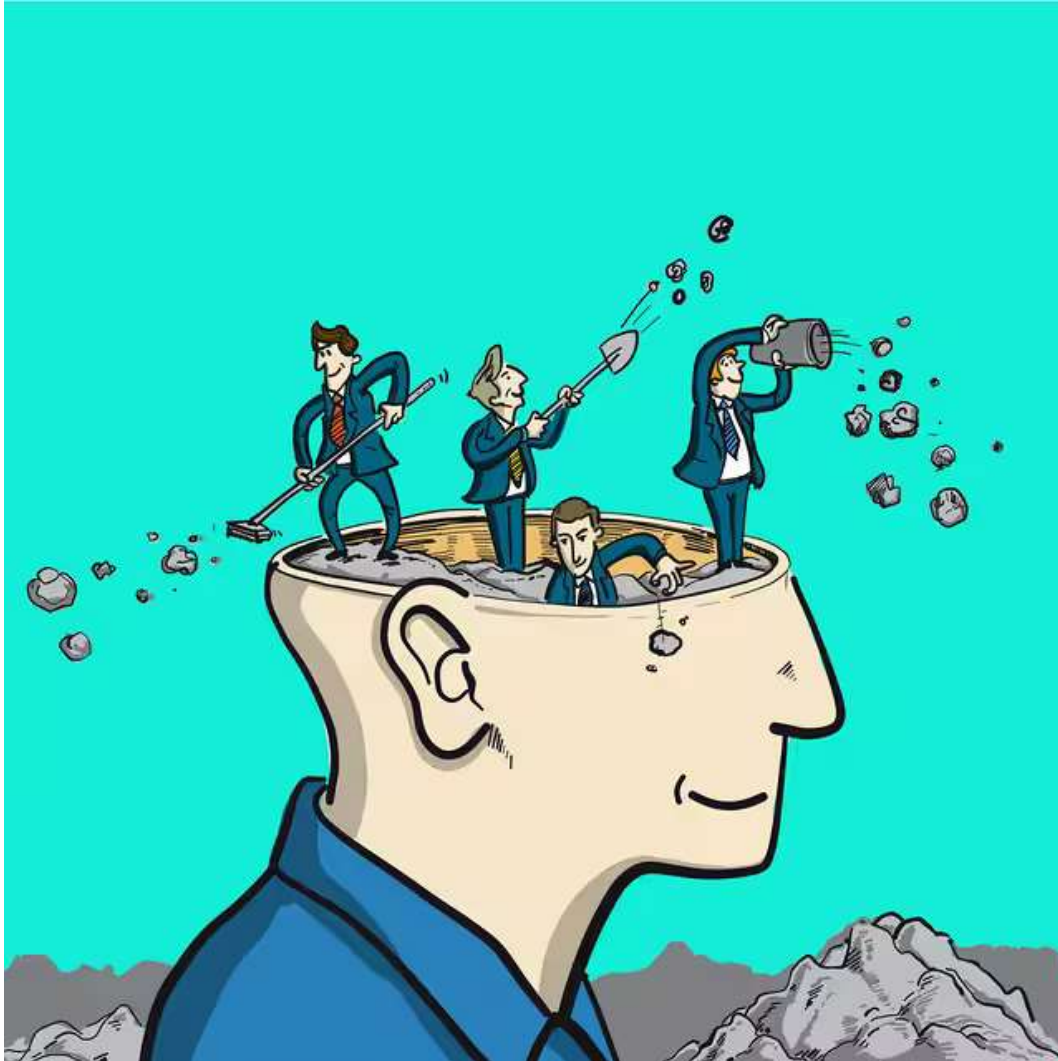
Xia L, Gildersleeve JC. Anti-glycan IgM repertoires in newborn human cord blood. *PloS One.* 2019; 1:e0218575.

Xu C, Owen JE, Gislason T, Benediktsdottir B, Robinson SR. Quantitative analysis of size and regional distribution of corpora amylacea in the hippocampal formation of obstructive sleep apnoea patients. *Sci Rep.* 2021; 11:20892.

VII. ANNEX

THE CONVERSATION

Rigor académico, oficio periodístico



Honza Hruby / Shutterstock

Así saca la basura el cerebro

15 enero 2020 21:50 CET

Jordi Vilaplana

Profesor Titular de Universidad. Departament de Bioquímica i Fisiologia, Universitat de Barcelona

Carme Pelegri

Profesora de Fisiologia, Grup de Recerca en Envel·liment i Neurodegeneració, Universitat de Barcelona

Elisabet Augé

Investigadora-Profesora Associada, Universitat de Barcelona

Marta Riba

Investigadora Predoctoral, Universitat de Barcelona

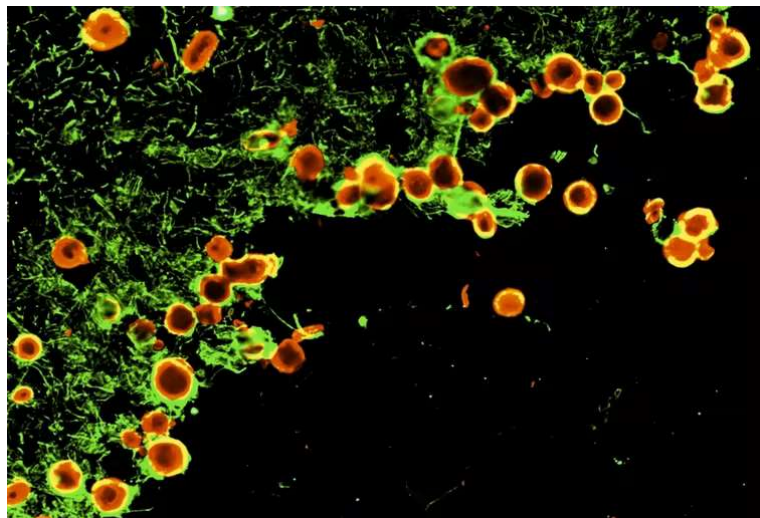
Si administrásemos un colorante vital como el azul de Evans a la sangre de una rata o un ratón, pasados unos minutos el animal tendría todos los órganos azulados, cual pitufo sin calzones, con excepción de su cerebro. La explicación es sencilla: en el cerebro existe una barrera, conocida como barrera hematoencefálica, que limita enormemente el intercambio de sustancias entre la sangre y dicho órgano.

Esta barrera provoca quebraderos de cabeza a los neurólogos, ya que dificulta la entrada de fármacos al cerebro y, por tanto, restringe los tratamientos disponibles para enfermedades como el alzhéimer y el párkinson. Pero ojo, porque esta barrera no solo limita la entrada de sustancias al cerebro. También frena su salida.

Entonces, ¿cómo hace el cerebro para sacar la basura?

Estudios recientes que hemos llevado a cabo junto con otros autores indican que el cerebro tiene un sistema propio de recogida de basura. En una primera fase, sin salir del cerebro, los desechos se vierten dentro de contenedores. Seguidamente, los contenedores abandonan el órgano pensante. Y en una tercera fase, ya fuera del cerebro, se eliminan esos contenedores.

Como veremos a continuación, esto nos va a permitir obtener información relevante acerca del estado del cerebro. Pero no nos adelantemos y describamos antes de nada cómo funciona el sistema de recogida de basura.



Contenedores siendo expulsados del cerebro. Riba, Augé, Pelegrí y Vilaplana / UB, Author provided

Los contenedores de basura del cerebro

En el cerebro existe un tipo de células llamadas astrocitos. Se caracterizan por tener forma estrellada, con digitaciones que se expanden a su alrededor. Son los responsables de generar los contenedores de basura, denominados en la jerga científica cuerpos amiláceos. Además, cual maleta facturada en un aeropuerto, los cuerpos amiláceos se etiquetan con unos marcadores denominados neo-epítomos que especifican cuál será su destino una vez expulsados del cerebro.

Generalmente, estos cuerpos amiláceos son estructuras esféricas y relativamente grandes. Pueden alcanzar diámetros de más de 20 micras, superando las 10 micras de los capilares sanguíneos. Demasiado tamaño para eliminarse a través de la sangre. Suerte que el cerebro tiene otros recursos para deshacerse de estos contenedores.

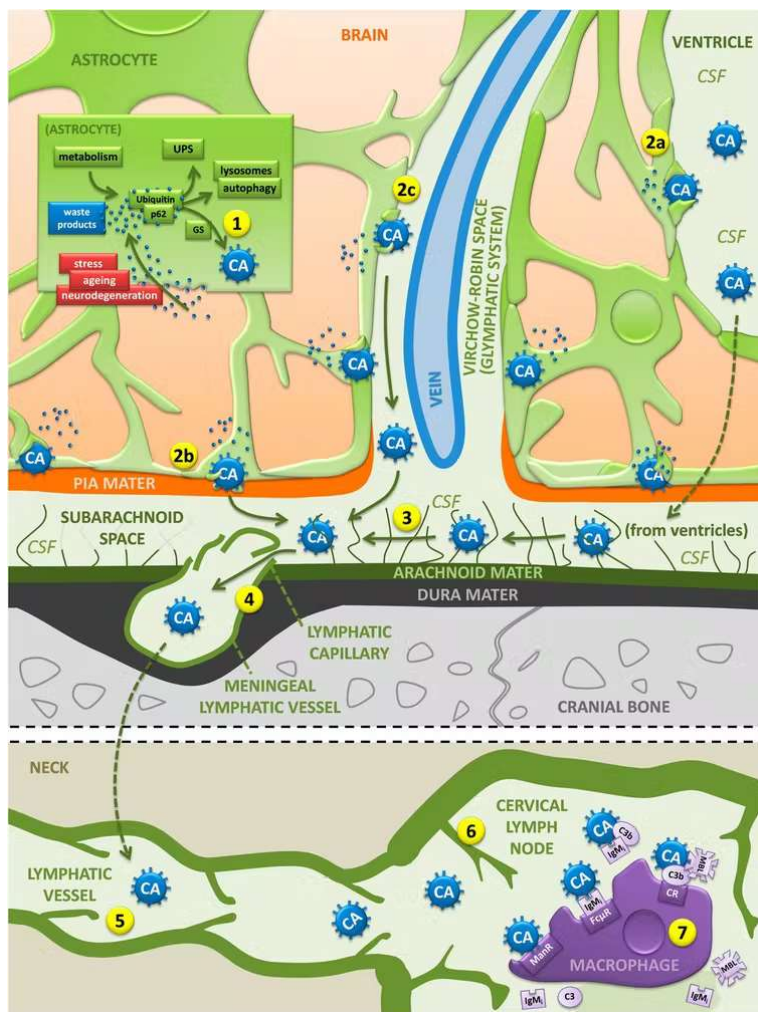
Físicamente el cerebro está muy bien protegido. Al igual que un pez de gran tamaño dentro de una pequeña pecera, “flota” dentro del cráneo suspendido en un medio acuoso llamado líquido cefalorraquídeo.

Pues bien, algunas sustancias de desecho cerebrales son vertidas directamente al líquido cefalorraquídeo, y este es el caso de los cuerpos amiláceos. Nuestros “contenedores”.

De ahí que, del mismo modo que es necesario limpiar de vez en cuando el agua de la pecera, sea necesario limpiar y renovar el líquido cefalorraquídeo, extrayendo los cuerpos amiláceos allí acumulados. Una tarea que está a cargo del sistema linfático de las meninges.

Cuestión de meninges

Entre el líquido cefalorraquídeo y los huesos del cráneo, así como entre el líquido cefalorraquídeo y el cerebro, existen unas membranas conocidas como meninges (la inflamación de estas membranas, la meningitis, es una enfermedad grave y en ocasiones mortal).



Ruta de eliminación de la basura cerebral. Marta Riba et al / PNAS 2019;116:51:26038-2604, Author provided

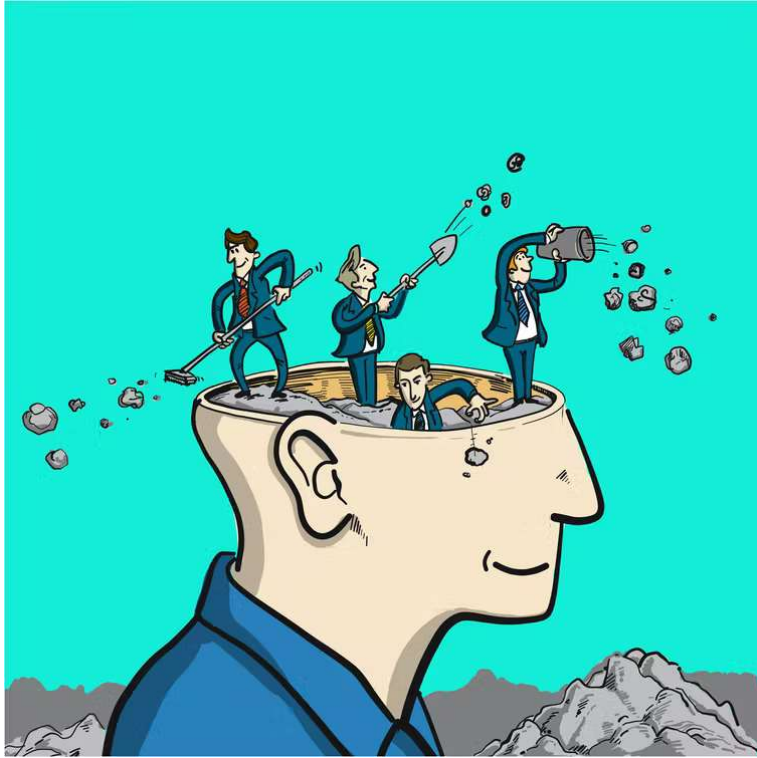
En las meninges encontramos el sistema linfático de las meninges, redescubierto recientemente. Los capilares linfáticos de las meninges recogen parte del líquido cefalorraquídeo y de los productos que contiene. Y los vasos linfáticos de las meninges descienden hacia el cuello. En el cuello se encuentran con nódulos linfáticos que filtran y limpian el líquido de productos indeseados.

Para llevar a cabo esta limpieza contamos unas células especializadas llamadas macrófagos. Los macrófagos, una vez leídas las etiquetas de destino o neo-epítomos presentes en los cuerpos amiláceos, se los “comen” (fagocitan) y proceden a su degradación química. De este modo, sustancias residuales cerebrales que no pueden ser degradadas en el propio cerebro ni pueden salir a través de la sangre encuentran una escapatoria y son eliminadas.

Una nueva herramienta para el estudio de enfermedades cerebrales

Lo más interesante del asunto es que, del mismo modo que el análisis del contenido de una bolsa de basura nos permite conocer los hábitos de las personas que las generaron, estudiando los productos de desecho presentes en los cuerpos amiláceos presentes en el líquido cefalorraquídeo podremos hacernos una idea de cómo está funcionando el cerebro.

Obtener líquido cefalorraquídeo es relativamente sencillo, por ejemplo mediante punción lumbar. Aislar los cuerpos amiláceos de este líquido también es fácil, debido a su relativamente gran tamaño, peso y densidad. Y en caso de padecer alguna enfermedad cerebral, los cuerpos amiláceos contendrán productos de desecho que nos pondrán sobre aviso. Por tanto, el análisis del contenido de los cuerpos amiláceos aislados puede ser una buena herramienta de diagnóstico.



Honza Hruby / Shutterstock

Resumiendo, en el cerebro algunos desechos se acumulan en contenedores de basura denominados cuerpos amiláceos. Estos cuerpos son expulsados al líquido cefalorraquídeo y transferidos al sistema linfático. Y ya en el sistema linfático, los macrófagos existentes en los nódulos linfáticos acaban definitivamente con ellos.

Se produce con todo ello un buen lavado de cerebro. Un lavado imprescindible para su correcto funcionamiento. Que además, ahora que lo conocemos, ofrece un nuevo enfoque para diagnosticar las enfermedades cerebrales.